00591
24

UNIVERSIDAD NACIONAL AUTONOMA DE MEXICO

INSTITUTO DE BIOTECNOLOGIA

Caracterización de un anticuerpo scFv que mimetiza el receptor natural de la proteína Cry1Ab de *Bacillus thuringienisis*

T E S I S

QUE PARA OBTENER EL GRADO DE

DOCTOR EN CIENCIAS BIOQUIMICAS

P R E S E N T A

ING. AMB. ISABEL GOMEZ GOMEZ

DIRECTOR DE TESIS

DR. MARIO SOBERON CHAVEZ

CUERNAVACA, MOR. SEPTIEMBRE 2002.

DEDICATORIAS

Dedico este trabajo a mis Padres quienes en todo momento han sabido impulsarme para alcanzar mis sueños. Gracias por este regalo tan maravilloso que es mi vida.

A mis hermanos y hermanas: Daniel, Rosa, Jorge Luis, Leobardo, Nadia, Juan Antonio y José Manuael con quienes disfruto momentos increíbles. Deseo de todo corazón que cada uno alcance sus sueños.

A quien inspiró todo este esfuerzo, quien ha luchado hombro con hombro y con quien seguiré hacia delante por siempre: Hugo Alejandro Ovando. Gracias por ser esta parte fundamental de mi vida. Te quiero.

AGRADECIMIENTOS

Deseo primeramente agradecer al Dr. Mario Soberón Chávez por abrirme esta oportunidad de desarrollo académico en su grupo, por su entusiasmo al dirigir esta Tesis y por todo el apoyo que recibí para realizar este trabajo.

A la Dra. Alejandra Bravo por la colaboración y apoyo a lo largo de todo este trabajo, por las discusiones que tanto aportaron a este trabajo y por creer en mí.

Al Dr. Juan Miranda Ríos por compartir conmigo su experiencia en Biología Molecular y por todos sus comentarios que enriquecieron este trabajo, pero sobre todo por su Amistad.

Al Dr. Baltazar Becerril por todo el apoyo brindado en la parte experimental que se refiere a Phage Display.

A los Dres. Baltazar Becerril y Alicia González por haber formado parte de mi comité tutoral durante mis estudios de doctorado, todas las discusiones aportaron algo valioso a este trabajo.

Al Dr. Enrique Rudiño por su valiosa colaboración en el modelo sobre la interacción entre la toxina Cry1Ab y el fragmento del receptor Bt-R_1.

A los Dres. José Luis Puente, Joel Osuna, Adela Rodríguez, Karen Manoutcharian, Enrique Rudiño y Lorenzo Segovia por la revisión del manuscrito y por sus sugerencias para mejorar el trabajo.

Al Biol. Jorge Sánchez por compartir toda su experiencia sobre toxinas Cry conmigo, por todos sus consejos para mejorar mis experimentos y por la extraordinaria Amistad que tenemos.

Al Ing. Guadalupe Peña con quien he compartido horas y horas de trabajo en el laboratorio, disfrutando de cada experimento exitoso y batallando con los que han resultado más latosos.

Al Dr. Carlos Muñoz quien se ha incorporado recientemente al grupo, pero con quien he discutido largamente para enfrentar nuevos retos sobre las toxinas Cry.

Gracias a Claudia Morera por ser tan paciente y por darme además de su apoyo técnico su increíble Amistad.

A Oswaldo López, Lizbeth Cabrera y a Laurita, quien ya no esta en nuestro grupo, por todo el apoyo técnico en diferentes partes de este trabajo.

Deseo agradecer muy especialmente todo el invaluable apoyo técnico que recibí de Sergio Blancas y Alejandro Uribe por el cual este trabajo resultó exitoso. Mil gracias por su Amistad.

A Graciela Domínguez por todo su apoyo en la parte administrativa.

A mis compañeros de laboratorio: Iván Arenas, Itzel Benítez, Giovanni Ríos, Claudia Pérez y Juan Conde con quienes comparto trabajo y amistad.

A la Unidad de Síntesis por los Oligos que utilizamos en diferentes partes de este trabajo.

A mis nuevos amigos: Santiago Becerra, Paul Gaytán, Gabriela Flores, Lidia Riaño, Luisa Fernández, y Adriana Valdéz.

Gracias a toda la gente que brinda su apoyo administrativo en nuestro Instituto. En especial quiero agradecer a Maribel y a Gloria, de Docencia, por ser tan amables y pacientes y por ayudarme a ver claro cuando la desesperación nubló mi mente.

Finalmente agradezco a CONACYT la Beca-Crédito, No de Registro 128488, que me permitó realizar mis estudios de Doctorado.

Este trabajo se realizó en el Departamento de Microbiología Molecular del Instituto de Biotecnología de la UNAM bajo la dirección del Dr. Mario Soberón Chávez.

TABLA DE CONTENIDO

INDICE DE FIGURAS

LISTA DE ABREVIATURAS

ANS	8-anilino-1-nafatalenosulfonato
APN	Aminopeptidasa-N
BSA	Albúmnina sérica
Bt	*Bacillus thuringiensis*
Bt-R_1	*Bacillus thuringiensis*-Receptor 1
Bt-R_{175}	*Bacillus thuringiensis*-Receptor de 175 kDa de *Bombix mori*
cDNA	Cadena sencilla de DNA
CDR3	Región determinante de complentariedad
Dis-C_3(5)	3,3'dipropiltiodicarbocianina
DNA	Acido desoxirribonucleico
DTT	Ditiotritiol
EDTA	Acido etilen diamino tetra-acético
EGTA	N, N, N',N'-ácido tetra acético Etilen glycol-bis-(β-aminoetil éter)
ELISA	Ensayo inmunoadsorbente ligado a enzimas
erm	Eritromicina
g	gramos
GalNAc	N-acetil-galactosamina
GPI	Glicosil-fosfatidil-inositol
h	horas
HEPES	Acido 4-(2-hidroxi etil)piperazina-1-etano sulfónico
IPTG	Isopropil-β-D-tiogalactopiranósido
LB	Medio de cultivo
LB-amp	Medio de cultivo adicionado con ampicilina
mM	Concentración mili molar
PBS	Solución amortiguadora de fosfatos
PCR	Reacción en cadena de polimerasa
pH	Potencial de hidrógeno
PMSF	Fenil metanosulfonil fluoruro
PVDF	Membrana de inmobilón-P. Polivinilideno difluoruro
RNA	Acido ribonucleico
scFv	Fragmento variable de cadena sencilla
SDS	Dodecil sulfato de sodio
SDS-PAGE	Electroforesis en gel de acrilamida en condiciones desnaturalizantes
SP	Medio de esporulación
TRM	Teoría de reconocimiento molecular
VMMA	Vesículas de la microvellosidad apical media

Caracterización de un anticuerpo scFv que mimetiza el receptor natural de la proteína Cry1Ab de *Bacillus thuringiensis*

ABSTRACT

The Cry proteins of *Bacillus thuringiensis* are potential bioinsecticides for the control of several pests and human vector diseases like mosquitoes. The Cry toxins exert their effect on midgut of sensitive insects. It has been described that specificity and toxicity correlates with binding of the toxins to receptors located in the insect midgut cells. For this reason, the study on the interaction between the Cry toxins and their receptors is very important for understanding the molecular basis of insect specificity.

In this work using Phage Display, we obtained scFv antibodies that interact with Cry1Ab toxin from *Bacillus thuringiensis*. One of these antibodies, designed scFv73, led us to identify a discrete region on cadherin like receptor Bt-R_1 from *Manduca sexta* that interact with Cry1Ab toxin. This interaction is very important in the mode of action since bioassays done with Cry1Ab toxin preincubated with an excess of scFv73 showed a significative toxicity decrease. The interaction of the toxin with the region ^{869}HITDTNNK^{876} from Bt-R_1 was confirmed by using synthetic peptides that inhibit the interaction between Cry1Ab toxin with Bt-R_1 receptor in toxin overlay assays. We tested that the interaction of the ^{869}HITDTNNK^{876} in Bt-R_1 is with loop 2 of domain II of Cry1Ab toxin and this interaction is determined by complementary hydropathic profiles like as suggested by the molecular recognition theory. Finally, we tested that interaction between Cry1Ab and Bt-R_1 facilities the proteolysis of helix α-1 in domain I with the subsequent oligomerization of four Cry1Ab monomers that probed to be insertion capability into brush border membrane vesicles *in vitro*.

A second site in Bt-R_1 that was recognized by the loop α-8 from domain II of Cry1Ab toxin, was also identified.

The scFv antibodies are powerful tools for the research of the interaction between Cry toxins and their receptors, for this reason we are working with the construction of immune libraries of scFv antibodies. With these repertories we could obtain new information about the interaction between different Cry toxins with their receptors and the role for this interaction on the mode of action for Cry toxins.

RESUMEN

Las proteínas Cry de *Bacillus thuringiensis* son bioinsecticidas con gran potencial de aplicación para el control de insectos plaga y de vectores de enfermedades como los mosquitos. Estas toxinas ejercen su efecto en las células del intestino de los insectos susceptibles y se ha demostrado que la interacción de las toxinas con los receptores localizados en estas células determina especificidad y toxicidad, por lo que el estudio de la interacción de las toxinas con sus receptores es importante para entender más acerca del mecanismo de acción de estas toxinas.

En este trabajo, haciendo uso de la técnica de despliegue en fagos "phage display" logramos obtener anticuerpos scFv que interactúan con la toxina Cry1Ab de *Bacillus thuringiensis*. Uno de estos anticuerpos, denominado scFv73, nos permitió identificar una región localizada en una proteína de tipo caderina de *Manduca sexta* (Bt-R_1) que interacciona con la toxina Cry1Ab. Dicha interacción es importante dentro del modo de acción ya que si se preincuba la toxina con un exceso del scFv73 se disminuye la toxicidad un 50%. La interacción de la toxina con la región ^{869}HITDTNNK^{876} del receptor Bt-R_1 se confirmó mediante el uso de péptidos sintéticos que inhibieron la interacción entre la toxina y el receptor Bt-R_1. También fue posible identificar que el asa 2 del dominio II de esta toxina es la que reconoce al epitope ^{869}HITDTNNK^{876} en el receptor. Esta interacción se da a través de perfiles de hidropatía complementarios como lo sugiere la teoría de reconocimiento molecular. Finalmente, observamos que la interacción entre el Bt-R_1 y la toxina Cry1Ab favorece el procesamiento proteolítico de la hélice α1 del dominio I y la oligomerización de esta, formándose un agregado de 4 subunidades capaces de insertarse en vesículas de membrana de *Manduca sexta in vitro*.

Además, también identificamos otro sitio de interacción de la toxina Cry1Ab con el receptor Bt-R_1 el cual corresponde con la asa α8.

Los anticuerpos scFv resultaron una herramienta valiosa para el estudio de las interacciones entre las toxinas Cry con sus receptores por lo que la construcción de nuevas librerías inmunes nos permitirá entender, más acerca del complejo mecanismo de interacción de

diferentes toxinas Cry con la membrana de los insectos blanco y de los diferentes pasos que estén involucrados en su toxicidad.

INTRODUCCION

ANTECEDENTES GENERALES

El control de plagas de insectos, que afectan cultivos de interés comercial o que son vectores de enfermedades en humanos, es uno de los principales intereses a nivel mundial en la producción de alimentos y en la salud humana. Se estima que hasta un 28% de la producción de alimentos en el mundo se pierde por plagas de insectos ya sea en el campo o durante su almacenamiento. Hasta la fecha el control de estas plagas se ha basado en el uso de insecticidas químicos; lo que ha provocado una serie de efectos no deseados como son: la acumulación de químicos carcinogénicos en los ecosistemas, la contaminación del agua, el desarrollo de resistencia por parte de los insectos y la destrucción indiscriminada de insectos benéficos. Todo esto, ha dado origen a la búsqueda de alternativas que no dañen al medio ambiente y que permitan un control adecuado de estas plagas (Rajamohan et al., 1998).

Los bioinsecticidas representan una alternativa potencial sobre los insecticidas químicos, particularmente cuando la resistencia de los insectos o los efectos no deseados en el medio ambiente están asociados con el uso de sustancias químicas. Los insecticidas químicos han dominado el mercado de control de plagas ya que presentan un gran número de ventajas entre las que se incluyen: su bajo costo de producción, un amplio espectro de especies blanco y su fácil aplicación. Por el contrario, los bioinsecticidas cuentan con un pequeño segmento dentro del mercado (<5%) a pesar de que en áreas donde se practica su aplicación ofrecen una alternativa ambientalmente segura y de bajo costo con respecto a los químicos. Sin embargo, en otras áreas los bioinsecticidas no tienen un costo accesible o bien, los bioinsecticidas apropiados aún no han sido identificados (Bishop, 1994).

Diversas toxinas bacterianas, virus y hongos son utilizados para el control de plagas de cultivos. Sin embargo, a nivel mundial, los bioinsecticidas son utilizados en unos cuantos millones de hectáreas de cultivos y bosques cada año (Bishop, 1994). Paradójicamente, la alta especificidad de los biopesticidas es a la vez una ventaja y desventaja. Por un lado, esta

especificidad significa que especies no blanco (insectos benéficos, otros invertebrados, vertebrados y plantas) no son afectados. Por el otro lado, su especificidad restringe su uso en donde, por ejemplo, varias plagas afectan a un cultivo particular. Su relativa baja velocidad de acción y sus altos costos de producción son también factores que limitan el uso de algunos bioinsecticidas como virus y hongos. La ingeniería genética esta investigando varios de estos problemas con el objetivo de resolverlos sin perder las características benéficas de estos insecticidas biológicos (Bishop, 1994; Van Rie, 2000). Entre los diferentes agentes de control biológico, las bacterias patógenas de insectos han sido una de las alternativas más estudiadas y con mayor potencial. Aún cuando diversas bacterias infectan y matan insectos, *Bacillus thuringiensis* es el agente de control biológico comercialmente más probado y utilizado sobre plagas de insectos a nivel mundial (Rajamohan et al., 1998).

Bacillus thuringiensis

Bacillus thuringiensis (Bt) es el nombre que se le da a una familia de bacterias encontradas alrededor de todo el mundo. La primera descripción de Bt apareció por primera vez en un artículo Japonés en 1901. La cepa fue aislada de larvas del gusano de la seda (*Bombix mori*), que morían rápidamente por una infección causada por la bacteria, así que fue considerada una plaga. La bacteria fue denominada *Bacillus sotto* ("sotto" significa colapso repentino en japonés) pues mataba rápidamente a las larvas. Unos diez años más tarde otra bacteria parecida fue encontrada en Alemania en larvas de *Anagasta kuhniella* y es a partir de este descubrimiento en la provincia de Thuringen que la bacteria se denominó *Bacillus thuringiensis*, un nombre que designa una gran familia de bacterias que producen cristales insecticidas, las cuales se clasifican en diferentes subespecies de acuerdo al serotipo flagelar (Yamamoto and Dean, 2000).

Bacillus thuringiensis es una bacteria aerobia gram positiva, caracterizada por la producción, durante su fase de esporulación, de una gran cantidad de proteínas insecticidas. Estas proteínas son acumuladas en inclusiones cristalinas las cuales al lisarse las células se liberan

junto con las esporas. Por su acumulación en forma de cristales, estas proteínas son designadas proteínas Cry o δ-endotoxinas (Yamamoto and Dean, 2000).

Las δ-endotoxinas se dividen en dos grandes familias con base en su identidad de secuencia: Cry y Cyt. Las toxinas de la familia Cyt se distinguen de las toxinas Cry en diversos aspectos: exhiben acción citolítica sobre una gran variedad de células eucarióticas y eritrocitos *in vitro* esto, a pesar de que ambos tipos de toxinas tienen la propiedad de formar poros en bicapas lipídicas (Knowles et al., 1989; Von Tersch et al., 1994). Otros reportes han demostrado sinergismo entre las toxinas Cyt y Cry con actividad contra mosquitos, lo que ha despertado el interés en entender más sobre el mecanismo de acción de esta familia de proteínas para su mejor aprovechamiento (Wu and Chang, 1985; Wu et al, 1994; Crickmore et al., 1995).

Las proteínas Cry, a diferencia de las Cyt, son tóxicas contra varias plagas de insectos de los órdenes Lepidóptera, Coleóptera y Díptera así como para algunos Nemátodos. Hay reportes más recientes de cepas de Bt activas contra otros órdenes de insectos (Himenóptera, Homóptera, Ortoptera y Mallofaga) así como contra moscas y protozoarios (Schnepf et al., 1998).

Además de las δ-endotoxinas, las cuales normalmente se expresan durante la fase estacionaria tardía y cristalizan en la célula durante la esporulación, algunas cepas de Bt también contienen toxinas insecticidas extracelulares o β-exotoxinas. Normalmente las exotoxinas son expresadas durante la fase vegetativa del desarrollo. Una clase de exotoxinas es denominada "Vip" (proteínas insecticidas vegetativas) y aunque el modo de acción de estas toxinas no se ha reportado, si se sabe que por ejemplo Vip1 y Vip2 son toxinas binarias tóxicas para *Diabrótica* y que Vip3 es activa contra algunos lepidópteros, especialmente del género *Spodoptera* (Yamamoto and Dean, 2000).

Proteínas Cry: Clasificación y Estructura

En 1989 Höfte y Whiteley presentaron una clasificación de las toxinas Cry basada en la identidad de secuencia y en el orden del insecto contra el que son específicas; de este modo las toxinas con actividad insecticida para lepidópteros se denominaron CryI, aquéllas que son tóxicas contra lepidópteros y dípteros se llamaron CryII, CryIII son tóxicas para coleópteros y las CryIV son específicas para dípteros. Al ir creciendo el número de secuencias reportadas se decidió que las proteínas Cry se clasificarían exclusivamente de acuerdo a la identidad de su secuencia de aminoácidos. Se propuso conservar el nombre Cry y a cada proteína se le asignó un nombre compuesto por 4 categorías. En la primera categoría se cambió el número romano por un número arábigo y a todo gen cuyo producto muestra una identidad menor al 45% respecto de las proteínas conocidas se le asigna un nuevo número arábigo. La segunda categoría es una letra mayúscula y se le asigna una nueva letra a todo gen cuya secuencia comparta menos del 75% de identidad pero más del 45%. La tercera categoría es una letra minúscula y se asigna a todas las proteínas que compartan menos del 95% de identidad pero más del 75%. Para diferenciar a las proteínas que varían solamente en algunos residuos, se asigna una cuarta categoría que consiste en un número arábigo y se le asigna a las proteínas que presentan una identidad entre el 95 y 100% (Crickmore et al., 1998).

La estructura tridimensional de tres proteínas Cry se ha resuelto mediante cristalografía de rayos X. Estas proteínas son específicas para lepidópteros: Cry1Aa (Grochulski et al., 1995), coleópteros: Cry3A (Li et al., 1991) y dípteros-lepidópteros: Cry2Aa (Morse et al, 2001). Para resolver las estructuras de las toxinas Cry1Aa y Cry3A se emplearon a las toxinas activadas con tripsina, mientras que para la Cry2Aa se utilizó a la protoxina completa sin digerir. Estas proteínas muestran características estructurales similares como se puede observar en la figura 1.

Las proteínas Cry se encuentran compuestas por tres dominios estructurales distinguibles entre sí, cada uno constituido por cerca de 200 aminoacidos. El Dominio I contiene siete hélices α, seis de las cuales son anfipáticas (α1, α2, α3, α4, α6 y el α7) y se encuentran

rodeando la hélice α5 que es la más hidrofóbica. El dominio II esta compuesto de tres láminas β arregladas en forma de un prisma piramidal, las cuales están unidas por asas que varían en tamaño y constituyen regiones hipervariables entre las diferentes toxinas Cry. Este arreglo de asas es muy parecido en estructura a los sitios de unión al antígeno en las inmunoglobulinas, por lo que se propusieron como candidatos de sitios de unión a los receptores y por lo tanto como responsables de la especificidad en las toxinas Cry. El dominio III constituye la región carboxilo terminal de la toxina, se compone de dos láminas β arregladas de forma antiparalela, integrando un β-sandwich (Rajamohan et al., 1998).

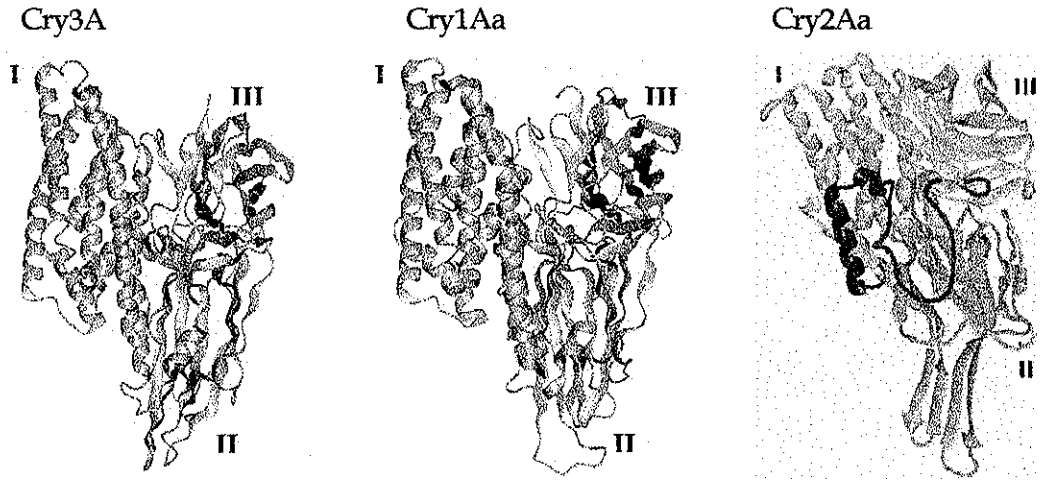

Figura 1. Estructura tridimensional de diferentes toxinas Cry.

A lo largo de las secuencias de las diferentes toxinas Cry se identificaron regiones con gran identidad en secuencia. Estas regiones designadas como "bloques conservados" (del 1 al 5), fueron identificadas en regiones estructuralmente importantes como el contacto entre dominios y en regiones dentro de la molécula en las toxinas, sugiriendo que toxinas que contengan estos bloques tendrán una estructura similar (Höfte and Whiteley, 1989; Li et al., 1991).

Mecanismo de acción de las toxinas Cry

Los cristales compuestos por las protoxinas Cry deben ser ingeridos y digeridos por los insectos para que desplieguen su acción insecticida. Aunque el mecanismo de acción

detallado aún no se ha descrito completamente, una cantidad importante de información se ha generado al respecto en los últimos años. También es importante mencionar que la mayor parte de la información se ha obtenido de insectos del orden lepidóptera por la facilidad que representa su tamaño y su cultivo en condiciones de laboratorio. En general, el mecanismo de acción de las toxinas Cry involucra la solubilización del cristal y liberación de las protoxinas, la activación proteolítica de la protoxina, la unión de la toxina Cry a receptores localizados en el intestino medio y la inserción de la toxina en la membrana para formar poros (Schnepf et al., 1998; Rajamohan et al., 1998; Li et al., 2001).

Solubilización y Activación

El blanco primario de las toxinas Cry es la membrana del intestino, lo que las convierte en venenos intestinales. Muchas proteínas Cry son insolubles en condiciones neutras o ligeramente ácidas lográndose solubilizar únicamente en pH alcalino y bajo condiciones reductoras debido a que la mayoría de las protoxinas contienen en su carboxilo terminal varios residuos de cisteína que forman puentes disulfuro. El intestino medio de muchos lepidópteros y dípteros se caracteriza por tener condiciones alcalinas y reductoras ideales para la solubilización de los cristales (Knowles, 1994).

La activación ocurre a través de proteólisis discreta por proteasas, del tipo tripsina o quimiotripsina, presentes en el intestino de los insectos susceptibles dando origen a una proteína activa capaz de matar al insecto. Las protoxinas pueden ser activadas *in vitro* con tripsina o con el jugo gástrico de los insectos susceptibles sin perder su efecto letal *in vivo*. Aproximadamente el 50% de la protoxina se remueve a través de cortes proteolíticos en el extremo carboxilo terminal. Mientras que en el extremo amino terminal se eliminan aproximadamente 28 aminoácidos. Dado que el extremo carboxilo de la protoxina no es esencial para la toxicidad, esta región podría estar involucrada en la estabilidad de la protoxina y podría también estar protegiendo a la toxina de la digestión proteolítica prematura (Knowles, 1994; Rajamohan et al., 1998).

Unión al receptor

A finales de los 80's se demostró que las toxinas Cry podían interactuar con gran afinidad con vesículas de membrana de la microvellosidad apical (VMMA) (Hofmann et al., 1988). Desde entonces la unión de la toxina a la microvellosidad del intestino medio ha sido unos de los pasos más estudiados dentro del modo de acción de las toxinas Cry por ser un paso necesario para la actividad insecticida.

Experimentos de inmunocitoquímica *in vivo* permitieron determinar que las toxinas Cry se unen a la membrana de células epiteliales, en los insectos susceptibles, sin internarse en ellas (Bravo et al, 1992).

In vitro, empleando toxinas marcadas con radioactividad y VMMA's de insectos susceptibles, se hizo posible estudiar la unión de las toxinas Cry a nivel molecular. Los resultados de estos experimentos revelaron lo complejo de este proceso porque la interacción se compone de dos pasos: la unión reversible al receptor y la inserción irreversible en la membrana (Liang et al., 1995). Una gran cantidad de estudios demostró que existe una relación entre la afinidad, la concentración de los sitios de unión y la actividad insecticida; sin embargo, algunas excepciones se han descrito a este respecto, un ejemplo es lo reportado por Wolfersberger, quien observó una relación inversa entre la unión y la toxicidad en *Lymantria dispar* con las toxinas Cry1Ab y Cry1Ac. El notó que la toxina con alta actividad insecticida Cry1Ab tiene una unión reducida, mientras que una toxina menos activa, Cry1Ac, se une con mayor afinidad (Wolfersberger, 1990). En otro caso, se demostró que las toxinas Cry1Aa y Cry1Ab tienen capacidades de unión similares en VMMA's de *B. mori.* Sin embargo, la actividad insecticida de Cry1Aa es 100 veces mayor que la de Cry1Ab en los insectos. (Ihara et al., 1993). En ambos casos se demostró que las toxinas con mayor actividad (Cry1Ab en el caso de *L. dispar* y Cry1Aa para *B. mori*) presentan un mayor porcentaje de la toxina asociada de forma irreversible en la membrana.

Estos ensayos de unión, además de permitir la comparación de la afinidad de toxinas nativas y mutantes diseñadas para identificar los sitios de la toxina involucrados en la interacción

con el receptor; también han hecho posible estudiar mecanismos de desarrollo de resistencia asociada con la variación en las propiedades de unión de las toxinas a las VMMA's de insectos resistentes (Van Rie et al., 1990; Ferre et al, 1991).

En años recientes, estudios sobre la naturaleza de los sitios de unión de las proteínas Cry permitió identificar proteínas del tipo aminopeptidasa y caderina como posibles receptores para estas toxinas (Denolf, 1999).

Oligomerización y formación de poro.

Después de que la toxina se ha unido a su receptor, se inserta rápida e irreversiblemente en la membrana de las células. Se propone que la unión de la toxina al receptor puede provocar un cambio conformacional que hace a la toxina competente para insertarse en la membrana, pero se desconoce si este evento puede promover una cadena de señalización intracelular que sumado a la formación del poro provoque la lisis y muerte celular (Rajamohan et al., 1998).

El siguiente paso involucra la formación del poro en la membrana (Lorence et al., 1995; Rajamohan et al., 1998). Existen evidencias de estudios *in vitro* que muestran que entonces las proteínas forman oligómeros de varias subunidades, aunque aún no esta claro si esto ocurre antes o después de la inserción (Yamamoto and Dean, 2000; Soberón et al., 1999).

En 1987 se determinó que diferentes proteínas Cry son capaces de formar poros de aproximadamente 10-20 Å en bicapas sintéticas (Knowles and Ellar, 1987). Hasta ahora las evidencias generadas han demostrado que las toxinas pueden formar agregados de aproximadamente 200 kDa y que se requieren al menos 4 monómeros de toxina para poder formar poros (Aronson, 1999; Schwartz and Laprade, 2000; Vié et al., 2001).

Relación estructura-función en las toxinas Cry

Basados en la estructura de las toxinas Cry, en experimentos de mutagénesis dirigida y mediante intercambio de fragmentos, se propuso la función de cada dominio: las hélices

anfipáticas del Domino I como responsables de la formación del poro, el Dominio II como el principal responsable de la interacción con los receptores, mientras que el Dominio III tiene un papel importante en la integridad de la proteína y en la interacción con el receptor.

El dominio I (Figura 2), compuesto por hélices α es el responsable de la inserción en la membrana. Cinco de las hélices externas (α3-α7) son lo suficientemente largas como para atravesar a la membrana. Un parecido estructural entre el dominio I de las proteínas Cry y dominios de otras toxinas capaces de atravesar membranas como el de la colicina A da soporte a esta teoría. El dominio I por si solo, expresado de un gene truncado es capaz de insertarse en vesículas de fosfolípidos, no obstante su actividad de formación de poro es muy diferente comparada con la obtenida con la toxina completa (Schnepf et al., 1998).

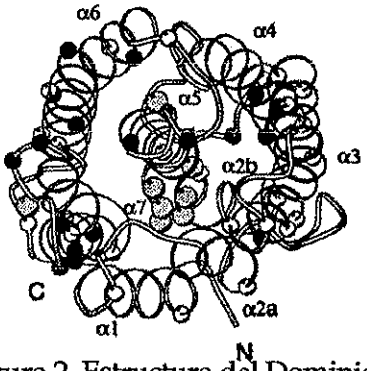

Figura 2. Estructura del Dominio I.

Los mecanismos de inserción de otras toxinas bacterianas diferentes a Bt, han ayudado a proponer dos modelos de inserción para las proteínas Cry. Los modelos denominados como el de "sombrilla" y el del "abrecartas", están basados en la idea de que solamente una parte del Dominio I es capaz de insertarse en la membrana. De acuerdo con el primer modelo (de sombrilla), el asa hidrofófica entre las hélices α4 y α5 inicia la inserción en la membrana. Se han reportado algunos datos experimentales que favorecen el modelo de sombrilla utilizando péptidos sintéticos en donde se muestra que las hélices α4 y α5 se insertan transversalmente en membranas lipídicas mientras que la hélice α7 sintética no reveló esta misma capacidad (Gazit and Shai, 1995; Gazit et al., 1998; Aronson and Shai, 2001). Otra evidencia a favor del modelo de la sombrilla son mutantes localizadas en la región del asa

que conecta las hélices α4 y α5, las cuales están afectadas en su capacidad de inserción, mientras que la mutantes localizadas entre las hélices α5 y α6 no presentan este problema (Chen et al., 1995; Hussian et al., 1996; Schwartz et al., 1997).

El modelo del abrecartas, propuesto por Hodgman y Ellar, es una adaptación del modelo de la colicina A, en el cual se formula que las hélices hidrofóbicas α5 y α6 sobresalen de la toxina insertándose como un abrecartas en la membrana mientras que el resto de la toxina permanece fuera de la membrana o unida al receptor (Hodgman y Ellar, 1990).

Existe aún gran controversia acerca de cual es el modelo que describe de manera sólida la inserción de la toxina en la membrana, por lo que los estudios sobre oligomerización y la estructura de la toxina insertada en la membrana ayudarán a entender más sobre problema.

En el dominio II se localizan regiones hipervariables expuestas que unen las láminas β que lo conforman (asas α8, 1, 2 y 3). Mediante mutagénesis sitio-dirigida y con intercambio de segmentos entre diferentes toxinas se han identificado algunos residuos involucradas en la unión específica a membranas de lepidópteros y coleópteros demostrándose su participación en la unión a los receptores (Dean et al., 1996; Wu and Aronson, 1992). Por ejemplo, la especificidad de la toxina Cry1Aa hacia *B. mori* se puede trasladar a la toxina Cry1Ac (la cual no presenta actividad contra este insecto) al intercambiar una región con poca similitud entre los genes de estas proteínas (residuos 332-450), que corresponden a un fragmento del dominio II (Ge et al., 1989). Otros estudios han permitido determinar que los residuos 335-450 de la toxina Cry1Ac son importantes para la actividad hacia *Trichoplusia ni* pero que la actividad contra *Heliothis virescens* requiere de la región comprendida entre los residuos 335-615 de esta misma toxina (Ge et al., 1991). Estos resultados indican que las regiones determinantes de especificidad no estan restringidas únicamente a las regiones hipervariables y además difieren dependiendo del insecto blanco.

De manera general, los residuos de las asas han sido considerados como los principales responsables de la interacción con el receptor, sin embargo las interacciones funcionales de residuos individuales difieren significativamente entre insectos blanco. Por ejemplo, la

mutación en el asa2 de Cry1Ab F371A reduce la toxicidad a *M. sexta* afectando la unión irreversible de la toxina, pero la misma mutación no tiene efecto en la unión ni sobre la toxicidad en *H. virescens*. De igual modo, aunque Cry1Ab reconoce diferentes receptores en *M. sexta* y *H. virescens* en VMMA's, el cambio por alanina de los residuos G439 y F440 localizados en el asa 3 afectan la unión inicial al receptor y reducen la toxicidad en ambos insectos (Rajamohan et al., 1996).

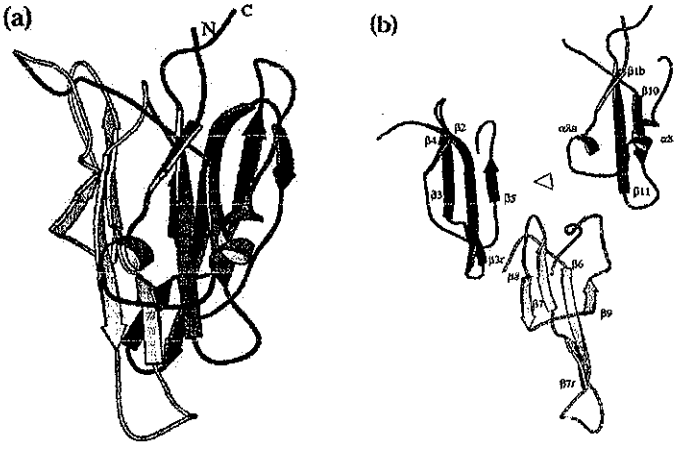

Figura 3. (a) Estructura del Dominio II. (b) Asas que unen las láminas β que lo conforman.

Mutaciones también localizadas en el dominio II, pueden mejorar la unión y toxicidad en algunos insectos. Una mutante triple de la toxina Cry1Ab (N372A, A282G, L283S), localizadas en las asas α8 y asa2, muestra un incremento de 18 veces en la unión a VMMA's y 36 veces en toxicidad contra *L. dispar*, una plaga de gran importancia en bosques (Rajamohan et al., 1996). Al cambiar los residuos del asa3, del dominio II en la toxina Cry3A, por alaninas se incrementó la toxicidad hacia *Tenebrio molitor* 2.4 veces (Wu and Dean, 1996). Mientras que otra mutación en el asa1 de esta misma toxina también incrementó la toxicidad hacia *T. Molitor* (11.4 veces), *Chrysomela scripta* (2.5 veces) y en *Leptinotarsa decemlineata* (1.9 veces) (Wu and Dean, 1996). Estos ejemplos nos ilustran como el entender más acerca de las interacciones toxina-receptor puede permitirnos la construcción de una segunda generación de toxinas más potentes.

Es interesante también que el dominio II tiene un plegamiento similar al de una lectina de plantas denominada jacalina, la cual es capaz de unir carbohidratos a través de las asas

expuestas en los ápices del β-prisma (Sankaranarayanan et al., 1996). A la fecha se sabe que la proteína Cry1Ac reconoce un motivo carbohidrato (N-acetil galactosamina) en uno de los receptores (la aminopeptidasa N) de *L. dispar*, sin embargo esta interacción se da a través del dominio III (residuos 509-513, 544-547) (Burton et al., 1999; de Maagd et al, 1999 ; Jenkins et al., 2000).

Originalmente, como ya se indicó anteriormente, se sugirió que el dominio III podría participar conservando la integridad de la toxina protegiéndola de posteriores proteólisis. Sin embargo, estudios posteriores con toxinas quiméricas y algunas mutantes demostraron que este dominio también se encuentra involucrado en la especificidad de la toxinas Cry. Varios grupos han generado evidencia sobre el papel en la especificidad del dominio III de Cry1Ac en *H. virescens* (Ge et al., 1991; Schnepf et al., 1990). Las mutaciones S503A y S504A en el dominio III de Cry1Ac provoca reducción de la toxicidad con la correspondiente disminución en la unión a VMMA's en *M. sexta* (Aronson et al., 1995).

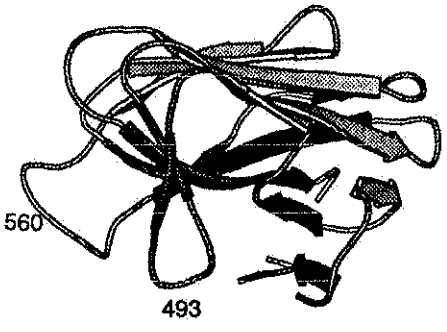

Figura 4. Estructura del Dominio III.

También se han contruído toxinas híbridas donde se intercambió el dominio III entre Cry1Aa y Cry1Ac, las proteínas que tienen el dominio III de Cry1Aa se unen a una proteína de 210 kDa mientras que aquellas que tienen el dominio III de Cry1Ac se unen a una de 120 kDa en *L. dispar* (Lee et al., 1995). El intercambio de dominios también ha sugerido un papel muy importante del dominio III en la unión a *Spodoptera exigua* (de Maagd et al., 1996).

De estudios con otras toxinas como la exotoxina A de *Pseudomonas aeruginosa* o la de la difteria, donde la interacción toxina-receptor lleva a la formación de poros, se sabe que la

estructura de láminas β puede participar en la unión al receptor (Allured et al., 1986; Choe et al., 1992), inserción en la membrana (Ojcius and Young, 1991) y en la función del canal (Yool, 1994). Ninguna de estas funciones se descarta para el dominio III de las toxinas Cry (Schnepf et al., 1998).

Análisis filogenético de las secuencias de toxinas Cry

Un análisis filogenético indicó que los tres dominios que componen las toxinas Cry han evolucionado independientemente, y la recombinación entre dominios III ha tomado lugar entre diferentes toxinas (Bravo, 1997; de Maagd et al., 2001, Figura 5). La combinación de estos dos procesos ha generado δ–endotoxinas con modos de acción similares pero con especificidades diferentes. Las secuencias del Dominio I parecen tener un origen común, mientras que los dominios II y III son comunes únicamente entre subgrupos de proteínas. Esto es consistente con el hecho de que el Dominio I compuesto de hélices α este involucrado con la formación del poro, mientras que los otros dos dominios sean responsables de la interacción con receptores específicos en la membrana. Además, la división filogenética entre los dominios I mostró una correlación con el tipo de insecto blanco por las toxinas, lo cual sugiere que diferentes tipos de dominios I se han seleccionado para actuar en ambientes de membranas particulares de distintos insectos blanco (Bravo, 1997; de Maagd et al, 2001).

A)

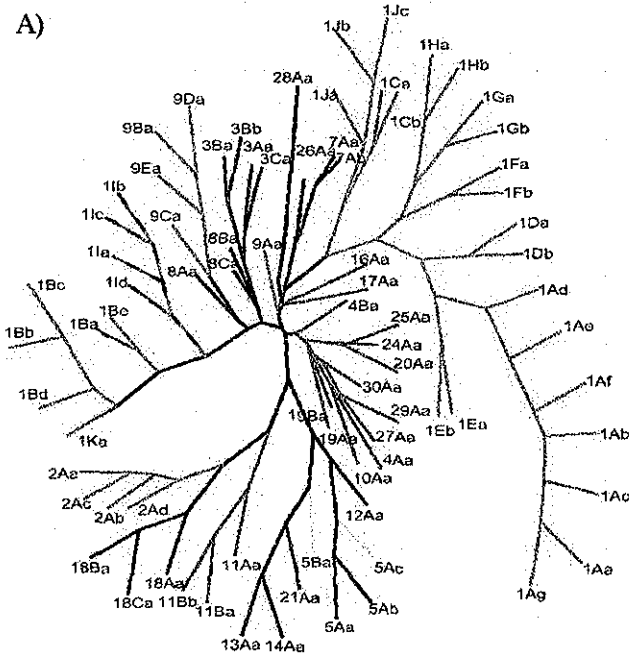

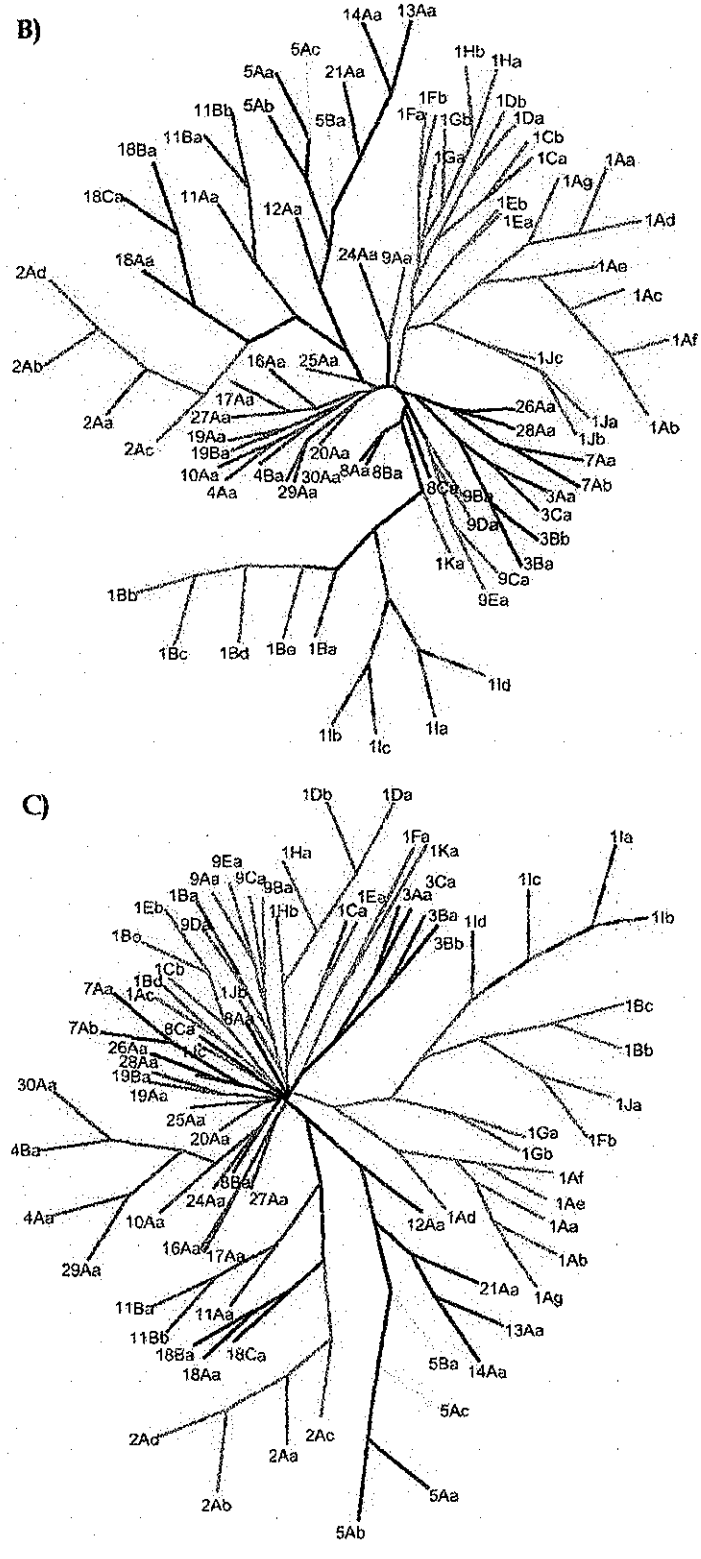

Figura 5. Arboles filogenéticos pertenecientes al dominio I (A), dominio II (B) y dominio III (C). (de Maagd et al., 2001).

ANTECEDENTES PARTICULARES

Los receptores de las toxinas Cry

El blanco biológico de las toxinas Cry es el epitelio del intestino medio de los insectos susceptibles. Para entender más sobre el mecanismo de toxicidad vale la pena conocer un poco más sobre la naturaleza de este blanco. Como ya se mencionó anteriormente, mucha de la investigación sobre el modo de acción de las toxinas de Bt se ha centrado en insectos lepidópteros, pero la investigación con otros órdenes de insectos también ha empezado ha desarrollarse. Sobre la estructura y función del intestino medio de los insectos (Down, 1986) solo se mencionarán algunos detalles sobresalientes para el modo de acción de Bt.

Algunas larvas de lepidópteros pueden incrementar su peso en tres órdenes de magnitud en tan solo dos semanas pues pasan la mayor parte del tiempo alimentándose. El intestino medio es la zona principal de digestión y absorción de los alimentos y es por lo tanto una de las partes de mayor importancia para la fisiología del insecto. El intestino medio de las larvas de lepidópteros es un tubo simple compuesto de una monocapa de células apoyadas en una membrana basal. Los dos principales tipos de células son las columnares, con una microvellosidad apical, y las células goblet, con una gran cavidad unida a la superficie apical por una válvula compleja. Una membrana peritrófica, compuesta principalmente por quitina y glicoproteínas limita al intestino, separando el contenido intestinal del epitelio (Knowles, 1994).

Para explicar el alto grado de especificidad de las toxinas Cry, Knowles y Ellar (1987) propusieron que en un paso anterior a la formación del poro, las toxinas Cry se unen a receptores específicos presentes en las células del intestino medio de los insectos susceptibles. Experimentos, empleando VMMA de insectos susceptibles (Hofmann et al, 1988; Van Rie et al, 1989, 1990) o mediante el uso de líneas celulares de insectos (Knowles and Ellar, 1987; Haider and Ellar, 1987) han proporcionado evidencias sobre la existencia de tales receptores.

La identificación de los receptores de las toxinas Cry, utilizando VMMA y toxinas marcadas mediante el uso de una técnica conocida como ensayo de unión de ligando, ha facilitado su purificación y clonación. El conocer cual de las proteínas que constituyen el intestino medio es el blanco de las toxinas Cry es crítico para iniciar la ingeniería genética de toxinas con propiedades de unión mejoradas.

A la fecha, dos tipos de proteínas de membrana, se han identificado como receptores de las proteínas Cry1A en diferentes insectos: una proteína parecida a la super-familia de las caderinas (Bt-R_1) y la enzima aminopeptidasa-N (APN). Recientemente, un receptor diferente para las toxinas Cry1A de *L. dispar* fue reportado. El análisis indicó que se trata de una proteína de alto peso molecular y altamente glicosilada, pero se sabe muy poco acerca de ella (Jenkins and Dean, 2000; Valaitis et al., 2001).

Bt-R_1 fue purificado y clonado originalmente a partir del intestino de *M. sexta* (Vadlamudi et al., 1993) y su peso molecular se estimó en 210 kDa (Vadlamudi et al., 1993; Vadlamudi et al., 1995). Este receptor presenta entre un 30-60% de identidad con otras proteínas de la super-familia de las caderinas, las cuales son glicoproteínas transmembranales dependientes de calcio, responsables de mantener la integridad de contactos célula-célula en organismos multicelulares (Angst et al., 2001). Esta proteína es capaz de unirse con las toxinas Cry1Aa, Cry1Ab y Cry1Ac (Francis and Bulla Jr, 1997). El tratamiento de Bt-R_1 con enzimas capaces de desglicosilar no tuvo efecto en sus propiedades de unión,sugiriendo una interacción proteína-proteína entre estas moléculas. La afinidad de la toxina Cry1Ab por Bt-R_1 se estimó en $7.9x10^{-10}$ M, que es similar al valor obtenido al medir la afinidad de la toxina por VMMA (donde la unión irreversible tiene lugar). Tanto cultivos de líneas celulares de insectos como de mamíferos, transfectados con Bt-R_1 presentan gran afinidad por las toxinas Cry1A (Keeton and Bulla Jr, 1997; Meng et al., 2001).

También se ha reportado una proteína de 175 kDa (Bt-R_{175}), con secuencia similar a Bt-R_1 (80%), purificada de *B. mori* que es capaz de unirse con gran afinidad a la toxina Cry1Aa. Cuando este receptor es expresado en la línea celular de insecto Sf9, hace sensibles a las células al efecto de esta toxina (Nagamatsu et al., 1998 y 1999).

Un receptor para la toxina Cry1Aa, de tamaño equivalente, también se ha reportado en ensayos de unión de ligando con VMMA's de *L. dispar*, sin embargo la proteína aún no ha sido purificada (Jenkins and Dean, 2000).

Recientemente, un reporte indicó que una mutación que interrumpe el gene de la caderina de *H. virescens* provoca resistencia en una población de insectos, revelando el papel funcional de este receptor (Gahan et al., 2001).

La presencia de un receptor de 120 kDa fue reportada en ensayos de unión de ligando con VMMA's de *M. sexta* (Garczynski et al., 1991). Antes de que este receptor fuera caracterizado se descubrió que la unión de la toxina Cry1Ac a este, era inhibida por N-acetilgalactosamina (GalNAc), sugiriendo la presencia de un motivo GalNAc en el receptor mismo (Knowles et al., 1994). La proteína fue identificada como una Aminopeptidasa-N (APN) y se demostró que funciona como un receptor de la toxina Cry1Ac cuando se reconstituye en vesículas de fosfolípidos (Sangadala et al., 1994; Knight et al., 1995). Su clonación reveló la presencia de varios sitios de glicosilación y se identificó que se encuentra anclada a la membrana a través de glicosil-fosfatidil-inositol (GPI) localizado en su extremo carboxilo terminal, el cual no es esencial para la unión de la toxina. Se determinó de igual modo que la actividad de la enzima no se ve afectada por la unión de la toxina (Denolf et al., 1997; Knight et al., 1995).

Con pocas excepciones las APN's son capaces de unir Cry1Ac. Sin embargo su expresión en células Sf-21 no induce toxicidad, quizás debido a una glicosilación defectuosa lo cual se ha sugerido al comparar el peso molecular de la proteína expresada en las células con la obtenida de VMMA's (Masson et al., 1995; Luo et al., 1999). En contraste con Cry1Ac, las toxinas Cry1Aa y Cry1Ab varían en sus propiedades de unión a las APN's pues se ha notado que la unión de estas toxinas no depende del motivo del azúcar (Masson et al., 1995).

Se han reportado dos aminopeptidasas para *M. sexta* y otras APN's se han identificado en otros insectos como *L. dispar, H. virescens, B. mori, Plutella xilostella,* y *Trichoplusia ni,* las cuales varían en tamaño entre 105-180 kDa. La afinidad de Cry1Ac por las APN's purificadas de *M. sexta* y *L. dispar* esta en el intervalo de 100-200 nM, aproximadamente 100 veces menor que la

observada con VMMA's (Sangadala et al., 1994). Sin embargo, aunque la afinidad de la APN purificada es 100 veces menor que la reportada para la caderina, no deja de especularse acerca del papel que puede estar jugando en la toxicidad de las proteínas Cry, pues en estudios *in vitro* se ha demostrado que cuando la APN de *M. sexta* es reconstituida en liposomas, se requieren de concentraciones menores de toxina para observar actividad (hasta 1000 veces menos) (Sangadala et al., 1994). Otra evidencia es el hecho de que en intestinos de *T. ni* tratados con fosfolipasa C, la cual corta los sitios de anclaje por GPI, ya no se forman poros en respuesta a la toxina Cry1Ac (Lorence et al., 1997).

Se han hecho varios esfuerzos para lograr identificar a las regiones en los receptores que están siendo reconocidas por las toxinas Cry1A's. Haciendo uso de deleciones sobre el gene de la caderina de *B. mori* (Bt-R_{175}) el grupo del Dr. Nagamatsu logró localizar un segmento de aproximadamente 600 aminoácidos capaces de unir a la toxina Cry1Aa (Nagamatsu et al., 1999). Haciendo uso de la misma estrategia se logró mapaer una región de 70 aminoácidos en el Bt-R_1 de *M. sexta* (Dorsch et al., 2002). Finalmente en las aminopeptidasas de *B. mori* y de *P. xilostella* se ha localizado una región de 63 aminoácidos comprendida entre los residuos I135 y P198 con capacidad de unir la toxina Cry1Aa (Yaoi et al., 1999; Nakanishi et al., 2002).

Se propone entonces que la especificidad de las toxinas Cry podría está determinada por proteínas de unión específicas localizadas en el intestino de los insectos susceptibles y por epítopes funcionalmente diferentes localizados en regiones hipervariables de las toxinas Cry.

Despliegue en Fagos ("Phage Display")

El "Phage Display" es una técnica poderosa que permite seleccionar y modificar polipéptidos con capacidades de unión específicas. El método se basa en el hecho de que si un gene que codifica para un polipéptido es fusionado a los genes de las proteínas de la cubierta del fago M13 estos "genes fusionados" pueden ser incorporados a los bacteriofagos, los cuales desplegarán las proteínas híbridas en su superficie. De este modo, se establece un

enlace físico entre el fenotipo y el genotipo (Figura 6) (Winter et al., 1994; Hoogenboom and Chames, 2000; Hoogenboom, 2002).

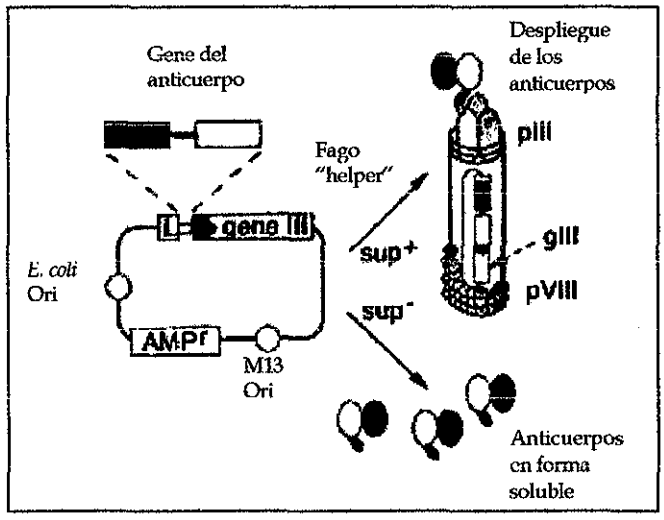

Figura 6. El fagémido pHEN1 para la expresión de anticuerpos en dos formatos diferentes.

Desde el primer reporte donde péptidos externos pueden ser desplegados en la superficie de fagos filamentosos, el despliegue de proteínas, dominios de éstas y péptidos en bacteriofagos, ha proporcionado una herramienta muy interesante para elucidar la naturaleza molecular de diferentes interacciones proteína-proteína (Smith, 1985). Los anticuerpos fueron las primeras moléculas en desplegarse exitosamente en la superficie de fagos (McCafferty et al., 1990) y es posible desplegar con éxito diferentes regiones de estas moléculas algunos de los cuales se representan en la figura 7.

Haciendo uso de técnicas de biología molecular se ha logrado generar bibliotecas de polipéptidos desplegadas en fagos. Los polipéptidos con una capacidad de unión específica pueden entonces ser seleccionados uniendo los fagos al ligando inmovilizado, eliminando mediante lavados los que no reconocen al ligando y examinando aquellos que quedaron unidos (Figura 8). Al igual que con otros métodos combinatorios, el éxito del "phage display" depende del tamaño y variabilidad de la biblioteca inicial (Winter et al., 1994; Li, 2000).

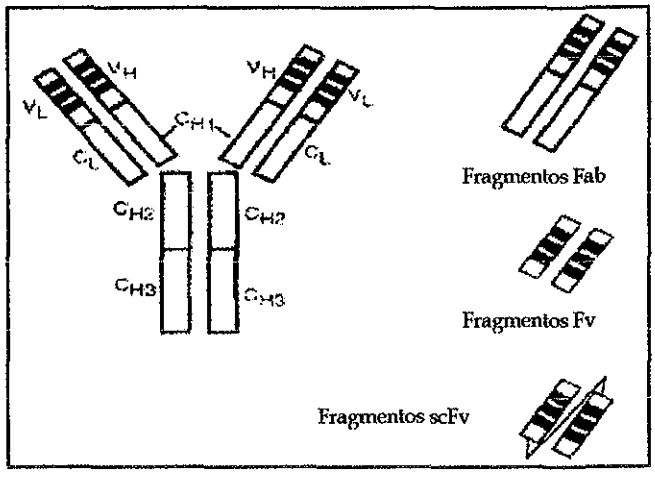

Figura 7. Esquema de una inmunoglobulina y diferentes formatos de fragmentos de anticuerpos que pueden ser desplegados en la superficie de fagos.

Las bibliotecas de péptidos desplegados en fagos pueden utilizarse para aislar péptidos que unan con alta especificidad y afinidad a casi cualquier proteína blanco. Estos péptidos pueden entonces utilizarse para entender más acerca del reconocimiento molecular, mimetizar receptores o como moléculas que permitan el diseño de fármacos (Cortese et al., 1994; Daniels and Lane, 1996; Sidhu, 2000; Coley et al., 2001).

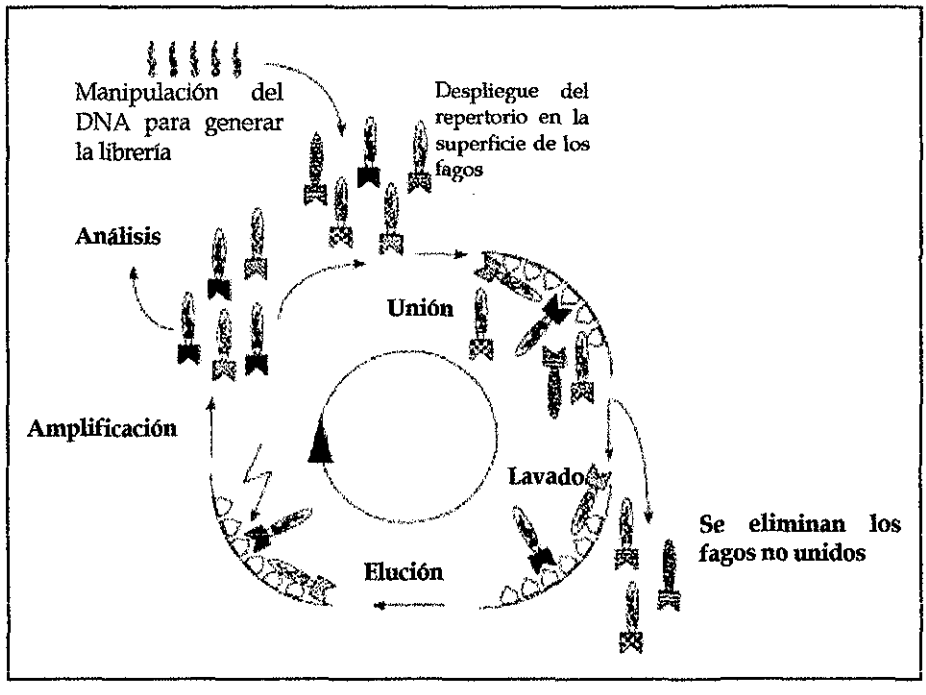

Figura 8. Diagrama general sobre la técnica de "Phage Display".

En nuestro laboratorio contamos con una biblioteca de fragmentos de anticuerpos en formato de scFv (fragmentos variables de cadena sencilla) que contiene una variabilidad de $1x10^8$ clonas. Se encuentra expresada en fagos filamentosos del tipo M13, la cual ha sido construída utilizando oligos que introducen secuencias al azar que varían en una longitud de 4 a 12 residuos de aminoácidos pertenecientes a la región determinante de complementariedad 3 (CDR_3) en la región variable de la cadena pesada (V_H-CDR_3) (Nissim, et al, 1994).

Previamente, con esta biblioteca se lograron recuperar anticuerpos scFv que interaccionan con la toxina CryIAb después de 8 rondas de selección, la afinidad hacia la toxina se comprobó mediante análisis de ELISA policlonal y monoclonal (Peralta, 1998). Es a partir de esta población con la que iniciamos la búsqueda de anticuerpos que nos permitieron estudiar la interacción entre la toxina Cry1Ab y su receptor natural en el lepidóptero *M. sexta.*

Teoría de Reconocimiento Molecular (TRM)

Aunque a la fecha se conocen las secuencias de una gran variedad de proteínas, aún no se han podido establecer conceptos que permitan, a partir estas, predecir su plegamiento y mucho más difícil aún, parece poder determinar las regiones a través de las cuales se establecen las interacciones con sus ligandos. La teoría de reconocimiento molecular, propuesta por Blalock y co-autores, propone que los puntos de contacto entre dos proteínas que interactúan pueden ser identificadas a través de perfiles de hidropatía complementarios, como se ilustra en la figura 9 (Blalock, 1990; Blalock, 1995; Blalock, 1999; Boquet et al., 1995).

Se ha acumulado evidencia que sugiere que un simple código binario de aminoácidos polares y no polares arreglado apropiadamente, es importante para determinar la forma y función de una proteína; es decir, que solamente su localización en la secuencia, más no la identidad de los grupos polares o no polares puede determinar la especificidad para la formación de una estructura estable o bien un péptido biológicamente activo. Este código de hidropatía se ha utilizado exitosamente para la síntesis de péptidos biológicamente activos,

en el diseño de proteínas que pueden plegarse como hélices α y para el desarrollo de programas de cómputo que pueden simular o predecir ciertos aspectos del plegamiento de proteínas. Esta teoría ha generado gran controversia, principalmente se cuestiona el hecho de si acaso ocurre *in vivo* (Root-Bernstein et al., 1998). Pero en contraposición también existen algunos ejemplos que la sustentan, los aspectos más relevantes donde se han centrado estos estudios han sido (1) la generación de péptidos antagonistas y (2) la función de dichos péptidos (Blalock, 1999). De los ejemplos más representativos a favor de esta teoría están las interacciones antígeno-anticuerpo. Se sabe que las secuencias de los CDR's son relativamente pequeñas (aproximadamente 10 aminoácidos), por lo que ofrecen una oportunidad interesante para el estudio de la TRM. Dos ejemplos caracterizados son: anticuerpos anti-sustancia P (Boquet et al., 1995) y anticuerpos anti-angiotensina II (Picard et al., 1986).

La crítica más relevante a esta teoría es, si las evidencias generadas son estadísticamente significativas. Aún no se puede generalizar al respecto, es cierto que varios ejemplos reportados sobre interacciones antígeno-anticuerpo parecen seguir esta teoría, pero todavía se requiere un análisis más exhaustivo para formular las generalidades necesarias (Boquet et al., 1995) a partir estas.

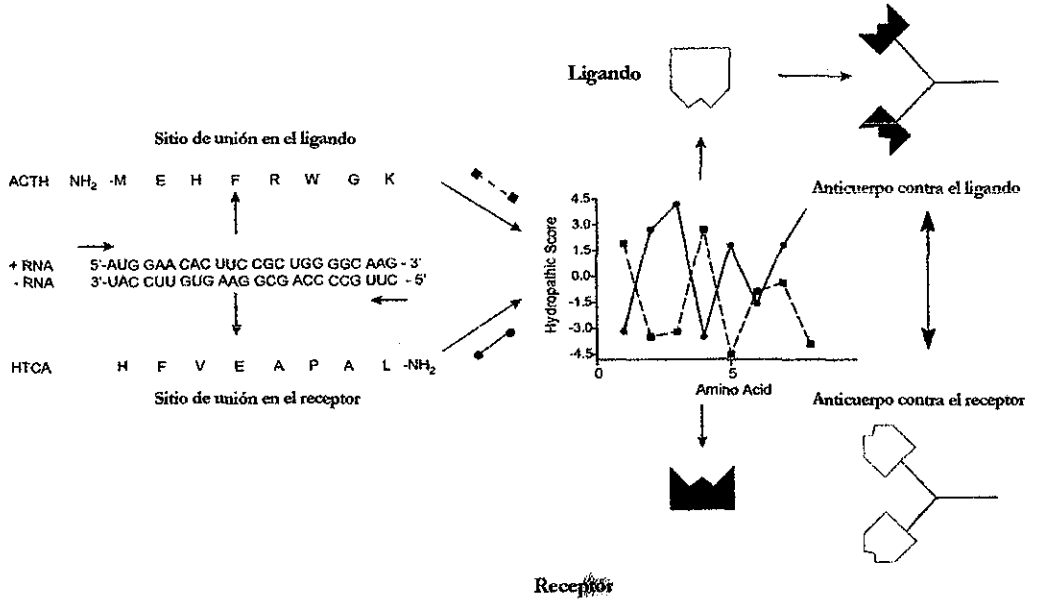

Figura 9. Teoría de Reconocimiento Molecular (TMR)

La unión de las toxinas a sus receptores específicos es considerada uno de los pasos clave para la toxicidad por diferentes razones. (A) La actividad de formación de poro *in vitro* en vesículas artificiales al incorporar los receptores purificados o VMMA's requiere de concentraciones menores de toxina que cuando estos no están presentes. (B) La resistencia en los insectos en la mayoría de los casos esta asociada con una reducción en la unión o con una baja concentración de los sitios de unión de los receptores.

Aunque ya se sabe de algunas proteínas que pueden funcionar como receptores de las toxinas Cry, se desconocen él o los epítopes necesarios para que se den las interacciones con las toxinas, tampoco se conoce el papel que estas interacciones tienen en la toxicidad y sobre el proceso de oligomerización aún no esta claro si éste depende del reconocimiento de las toxinas Cry con sus receptores, por lo que en este trabajo nos propusimos los siguientes objetivos:

OBJETIVO GENERAL

Obtener anticuerpos scFv que permitan estudiar la interacción entre la toxina Cry1Ab de *Bacillus thuringiensis* y su receptor natural en el lepidóptero *Manduca sexta*.

OBJETIVOS PARTICULARES

1) Caracterizar anticuerpos scFv, obtenidos a partir de una biblioteca no-inmune, que interfieran con la unión de la toxina Cry1Ab de *Bacillus thringiensis* a su receptor natural en *Manduca sexta*.

2) Identificar región o regiones en el receptor natural que están siendo reconocidas por la toxina Cry1Ab de *Bacillus thringiensis*.

3) Identificar región o regiones en la toxina Cry1Ab de *Bacillus thringiensis* que interaccionan con el receptor natural de *Manduca sexta*.

4) Estudiar el papel que tiene la interacción toxina-receptor en la toxicidad de la proteína Cry1Ab.

MATERIALES Y METODOS

CEPAS

Durante el desarrollo de este trabajo se utilizaron las siguientes cepas de *Bacillus thuringiensis*:

1. *Bacillus thuringiensis* variedad *berliner*/1715 que contiene el gene de la proteína Cry1Ab en el plásmido pHcPP con resistencia a eritromicina.
2. *Bacillus thuringiensis* variedad *kurstaki*/HD-1 que contiene el gene de la proteína Cry1Aa en el plásmido pHT409 con resistencia a eritromicina.
3. *Bacillus thuringiensis* variedad *kurstaki*/HD-73 que contiene el gene de la proteína Cry1Ac.
4. *Bacillus thuringiensis* variedad *tenebrionis*/BTS1 que contiene el gene de la proteína Cry3A.
5. *Bacillus thuringiensis* variedad *israelensis*/CG6 que contiene el gene de la proteína Cry11A con resistencia a eritromicina.

Además se utilizaron las siguientes cepas de *Escherichia coli*:

1. *E. coli* F371A, donada al laboratorio por el Dr. D. Dean, la cual contiene clonado el gene de la proteína Cry1Ab con la mutación F371A localizada en el dominio II, en el plásmido pBluescrip KS con resistencia a ampicilina (Rajamohan et al., 1995).
2. Dos cepas que expresan por separado al dominio I y al dominio II-III de la proteína Cry1Ab con resistencia a ampicilina (Flores et al., 1997).
3. *Escherichia coli* TG1, cepa utilizada para la producción de los anticuerpos scFv.

Las cepas se crecen en medio LB sólido con la concentración del antibiótico correspondiente durante 12 h a 30°C para el caso de Bt o 37°C para *E. coli* y posteriormente ser transferidas al medio líquido adecuado para su crecimiento.

PURIFICACION DE LAS TOXINAS Cry1A's

Para obtener los cristales de las proteínas Cry1Aa y Cry1Ab utilizamos medio de esporulación (SP) (Lereclus et al., 1995) adicionado con 7.5 μg de erm/ml. Para la proteína Cry11A se utilizan 25 μg de erm/ml y en el caso de las proteínas Cry1Ac y Cry3A el medio no requiere antibiótico. Después de inocular con una asada de la cepa correspondiente, los cultivos se dejaron crecer durante 3 o 4 días a 30°C hasta que por observación al microscopio notamos esporulación completa del cultivo y la producción de los cristales correspondientes.

Para la purificación de los cristales, primero se recupera la mezcla de esporas-cristales, los cuales se lavan exhaustivamente con una solución: NaCl 0.3 M, EDTA 0.01 M pH 8 para posteriormente ser purificados mediante un gradiente discontinuo de sacarosa (84%, 79%, 72% y 67%) complementado con NaCl 10 mM, Tris-HCl pH 8 50 mM y Tritón 0.01%. Las fracciones que contienen los cristales se lavan exhaustivamente con agua milli-Q para eliminar el exceso de sacarosa y se resuspenden para su conservación en Tris-HCl 50 mM adicionado con PMSF 1 mM.

Los cristales se solubilizan en una solución amortiguadora de carbonatos 50 mM pH 9.5 en presencia de 0.02% de mercaptoetanol durante 2 h a 37°C con agitación suave. Se recupera el sobrenadante mediante centrifugación a 10,000g x 10 min.

PURIFICACION DE PROTEINAS DE *E. coli.*

Se utilizó el protocolo reportado por Lee et al., 1992. Se parte de un inóculo de 50 ml de medio LB-amp (50 μg/ml) de la cepa correspondiente de *E. coli* y se dejan crecer a 37° C durante 12 h. Se inoculan 500 ml de LB-amp (100 μg/ml) con 5 ml del cultivo anterior y se dejan crecer durante 48 h a 37°C.

Se recuperan las células centrifugando (10,000g x 10 min) y el paquete celular se resuspende en: Tris-HCl 50 mM; EDTA 50 mM pH 8; sacarosa 15% y lisozima 2 mg/ml y se sonica en hielo (3 veces durante 3 minutos). Centrifugar (15000g x 15 min). Lavar la pastilla con tritón X-100 2% frío. Lavar 3 veces con NaCl 0.5 M y 2 veces más con agua destilada.

La solubilización de las proteínas se realiza en una solución amortiguadora de carbonatos 50 mM pH 9.5 en presencia de DTT 10 mM durante 2 h a 37°C con agitación suave. Recuperar el sobrenadante centrifugando a 10,000g x 10 min.

La activación se realiza con tripsina 1:50 (m/m) a 37°C durante 1 h con agitación suave, al final se adiciona PMSF 1 mM concentración final. Se recupera el sobrenadante centrifugando a 10,000g x 10 min.

PURIFICACION DE LOS ANTICUERPOS scFv

Se prepara un inóculo de cada clona a purificar en 50 ml de medio 2xYT adicionado con glucosa al 2% y 50 μg/ml de ampicilina. Incubar 12 h a 25°C y 250 rpm. Transferir 5 ml del precultivo a 500 ml de medio 2xYT fresco adicionado con 0.1% de glucosa y 100 μg/ml de ampicilina. Incubar a 37°C y 200 rpm hasta alcanzar una densidad óptica de 0.7 medida a 600 nm. La expresión de los anticuerpos se induce con 0.5 mM de IPTG incubando a 25°C durante 4 h a 200 rpm.

Recuperar las células centrifugando el cultivo a 5,000 g x 15 min. La pastilla se resuspende en 1/40 (v/v) de una solución que contiene: sacarosa 200 mg/ml; EDTA 1 mM y Tris-HCl 30 mM pH 8. Incubar en hielo 20 min. Centrifugar a 5,000g x 15 min y recuperar el sobrenadante. La pastilla se resuspende en 1/40 (v/v) de una solución de $MgSO_4$ 5 mM y se incuba en hielo por 20 min. Tanto el primer sobrenadante como la segunda suspensión se centrifugan a 15,000g x 15 min y se recuperan los sobrenadantes, los cuales se dializan toda la noche a 4°C en PBS.

Para purificar los anticuerpos scFv se prepara una columna con 1 ml de resina níquel-agarosa (Quiagen). La resina se equilibra con 5 ml de una solución de imidazol 20 mM en PBS. Los sobrenadantes, previamente dializados, se pasan por las columnas. Lavar con una solución de imidazol 35 mM en PBS. La muestra se eluye con 2 ml de imidazol 250 mM en PBS más 0.02% de azida de sodio. Finalmente, las columnas se regeneran con una solución de imidazol 500 mM en PBS, y se almacenan con 2 ml de PBS y azida de sodio al 0.02%.

La purificación se verifica mediante SDS-PAGE al 12%. Y la concentración de proteína se determina midiendo la absorbancia a 280 nm, considerado que 1 DO = 0.7 mg/ml (Amersdorfer et al., 1997).

RECUPERACION DE LOS INTESTINOS DE *Manduca sexta* Y PURIFICACION DE LAS VESICULAS DE LA MICROVELLOSIDAD APICAL MEDIA

Se parte de larvas recién mudadas al 5° instar de *M. sexta* las cuales se mantienen en hielo para su disección. Después de fijar cada uno de los extremos de la larva sobre una base de disección de unicel se realiza un corte longitudinal para dejar expuesto el intestino. Se eliminan los 3 primeros segmentos de cada extremo y la porción media se extrae cuidadosamente. Se realiza un segundo corte longitudinal en esta porción para eliminar los restos de comida junto con la membrana peritrófica. El tejido se enjuaga exhaustivamente en una solución de: manitol 300 mM; Tris-HCl 17 mM; EGTA 5 mM; DTT 2 mM y PMSF 0.5 mM ajustado a un pH de 7.4. El tejido se recupera en un tubo inmerso en hielo seco y se conserva a -70°C.

Para realizar la purificación de las VMMA's se utilizó el protocolo reportado por Wolfersberger y co-autores (Wolfersberger et al., 1987). Se descongelan en hielo los intestinos y se pesan 3 g de tejido. La muestra se coloca en un homogeneizador, previamente sumergido en hielo, y se agregan 30 ml de solución I (manitol 300 mM; Tris-HCl 17 mM; EGTA 5 mM; DTT 2 mM; HEPES 10 mM; EDTA 1 mM; PMSF 0.5 mM; leupeptina 100 μg/ml, pepstatina 100 μg/ml y neomicina 100 μg/ml ajustado a un pH de 7.4). Se coloca el émbolo de teflón en el taladro y se dan 9 golpes suaves a 2,250 rpm. Agregar suavemente 30 ml de la solución II ($MgSO_4$ 24 mM) por las paredes del homogeneizador. Se cubre con parafilm la boca del homogeneizador y se mezcla suavemente por inversión. Incubar en hielo durante 15 min agitando por inversión 3 o 4 veces. En este paso tomar 200 μl de muestra para hacer las determinaciones correspondientes al homogenizado inicial.

Centrifugar a 2,500g x 15 min a 4°C y descartar la pastilla. Cambiar el sobrenadante a otro tubo limpio y centrifugar a 30,000g x 30 min a 4°C, descartar ahora el sobrenadante. La pastilla se resuspende en ½ volumen de la solución I fría y ½ volumen de la solución II.

Repetir los pasos de centrifugación de la misma forma ya descrita. Resuspender la pastilla final en la solución I diluida con agua destilada 1:1 (1 ml); dar tres golpes a 2,250 rpm utilizando nuevamente el homogenizador. Finalmente dializar la preparación en 1000 volúmenes de una solución: KCl 150 mM y HEPES 10 mM ajustada a pH de 7.4 durante 12 h a 4°C.

DETERMINACION DE LA CONCENTRACION DE PROTEINA

La cuantifcación de la cantidad de proteína en las VMMA's y el homogenizado se realizó por el método de Lowry. 5 y 10 µl de muestra (homogenizado inicial o VMMA) se llevan a un volumen final de 1 ml con agua destilada. Se agregan 3 ml de la solución AB+C (100:1). La solución AB contiene: Na_2CO_3 2 g; SDS 1 g; NaOH 0.4 g y $KNaC_4H_4O_6 \cdot 4H_2O$ 0.16 g en 100 ml de agua y la solución C: $CuSO_4 \cdot 5H_2O$ 0.25 g en 50 ml de agua. Se incuba 1 h a temperatura ambiente y se agregan 0.3 ml del reactivo de folin (Sigma) diluido 1:1 con agua, se incuba 45 min a temperatura ambiente. Se hace la determinación en un espectrofotómetro a 625nm y los valores se referencian a una curva estándar preparada con BSA.

DETERMINACION DE ACTIVIDADES ENZIMATICAS

Actividad de aminopeptidasa

Se prepara una solución de L-leucina-p-nitroanilida (Sigma) 10 mM. En una celda de poliestireno se ponen los siguientes volúmenes de las soluciones indicadas: 400 µl de agua mili-Q; 200 µl de Tris-HCl pH 8 200 mM; 250 µl de NaCl 1M y 2 µl de la muestra de homogenizado o VMMA's. A esta mezcla de reacción se adicionan 100 µl de la solución de L-leucina-p-nitroanilida y se agita por inversión. Se sigue la cinética de la reacción por 2, 4 y 6 min midiendo la absorbancia a 405 nm.

Se considera que 0.1 unidades de absorbancia a 405 nm equivalen a 1 µmol/min.

Actividad de fosfatasa alcalina

Se prepara el sustrato, p-nitrofenol fosfato (Sigma), en una solución de: Tris-HCl pH 9 100 mM y $MgCl_2$ 0.5 mM, a una concentración de 1 mg/ml. Repetir esta misma solución pero ahora incluir además tritón X-100 al 0.02%. Dispersar 20 µg de cada muestra en 500 µl de cada una de estas soluciones y mezclar muy bien. Incubar 15 min a temperatura ambiente. Se detiene la reacción añadiendo 500 µl de EDTA 250 mM pH 8. Se realizan las lecturas en un espectrofotómetro a 405 nm utilizando celdas de poliestireno de 1 cm de longitud y los valores se refieren a una curva estándar de p-nitrofenol (Merck).
La actividad enzimática específica se calcula considerando la cantidad de proteína necesaria para transformar 1 nmol de p-nitrofenol fosfato en un minuto.
La cantidad de fosfatasa alcalina se calcula en presencia y ausencia de triton-X 100 para calcular la proporción de vesículas con orientación positiva (fosfatasa orientada hacia el exterior).

"WESTERN BLOT"

Se separan en SDS-PAGE las muestras por analizar. Se transfieren las proteínas del gel en una membrana de PVDF. La transferencia se comprueba tiñendo la membrana con rojo de punceau 0.5% en ácido acético 2%. A continuación, se bloquea con leche descremada al 5% en PBS durante 1 h. Se lava la membrana 5 veces con PBS-Tween 20 0.05% (PBS-T). Se incuba con el anticuerpo primario a la dilución apropiada durante 2 h y se lava 5 veces con PBS-T para incubar con el anticuerpo secundario peroxidado por 2 h. Lavar 5 veces con PBS-T y una vez con PBS. Revelar usando los reactivos de quimioluminiscencia (Pierce) de acuerdo con las especificaciones recomendadas por el fabricante.

EXPERIMENTOS DE UNION EN SOLUCION

Previamente se marcan las toxinas con biotina (Amersham) siguiendo las indicaciones recomendadas por el fabricante. Las proteínas marcadas se purifican utilizando una columna

empacada con Sephadex G-25 (Sigma). La marca se verifica después de haber transferido las proteínas en membranas de nitrocelulosa revelando la señal con estreptavidina acoplada a peroxidasa.

Para el experimento de unión, se incuban 10 μg de VMMA's de *M. sexta* con 10 nM (concentración final) de la toxina marcada con biotina. Las muestras se llevan a un volumen final de 100 μl con una solución de BSA 0.1% en PBS-Tween 20 0.1%. Se incuban durante 1 h a temperatura ambiente. Centrifugar las muestras a 14,000 rpm durante 10 min. Lavar 2 veces con 100 μl de la solución de BSA 0.1% en PBS-Tween 20 0.1%. Se elimina el sobrenadante y la pastilla se resuspende en 15 μl de PBS. Se separan las proteínas en SDS-PAGE y se transfieren a membrana de nitrocelulosa (ECL-Amersham).

Después de la transferencia la membrana se lava con PBS y se incuba con PBS-Tween 20 2% por 20 min. Lavar 2 veces con PBS-Tween 20 al 0.05%. Incubar con estreptavidina acoplada a peroxidasa (1:7500) 1 h. Lavar 2 veces con PBS-Tween 20 al 0.05%. Revelar la señal con los reactivos de quimioluminiscencia de acuerdo a las especificaciones del fabricante.

EXPERIMENTOS DE UNION DE LIGANDO

Separar en un SDS-PAGE preparativo al 9% 100 μg de VMMA's de *M. sexta* y se transfieren las proteínas a una membrana de nitrocelulosa (ECL-Amersham). Lavar la membrana con PBS-Tween 20 0.1% y bloquear una hora con BSA 0.2% en PBS-Tween 20 0.1%. Se lava nuevamente con PBS-Tween 20 0.1% y se incuba durante dos horas con 10 nM de toxina marcada con biotina en una solución de BSA 0.1% en PBS-Tween 20 0.1%. Se lava con PBS-Tween 20 0.1% y se incuba durante una hora con estreptavidina acoplada a peroxidasa. Se lava nuevamente con PBS-Tween 20 0.1% y dos veces con PBS antes de detectar la unión con los reactivos de quimioluminoscencia.

ACTIVACION DE LA TOXINA Cry1Ab EN PRESENCIA DEL ANTICUERPO scFv73

Se toman 300 μl de la protoxina solubilizada en un intervalo de concentración de 1.5-2 μg/μl que se incuban con el anticuerpo scFv73 en una proporción 1:1 (m/m) durante 1 h a

temperatura ambiente. Una vez terminado este tiempo se adicionan las proteasas en una relación 1:20 (m/m) cuando se utiliza tripsina y al 5% si se trata de jugo gástrico de *M. sexta*. Las muestras se incuban durante 1 h a 37°C con agitación suave. Las proteasas se inactivan agregando PMSF a una concentración final de 1 mM. Centrifugar 10 min a 10,000 rpm y guardar el sobrenadante a 4°C hasta su uso.

ACTIVACION DE LA TOXINA Cry1Ab CON VESICULAS DE LA MICROVELLOSIDAD APICAL MEDIA

Mezclar 10 μg de la preparación de VMMA's de *M. sexta* con 100 nM de la protoxina solubilizada. Incubar 15 min a temperatura ambiente. Inactivar las proteasas con PMSF a una concentración final de 1 mM y centrifugar las muestras a 10,000 rpm durante 10 min. Se recuperan los sobrenadantes y se conservan a 4°C hasta su uso.

ENSAYOS DE FORMACION DE PORO

En una celda para el fluorómetro, se colocan 0.9 ml de una solución de cloruro de metil-glucamina 150 mM y HEPES 10 mM a pH 8 y se agrega 1 μl del colorante 3,3'dipropiltiodicarbocianina (Dis-C_3(5)). Los cambios de fluorescencia se miden a 620/670 nm de longitud de onda de exitación/emisión respectivamente (Lorence, et al., 1995). La celda se introduce en el espectrofotómetro. Se adicionan 10 μg de VMMA's y se permite la homogenización del sistema (aproximadamente 30 seg). La calibración se realiza agregando 1 μl de valinomicina (ionóforo específico para potasio, que nos indica si la preparación de VMMA's esta correctamente cargada con este ión). La toxina que se desea probar se agrega en una concentración final de 50 nM. Para realizar los registros de cambio de potencial se realizan adiciones crecientes de KCl 3 M. El análisis de los datos se realiza graficando la diferencia de fluorescencia (ΔF) contra el potencial de potasio (K^+), el cual se calcula haciendo uso de la ecuación de Nerst, como se representa en el siguiente esquema.

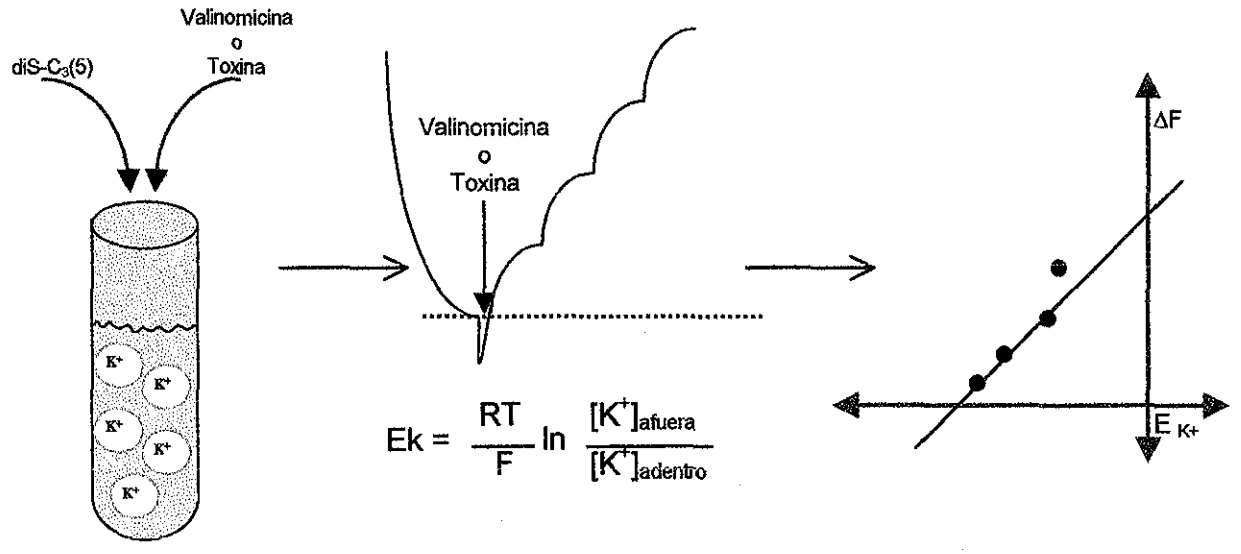

EXPERIMENTOS DE UNION AL 8-ANILINO-1-NAFTALENSULFONATO (ANS)

En los experimentos de unión al colorante ANS, con las muestras de toxinas activadas, se midieron los cambio de fluorescencia utilizando una longitud de onda de exitación/emisión de 380/480 nm respectivamente. Los registros se realizaron a temperatura ambiente y agregando 1.5 μg de toxina en 1.8 ml de una solución de citrato de sodio 50 mM; NaCl 100 mM ajustada a pH 6. La concentración final del ANS fue 15 μM.

BIOENSAYOS

Para la realización de los bioensayos se utilizó la técnica de contaminación de superficie con larvas de *M. sexta* del primer estadío de crecimiento. En placas de 24 pozos con una capacidad de 4 ml se vacía la dieta la cual es contaminada con 35 μl de la toxina en las concentraciones deseadas. Se dejan secar muy bien las cajas y entonces se coloca una larva en cada pozo. Después de 7 días se cuentan las larvas muertas y se calcula el porcentaje de mortalidad con respecto al control que consiste solamente de agua con la que se prepararon las diluciones de la toxina.

CONSTRUCCION, CLONACION Y PURIFICACION DE LOS FRAGMENTOS DEL Bt-R_1

Primero se recuperó el RNA total, de aproximadamente 5 g de intestino medio de larvas de *M. sexta* de quinto instar, utilizando la metodología reportada por Chomczynski y Sacchi (1987). A continuación se realizó la síntesis de cDNA con los siguientes oligos, TBRGIL: AGT-GAC-CAC-CTC-GTC-TAA y TBRBL: TGT-TGA-TAT-CCC-TGC-GGT con el Kit de RT-PCR(AMV) de acuerdo con las especificaciones del fabricante (Roche). Esta primera hebra de cDNA se utilizó como templado para amplificar por PCR los dos fragmentos deseados, para lo cual se emplearon los siguientes pares de oligos; TBRGIU: GAC-GCG-GAT-ACT-CCT-CCA; TBRGIL: AGT-GAC-CAC-CTC-GTC-TAA; TBRBU: GAT-GGC-AAC-AGC-GAA-GGT y TBRBL: TGT-TGA-TAT-CCC-TGC-GGT. Se purificaron los productos del tamaño esperado (230 pb), los cuales se reamplificaron en una segunda reacción de PCR donde además se introdujeron los sitios de restricción *Sfi I* y *Not I* con los siguientes oligos: GI-Sfi: $(GA)_{10}$G-GCC-CAG-CCG-GCC-GAC-GCG-GAT-ACT-CCT-CCA; GI-Not: $(GA)_{10}$G-CGG-CCG-C-AGT-GAC-CAC-CTC-GTC-TAA; BU-Sfi: $(GA)_{10}$G-GCC-CAG-CCG-GCC-GAT-GGC-AAC-AGC-GAA-GGT y BU-Not: $(GA)_{10}$G-CGG-CCG-C-TGT-TGA-TAT-CCC-TGC-GGT. Estos sitios se utilizaron para clonarl en el plásmido pSyn 1, el cual permite agregar una cola de histidinas y que además posee un c-myc, que facilita la detección de la proteínas con el anticuerpo monoclonal anti c-myc (Sigma). Los productos finales, con la talla esperada 300 bp, se purificaron y digirieron con las enzimas correspondientes. Se ligaron en el plásmido previamente digerido y los productos ligados se electroporaron en células TG1 de *E. coli*.

La purificación de los fragmentos se realizó de la misma forma anteriormente indicada para los anticuerpos scFv.

CONSTRUCCION DE BIBLIOTECAS INMUNES DE ANTICUERPOS scFv

Para la construcción de estas bibliotecas previamente se inmunizaron 2 conejos (Cepa Nueva Zelanda) con las toxinas Cry1Ab o Cry11A. Se efectuaron 4 aplicaciones a cada animal de aproximadamente 1 mg de la toxina correspondiente; después de la primera aplicación

(hecha en adyuvante de Freund's completo) se dejaron pasar 5 días para realizar la segunda aplicación, mientras que la tercera y cuarta se realizaron cada 10 días cada una. Las tres últimas aplicaciones se realizaron en adyuvante incompleto (Melox). Antes y durante cada una de las aplicaciones se tomaron muestras del suero para comparar los títulos de anticuerpos obtenidos durante la inmunización. Después de la cuarta aplicación ya no se observó variación en los títulos, los cuales se verificaron mediante ELISA. Se dejaron pasar 5 días más antes de sacrificar a los animales. De cada uno de ellos se recuperaron el bazo y la médula ósea a partir del fémur.

De estos tejidos se recupera inmediatamente el RNA total siguiendo la metodología reportada por Chomczynski y Sacchi (1987). Con este RNA se procede a la síntesis de cDNA haciendo uso del Kit de RT-PCR(AMV) de acuerdo con las especificaciones del fabricante (Roche). Este cDNA sirve como templado para la amplificación de las cadenas pesadas y ligeras con las cuales se conformará el repertorio de anticuerpos scFv. Para lograr esto último se utilizaron los oligos reportados por Hawlisch y colaboradores (Hawlisch et al., 2000). Las condiciones de PCR, digestión de los productos y su ligación en el vector pSyn 2, fueron las mismas que las reportadas por Hawlisch y colaboradores, excepto que las dos primeras reacciones de PCR se realizaron con Vent-Polimerasa. Los productos ligados se electroporaron en células TG1 de *E. coli*.

RESULTADOS

SITIO DE INTERACCION EN EL Bt-R_1 CON LA TOXINA Cry1Ab

Caracterización y purificación de anticuerpos scFv que unen a la toxina Cry1Ab.

A partir de una biblioteca de anticuerpos scFv, obtenidos de un humano no inmunizado con un tamaño aproximado de 10^8 variantes y con una variabilidad localizada en el CDR3, se seleccionaron mediante la técnica de "Phage Display" una colección de fagos que reconocen a la toxina Cry1Ab de *Bacillus thuringiensis*. Para la caracterización de estos fagos, se amplificaron por PCR las regiones variables y los productos se digirieron con la enzima de restricción *Bst*NI. El análisis de los patrones de restricción de 50 clonas seleccionadas al azar, nos permitió observar que existían al menos tres anticuerpos diferentes, de los cuales la clona correspondiente al scFv45 fue la mas representada (95%) y las otras dos clonas quedaron designadas como la scFv19 y scFv73. La secuencia de DNA de estas clonas mostró diferencias en la región correspondiente al CDR3, como se muestra en la figura 10.

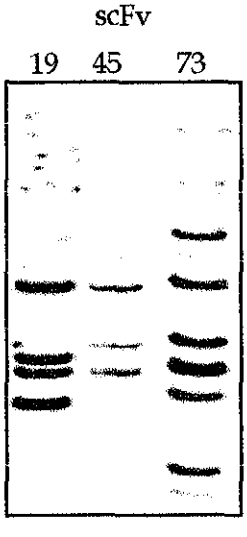

CDR3 del scFv 19: RTSPRLTPKHR

CDR3 del scFv 45: NPRIPP

CDR3 del scFv 73: ITQTTNR

Figura 10. Patrones de restricción de los tres scFv's seleccionados y secuencias de sus CDR's 3.

En "Western blot" determinamos a que dominio de la toxina Cry1Ab se estaban uniendo estos anticuerpos scFv. Para este análisis se utilizaron extractos de *E. coli* que expresan por separado el dominio I o el dominio II-III de la toxina Cry1Ab, los cuales fueron separados

por SDS-PAGE y transferidos en membranas de PVDF para ser incubados con los correspondientes scFv's. La figura 11 muestra que las tres clonas reconocen un fragmento de aproximadamente 44 kDa correspondiente al dominio II-III, pero no al fragmento de 30 kDa del dominio I.

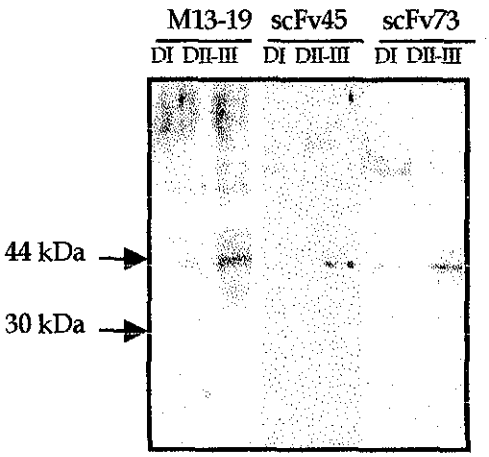

Figura 11. Unión de los anticuerpos scFv a los dominios de la toxina Cry1Ab.

Mediante ELISA se determinó si era el dominio II o el III reconocido por estas clonas para lo cual, se utilizó la toxina Cry1Ac que muestra un 98% de identidad con la toxina Cry1Ab en el dominio II pero solamente un 38% de identidad en el dominio III. El resultado del ELISA indicó que las tres clonas reconocen a la toxina Cry1Ac sugirendo que los anticuerpos scFv analizados se unen al dominio II de la toxina Cry1Ab.

A continuación, los tres genes correspondientes a los anticuerpos scFv19, scFv45 y scFv73 fueron subclonados en el vector pSyn1 que nos permitió unirles una cola de histidinas lo cual nos facilitó su purificación utilizando una columna de níquel-agarosa. Después de expresar las clonas en la cepa TG1 de *E. coli*, solamente fue posible purificar las clonas de los anticuerpos scFv45 y scFv73 (Figura 12) y fue con estos con los que se continuo el trabajo experimental.

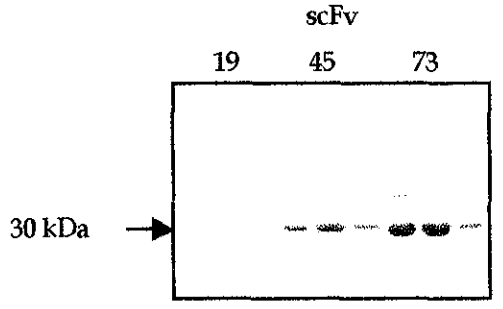

Figura 12. Purificación de los scFv's.

Ensayos de unión de la toxina Cry1Ab a VMMA de *M. sexta* utilizando los anticuerpos scFv como competidores

A) Ensayo de unión en solución.

Para saber si los anticuerpos scFv purificados podían competir la unión de la toxina Cry1Ab a sus receptores naturales, que se encuentran localizados en el intestino medio de los insectos blanco, se utilizó un protocolo de unión en solución, el cual es un ensayo cualitativo que permite observar interacción entre la toxina y vesículas aisladas a partir del intestino medio de *Manduca sexta*. En este experimento, las vesículas se incubaron con la toxina Cry1Ab previamente marcada con biotina e incubada en presencia o ausencia de excesos molares (indicado en cada caso) de cada uno de los anticuerpos scFv. La toxina que no se une se separa mediante centrifugación y la toxina unida se visualiza después de separar por SDS-PAGE y transferir el complejo en membranas de nitrocelulosa. El resultado se muestra en la figura 13, donde se aprecia que tanto el anticuerpo scFv45 como el scFv73 compiten la interacción entre la toxina Cry1Ab y las vesículas; sin embargo, el scFv73 compite mejor que el anticuerpo scFv45, pues con un exceso de 250 veces se aprecia un efecto más importante.

B) Ensayo de unión de ligando

En el ensayo de unión de ligando es posible observar la interacción de la toxina con sus receptores presentes en las vesículas del insecto blanco. Primero se separan las proteínas de las vesículas en SDS-PAGE y se transfieren a membranas de nitrocelulosa que se incuban con la toxina marcada con biotina, finalmente la detección se realiza con estreptavidina

acoplada a peroxidasa. Para nuestro experimento, la toxina marcada se preincubó con un exceso de los anticuerpos scFv y se observó si tenían algún efecto sobre la interacción con alguno de los receptores de *M. sexta*. La figura 14 muestra que la toxina Cry1Ab se une a la proteína de 120 kDa (Aminopeptidasa-N) y la de 210 kDa (Caderina o Bt-R_1) como ya se ha reportado en otros trabajos (Jenkins and Dean, 2000). El anticuerpo scFv45 preincubado con la toxina no tiene ningún efecto sobre la interacción entre esta y los receptores de 120 o 210 kDa. En cambio, el anticuerpo scFv73 es capaz de competir la unión entre la toxina Cry1Ab y la proteína de 210 kDa pero no tiene efecto sobre la unión a la de 120 kDa. Los números que se encuentran sobre cada banda en los siguientes experimentos representan los valores de densitometría de cada resultado analizado.

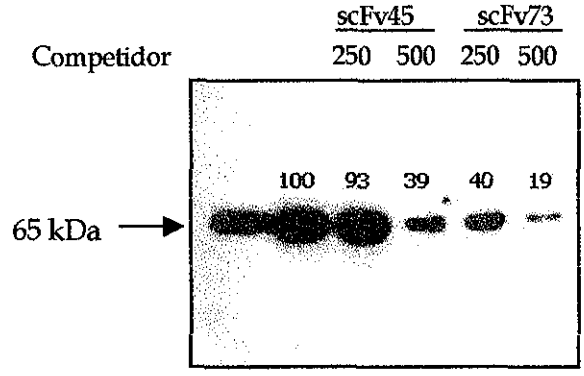

Figura 13. Ensayo de unión en solución con los anticuerpos scFv 45 y 73 como competidores.

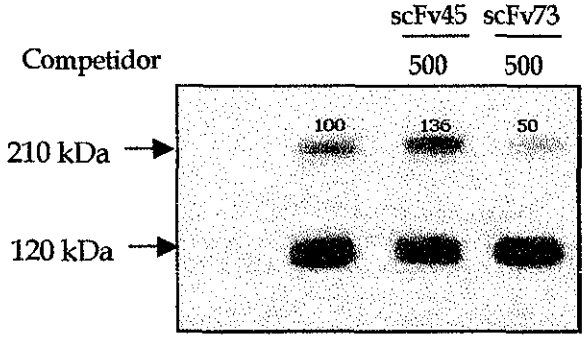

Figura 14. Ensayo de unión de ligando compitiendo la interacción entre la toxina Cry1Ab y sus receptores con los anticuerpos scFv.

El CDR3 del scFv73 presenta homología con una región discreta presente en las caderinas de los lepidópteros *M. sexta* y *B. mori*

Dado que el anticuerpo scFv73 es capaz de competir la interacción entre la toxina Cry1Ab y el Bt-R_1 que es un receptor natural de *M. sexta*, procedimos a comparar la secuencia del CDR3 del anticuerpo scFv73 con las secuencias ya reportadas de los receptores naturales localizados en el intestino medio de *M. sexta*: la aminopeptidasa-N y la caderina (BT-R_1). Dicho análisis nos permitió obtener una región de 8 aminoácidos localizados en el Bt-R_1 que presentan un 71% de identidad con el CDR3 del anticuerpo scFv73; mientras que el análisis con la aminopeptidasa-N no presentó ninguna región con identidad de secuencia significativa. El mismo análisis se realizó con la caderina de *B. mori*, otro lepidóptero sensible a las toxinas Cry1A, indicando la presencia de la misma secuencia identificada en *M. sexta*, pero además identificamos un segundo sitio en la caderina de *B. mori* que mostró 70% de identidad con el CDR3 del scFv73.

Ensayos de unión de ligando con las toxinas Cry1Aa y Cry1Ab utilizando péptidos sintéticos como competidores para identificar las regiones de unión al Bt-R_1 y Bt-R_{175}

Con el propósito de determinar si la secuencia identificada en el Bt-R_1 era el sitio de unión a la toxina Cry1Ab se mandaron a sintetizar péptidos correspondientes con las secuencias indicadas en la siguiente tabla:

Péptido sintético	Correspondencia con	Secuencia
CDR3-73	CDR3 del anticuerpo scFv73	RITQTTNR
BtR1-Cry	Región en el Bt-R_1	^{869}HITDTNNK^{876}
BtR175-Cry1	Región 1 en el Bt-R_{175}	^{873}IIDTNNK^{879}
BtR175-Cry2	Región 2 en el Bt-R_{175}	^{1296}LDETTN^{1301}

Para demostrar que las regiones identificadas dentro de las secuencias de Bt-R_1 y Bt-R_{175}, están involucradas en la interacción con la toxina Cry1Ab, se realizaron experimentos de unión de ligando empleando como competidores a los péptidos sintéticos que corresponden

con las regiones indicadas en la tabla anterior. En estos experimentos (Figura 15A) también se observó disminución de la señal en la proteína de 210 kDa cuando se utilizaron los péptidos sintéticos como competidores, siendo mayor el efecto del péptido BtR1-Cry que el del CDR3-73. No tuvimos un efecto considerable sobre la proteína de 120 kDa. En la figura 15B se muestra que al igual que para la toxina Cry1Ab, los péptidos sintéticos también interfieren en la interacción de la toxina Cry1Aa y la proteína de 210 kDa. Sin embargo al comparar el efecto que muestran con la toxina Cry1Ab, el péptido CDR3-73 muestra mayor efecto que el péptido BtR1-Cry.

Como se mencionó previamente, además de la región localizada dentro del Bt-R_1 también logramos localizar dos regiones presentes en el Bt-R_{175}, que es la caderina de *B. mori*. Estas 2 regiones podrían estar involucradas en la interacción con las toxinas Cry1A. Esto se demostró utilizando los péptidos sintéticos correspondientes con estas regiones que fueron designados como BtR175-Cry1 y BtR175-Cry2. En la unión de la toxina Cry1Ab (Figura 13A), el péptido sintético BtR175-Cry2 compite más eficientemente por la proteína de 175 kDa que con la toxina Cry1Aa (Figura 13B). En contraste el péptido sintético BtR175-Cry1 no mostró competencia significativa por la unión de ambas toxinas a la proteína de 175 kDa (Figuras 16 A y B).

A) Toxina Cry1Ab

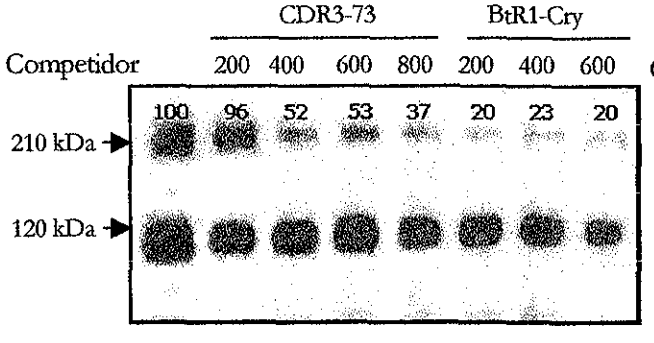

B) Toxina Cry1Aa

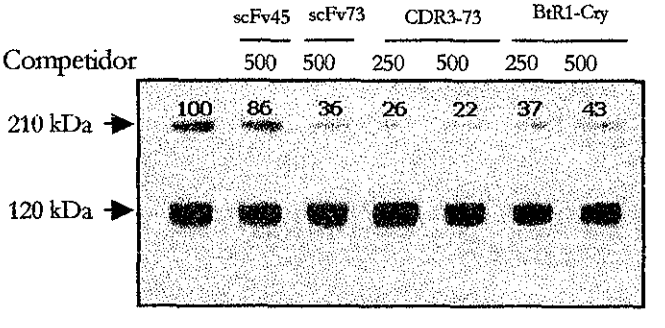

Figura 15. Ensayo de unión de ligando empleando péptidos sintéticos para competir la interacción entre las toxinas Cry1Ab y Cry1Aa con los receptores de *M. sexta*.

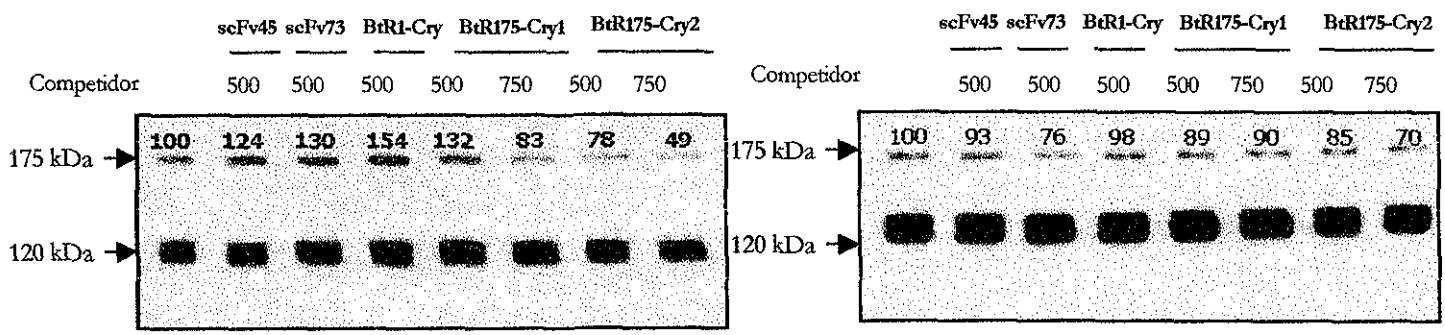

Figura 16. Ensayo de unión de ligando empleando péptidos sintéticos para competir la interacción entre las toxinas Cry1Ab y Cry1Aa y los receptores de *B. mori*.

Afinidad del anticuerpo scFv73 por las toxinas Cry1A's

Originalmente la afinidad de la toxina Cry1Ab por el receptor Bt-R_1 purificado se reportó de 0.7 nM (haciendo uso de toxina marcada con radioactividad) (Vadlamudi et al., 1995). Para conocer la afinidad del anticuerpo scFv73 por las toxinas Cry1A's empleamos SPR (Surface Plasmon Resonance), la cual es una metodología que permite medir interacción entre 2 moléculas en tiempo real. En la figura 17A solamente se muestran los datos obtenidos al medir la interacción entre el anticuerpo scFv73 inmovilizado con diferentes concentraciones de la toxina Cry1Ab, se graficaron los valores experimentales y teóricos (líneas punteadas) y podemos notar que el ajuste obtenido es bastante bueno (utilizando el modelo de un sitio de unión). El análisis reveló que las toxinas Cry1Aa, Cry1Ab y Cry1Ac se unen al anticuerpo inmovilizado y el ajuste de las curvas obtenidas reveló una estequiometría 1:1 toxina/receptor. Las afinidades de las toxinas por el anticuerpo scFv73 resultaron en el orden nanomolar y son las siguientes:

Cry1Aa K_d = 51.1 nM

Cry1Ab K_d = 39.7 nM

Cry1Ac K_d = 20.5 nM

Otro dato interesante que nos indicó que los dos anticuerpos (scFv45 y scFv73) se unen a través de sitios diferentes a la toxina Cry1Ab lo obtuvimos en SPR inyectando la toxina Cry1Ab con el anticuerpo scFv73 sobre el scFv73 inmovilizado. Podemos observar en la figura 17B como se inhibe completamente la interacción, es decir, la toxina ya no es capaz de unirse al scFv73 inmovilizado, por estar interaccionando con el que se encuentra en el flujo. En contraste, el anticuerpo scFv45 solo inhibió en un 5% la unión de la toxina Cry1Ab al scFv73 inmovilizado.

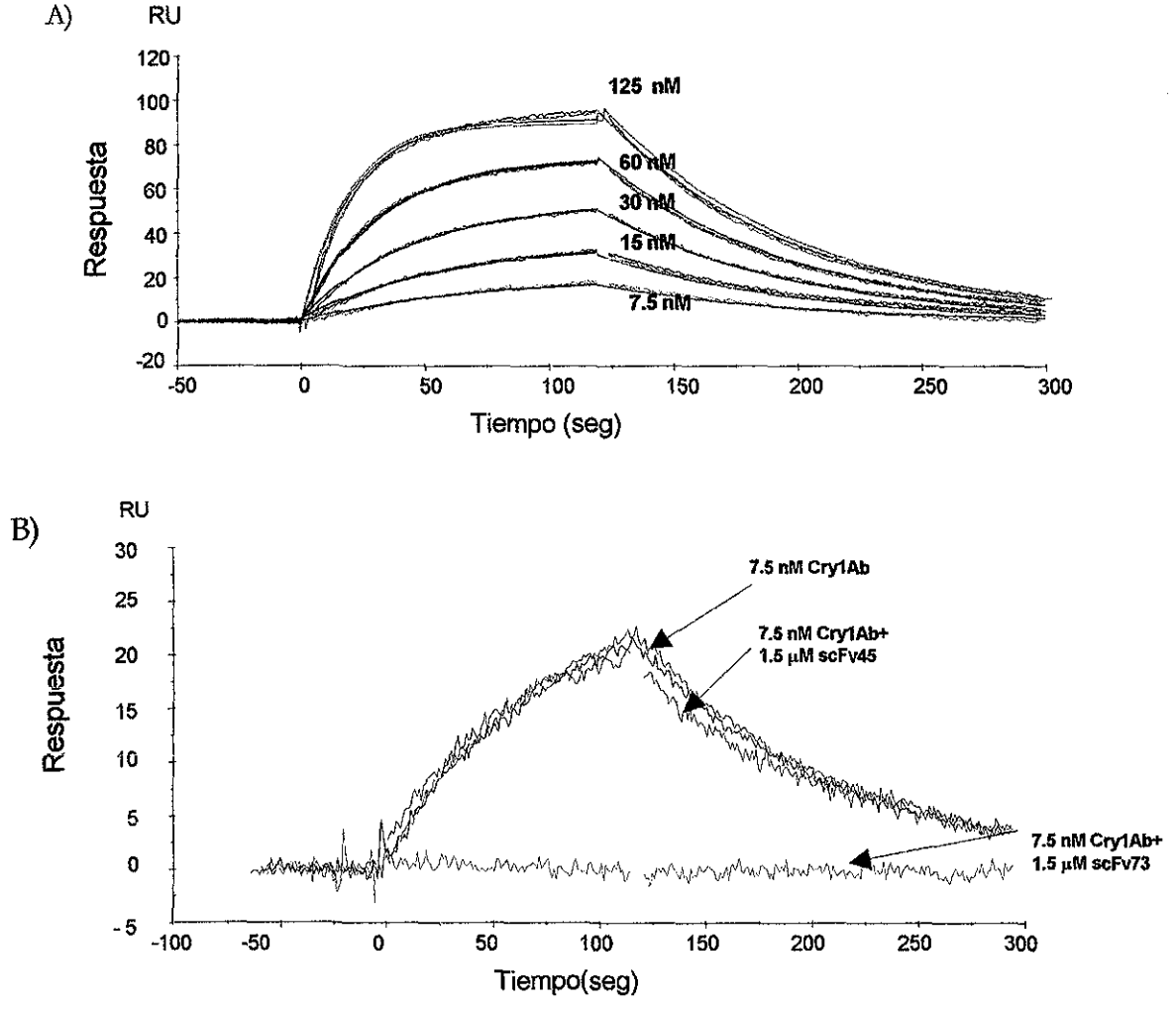

Figura 17. Análisis de la unión en SPR de la toxina Cry1Ab al scFv73. A) Unión de diferentes concentraciones de Cry1Ab al scFv73 inmovilizado. B) Unión de Cry1Ab al scFv73 inmovilizado en presencia de los scFv45 y scFv73.

Papel del epítope mapeado en Bt-R_1 en la toxicidad de Cry1Ab

Se realizaron bioensayos para demostrar que el epítope mapeado dentro del Bt-R_1, involucrado en la interacción con la toxina Cry1Ab, tiene un efecto sobre la toxicidad de Cry1Ab en larvas de *M. sexta*. Los bioensayos se realizaron preincubando la toxina Cry1Ab con los anticuerpos scFv o bien con los péptidos sintéticos correspondientes al CDR3 del scFv73 y a la región identificada en el Bt-R_1. Se utilizaron larvas de primer instar, las cuales se alimentaron con dieta artificial en la que previamente fue aplicada la toxina Cry1Ab sola o mezclada con un exceso molar de 300 veces de los anticuerpos scFv o los péptidos sintéticos. La tabla I muestra que la toxicidad de Cry1Ab se reduce hasta en un 50% cuando la toxina se preincuba con el anticuerpo scFv73 o los péptidos sintéticos CDR3-73 o con el BtR1-Cry. Mientras que el anticuerpo scFv45 presenta efecto menor (10%) sobre la toxicidad de Cry1Ab. Ninguno de los anticuerpos o péptidos mostró por si solos efecto tóxico sobre las larvas de *M. sexta* (datos no mostrados).

Tabla I. Toxicidad de la proteína Cry1Ab contra larvas de *M. sexta* en presencia o ausencia de competidores.

Tratamiento	Mortalidad en %
Cry1Ab (9 ng/cm^2)	97±2.3
Cry1Ab + scFv45	89±4.6
Cry1Ab + scFv73	55±1.1
Cry1Ab + CDR3-73	48±5.9
Cry1Ab + BtR1-Cry	49±4.2
Control	0

SITIO DE INTERACCION EN LA TOXINA Cry1Ab CON EL Bt-R_1

Durante el desarrollo de este trabajo, surgió la idea de mutagenizar el anticuerpo scFv73, para lo cual, no era suficiente la secuencia del CDR3 que nosotros teníamos ya que además

de ser muy corta solo correspondía a una hebra de DNA. La secuencia completa nos indicó que lo que habíamos tomado como el CDR3 (RITQTTNR), en realidad pertenecía a la hebra no codificante de DNA (5'-3') y la secuencia correspondiente con la hebra codificante: TVGSLSNS, no presenta identidad en secuencia con el epítope que habíamos localizado en el Bt-R_1 (^{869}HITDTNNK^{876}) Figura 18.

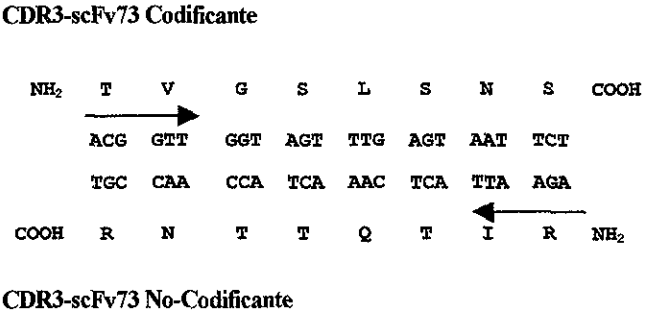

Figura 18. Secuencias de la hebras codificante y no codificante del CDR3 del scFv73.

Para confirmar que el scFv73 y Bt-R_1 se unen a la toxina Cry1Ab a través del mismo sitio, se sintetizaron péptidos con las secuencias del CDR3 del scFv73, correspondientes con la hebra codificante y no codificante, así como del epítope en Bt-R_1 ya idenficado previamente. La competencia en la unión del scFv73 por la toxina con estos péptidos nos indicó que, a pesar de la secuencia, los tres péptidos eran capaces de inhibir la interacción entre la toxina y el scFv73, por lo que se unen a la toxina a través del mismo sitio. Otro péptido con la secuencia del CDR3 del scFv73 en otro orden (péptido "scramble") no compitió con esta interacción (Figura 19).

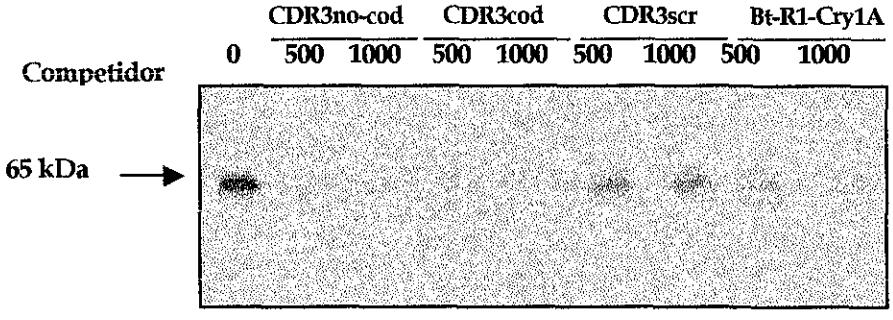

Figura 19. El CDR3 del scFv73 y el epítope de Bt-R_1 se unen al mismo sitio en la toxina Cry1Ab.

El scFv73 se une al asa2 de la toxina Cry1Ab

La predicción de que el dominio II de las toxinas Cry esta involucrado en la unión con el receptor ha provocado estudios exhaustivos en esta región; sobre todo dirigida sobre las asas localizadas en el ápice en la parte inferior que conectan las láminas β (Dean et al., 1996), por lo que no se descartó la posibilidad de que el anticuerpo scFv73 reconociera a la toxina Cry1Ab a través de alguna estas regiones. Con la finalidad de saber cual era el sitio de interacción entre el anticuerpo scFv73 y la toxina Cry1Ab, y tomando en cuenta que previamente ya habíamos observado que el anticuerpo scFv73 reconocía al Dominio II de la toxina Cry1Ab; se decidió sintetizar péptidos correspondientes con las secuencias de las asas del dominio II de las toxinas Cry1Aa y Cry1Ab. El alineamiento de las secuencias de estas toxinas nos permite observar que ambas presentan la misma secuencia en el asa 1 pero muestran diferencias significativas en las secuencias correspondientes a las asas2 y 3; sin embargo ambas toxinas tienen actividad tóxica contra el lepidóptero *M. Sexta* y reconocen tanto a Bt-R_1 como la APN en ensayos de unión de ligando.

Asa 1:

Cry1Aa TDVH RG FNYW

Cry1Ab TDAH RG EYYW

Asa 2:

Cry1Aa PLY RRIILGSGP NNQE

Cry1Ab TLY RRPFNI GI NNQQ

Asa 3:

Cry1Aa TMLS QAAGAVY TLR

Cry1Ab SMFR SGFSNS SVSI

Estos péptidos se emplearon en experimentos de "Western blot", donde se compitió la unión del anticuerpo scFv73 a la toxina Cry1Ab con diferentes excesos de dichos péptidos. De este modo logramos observar que el anticuerpo scFv73 previamente incubado con el péptido del asa 2 era incapaz de unirse a la toxina Cry1Ab, lo que indicó que esta asa del dominio II debe

estar reconociendo al scFv73 (Figura 20A). El mismo efecto se observó al realizar el mismo experimento pero ahora utilizando la toxina Cry1Aa con los péptidos sintéticos correspondientes a las asas de esta toxina (20B).

A) Cry1Ab

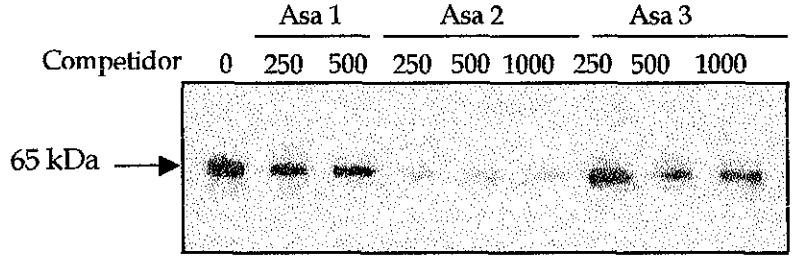

B) Cry1Aa

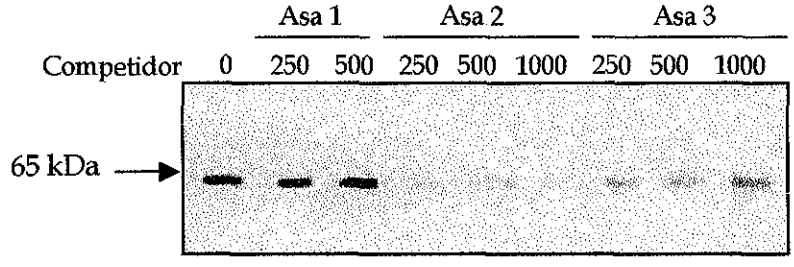

Figura 20. El péptido sintético correspondiente con el asa2 de las toxinas Cry1Aa y de Cry1Ab inhiben la interacción entre el anticuerpo scFv73 y las toxinas Cry1A.

Mutaciones en el asa2 de Cry1Ab que afectan la unión y toxicidad de esta proteína también afectan la unión al anticuerpo scFv73

Las mutaciones F371A y RR368-9EE localizadas en el asa2 de la toxina Cry1Ab tienen efecto sobre las propiedades de unión a VMMA de *M. sexta* y además están afectadas en toxicidad (Dean et al., 1996; Rajamohan et al., 1998). Con el propósito de investigar un poco más sobre el papel de esta asa en la unión a la toxina Cry1Ab, decidimos sintetizar péptidos correspondientes al asa2 que presentaran estas mutaciones y utilizando experimentos de tipo "Western blot" analizar que efecto tienen sobre la interacción del anticuerpo scFv73 con la toxina Cry1Ab. Lo que observamos fue que, en concordancia con las toxinas mutantes,

ninguno de los dos péptidos sintéticos que contienen las mutaciones RR368,369AA y F371A fueron capaces de competir la interacción entre la toxina Cry1Ab y el scFv73 reafirmando así el papel que juegan estos residuos en dicha interacción. Además de este experimento, se cuenta con la cepa de la mutante F371A localizada el asa2 del dominio II en la toxina Cry1Ab (Rajamohan et al., 1995). Después de la purificación de la toxina mutante, se analizó su capacidad de unión al scFv73 y al mismo tiempo se compitió dicha interacción con el asa2 de Cry1Ab que no presenta ningún cambio en la secuencia, como control se realizó el mismo experimento con la toxina Cry1Ab silvestre. En este experimento observamos que la unión del scFv73 a la toxina mutante se inhibe con excesos menores del péptido sintético, a diferencia de la toxina silvestre (Figura 21). Estos datos, muestran que esta mutación sencilla tiene un efecto importante en la interacción con el anticuerpo scFv73.

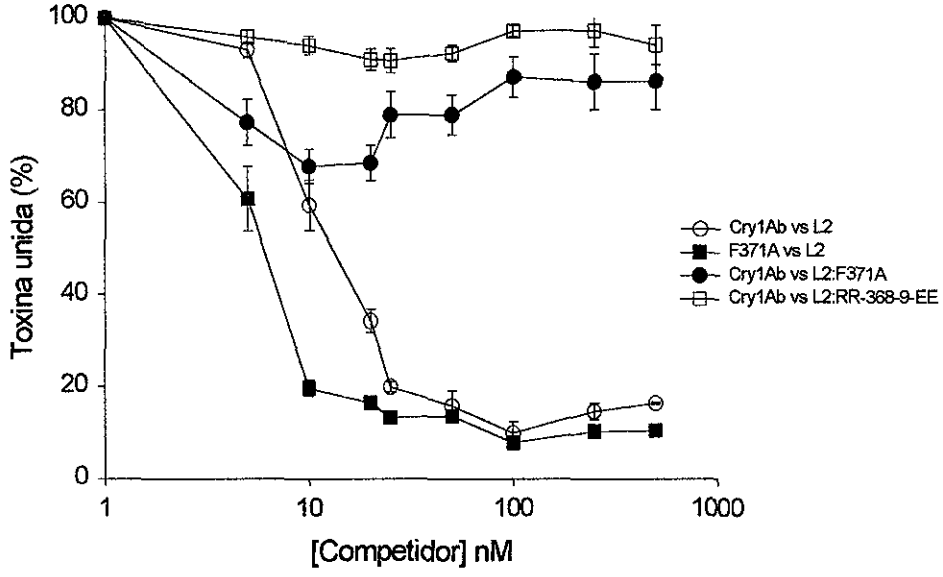

Figura 21. Competencias con péptidos sintéticos correspondientes al asa2 de la toxina Cry1Ab con mutaciones en los residuos 371 o 368-369.

Se comparó la afinidad de las toxinas Cry1Ab y Cry1Ab-F371A por el anticuerpo scFv73 utilizando el SPR y podemos observar en la figura 22 los sensogramas obtenidos. La afinidad de la toxina Cry1Ab-F371A (115 nM) fue menor que la obtenida para la Cry1Ab silvestre (55.8 nM) indicando que la mutación F371A afecta la interacción con el scFv73.

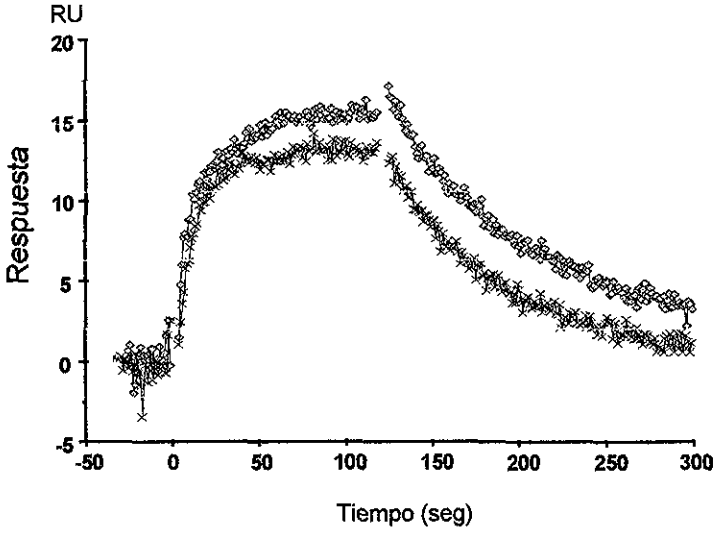

Figura 22. Comparación de la unión de las toxinas Cry1Ab (gris) y F371A (negro) al anticuerpo scFv73 inmovilizado.

Los péptidos correspondientes al asa2 de las toxinas Cry1Aa y Cry1Ab compiten la unión por el Bt-R_1 en ensayos de unión de ligando

Sabiendo que el anticuerpo scFv73 presenta homología con una región discreta en la caderina de *M. sexta* (Bt-R_1) y además que el asa2 de Cry1Ab inhibe la interacción entre el anticuerpo scFv73 y las toxinas Cry1Aa y Cry1Ab, procedimos a realizar experimentos de unión de ligando donde se compitiera la unión de las toxinas marcadas con biotina al receptor Bt-R_1 utilizando diversos excesos de los péptidos sintéticos correspondientes a las asas de las toxinas Cry1Aa y Cry1Ab.

El experimento correspondiente a la unión de la toxina Cry1Ab muestra como el asa2 inhibe la unión de la toxina Cry1Ab a la proteína de 210 kDa (Bt-R_1) pero no tiene efecto sobre la proteína de 120 kDa (Aminopeptidasa-N) (Figura 23A). Sin embargo el mismo experimento pero ahora con la toxina Cry1Aa nos muestra que además del asa2, el asa3 también tiene un efecto en la interacción (Figura 23B). Este dato nos permite sugerir que posiblemente existe otro sitio de reconocimiento entre el Bt-R_1 y el dominio II de Cry1Aa localizado en el asa3. De la misma manera que con Cry1Ab, ningún exceso del asa2 o asa3 de Cry1Aa tiene efecto

sobre la proteína de 120 kDa. Finalmente, el asa1 no afectó en la unión de las toxinas Cry1Aa o Cry1Ab con ninguno de los 2 receptores (Figuras 23 A y B).

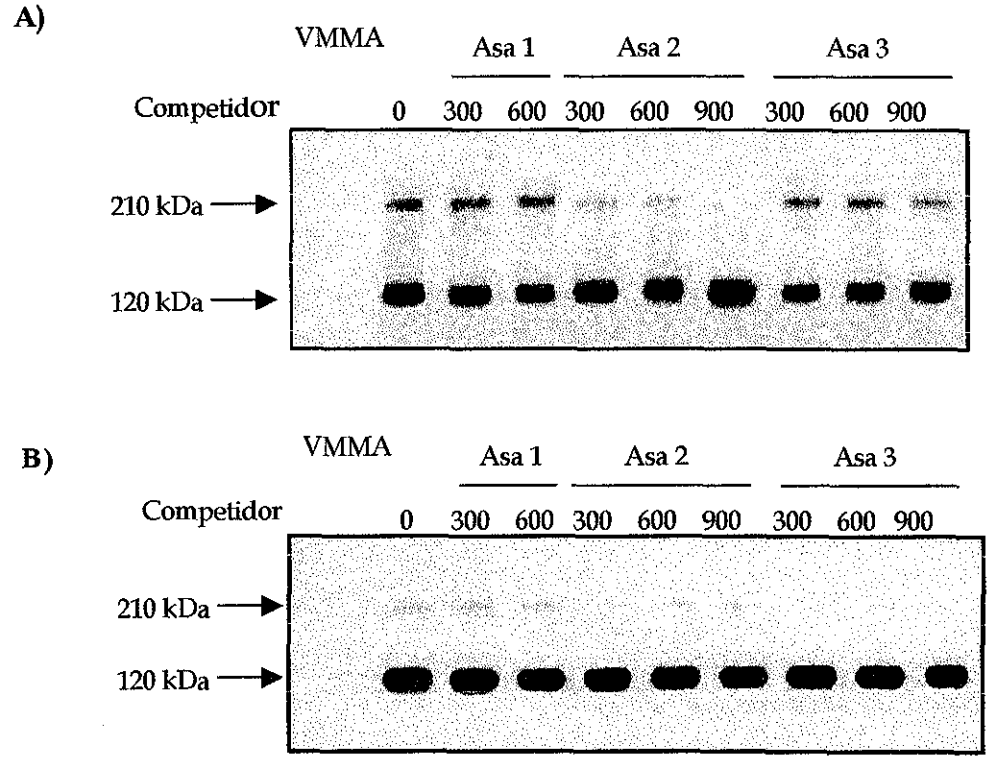

Figura 23. El asa2 de Cry1Ab o Cry1Aa desplaza la interacción entre el Bt-R_1 y las toxinas Cry1Ab (A) o Cry1Aa (B).

Perfiles de hidropatía inversos determinan la interacción entre el asa2 y Bt-R_1

Después de observar que el epítope identificado en el Bt-R_1 se une a las toxinas Cry1Aa y Cry1Ab por el asa2, a pesar de que en secuencia comparten poca identidad, surgió la pregunta de cómo un mismo epítope podría ser reconocido por secuencias diferentes. Con respecto a esto, se ha visto en otros trabajos que la interacción entre proteínas se puede dar a través de perfiles de hidropatía complementarios (Blalock, 1999). Al comparar los perfiles de hidropatía de las secuencias de las asas2 de las toxinas Cry1Aa y Cry1Ab con el epítope del Bt-R_1. Lo primero que observamos fue que los perfiles de hidropatía del CDR3 del anticuerpo scFv73; tanto de la hebra codificante como de la no codificante y del epítope del Bt-R_1 eran muy parecidos entre ellos (figura 24), sugiriendo que las tres secuencias pueden

interaccionar con un mismo ligando, esto de acuerdo con la teoría de reconocimiento molecular (Blalock, 1999). La segunda observación fue que las asas2 de las toxinas Cry1Aa y Cry1Ab tienen un perfil de hidropatía inverso con respecto al del epítiope de Bt-R_1, siendo más complementario el perfil del asa2 de Cry1Ab que el de Cry1Aa (Figura 25). También notamos que la porción de las toxinas que mostró perfil de hidropatía inverso con el epítope de Bt-R_1 incluía 5 residuos localizados en la β6 más 5 residuos localizados en el asa2; mientras que el epítope del Bt-R_1 se amplió hacía los residuos ^{865}NITIHITDTNN^{875}. Finalmente, la identidad entre las regiones de las toxinas Cry1Aa y Cry1Ab que tienen este perfil de hidropatía complementario al de Bt-R_1 es del 54% donde 5 de 6 residuos idénticos están ubicados en la región de la β6.

Finalmente, se preparó un modelo teórico que representa la interacción de la toxina Cry1Ab y la secuencia identificada en el receptor Bt-R_1. Para la construcción del mismo se prepararon, por separado, los modelos correspondientes a la toxina Cry1Ab y a la secuencia que identificamos mediante el perfil de hidropatía del receptor Bt-R_1.

Para la construcción del modelo de Cry1Ab se tomó como base la estructura de la toxina Cry1Aa, la cual ya ha sido determinada mediante cristalografía de rayos X (Grochulski et al., 1995). Estas dos toxinas tienen 89% de identidad en su secuencia de aminoácidos. A continuación, haciendo uso del módulo Builder de Insigh II (MSI, actualmente Accelrys) se "rasuraron" las cadenas laterales del modelo de la toxina Cry1Aa para entonces cargar la secuencia de la toxina Cry1Ab. Se asignaron los residuos de la secuencia de Cry1Ab a la cadena principal de Cry1Aa. Este primer modelo se exportó en formato PDB y se minimizó dentro del programa CNS teniendo cuidado de que la posición del modelo de Cry1Ab no fuera modificado de forma considerable con respecto de la posición en la estructura de la toxina Cry1Aa (RMSD entre carbonos α). Finalmente, el modelo de la toxina Cry1Ab se revisó residuo por residuo (utilizando el programa O) realizando ajustes en las regiones y favoreciendo las interacciones con átomos vecinos. La calidad final del modelo se verificó con una gráfica de Ramachandran, que indicó menos del 5% de los residuos en conformaciones no comunes.

El siguiente paso fue la construcción de un "modelo" para la secuencia identificada en el receptor Bt-R_1. Esta se preparó utilizando tres rutas diferentes. (A) Se consideró una estructura "lineal". (B) Se realizó una búsqueda por similitud en la base de datos del PDB, la cual proporcionó una región en una caderina-E con estructura de "asa". En este mismo apartado se estructuró la secuencia del Bt-R_1 como una estructura de tipo α y también como β. (C) Finalmente se realizó una predicción de estructura secundaria, obteniéndose un resultado de: No estructurado–ASA-No estructurado. El cual se combinó con la secuencia obtenida a partir de la caderina-E para tomar esta "estructura" de No estructurado–ASA-No estructurado.

Finalmente, haciendo uso del programa Gramm se realizó un Docking geométrico entre la toxina Cry1Ab, la cual se mantuvo fija todo el tiempo, y las diferentes posibilidades del fragmento del Bt-R_1 (lineal, α, β y No estructurado–ASA-No estructurado). De este Docking se seleccionaron los resultados que más acercaron a las zonas que identificamos experimentalmente (El Dominio II de la toxina Cry1Ab) y se realizaron ajustes de posición con el programa CNS. Esto se repitió varias veces hasta que la mayoría de los resultados se localizaron en Dominio II y especialmente en la zona correspondiente con el asa2.

Uno de los modelos resultantes, que más se ajusta a la evidencia experimental generada y discutida anteriormente, se presenta en la figura 26. En esta representación podemos notar que la región del Bt-R_1 se une a la toxina Cry1Ab a través de la región comprendida desde la β6 y el asa2 lo cual nos indica que estas dos regiones pueden establecer una interacción entre ellas, el contexto final de la interacción entre el receptor completo y la toxina aún esta por determinarse.

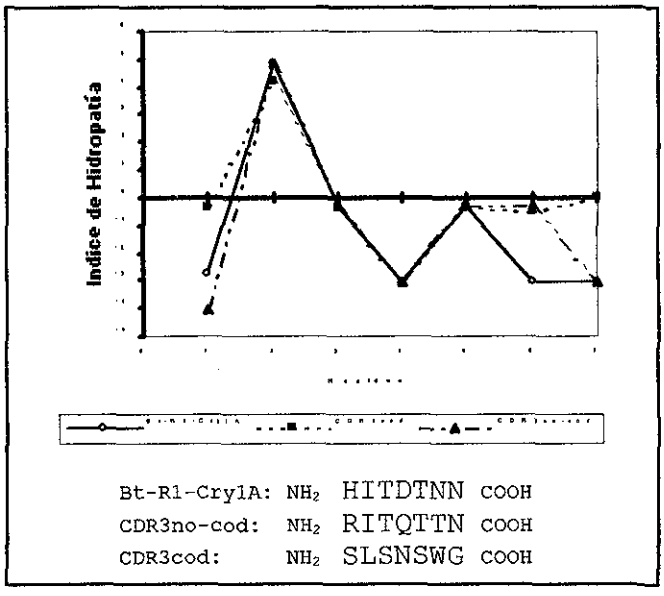

Figura 21. Perfiles de hidropatía entre el CDR3 del scFv73 y Bt-R_1.

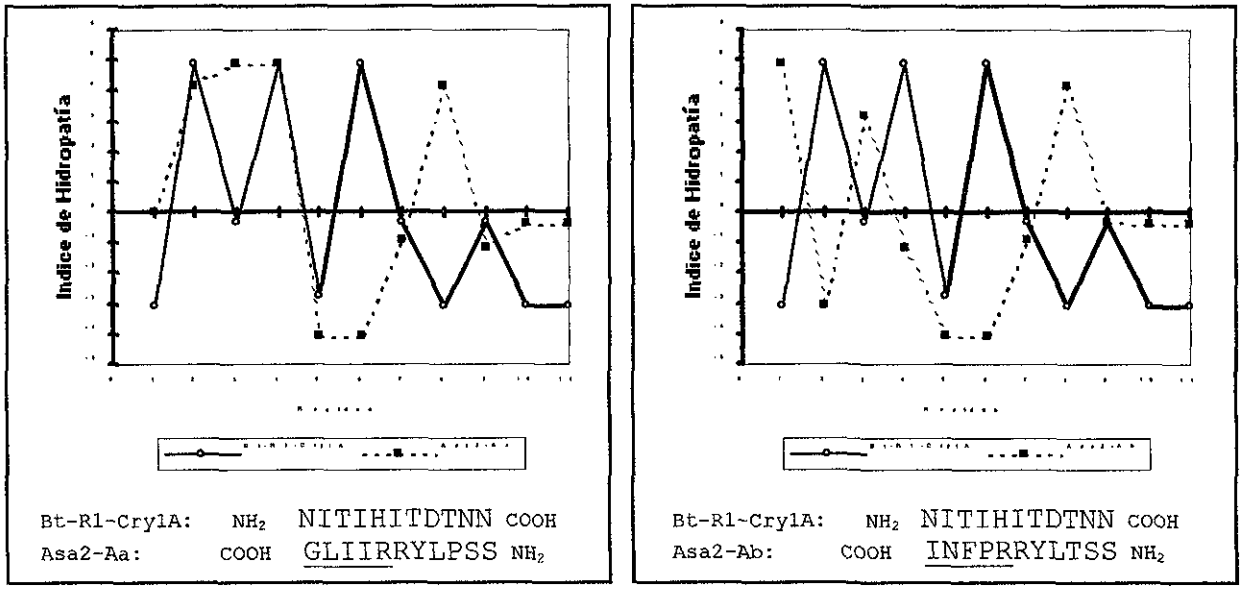

Figura 22. Perfiles de hidropatía complementarios entre las asas2 de Cry1Aa y Cry1Ab con un fragmento del Bt-R_1.

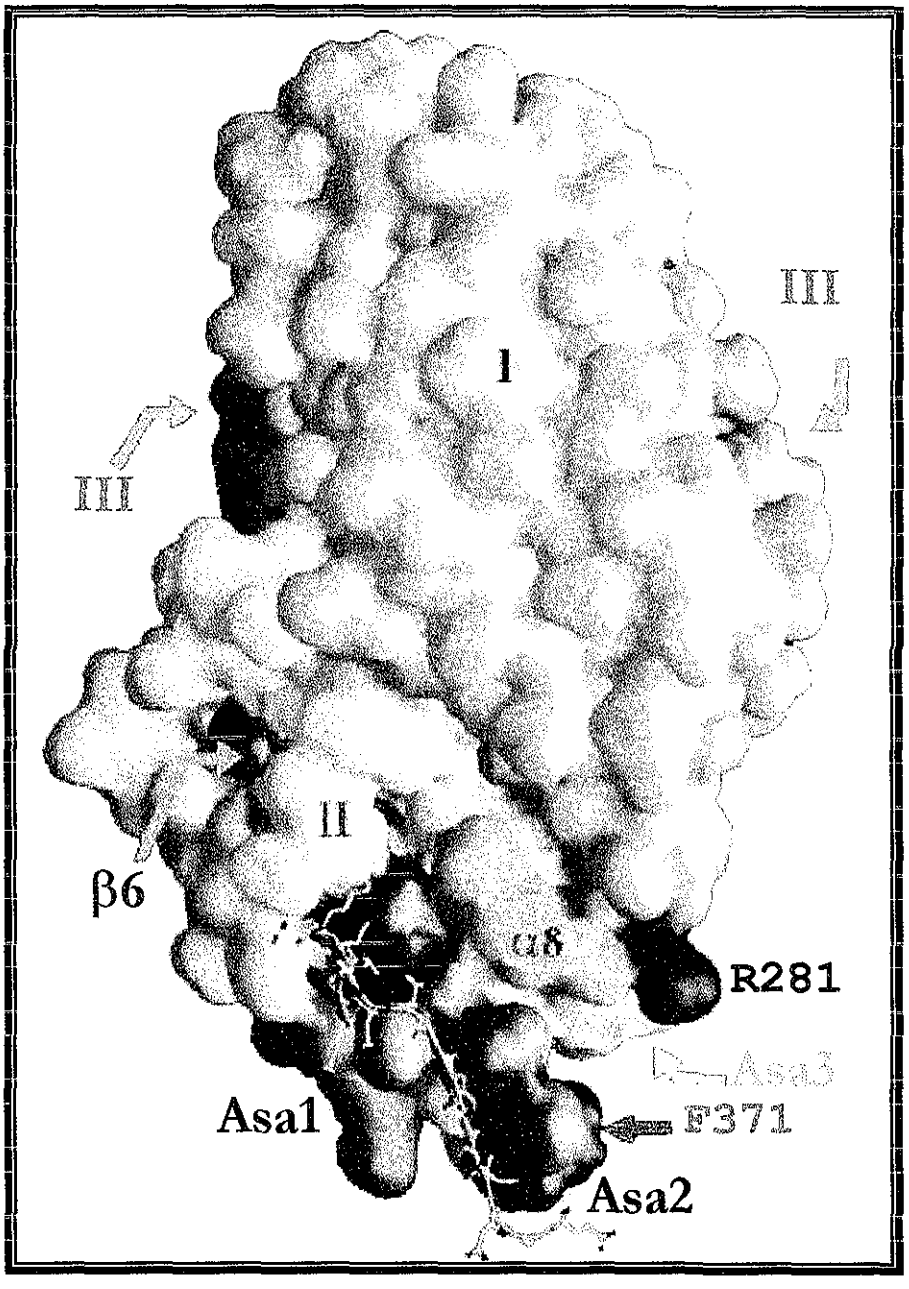

Figura 26. Modelo de interacción entre la toxina Cry1Ab y el fragmento ^{865}NITIHITDTNN^{875} del Bt-R_1.

El asa α8 localizada el dominio II de la toxina Cry1Ab reconoce un segundo epítope en el receptor Bt-R_1

Existe otra asa (α8), localizada en el dominio II que conecta la β1 con la β2 y que se encuentra muy cercana al dominio I, la cual se ha demostrado mediante mutagénesis sitio dirigida que también participa en la unión de la toxina a VMMA's de *M. sexta* (Lee et al., 2000; Lee et al., 2001), por lo que analizamos si un péptido sintético con la secuencia correspondiente a esta asa (^{279}SFRGSAQGIEGS^{290}) es capaz de afectar la interacción entre la toxina Cry1Ab y el anticuerpo scFv73. Como se puede observar en la figura 27A, este péptido fue capaz de competir la interacción entre la toxina y el anticuerpo scFv73. También inhibió la interacción entre el Bt-R_1 y la toxina Cry1Ab, pero no tuvo efecto sobre la unión a la APN, figura 27B, lo cual sugiere que tanto el asa2 como el α8 tienen capacidades de unión similares, la pregunta entonces fue si reconocen el mismo sitio en el receptor Bt-R_1 o si reconocen epítopes diferentes.

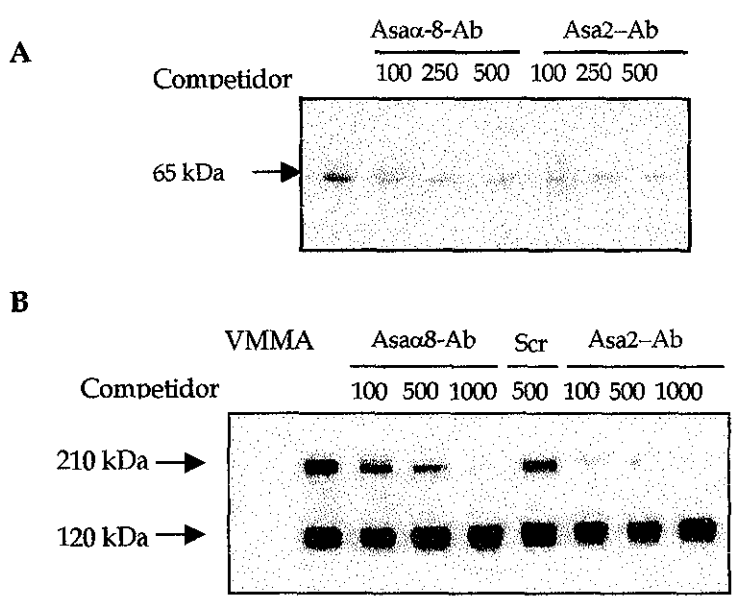

Figura 27. El asa α8 y 2 de Cry1Ab compiten la interacción del anticuerpo scFv73 con la toxina Cry1Ab (A) y también su interacción con el Bt-R_1 (B).

Para identificar las regiones reconocidas por el asa α8 y asa2 de la toxina Cry1Ab en el receptor Bt-R_1, clonamos dos fragmentos de 70 aminoácidos de este receptor por separado. El primer fragmento corresponde los residuos 831-900 (TBR1) y contiene el epítope que previamente identificamos (^{865}NITIHITDTNNK^{876}); mientras que el segundo abarca los residuos 1291-1360 (TBR2) que fue caracterizado por Dorsch y co-autores (Dorsch et al., 2002). La estrategia utilizada para clonar los productos de PCR fue la misma que se utlizó para sub-clonar los anticuerpos scFv, es decir, nos valimos de la "cola de histidinas" para la purificación utilizando una columna de níquel-agarosa.

Después de la purificación se obtuvieron dos péptidos de aproximadamente 30 kDa, los cuales se separaron en SDS-PAGE y se transfirieron en membrana de PVDF. Para saber si eran reconocidos por las toxinas Cry1Aa, Cry1Ab y Cry1Ac, la membrana de PVDF se incubó con 10 nM de cada una de las toxinas correspondientes marcadas con biotina y se reveló la unión con estreptavidina acoplada a peroxidasa. La figura 28 muestra que las tres toxinas Cry1A son capaces de unir ambos péptidos. Sin embargo, la toxina Cry3A, que no es tóxica para *M. sexta*, no es capaz de reconocer ninguno de los 2 fragmentos, indicando así la especificidad de estas regiones del Bt-R_1 en su interacción con las toxinas Cry1A's.

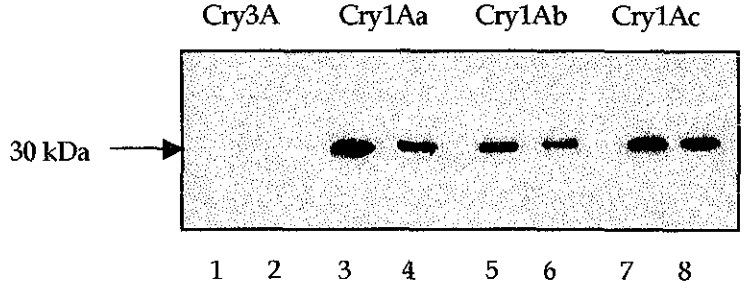

Figura 28. Las toxinas Cry1A's unen a los 2 sitios clonados del Bt-R_1 de *M. sexta*. (1, 3, 5 y 7: TBR1; 2, 4, 6 y 8: TBR2)

Después de observar la unión de la toxina Cry1Ab a ambos fragmentos se compitió esta interacción con excesos de péptidos sintéticos correspondientes con el asa α8 y asa2 de la toxina Cry1Ab. La figura 29A nos muestra que la interacción entre el TBR1 y la toxina Cry1Ab se compite solamente con el asa2 pero no con el asa α8, mientras que la interacción

de la toxina con el TBR2 se inhibe tanto con el asa2 como el asa α8, figura 29B. Estos datos sugieren que mientras el TBR1 interacciona con el asa2 del dominio II de la toxina Cry1Ab, como previamente habíamos observado, el TBR2 puede hacerlo con el asa α8 y con el asa2, indicando dos posibles sitios en la toxina involucrados en el reconocimiento del Bt-R_1 de *M. sexta*. Un péptido con una secuencia irrelevante no tiene efecto sobre esta interacción.

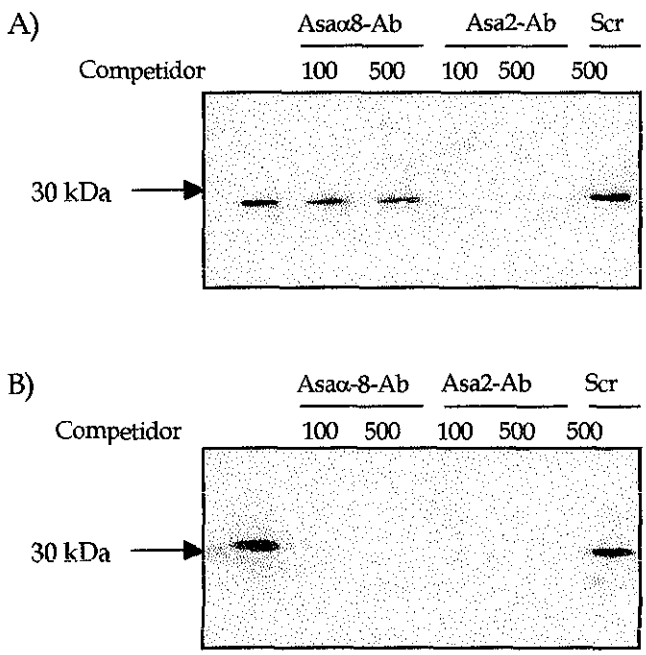

Figura 29. Competencias con péptidos sintéticos de las asas de Cry1Ab y su efecto en la interacción de esta toxina con los TBR's del Bt-R_1.

Con estos datos podemos sugerir la presencia de dos sitios de interacción en el receptor Bt-R_1 con la toxina Cry1Ab. Aún falta determinar el papel que tienen en la toxicidad en bioensayos, su afinidad por la toxina y su efecto en la activación de la protoxina Cry1Ab (Molecular basis for *Bacillus thuringiensis* Cry1A toxin specificity: Domain II loop α-8 and loop 2 of Cry1Ab toxin recognize different sites in the *Manduca sexta* Bt-R_1 receptor. **Isabel Gómez**, Alejandra Bravo, and Mario Soberón. Artículo en preparación).

ENSAYOS DE ACTIVACION DE LA PROTOXINA Cry1Ab EN PRESENCIA DEL ANTICUERPO scFv73

Hasta el momento no se sabe con toda certeza cual es el papel que juega el receptor en la actividad tóxica de las proteínas Cry, se piensa que ancla a la toxina a la membrana y esto permite su inserción y oligomerización, pero aún hacen se requieren más estudios para confirmar estas hipótesis.

Por otro lado, hemos observado en el laboratorio que los cristales de las proteínas Cry1A una vez que se activan *in vitro* para obtener las toxinas, mediante tratamiento con tripsina, son capaces de unirse a sus receptores cuando se marcan con biotina y son tóxicas *in vivo*, ya que si alimentamos larvas de insectos susceptibles con estas toxinas, los insectos mueren. Sin embargo, si estas mismas preparaciones se utilizan en experimentos donde se mide la formación de poro inducida por estas toxinas en VMMA's, no siempre observamos este efecto, lo cual nos hace suponer que durante el procesamiento *in vitro* con tripsina algún paso de la proteólisis posiblemente esta incompleto.

Los resultados previos nos han permitido obtener un anticuerpo scFv que se une a la toxina Cry1Ab por un sitio similar localizado en el receptor natural Bt-R_1. Utilizando este anticuerpo scFv como un "receptor", investigamos si la interacción toxina-receptor tiene algún papel en el proceso de toxicidad de estas proteínas.

Se realizaron experimentos de activación proteolítica con la protoxina Cry1Ab en presencia del anticuerpo scFv73. Con este objetivo preincubamos la protoxina soluble con los anticuerpos scFv45 o scFv73 a temperatura ambiente durante una hora y después de este paso realizamos la activación proteolítica con tripsina o jugo gástrico de *M. sexta*. El anticuerpo scFv45 se utilizó como control, pues ya sabíamos que se une a la toxina Cry1Ab pero no tiene ningún efecto en su interacción con el Bt-R_1 ni sobre la toxicidad. La actividad de formación de poro de las toxinas activadas *in vitro* se midió registrando los cambios de fluorescencia empleando BBMV de *M. sexta* y la cianina Dis-C_3-(5) que es sensible a los cambios de potencial de la membrana, como se describe en materiales y métodos. Algunos trazos representativos de estos experimentos se muestran en la figura 30.

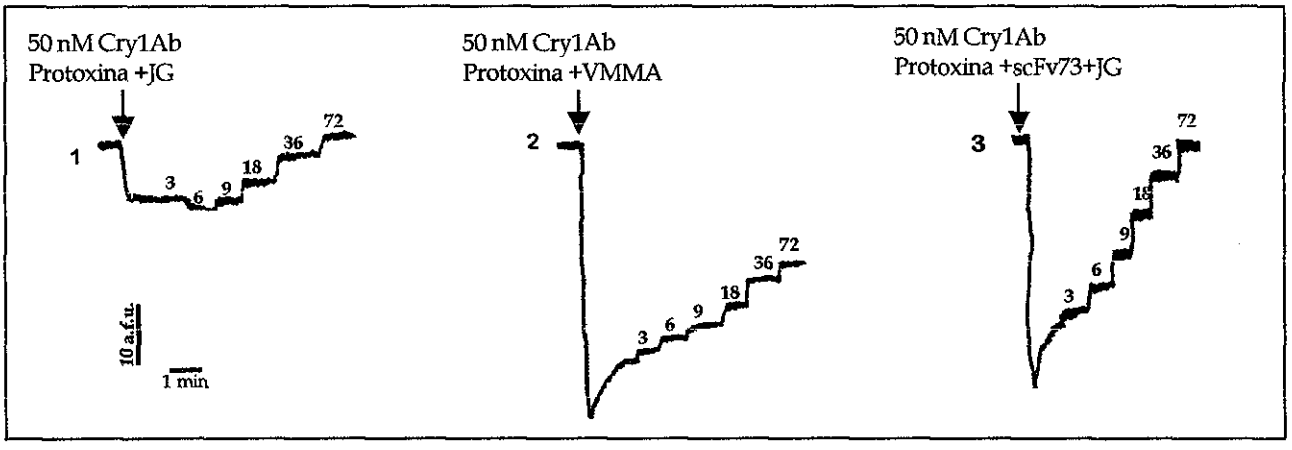

Figura 30. Permeabilidad a K^+ a través de VMMA inducida por la toxina Cry1Ab obtenida con diferentes tratamientos. Las flechas indican la adición de la toxina y los números sobre los trazos indican la concentración final de K^+ después de cada adición.

Para comparar la actividad de las diferentes preparaciones se hace un análisis graficando la diferencia de fluorescencia (ΔF) contra el potencial de membrana (E_m) como se indica en materiales y métodos. Al comparar las pendientes de cada registro obtenido, entre mayor sea este valor mayor es la permeabilidad a K^+. Los datos que se resumen en la tabla 2 nos muestran que el tratamiento de la protoxina con el scFv73 previo a la adición de las proteasas resultó en una mayor actividad de formación de poro, comparada con los otros tratamientos realizados. La protoxina, los scFv's solos o una mezcla de ambos no presentaron actividad de formación de poro. También notamos que la preincubación de la protoxina con el scFv73 es un paso necesario pues si se incuban y mezclan la protoxina, el scFv73 y la proteasa al mismo tiempo, resulta en una preparación sin actividad de formación de poro. Esta actividad mejoró cuando la incubación entre el anticuerpo scFv73 y la protoxina se realizó a 37°C lo que sugiere una mejor interacción entre ellos.

También notamos que la activación proteolítica, utilizando jugo gástrico de *M. sexta*, proporciona mejores resultados que la tripsina, probablemente porque en el jugo gástrico se encuentra una proteasa con características diferentes a las de la tripsina, lo que produce un mejor procesamiento de la protoxina.

La incubación de la protoxina Cry1Ab con el scFv73 y el tratamiento de esta mezcla con jugo gástrico, nos permitió obtener preparaciones con una actividad mejorada de formación de poro. Estos datos nos hablan de que la interacción con el receptor es un paso importante para que la toxina logre insertarse en la membrana de los insectos blanco.

Las vesículas que se preparan a partir del intestino medio de los insectos blanco contienen los receptores naturales y también tienen actividad proteolítica. Por esta razón probamos si la protoxina se podía activar con las vesículas del intestino medio de *M. sexta* sin la adición de proteasas. La figura 30 y tabla 2 muestran que la incubación de la protoxina Cry1Ab con VMMA resulta en preparaciones con actividad de formación de poro apoyando nuestra hipótesis sobre una interacción previa con el receptor previa al procesamiento proteolítico.

Bioensayos realizados con las preparaciones indicadas en la tabla 3 muestran que tanto la protoxina sola como la activada en presencia de scFv73 tienen valores de LC_{50} parecidos, mientras que la protoxina activada con jugo gástrico presenta un valor 10 veces mayor.

Tabla 2. Permeabilidad a K^+ producida por la toxina Cry1Ab activada mediante diferentes tratamientos.

Muestra	$m\text{-}m_{int}$[a] [Permeabilidad a K^+]	% de permeabilidad a K^+
Protox. Cry1Ab + scFv73 + Tripsina	0.202	41
Protox. Cry1Ab + scFv73 + Jugo gástrico (JG)	0.392	78
Protox. Cry1Ab + scFv45 + Tripsina	0.049	10
Protox. Cry1Ab + scFv45 + JG	0.027	5
Protox. Cry1Ab + Jugo gástrico	0.045	9
Protox. Cry1Ab + scFv73 + JG a 37°C	0.498	100
Protox. Cry1Ab + scFv73 + JG (Mezcla)	0.087	18
Protox. Cry1Ab + BBMV	0.143	29
Protox. Cry1Ab + JG (Monómero)	0.049	10
Protox. Cry1Ab + scFv73 + JG (Monómero)	0.047	10
Protox. Cry1Ab + scFv73 + JG (Oligómero)	0.122	25

a El valor de la pendiente indicada, es la diferencia de la pendiente de la toxina menos la pendiente de la permeabilidad intrínseca en las vesículas. (JG. Jugo gástrico)

Tabla 3. Bioensayo con larvas de *M. sexta* utilizando toxina Cry1Ab activada en presencia o ausencia del scFv73.

Muestra	LC_{50} (ng/cm^2)
Protoxina Cry1Ab	1 (0.5-1.7)
Protoxina Cry1Ab + scFv73 + Jugo gástrico	1.6 (0.78-3.01)
Protoxina Cry1Ab + Jugo gástrico	20.7 (14.3-67.48)

La actividad de formación de poro *in vitro* correlaciona con la presencia de oligomeros de la toxina Cry1Ab

Una vez que observamos la actividad de formación de poro *in vitro*, examinamos si esta, se encuentra asociada con la formación de oligómeros como sucede con otras toxinas bacterianas, como la aerolisina o la toxina del cólera, las cuales para poderse insertar en su membrana blanco primero deben interaccionar con sus receptores, lo que les permite oligomerizar y formar entonces una estructura capaz de insertarse y formar el poro en la membrana blanco.

El análisis se realizó en "Western blot" detectando con un anticuerpo policlonal anti-Cry1Ab. La figura 31 muestra que las preparaciones que presentan actividad de formación de poro presentan un agregado de aproximadamente 250 kDa, que correspondería con un oligómero formado por cuatro monómeros de la toxina. La preparación correspondiente a la protoxina tratada con jugo gástrico no muestra tales agregados y además no tiene actividad de formación de poro.

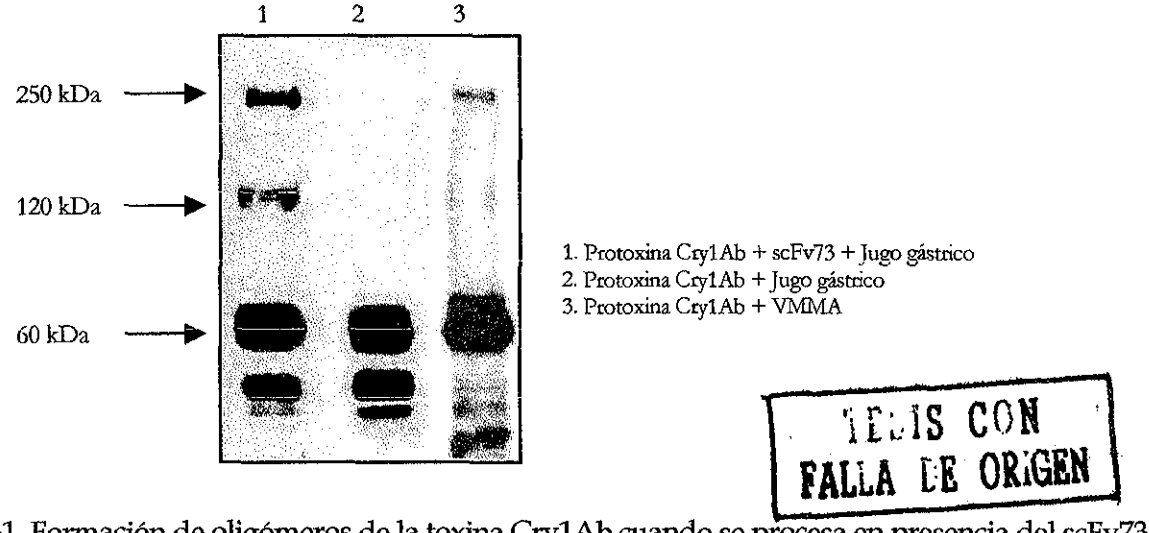

Figura 31. Formación de oligómeros de la toxina Cry1Ab cuando se procesa en presencia del scFv73 o VMMA.

Para confirmar que la actividad de formación de poro esta directamente relacionada con la formación del agregado de 250 kDa, se procedió a la separación del oligómero mediante cromatografía de exclusión por tamaño. La cromatografía se realizó en una columna

Superdex 200, con dos preparaciones de toxina: la correspondiente a toxina activada en presencia del scFv73 y la otra activada con jugo gástrico.

Después de la cromatografía se obtuvieron dos poblaciones de peso molecular distinto, las cuales se analizaron en "Western blot" detectando con un anticuerpo monoclonal (que reconoce una región localizada dentro del dominio I) o con un anticuerpo policlonal. Los resultados se muestran en al figura 32 donde se observa que al revelar con el anticuerpo policlonal es posible observar la banda de aproximadamente 250 kDa, correspondiente a la toxina Cry1Ab oligomerizada; los monómeros de ambas preparaciones se revelan tanto con el anticuerpo monoclonal como con el policlonal. Estos datos sugieren que la toxina podría estar sufriendo un cambio conformacional al oligomerizar, pues el anticuerpo monoclonal no es capaz de detectar al oligómero pero si los monómeros. La protoxina activada con jugo gástrico sin el scFv73 no contiene ningún agregado pero si presenta la banda de 65 kDa correspondiente al monómero, los cuales se detectan tanto con el anticuerpo monoclonal como policlonal.

A)Revelado con anticuerpo policlonal.

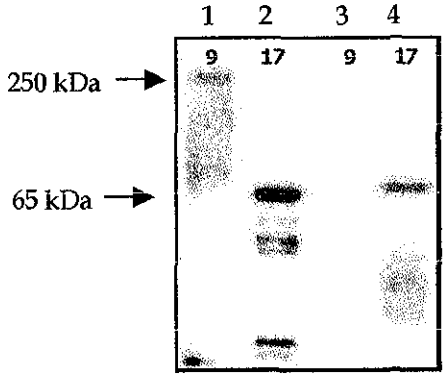

B) Revelado con anticuerpo monoclonal.

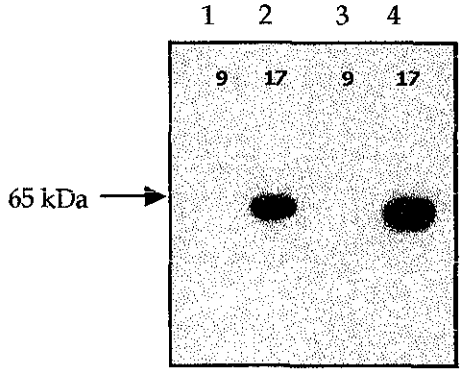

1 y 2 en ambas figuras corresponden a las fracciones recuperadas de la preparación de toxina activada en presencia del scFv73.

3 y 4 corresponden a las fracciones recuperadas de la preparación de toxina obtenida al activar la protoxina con jugo gástrico.

9 y 17 indican el número de la fracción donde se recuperaron estas muestras.

Figura 32. "Western blot" de las fracciones recuperadas de la cromatografía de exclusión por tamaño.

Finalmente, se realizaron experimentos de formación de poro con el oligómero de 250 kDa y los monómeros, recuperados de la cromatografía de exclusión por tamaño. Los valores de la actividad de formación de poro tanto del oligómero como de los monómeros se encuentran incluidos en la tabla 2. Debemos notar que después de la separación en la cromatografía, se obtuvo una concentración baja del oligómero por lo que el experimento se realizó con una concentración final de 6 nM de esta muestra. Sin embargo, esta concentración fue suficiente para registrar actividad, mientras que los monómeros purificados, no muestran este efecto aún cuando se utilizaron 30 nM de concentración final de cada uno.

La pérdida del α1 del Dominio I promueve la oligomerización de la toxina Cry1Ab

El análisis de las secuencias del amino terminal de la fracción correspondiente al oligómero y la de los monómeros por separado, nos reveló que estos últimos en ambas preparaciones, son iguales; sin embargo, el oligómero presenta una diferencia en la secuencia con los monómeros la cual consiste en la pérdida del α1 del Dominio I en la toxina.
Este procesamiento podría estar favoreciendo interacciones toxina-toxina que la llevarán a oligomerizar y finalmente insertarse en la membrana.

Amino terminal de los monómeros: ^{29}IETGYTP
Amino terminal del oligómero: ^{51}VPGAG

Unión del oligómero al colorante ANS

El 8-anilino-1-naftalenosulfonato (ANS) es un colorante fluorescente capaz de unirse a regiones hidrofóbicas expuestas, las cuales no son comunes en proteínas que se encuentran en solución. Al analizar la unión de este colorante con las preparaciones obtenidas en presencia del scFv73 o sin él (Figura 33) notamos que la fluorescencia del colorante aumenta únicamente al hacer la adición de toxina que se obtuvo en presencia del scFv73, la cual presenta la formación del oligómero y no se observa ningún efecto con la toxina activada con

jugo gástrico. Estos datos sugieren que la toxina al interactuar con su receptor y oligomerizar sufre un cambio conformaconal que la hace competente para la inserción.

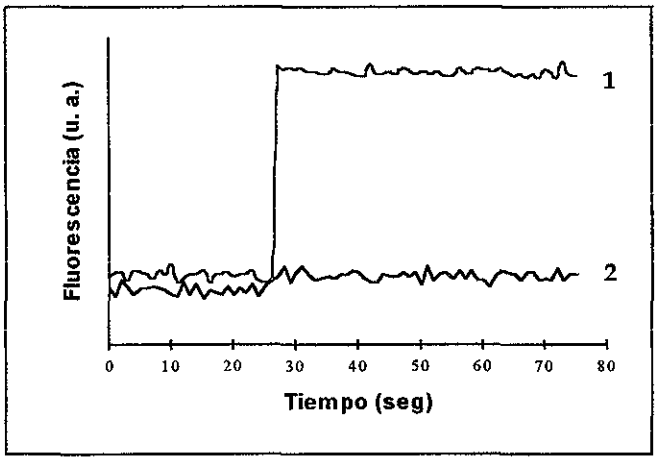

1. Cry1Ab activada en presencia del scFv73.
2. Cry1Ab activada en ausencia del scFv73

Figura 33. Unión de la toxina Cry1Ab activada en presencia o ausencia del anticuerpo scFv73 al colorante ANS.

DISCUSION

Las proteínas insecticidas de *Bacillus thuringiensis* ejercen su efecto tóxico cuando las larvas de insectos susceptibles ingieren los cristales que las contienen. El proceso mediante el cual estas proteínas logran intoxicar a los insectos susceptibles involucra diferentes pasos: la solubilización, la activación proteolítica, la unión al receptor, la inserción en la membrana, la oligomerización y la formación del poro. Se sabe que la toxicidad esta relacionada, en la mayoría de los estudios reportados, con la capacidad de unión de estas toxinas con receptores específicos localizados en el intestino de estos insectos.

A la fecha se han reportado 2 proteínas identificadas en diferentes insectos del orden lepidótera, que son capaces de unir a las toxinas Cry1A, la aminopeptidasa-N de 120 kDa (APN) que se encuentra anclada a la membrana por GPI y la caderina de 210 kDa (Bt-R_1). Más recientemente se identificó una tercera proteína de 270 kDa con un alto grado de glicosilación. Sin embargo, aún no se ha descrito el papel que los receptores tienen dentro del modo de acción de las proteínas Cry ni tampoco si todos se requieren para que las toxinas Cry tengan efecto tóxico sobre los insectos blanco (Jenkins and Dean, 2000).

Se sabe que la caderina tiene una participación importante, ya que en una población de insectos de *H. virescens,* la resistencia a la toxina Cry1Ac se debe a una mutación que interrumpe el gene de la caderina, mientras que la APN no se encuentra afectada (Gahan et al, 2001). El conocer cuales son las proteínas con las que interaccionan las toxinas Cry para que estas ejerzan su efecto tóxico, permitirá diseñar toxinas mejoradas y tener un manejo más adecuado de la resistencia en diferentes poblaciones de insectos.

En el presente trabajo, utilizando anticuerpos scFv aislados mediante "Phage Display", se logró identificar una región de 8 residuos localizada en la caderina de *M. sexta* que esta involucrada en la interacción con las toxinas Cry1Aa y Cry1Ab. Esta región es importante para que la toxina Cry1Ab tenga su efecto tóxico, pues si se alimentan las larvas con la toxina preincubada con péptidos correspondientes con esta región, la toxicidad disminuye. La participación de esta región en la interacción con las toxinas Cry1Aa y Cr1Ab quedó confirmada al utilizar un péptido sintético correspondiente con la secuencia identificada en Bt-R_1 (^{869}HITDNNK^{876}) que fue capaz de inhibir la interacción de las toxinas Cry1Aa y

Cry1Ab con las caderinas de *M. sexta* y *B. mori*. Es importante notar que las competencias en ensayos de unión de ligando con los péptidos sintéticos fueron mejores con *M. sexta* que con *B.* , cual indica que las condiciones desnaturalizantes utilizadas pueden estar afectando los sitios de reconocimiento entre estas proteínas, lo cual esta de acuerdo con lo reportado previamente para *B. mori* (Nagamatsu et al., 1999). Esto nos sugiere que en la interacción entre esta región del Bt-R_1 con la toxina Cry1Ab no esta comprometida la estructura y que la secuencia es suficiente. Gracias a esta característica, los péptidos lineales utilizados durante nuestro desarrollo experimental fueron herramientas útiles.

Con la secuencia del CDR3 del anticuerpo scFv73 logramos identificar en la caderina de *M. sexta* una región capaz de interactuar con la toxina Cry1Ab y Cry1Aa, esta región también esta presente en la secuencia de la caderina de *B. mori*, pero además en esta caderina identificamos una segunda región que no localizamos en la caderina de *M. sexta*. Estos insectos lepidópteros presentan diferente sensibilidad a las toxinas Cry1Aa y Cry1Ab, *B. mori* es más sensible al efecto de la toxina Cry1Aa que a Cry1Ab y en *M. sexta* no hay mucha diferencia en la sensiblidad. Dichas diferencias pueden deberse a que los sitios de unión para las toxinas son diferentes o también que algún sitio que es requerido para una toxina y no lo sea para otras. Esto nos habla de lo complejo que puede resultar la interacción de estas toxinas con sus receptores, por lo que la identificación de los sitios de reconocimiento entre estas moléculas adquiere gran importancia.

Diversos reportes han indicado el papel del dominio II de las toxinas Cry en el reconocimiento de los receptores en insectos sensibles y resistentes, a través de estudios de mutagénesis sitio dirigida en las asas que conectan las láminas β2-β3; β6-β7 y β10-β11. Además estas asas presentan gran variabiliad en secuencia entre las diferentes toxinas Cry por lo que han sido propuestas como las responsables de la especificidad de estas toxinas. Diferentes mutaciones ubicadas a lo largo de estas regiones dan como resultados proteínas afectadas en sus propiedades de unión a los receptores y en diferentes grados en su toxicidad dependiendo del insecto blanco, lo cual indica que diferentes regiones en diferentes toxinas podrían reconocer la misma o diferentes partes del o de los receptores (Dean et al., 1996).

En la segunda parte de trabajo, logramos identificar que la región ^{869}HITDNNK^{876} en la caderina de *M. sexta* interacciona con el asa2 de la toxina Cry1Ab. Esto también fue comprobado mediante el uso de péptidos sintéticos que corresponden con las secuencias de las asas del dominio II de esta toxina. Notamos que para el caso de Cry1Aa, en ensayos de unión de ligando, además del asa2 y el asa3 también era capaz de inhibir la interacción con el Bt-R_1, lo cual nos sugiere un segundo sitio en la caderina reconocido por esta secuencia. Es importante señalar que el asa3 de Cry1Aa es completamente diferente del asa3 de Cry1Ab. Por lo tanto, aún quedan regiones en el receptor por ser analizadas, lo mismo sucede para la toxina, pues no debemos olvidar que existen otras regiones expuestas localizadas en los dominios II y III que pueden estar involucradas en el reconocimiento en los diferentes pasos que conforman el mecanismo de acción de estas toxinas.

Otra herramienta que resultó valiosa para la identificación de regiones que están interactuando entre la toxina y el receptor, fué el análisis de los perfiles de hidropatía de las secuencias de aminoácidos que se proponían como candidatas, con base en los resultados experimentales. La teoría del reconocimiento molecular descrita por Blalock, habla de que dos proteínas pueden interactuar si sus perfiles de hidropatía son complementarios. Valiéndonos de este concepto, se pueden idenficar secuencias sin limitarnos a la identidad en las mismas; además abre la posibilidad de ingenierar proteínas mediante mutagénesis que nos permitan hacer más completarios los perfiles de hidropatía, lo cual se vería reflejado en toxinas con afinidad mejorada y por lo tanto con mayor efecto tóxico. Esta es otra posiblidad para contender con los insectos resistentes, pues podrían ser tratados con mezclas de toxinas que unan a diferentes receptores con mayor afinidad que las toxinas silvestres.

Después de realizar el análisis de los perfiles de hidropatía entre las asas de las toxinas Cry1Aa y Cry1Ab contra la región del Bt-R1, notamos que son complementarios, sugiriendo que estas regiones pueden interactuar siguiendo lo propuesto por la TRM propuesta por Blalock y colaboradores. También notamos que la región que identificamos se extendió 4 residuos más y que la región en las toxinas abarcó también residuos comprendidos en la lámina β6. Esto también sugiere que los sitios de reconocimiento en la toxina no están limitados a las secuencias de las asas, si no que también hay participación de otras regiones de las toxinas Cry1A.

En nuestros experimentos, el uso de péptidos sintéticos, correspondientes con la secuencia del asa2 de la toxina Cry1Ab, que contienen mutaciones ya reportadas que afectan unión y toxicidad a *M. sexta* (F371A y RR368-369EE), no son capaces de competir la unión entre el anticuerpo scFv73 y la toxina Cry1Ab, lo cual correlaciona con los datos reportados y muestra que estos residuos estan involucrados en el reconocimiento de la toxina con el receptor Bt-R1 (caderina) de *M. sexta*.

Después de unirse a sus receptores se piensa que la toxina sufre cambios conformacionales que la convierten en una estructura competente para insertarse en la membrana, pero aún existen varias preguntas sobre este tópico: ¿la toxina primero interactúa con sus receptores y entoces se inserta en la membra, lo cual le permite oligomerizar? ó ¿La toxina al unirse al receptor se oligomeriza, formando una estructura competente para la inserción? ó tal vez el receptor solo ayuda a concentrar localmente a la toxina lo cual favorece la inserción de algunas moléculas y posiblemente su oligomerización.

Algunos reportes previos aceptan que las toxinas Cry para insertarse en la membrana deben agregarse, un trabajo de nuestro grupo aportó evidencias sobre este aspecto. Haciendo uso de dos toxinas afectadas en diferentes pasos en el modo de acción (una no es capaz de unirse al receptor y la segunda no puede formar poro, pero si puede unirse a su receptor), mediante experimentos de unión y de formación de poro *in vitro* se demostró que cuando se mezclan las dos toxinas mutantes la activiad tóxica se recupera, lo cual sugiere interacciones toxina-toxina (Soberón et al., 1999).

Sin embargo se ha visto que en solución, el fenómeno de oligomerización no se presenta (Guereca and Bravo, 1999). Po esta razón, se propone que para que las toxinas se agreguen, deben unirse a la membrana de los insectos blanco (Aronson et al., 1999; Aronson, 2000), aunque no queda clara la participación de los receptores en el fenómeno de oligomerización ni sobre cuantas moléculas deben agregarse para lograr una inserción efectiva. Tampoco esta claro si la agregación ocurre antes o después de la unión a los receptores.

En nuestro trabajo, al estudiar el papel de la interacción entre la toxina Cry1Ab y la región del Bt-R_1 identificada, demostramos que la interacción entre el receptor Bt-R_1 y la toxina Cry1Ab juega un papel en la toxicidad de esta proteína. Para esto, utilizamos al anticuerpo scFv73 como "receptor modelo" y obtuvimos diferentes preparaciones de toxina

incubándola con o sin este anticuerpo. El análisis de las muestras con "Western blot", formación de poro *in vitro* y el análisis de secuencia del amino terminal nos indicaron que para que la toxina pueda insertarse en la membrana y formar poros, primero debe interactuar con su receptor, lo cual permitirá la pérdida de la hélice α1 en el dominio I, lo cual favorece interacciones toxina-toxina que finalmente darán origen a un oligomero compuesto por 4 subunidades capaz de insertarse en la membrana. Hay evidencias de otros grupos que indica que la toxina debe oligomerizar para formar el poro y un reporte indica que este poro podría estar formado por 4 subunidades, tal y como lo estamos viendo nosotros (Vié et al., 2001). Nuestros datos muestran que el proceso de oligomerización ocurre después de que la toxina se une al receptor Bt-R_1 y antes de insertarse en la membrana. Posiblemente la interacción con el receptor provoca un cambio conformacional en la toxina que deja expuesta la hélice α1 para ser digerida, lo cual no se da en ausencia del receptor, por lo tanto en solución sin el receptor este fenómeno no es posible. Otra observación fue que el procesamiento proteolítico se dio más eficientemente con el jugo gástrico del insecto susceptible que con la tripsina, lo que habla de una proteasa aún no identificada que realiza este procesamiento.

Otros reportes también hablan del papel de las proteasas en el modo de acción, varios trabajos han dejado ver que cada insecto contiene proteasas que actúan sobre las proteínas Cry con efectos de activación o degradación y también se ha descrito su papel en el desarrollo de resistencia, pues insectos resistentes degradan la toxina más rápidamente impidiendo su efecto tóxico (Lightwood et al., 2000; Miranda et al., 2001).

A pesar de que nuestros datos apoyan el papel del receptor Bt-R_1, en la oligomerización de la toxina, no descartamos que la aminopeptidasa-N pueda tener un papel importante en la toxicidad de estas proteínas o bien, la presencia de otras moléculas que puedan tener esta función de "receptor" en los insectos susceptibles. Es claro, que aún cuando logramos obtener preparaciones de toxina con capacidad de formar poro *in vitro*, nuestras concentraciones de toxina oligomerizada son bajas y nuestros experimentos de "Western blot" nos indican que mucha toxina permanece como monómero, posiblemente debido a que

se requieren de otros sitios de contacto con la membrana que en nuestros experimentos *in vitro* no tenemos representados.

El identificar otras regiones en el receptor mediante el uso de la técnica de "Phage Display", es una alternativa con gran potencial que nos permitirá entender más sobre el modo de acción de la toxinas Cry y podría aportar evidencias sobre la presencia de otros receptores. También nos ayudará a identificar que regiones en la toxina son las que participan en dichas interacciones. Resulta interesante que nuestro anticuerpo scFv73, que nos sirvió como receptor modelo durante este trabajo, proviene de una biblioteca de anticuerpos no-inmune, lo que hace pensar que una biblioteca inmune podria resultar una fuente de anticuerpos que permitan explorar exhaustivamente diferentes regiones de la toxina que parecen blanco de interacción con los receptores, como en este caso lo es el asa 3 de las toxinas Cry1A's.

El papel que tienen otros receptores como la APN no deja llamar la atención. Recientemente se ha descrito la presencia de microdominios ordenados en la membrana de los lepidópteros *M. sexta* y *H. virescens*, en los cuales se pueden encontrar proteínas asociadas a la membrana por GPI, como es el caso del receptor APN de las toxinas Cry. Experimentos donde se utilizaron membranas enriquecidas en estos dominios designados, como "rafts", mostraron actividad de poro cuando se agregaron las toxinas Cry1Ab o Cry1Ac. El tratamiento de estas membranas con ciclodextrina, un agente que secuestra colesterol, afectó drásticamente la actividad de formación de poro sugiriendo, de forma importante, el papel que pueden tener estos dominios de la membrana dentro del mecanismo de acción de estas toxinas.

Actualmente en el grupo se estan abordando preguntas sobre este respecto que nos permiten sugerir que la APN tiene un papel tan importante como la caderina dentro del mecanismo de acción de las toxinas Cry. Esto lo esquematizamos en el diagrama de las conclusiones de este trabajo (D).

CONCLUSIONES

Se caracterizó un anticuerpo scFv cuyo CDR3 presenta homología con una región de 8 aminoácidos presente en las caderinas de insectos sensibles a las toxinas Cry1A. (A)

Se identificó a la asa2 de la toxina Cry1Ab como el sitio que reconoce a la secuencia de 8 aminoacidos localizada en la caderina (Bt-R_1) de *Manduca sexta.* (B)

La oligomerización involucra la unión al receptor lo que provoca la pérdida de la hélice $\alpha 1$ del dominio I de la toxina, esto favorece las interacciones toxina-toxina y la agregación de 4 subunidades. (C)

Para insertarse en la membrana, la toxina Cry1Ab debe oligomerizar. (D)

La secuencia identificada en las caderinas es importante para la interacción con las toxinas Cry1A, pues si se alimentan larvas con la toxina incubada con los péptidos correspondientes a esta región, la toxicidad se ve disminuida.

Para la toxina Cry1Aa, además del asa2 esta participando el asa3 en el reconocimiento de la caderina de *M. sexta.*

El asa $\alpha 8$ de la toxina Cry1Ab también interacciona con el Bt-R_1 a través de un segundo sitio localizado en el repetido 11 de este receptor.

Estas conclusiones se encuentran incluidas en el siguiente diagrama sobre el modo de acción de las toxinas Cry. Los números indican los pasos generales ya descritos, que incluyen:

1. Solubilización del cristal.
2. Activación proteolítica.
3. Unión al receptor.
4. Formación del poro.

Dentro de estos, con este trabajo incluimos que la activación proteolítica involucra dos pasos: la pérdida de aproximadamente el 50% de la protoxina y después la pérdida de la hélice α1 del dominio I, esta activación proteolítica depende de la interacción de la toxina con el receptor Bt-R_1 (3A). Se favorecen entonces interacciones toxina-toxina que darán lugar a la formación de un oligómero funcional capaz de insertarse en la membrana (3B).

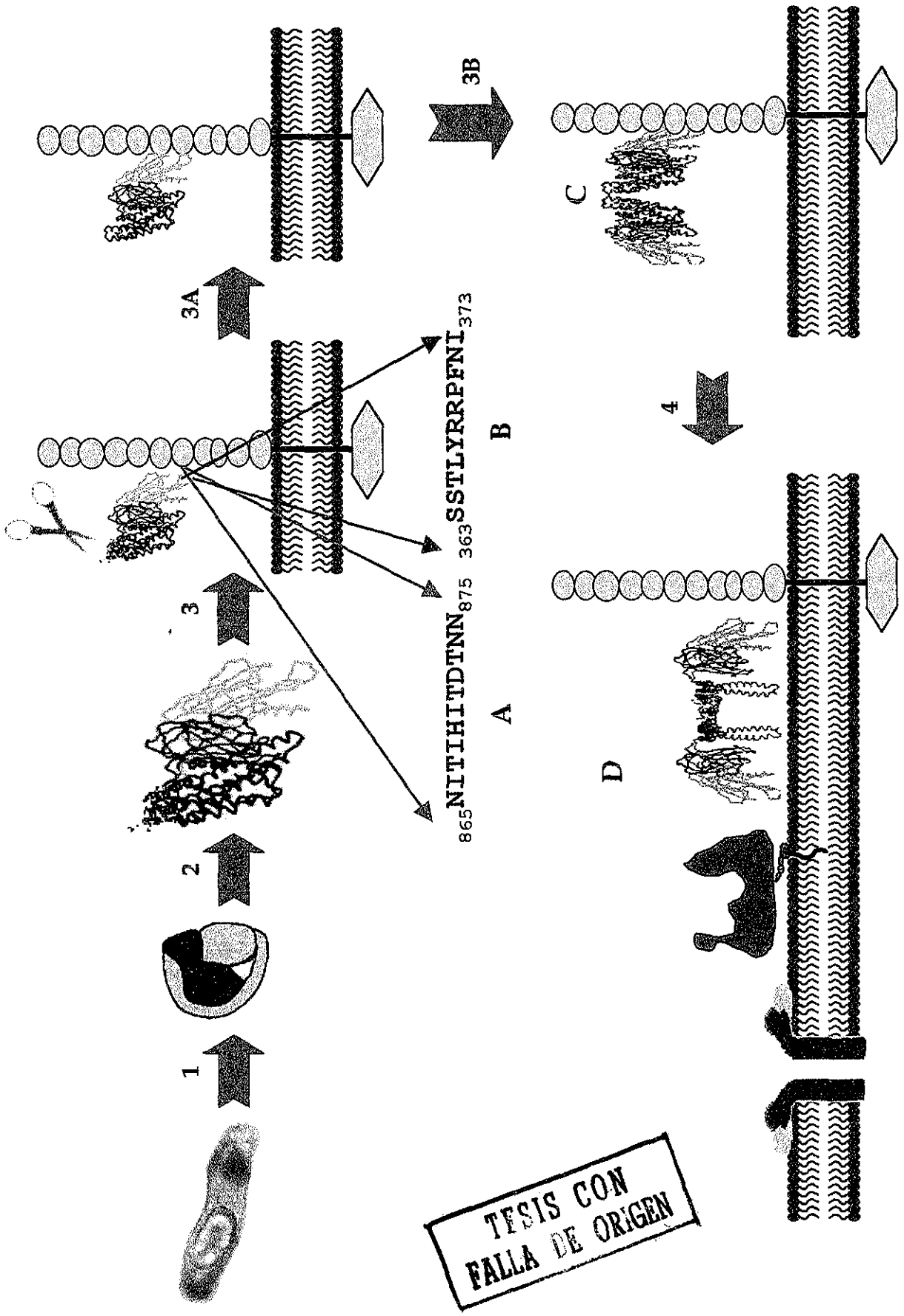

PERSPECTIVAS

CONSTRUCCION DE BIBLIOTECAS INMUNES DE ANTICUERPOS scFv DE LAS TOXINAS Cry1Ab Y Cry11A

Aún existen otras regiones en la toxina que pueden estar interactuando con los receptores presentes en los insectos sensibles (por ejemplo el asa3) y que pueden ser importantes para la actividad de estas toxinas, estas regiones no se lograron identificar con los anticuerpos que hemos aislado, los cuales provienen de una biblioteca de anticuerpos de humano no inmunizado. Con la intención de aislar nuevos scFv's que nos permitan identificar y estudiar el papel de otras regiones, nos propusimos la construcción de bibliotecas inmunes de anticuerpos scFv para las toxinas Cry1Ab y Cry11A.

La toxina Cry11A resulta de gran interés porque aún no se ha descrito la naturaleza del receptor. Además se trata de una toxina específica para mosquitos, los cuales son vectores de enfermedades, por lo que estudiar la interacción con sus receptores y entender más sobre la especificidad toma importancia desde el punto de vista biológico y de la salud. Continuaremos también con el análisis de la toxina Cry1Ab, que ha sido nuestro modelo, tratando de ampliar nuestros conocimientos sobre el modo de acción de estas toxinas.

Para la construcción de destas bibliotecas inmunes de anticuerpos scFv primero inmunizamos dos conejos con las toxinas Cry1Ab o Cry11A, la presencia de los anticuerpos deseados se confirmó utilizando "Western blot" y ELISA's, los cuales nos indicaron títulos constantes para ambas toxinas después de 4 aplicaciones de cada una de ellas.

A continuación realizamos una extracción de RNA total de la médula ósea y del bazo como se detalla en materiales y métodos, al finalizar el procedimiento se checaron las muestras en un gel de agarosa con tiocianato de guanidina (Figura 34). El procedimiento general que utilizamos para la construcción de las bibliotecas se resume en la figura 35 y geles de agarosa representativos de cada rección de PCR se muestran en la figura 36.

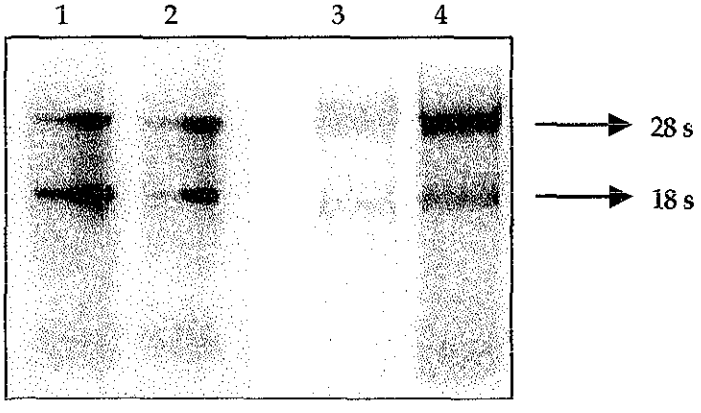

Figura 34. RNA total del bazo y médula ósea de los conejos inmunizados con las toxinas Cry1Ab (1 y 2) y Cry11A (3y 4)

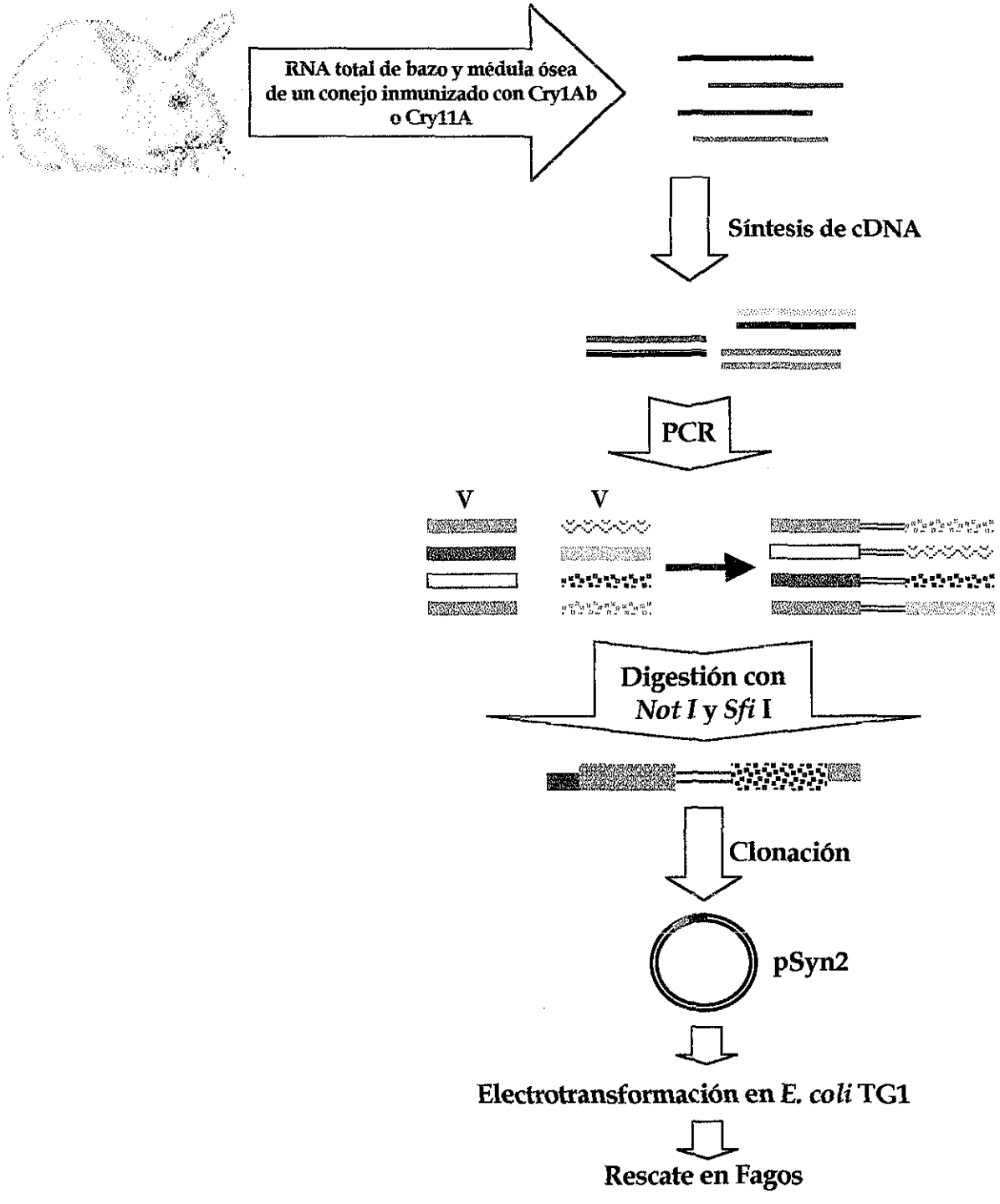

Figura 35. Esquema general utilizado para la construcción de las bibliotecas inmunes de anticuerpos scFv de las toxinas Cry1Ab y Cry11A.

PCR1 Amplificación de las V_H's y V_k's

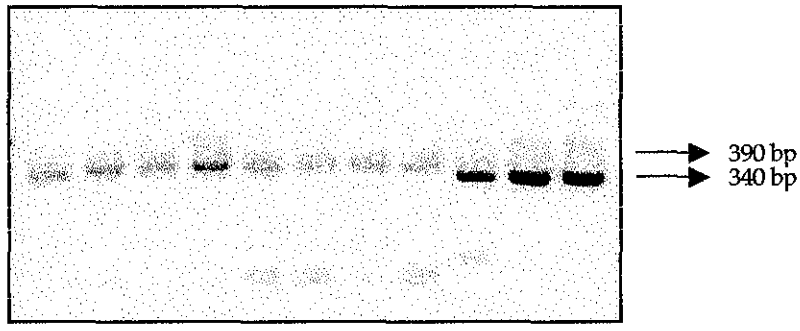

PCR2 Introducción de un conector en las V_H's y V_k's

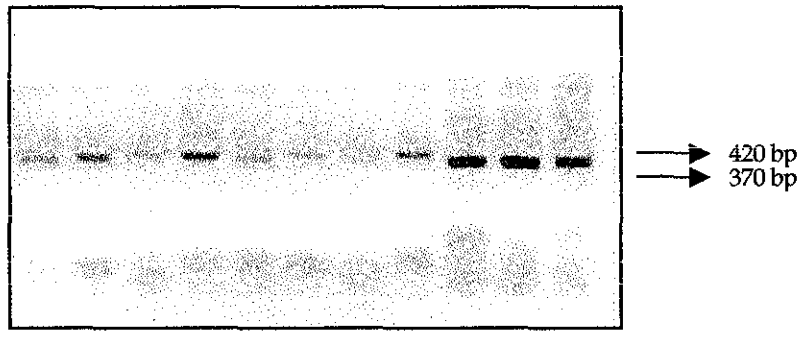

PCR3 Ensamble de las V_H's y V_k's e introducción de los sitios de restricción

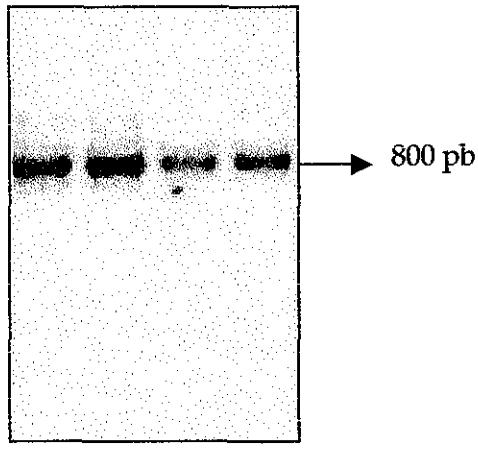

Figura 36. Productos característicos obtenidos en las reacciones de PCR para obtener los repertorios de scFv´s.

Después de haber obtenido los productos de la reacción del PCR3, se realizó la doble digestión Sfi-Not de los mismos y se clonaron los productos en el vector pSyn2 para finalmente transformar en la cepa TG1 de *E. coli*.

Hasta el momento hemos logrado obtener las dos bibliotecas correspondientes de la toxina Cry1Ab, mientras que las correspondientes a Cry11A estan por ser transformadas. Para el caso de Cry1Ab obtuvimos un título de aproximadamente 10^6 variantes, con las cuales continuaremos el análisis para explorar otras regiones de la toxina que puedan estar involucradas en interacción con los receptores y la toxicidad.

BIBLIOGRAFIA

Allured, V. S., Collier, R. J., Carrol, S. F. and McKay, D. B. 1986. Structure of exotoxin A of *Pseudomonas aeruginosa* at 3.0-Angstrom resolution. Proc. Natl. Acad. Sci. USA 83:1320-1324.

Amersdorfer, P., Wong, C., Chen, S., Smith, T., Deshpande, S., Sheridan, R., Finnern, R. and Marks, J. 1997. Molecular characterization of murine humoral immune response to botulinum neurotoxin type A binding domain as assessed by using phage antibody libraries. Infection and Immunity. 65:3743-3752.

Angst, B. D., Marcozzi, C. and Magee, A. I. 2001. The cadherin super-family. J. Cell. Sci. 114:625-626.

Aronson, A. I., Wu, D. and Zhang, C. 1995. Mutagenesis of specific and toxicity regions o f a *Bacillus thuringiensis* protoxin gene. J. Bacteriol. 177:4059-4065.

Aronson, A. I. 2000. Incorporation of protease K into larval insect membrane vesicles does not result in disruption of integrity or function of the pore-forming *Bacillus thuringiensis* δ-endotoxin. Appl. Environ. Microbiol. 66:4568-4570.

Aronson, A. I., Geng. C. and Wu L. 1999. Aggregation of *Bacillus thuringiensis* Cry1A toxins upon binding to target insect larval midgut vesicles. Appl. Environ. Microbiol. 65:2503-2507.

Aronson, A. I. and Shai, Y. 2001. Why *Bacillus thuringiensis* insecticidal toxins are so effective: unique features of their mode of action. FEMS Microbiol. Lett. 195:1-8.

Bishop, D. H. L. 1994. Biopesticides. Curr. Opin. Biotech. 5:307-311.

Blalock, J. E. 1990. Complementary of peptides specified by "sense" and "antisense" strands of DNA. Trends Bitech. 8:140-144.

Blalock, J. E. 1995. Genetic origins of protein shape and interaction rules. Nature Med. 1:876-879.

Blalock, J. E. 1999. On the evolution of ligands: did peptides functionally precede metals and small organic molecules? Cell Mol. Life Sci. 55:513-518.

Boquet, D., Dery, O., Frobert, Y., Grassi, J. and Counrad, J. Y. 1995. Is hydropathic compleentary involved in antigen-antibody binding? Mol. Immunol. 32:303-308.

Bravo, A. 1997. Phylogenetic relationships of *Bacillus thuringiensis* δ-endotoxin family proteins and their functional domains. J. Bac. 179: 2793-2801.

Bravo, A., Jansens, S. and Peferoen, M. 1992. Immunocytochemical localization of *Bacillus thuringiensis* insecticidal crystal proteins in intoxicated insects. J. Invert. Pathol. 60:237-246.

Bravo, A., Hendrickx, K., Jansens, S. and Peferoen, M. 1992. Immunocytochemical analysis of specific binding of *Bacillus thuringiensis* insecticidal crystal proteins to lepidopteran and coleopteran midgut membranes. J. Invert. Pathol. 60:247-253.

Burton, S. L, Ellar, D. J., Li, J., and Derbyshire, D. J. 1999. N-acetilgalactosamine on the putative insect receptor aminopeptidase N is recognosided by a site on domain III lectin-like fold of a *Bacillus thuringiensis* insecticidal toxin. JMB 287: 1011-1022.

Chen, X. J., Curtis, A., Alcantara, E. and Dean, D. H. 1995. Mutations in Domain I of a *Bacillus thuringiensis* δ-endotoxin CryIAb reduce the irreversible binding to toxin to *Manduca sexta* brush border membrane vesicles. J. Biol. Chem. 270:6412-6419.

Choe, S., Bennett, M. J., Fujji, G., Curmi, P. M. G., Kantardjieff, K. A., Collier, R. J. and Eisenberg, D. 1992. The crystal structure of diphteria toxin. Nature. 357:216-222.

Chomczynski, P. and Sacchi, N. 1987. Single-step method of RNA isolation by acid guanidinium thiocyanate-phenol-chloroform extraction. Anal. Biochem. 162:156-159.

Coley, A. M., Campanele, N. V., Casey, J. L., Hodder, A. N., Crewther, P. E., Anders, R. F., Tilley, L. M. and Foley, M. 2001. Rapid and precise epitope mapping of monoclonal antibodies against *Plasmodium falciparum* AMA1 by combined phage display of fragments and random peptides. Protein Eng. 14:691-698.

Cortese R., Felice, F., Galfre, G., Luzzago, A., Monaci, P. and Nicosia, A. 1994. Epitope discovery using peptide libraries displayed on phage. TIBTECH. 12:262-267.

Crickmore, N., Bone, E. J., Williams, J. A. and Ellar, D. J. 1995. Contribution of the individual components of the δ-endotoxin crystal to the mosquitocidal activity of *Bacillus thuringiensis* subsp. *israelensis*. FEMS Microbiol. Lett. 131:249-254.

Crickmore, N., Zeigler, D.R., Feitelson, J., Schnepf, E., Van Rie, J., Lereclus, D., Baum, J., and Dean, D.H. 1998. Revision of the nomenclature for the *Bacillus thuringiensis* pesticidal crystal proteins. Microbiol. Mol. Biol. Rev. 62:807-13.

de Maagd, R.A., Bakker, P. L., Masson, L., Adang, M. J., Sangadala, S., Stiekema, W. and Bosh, D. 1999. Domain III of *Bacillus thuringiensis* delta-endotoxin Cry1Ac is involved in binding to *Manduca sexta* brush border membranes and its purified aminopeptidase N. Mol. Microbiol. 31:463-471.

de Maagd, R.A., Bravo, A. and Crickmore, N. 2001. How *Bacillus thuringiensis* has evolved specific toxins to colonize the insect world. Trends Genet. 17: 193-9.

de Maagd, R.A., Kwa, M. S. G., van der Klei, H., Yamamoto, T., Scipper, B., Vlak, J. m:, Stiekema, W. J. and Bosch, D. 1996. Domain III substitution in *Bacillus thuringiensis* CryIA(b) results in superior

toxicity for *Spodoptera exigua* and altered membrane protein recognition. Appl. Environ. Microbiol. 62:1537-1543.

Daniels D. A. and Lane, D. P. 1996. Phage peptide libraries. Methods. 9:494-507.

Dean, D. H., Rajamohan, F., Lee, M. K., Wu, S. J., Chen, . J, Alcantara, E. and Hussain, S. R. 1996. Probing the mechanism of action of *Bacillus thuringiensis* insecticidal proteins by site-directed mutagenesis-a minireview. Gene 179:111-117.

Denolf, P. 1999. Molecular characterization of *Bacillus thuringiensis* δ-endotoxin receptor in the insect midgut. Recent Res. Devel. Microbiol. 3:235-267.

Denolf, P., Hendrickx, K., Vandamme, J., Jansens, S., Peferoen, M., Degheele, D. and van Rie, J. 1997. Cloning and characterization of *Manduca sexta* and *Plutella xylostella* midgut Aminopeptidase N enzymes related to *Bacillus thuringiensis* binding proteins. Eur. J. Biochem. 248:748-761.

Dorsch, J. A., Candas, M., Griko, N. B., Maaty, W. S. A., Midboe, E. G., Vadlamudi, R. K. and Bulla Jr., L. A. 2002. Cry1A toxins of *Bacillus thuringiensis* bind specifically to a region adjacent to the membrane-proximal extracellular domain of Bt-R_1 in *Manduca sexta*: involvement of a cadherin in the entomopathogenicity of *Bacillus thuringiensis*. Insect Biochem. Mol. Biol. 32:1025-1036.

Dow, J. A. T. 1986. Insect midgut function. Adv. Insect. Physiol. 19:187-238.

Ferré, J., Real, M. D., Van Rie, J., Jansens, S. And Peferoen, M. 1991. Resistance to the *Bacillus thuringiensis* bioinsecticide in a field population of *Plutella xylostella* is due to a change in a midgut membrane receptor. Proc. Natl. Acad. Sci. USA 88:5119-5123.

Flores, H., Soberón, X., Sánchez, J. and Bravo, A. 1997. Isolated domain II and III from the *Bacillus thuringiensis* Cry1Ab δ-endotoxin binds to lepidopteran midgut membranes. FEBS Lett. 414:313-318.

Francis, B. R. and Bulla Jr., L. A. 1997. Further characterization of Bt-R_1, the cadherin-like receptor for Cry1Ab toxin in Tobacco hornworm (*Manduca sexta*) midguts. Insect Biochem. Molec. Biol. 27:541-550.

Garczynski, S. F., Crim, J. W. and Adang M. J. 1991. Identification of putative insect brush border membrane-binding molecules specific to *Bacillus thuringiensis* δ-endotoxin by protein blot analysis. Appl. Environ. Microbiol. 57:2816-2820.

Gazit, E., La Rocca, P., Sansom, M. S. P. and Shai, Y. 1998. The structure and organization within the membrane of the helices composing the pore-forming domain of *Bacillus thuringiensis* δ-endotoxin are consistent with an "umbrella-like" structure of the pore. Proc. Natl. Acad. Sci. USA 95:12289-12294.

Gazit, E., and Shai, Y. 1995. The assembly and organization of the α5 and α7 helices from the pore-forming domain of *Bacillus thuringiensis* δ-endotoxin. J. Biol. Chem. 270:2571-2578.

Ge, A. Z., Rivers, D., Milne, R. and Dean, D. H. 1991. Functional domain of *Bacillus thuringiensis* inscticidal crystal proteins: refinement of *Heliothis virescens* and *Trichoplusia ni* specificity domains on CryIA(c). J. Biol. Chem. 266:17954-17958.

Ge, A. Z., Shivarova, N. I. and Dean, D. H. 1989. Location of the Bombix mori specificity domain on a *Bacillus thuringiensis* δ-endotoxin protein. Proc. Natl. Acad. Sci. USA 86:4037-4041.

Grochulski, P., Masson, L., Borisova, S., Pusztai-Carey, M., Schwartz, J-L., Brousseau, R., and Cygler, M. 1995. *Bacillus thuringiensis* Cry1A(a) insecticidal toxin:crystal structure and channel formation. J. Mol. Biol. 254:447-464.

Güereca, L. and Bravo, A. 1999. The oligomeric state of *Bacillus thuringiensis* Cry toxins in solution. Biochimia et Biophysica Acta.1429: 342-350.

Gahan, L. J., Gould, F. and Heckel, D. G. 2001. Identification of a gene associated with Bt resistance in *Heliothis virescens*. Science. 293:857-860.

Haider, M. Z. and Ellar, D. J. 1987. Analysis of the molecular basis of insecticidal specificity of *Bacillus thuringiensis* crystal δ-endotoxin. Biochem. J. 248:197-201.

Hawlisch, H., zu Vilsendorf, A. M., Bautsch, W., Klos, A. and Köhl, J. 2000. Guinea pig C3 specific rabbit single chain Fv antibodies from bone marrow, spleen and blood derived phage libraries. J. Immunol. Meth. 236:117-131.

Hodgman, T. C. and Ellar, D. J. 1990. Models for the structure and function of the *Bacillus thuringiensis* δ-endotoxins determined by compilational analysis. DNA Seq. 1:97-106.

Hofmann, C., Lüthy, P., Hütter, R. and Pliska, V. 1988. Binding of the delta-endotoxin from *Bacillus thuringiensis* to brush-border membrane vesicles of the cabbage butterfly (*Pieris brassicae*). Eur. J. Biochem. 173:85-91.

Hofmann, C., Vanderbruggen, H., Höfte, H., van Rie, J., Jansens, S. and Van Mellaert. 1988. Specificity of *Bacillus thuringiensis* delta-endotoxins is correlated with the presence of high-affinity binding sites in the brush border membrane of the target insect midguts. Proc. Natl. Acad. Sci. USA. 85:7844-7848.

Höfte, H., and Whiteley, R. 1989. Insecticidal crystal proteins of *Bacillus thuringiensis*. Microbiol. Rev. 53: 242-255.

Hoogenboom, H. R. 2002. Overview of antibody phage-display technology and its applications. Methods Mol. Biol. 178:1-37.

Hoogenboom, H. R. and Chames, P. 2000. Natural binding designer sites made by phage display technology. Immunol. Today. August.

Hussian, S.-R. A., Aronson, A. I. and Dean, D. H. 1996. Substitution of residues on the proximal side of Cry1A *Bacillus thuringiensis* δ-endotoxins affects irreversible binding to *Manduca sexta* midgut membrane. Biochem. Biophys. Res. Commun. 226:8-14.

Ihara, H., Kuroda, E., Wadano, A. and Himeno, M. 1993. Specificity toxicity of δ-endotoxin from *Bacillus thuringiensis* to *Bombix mori*. Biosci. Biotechnol. Biochem. 57:200-204.

Jenkins, L. L. and Dean, D. H. 2000. Exploring the mechanism of action of insecticidal proteins by genetic engineering methods. In Genetic Engineering: Priciples and Methods. Setlow, J. K. (ed) New York: Plenum Press, pp 33-54.

Jenkins, J.L., Lee M.K., Valaitis, A.P., Curtiss, A., and Dean D.2000. Bivalente sequential binding model of a *Bacillus thuringiensis* toxin to gypsy moth aminopeptidase N receptor. J.Biol. Chem. 275:14423-14431.

Keeton, T. P. and Bulla Jr., L. A. 1997. Ligand specificity and affinity of Bt-R_1, the *Bacillus thuringiensis* Cry1A toxin receptor from *Manduca sexta*, expressed in mammalian and insect cell cultures. App. Envirion. Microbiol. 63:3419-3425.

Knigth, P. J., Crickmore, N. and Ellar, D. 1994. The receptor for *Bacillus thuringiensis* Cry1A(c) delta-endotoxin in the brush border membrane of the lepidopteran *Manduca sexta* is aminopeptidase N. Mol. Microbiol. 11:429-436.

Knigth, P. J., Knowles, B. and Ellar, D. 1995. Molecular cloning of an insect aminopeptidase N that serves as a receptor for *Bacillus thuringiensis* Cry1A(c) toxin. J. Biol. Chem. 270:17765-17770.

Knowles, B. H. 1994. Mechanism of action of *Bacillus thuringiensis* insecticidal δ-endotoxins. Adv. Insect Physiol. 24:275-308.

Knowles, B. H., Blatt, M. R., Tester, M., Horsnell, J. M., Carroll, J., Menestrina, G. and Ellar, D. J. 1989. A cytolytic δ-endotoxin from *Bacillus thuringiensis* var. *israelensis* forms cation-selective channels in planar lipid bilayers. FEBS Lett. 244:259-262.

Knowles, B. H. and Ellar, D. J. 1987. Colloid-osmotic lysis is a general feature of the mechaninsm of action of *Bacillus thuringiensis* δ-endotoxins with different insect specificity. Biochim. Biophys. Acta. 924:509-518.

Knowles, B. H., Thomas, W. E. and Ellar, D. J. 1984. Lectin-like binding of *Bacillus thuringiensis* var. *kustaki* lepidopteran-specific toxin in an initial step in insecticidal action. FEBS Lett. 168:197-202.

Lee, M. K., Jenkins, J. L., You, T. H., Curtiss, A., Son, J. J., Adang, M. J. and Dean, D. H. 2001. Mutations at the arginine residues in α8 loop of *Bacillus thuringiensis* δ-endotoxin Cry1Ac affect toxicity and binding to *Manduca sexta* and *Lymantria dispar* aminopeptidase N. FEBS Lett. 497:108-112.

Lee, M. K., Milne, R. E., Ge, A. Z. and Dean, D. H. 1992. Location of a *Bombix mori* receptor binding region a *Bacillus thuringiensis* d-endotoxin. J. Biol. Chem. 267:3115-3121.

Lee, M. K., Rajamohan, F., Gould, F. and Dean, D. H. 1995. Resistance to *Bacillus thuringiensis* CryIA δ- endotoxins in a laboratory-selected *Heliothis virescens* strain is related to receptor alteration. Appl. Environ. Microbiol. 61:3836-3842.

Lee, M. K., Rajamohan, F., Jenkins, J. L., Curtss, A. and Dean, D. H. 2000. Role of two arginine residues in domain II, loop 2 of Cry1Ab and Cry1Ac *Bacillus thuringiensis* δ- endotoxin in toxicity and binding to *Manduca sexta* and *Lymantria dispar* aminopeptidase N. Mol. Microbiol. 38(2):289-298.

Lereclus, D., Agaisse, H., Gominet, M. and Chaufaux, J. 1995. Overproductionof encapsulated insecticidal crystal proteins in a *Bacillus thuringiensis spo*OA mutant. Bio/Technol. 13:67-71.

Li, M. 2000. Applications of display technology in protein analysis. Nature Biotechnol. 18:1251-1256.

Li, J., Carrol, J. and Ellar, D.J. 1991 Crystal structure of insecticida d-endotoxin from *Bacillus thuringiensis* at 2.5 A resolution. Nature 353: 815-821

Li, J., Derbyshire, D. J., Promdonkoy, B. and Ellar, D. J. 2001. Structural implications for the transformation of the *Bacillus thuringiensis* δ-endotoxins from water-soluble to membrane-inserted forms. Biochem Soc. Trans. 29:571-577.

Liang, Y., Patel, S. S. And Dean, D. H. 1995. Irreversible binding kinetics of *Bacillus thuringiensis* CryIA δ-endotoxins to gypsy moth brush border membrane vesicles is directly correlated to toxicity. J. Biol. Chem. 270:24719-24724.

Lightwood, D. J., Ellar, D. J. and Jarrett, P. 2000. Role of proteolysis in determining potency of *Bacillus thuringiensis* Cry1Ac δ-endotoxin. Appl. Environ. Microbiol. 66:5174-5181.

Lorence, A., Darszon, A., Díaz, C., Liévano, A., Quintero, R. and Bravo A. 1995. δ-Endotoxin induce cation channels in *Spodoptera frugiperda* brush border membranes in suspensión and in lipid bilayers. FEBS Lett. 360:217-222.

Lorence, A., Darszon, A., and Bravo A. 1997. Aminopeptidase dependent pore formation of *Bacillus thuringiensis* Cry1Ac toxin on *Trichoplusis ni* membranes. FEBS Lett. 414:303-307.

Lou, K., McLachlin, J. R., Brown, M. R. and Adang, M. J. 1999. Expression of a glycosylphosphatidylinositol-linked *Manduca sexta* Aminopeptidase N in insect cells. Prot. Express. Purif. 17:113-122.

McCafferty, J., Griffiths, A. D., Winter, G. and Chiswell, D. J. 1990. Phage antibodies: filamentous phage displaying antibody variable domains. Nature. 348:552-554.

Masson, L., Lu, Y., Mazza, A., Brousseau, R. and Adang, M. J. 1995. The Cry1A(c) receptor purified from *Manduca sexta* displays multiple specificities. J. Biol. Chem. 270:20309-20315.

Meng, J., Candas, M., Keeton, T. P. and Bulla Jr., L. A. 2001. Expression on *Spodoptera frugiperda* (Sf21) insect cells of Bt-R_1, a cadherin-related receptor from *Manduca sexta* for *Bacillus thuringiensis* Cry1Ab toxin. Protein Express. Purific. 22:141-147.

Miranda, R., Zamudio, F., and Bravo, A. 2001. Processing of Cry1Ab δ-endotoxin from *Bacillus thuringiensis* by *Manduca sexta* and *Spodoptera frugiperda* midgut proteases: role in protoxin activation and toxin inactivation. Insect Biochem. Mol. Biol. 31:1155-1163.

Morse, R. J., Yamamoto, T. and Stroud, R. M. 2001. Structure of Cry2Aa suggests an unexpected receptor binding epitope. Structure. 9:409-417.

Nagamatsu, Y., Koike, T., Sasaki, K., Yoshimoto, A. and Furukawa, Y. 1999. The cadherin-like protein is essential to specificity determination and cytotoxic action of the *Bacillus thuringiensis* insecticidal Cry1Aa toxin. FEBS Lett. 460:385-390.

Nagamatsu, Y., Toda, S., Koike, T., Miyoshi, Y., Shigematsu, S. and Kogure, M. 1998. Cloning, sequencing, and expression of the *Bombix mori* receptor for *Bacillus thuringiensis* insecticidadl Cry1A(a) toxin. Biosci. Biotech. Biochem. 62:727-734.

Nakanishi, K., Yaoi, K., Nagino, Y., Hara, H., Kitami, M., Atsumi, S., Miura, N. and Sato, R. 2002. Aminopeptidase N isoforms from the midgut of *Bombix mori* and *Plutella xylostella*- their classification and the factors that determine their binding specificity to *Bacillus thuringiensis* Cry1A toxin. FEBS Lett. 519:215-220.

Nissim, A., Hoogenboom, H. R., Tomlinson, I. M., Flynn, G., Midgley, D. L. and Winter, G. 1994. Antibody fragments from a "single pot" phage display library as immnochemical reagents. EMBO J. 13:692-698.

Ojcius, D. M. and Young, J. D. E. 1991. Cytolytic pore-forming proteins and peptides-is there a common structural motif? Trends Biochem. Sci. 16:225-229.

Picard, C., Ronco, p., Mollier, P., Yao, J., Baudouin, B., Geniteau- Legendre, M. and Verroust, P. 1986. Epitope diversity of angitensin II analysed with monoclonal antibodies. Immunol. 57:19-24.

Peralta, M. 1998. Tesis de Licenciatura. Facultad de Ciencias. UNAM.

Rajamohan, F., Alcantara, E., Lee, M. K., Chen, X. J., Curtiss, A. And Dean, D. H. 1995 Single amino acid changes in Domain II of *Bacillus thuringiensis* Cry1Ab δ-endotoxin affect irreversible binding to *Manduca sexta* midgut membrane vesicles. J. Bact. 177(9):2276-2282.

Rajamohan, F., Cotrill, J. A., Gould, F. and Dean, D. H. 1996. Role of domain II, Loop 2 residues of *Bacillus thuringiensis* Cry1Ab δ-endotoxin in reversible and irreversible binding to *Manduca sexta* and *Heliothis virescens*. J. Biol. Chem. 271(5):2390-2396.

Rajamohan, F., Hussain, S. A., Cotrill, J. A., Gould, F. and Dean, D. H. 1996 Mutations at domain II, loop 3 of *Bacillus thuringiensis* Cry1Aa and Cry1Ab δ-endotoxins suggest loop 3 is involved in initial binding to lepidopteran midgets. J. Biol. Chem. 271(41)25220-25226.

Rajamohan, F., Alzate, O., Cotrill, J. A., Curtiss, A. And Dean, D. H. 1996. Protein engineering of *Bacillus thuringiensis* d-endotoxin: mutations at domain II of Cry1Ab enhance receptor affinity and toxicity toward gypsy moth larvae. Proc. Natl. Acad. Sci. 93:14338-14343.

Rajamohan, F., Lee, M. K. and Dean, D. H. 1998 *Bacillus thuringiensis* Insecticidal proteins: Molecular mode of action. Prog. Nucl. Ac. Res. 60:1-27.

Root-Bernstein, R. S. and Holsworth, D. D. 1998. Antisense peptides: A critical mini-review. J. Theor. Biol. 190:107-119.

Sangadala, S., Walters, F. S., English, L. H. and Adang M. J. 1994. A mixture of *Manduca sexta* aminopeptidase and phosphatase enhances *Bacillus thuringiensis* insecticidal Cry1A(c) toxin binding and $^{86}Rb^{+}$-K^{+} efflux in vitro. J. Biol. Chem. 269: 10088-10092.

Sankaranarayanan, R., Sekar, K., Banerjee, R., Sharma, V., Surolia, A and Vijayan, M. 1996. A novel mode of carbohydrate recognition in jacalin, a Moraceae plant lectin with a β-prism fold. Nat. Struct. Biol. 3:596-503.

Schnepf, E., Tomczak, K., Ortega, J. P. and Whiteley, H. R. 1990. Specificity-determining regions of a lepidopteran-specific insecticidal protein produced by *Bacillus thuringiensis*. J. Biol. Chem. 265:20923-20930.

Schnepf, E., Crickmore, N., Van Rie, J., Lereclus, D., Baum, J., Feitelson, J., Zeigler, D.R., and Dean, D.H. 1998. *Bacillus thuringiensis* and its pesticidal crystal proteins. Microbiol. Mol. Biol. Rev. 62:775-806.

Schwartz, J-L., Juteau, M., Grochulski, P., Cygler, M., Prefontaine, G., Brousseau, R., and Masson, L. 1997. Restriction of intramolecular movements within the Cry1Aa toxin molecule of *Bacillus thuringiensis* through disulfide bond engineering. FEBS Lett. 410:397-402.

Schwartz, J-L. and Laprade, R. 2000. Membrane permeabilisation by *Bacillus thuringiensis* toxins: protein insertion and pore formation. Entomopathogenic Bacteria: From laboratory to field application. Kluwer Academic Publishers. Printed in the Netherlands. 199-217.

Sidhu, S. S. 2000. Phage display in pharmaceutical biotechnology. Curr. Opin. Biotechnol. 11:610-616.

Smith, G. P. 1985. Filamentous fusion phage: novel expression vectors that display cloned antigens on the virion surface. Science. 228:1315-1317.

Soberón, M.,Pérez, R.V., Nuñez-Valdez, M. E., Lorence A. Gómez, I., Sánchez J and Bravo, A. 1999. Evidence for intermolecular interaction as a necessary step for pore-formation activity and toxicity of *Bacillus thuringiensis* Cry1Ab toxin. FEMS Microbiology Letters 191:221-225.

Vadlamudi, R. K., Ji, T. H. and Bulla Jr, L. A. 1993. A specific binding protein from *Manduca sexta* for the insecticidal toxin of *Bacillus thuringiensis* subsp. *berliner*. J. Biol. Chem. 268:12334-12340.

Vadlamudi, R. K., Weber, E., Ji, T. H., and Bulla Jr, L. A. 1995. Cloning and expression of a receptor for a insecticidal toxin of *Bacillus thuringiensis*. J. Biol. Chem. 270:5490-5494.

Valaitis, a. P., Jenkins, J. L., Dean, D. H. and Garner, K. J. 2001. Isolation and partial characterization of Gypsy moth BTR-270, an anionic brush border membrane glycoconjugate that binds *Bacillus thuringiensis* Cry1A toxins with high affinity. Archives Insect Biochem. Physiol. 46:186-200.

Van Rie, J. 2000. *Bacillus thuringiensis* and its use in transgenic insect control technologies. Int. J. Med. Microbiol. 290:463-469.

Van Rie, J., Jansens, S., Höfte, H., Degheele, D., Van Mellaert, H. 1990. Receptors on the brush border membrane of the insect midgut as determinants of the specificity of *Bacillus thuringiensis* delta-endotoxins. Appl. Environ. Microbiol. 56:1378-1385.

Van Rie, J., Jansens, S., Höfte, H., Degheele, D., Van Mellaert, H. 1989. Specificity of *Bacillus thuringiensis* δ-endotoxin: importance of specific receptors on the brush border membrane of the midgut of target insects. Eur. J. Biochem. 186:239-247.

Vié, V., Van Mau, N., Pomarède, P., Dance, C., Schwart, J. L., Laprade, R., Frutos, R., Rang, C., Masson, L., Heitz, F. and Le Grimellec, C. 2001. Lipid-induced pore formation of the *Bacillus thuringiensis* Cry1Aa isecticidal toxin.J. Membrane. Biol. 180:195-203.

Von Tersch, M. A., Slatin, S. L., Kulesza, C. A. and English, L. H. 1994. Membrane-permeabilizing activities of *Bacillus thuringiensis* coleopteran-active toxin CryIIIB2 and CryIIIB2 domain I peptide. Appl. Environ. Microbiol. 60:3711-3717.

Winter, G., Griffths, A. D., Hawkins, R. E. and Hoogenboom, H. R. 1994. Making antibodies by phage display technology. Annu. Rev. Immunol. 12:433-455.

Wolfersberger, M. G. 1990.The toxicity of two *Bacillus thuringiensis* δ-endotoxins to gypsy moth larvae is inversely related to the affinity of binding sites on midgut brush border membranes for the toxins. Experientia. 46:475-477.

Wolfersberger, M. G., Luethy, P., Maurer, A., Parenti, P., Sacchi, F. V., Giordana, B. and Hanozett, G. M. 1987. Preparation and partial characterization of amino acid transporting brush border membrane vesicles from the larval midgut of the cabbage butterfly (*Pieris brassicae*). Comp. Biochem. Physiol. 86A:301-308.

Wu, D. and Aronson, A. I. 1992. Localized mutagenesis defines regions of the *Bacillus thuringiensis* δ-endotoxin involved in toxicity and specificity. J. Biol. Chem. 267:2311-2317.

Wu, D. and Chang, F. N. 1985.Synergism in mosquitocidal activity of 26 and 65 kDa proteins from *Bacillus thuringiensis* subsp. *israelensis* crystal. FEBS Lett. 190:232-236.

Wu, D., Johnson, J. J., and Federeci, B. A. 1994. Synergism of mosquitocidal toxicity between CytA and CryIVD proteins using inclusions produced from cloned genes of *Bacillus thuringiensis.* Mol. Microbiol. 13:965-972.

Wu, D. and Dean, D. H. 1996. Functional significance of loops in the receptor binding domain of *Bacillus thuringiensis* CryIIIA δ-endotoxin. J. Mol. Biol. 255:628-640.

Yamamoto, T. and Dean, D. H. 2000. Insecticidal proteins produced by bacteria pathogenic to agricultural pests. Entomopathogenic Bacteria: from laboratory to field application. 81-100.

Yaoi, K., Nakanishi, K., Kadotani, T., Imamura, M., Koizumi, N., Iwahana, H. and Sato, R. 1999. *Bacillus thuringiensis* Cry1Aa toxin-binding region of *Bombix mori* aminopeptidase N. FEBS Lett. 463:221-224.

Yool, A. J. 1994. Block of the inactivating potassium channel by clofilium and hydroxylamine depends on the sequence of the pore region. Mol. Pharmacol. 46:970-976.

ANEXO I

Mapping the epitope in cadherin-like receptors involved in *Bacillus thuringiensis* Cry1A toxins interaction using phage display.

Gómez, I., Oltean, D., Gill, S., Bravo, A., and Soberón M.

Journal of Biological Chemistry. (2001). 276:28906-28912.

THE JOURNAL OF BIOLOGICAL CHEMISTRY
Vol. 276, No. 31, Issue of August 3, pp. 28906–28912, 2001
Printed in U.S.A.

Mapping the Epitope in Cadherin-like Receptors Involved in *Bacillus thuringiensis* Cry1A Toxin Interaction Using Phage Display*

Received for publication, April 5, 2001, and in revised form, May 29, 2001
Published, JBC Papers in Press, May 30, 2001, DOI 10.1074/jbc.M103007200

Isabel Gómez‡, Daniela I. Oltean§, Sarjeet S. Gill§, Alejandra Bravo‡, and Mario Soberón‡¶

From the ‡Instituto de Biotecnología, Departamento de Microbiología Molecular, Universidad Nacional Autónoma de México, Apdo postal 510-3, Cuernavaca, Morelos 62250, México and §Department of Cell Biology and Neuroscience, University of California, Riverside, California 92521

In susceptible lepidopteran insects, aminopeptidase N and cadherin-like proteins are the putative receptors for *Bacillus thuringiensis* (Bt) toxins. Using phage display, we identified a key epitope that is involved in toxin-receptor interaction. Three different scFv molecules that bind Cry1Ab toxin were obtained, and these scFv proteins have different amino acid sequences in the complementary determinant region 3 (CDR3). Binding analysis of these scFv molecules to different members of the Cry1A toxin family and to *Escherichia coli* clones expressing different Cry1A toxin domains showed that the three selected scFv molecules recognized only domain II. Heterologous binding competition of Cry1Ab toxin to midgut membrane vesicles from susceptible *Manduca sexta* larvae using the selected scFv molecules showed that scFv73 competed with Cry1Ab binding to the receptor. The calculated binding affinities (K_d) of scFv73 to Cry1Aa, Cry1Ab, and Cry1Ac toxins are in the range of 20–51 nM. Sequence analysis showed this scFv73 molecule has a CDR3 significantly homologous to a region present in the cadherin-like protein from *M. sexta* (Bt-R_1), *Bombyx mori* (Bt-R_{175}), and *Lymantria dispar*. We demonstrated that peptides of 8 amino acids corresponding to the CDR3 from scFv73 or to the corresponding regions of Bt-R_1 or Bt-R_{175} are also able to compete with the binding of Cry1Ab and Cry1Aa toxins to the Bt-R_1 or Bt-R_{175} receptors. Finally, we showed that synthetic peptides homologous to Bt-R_1 and scFv73 CDR3 and the scFv73 antibody decreased the *in vivo* toxicity of Cry1Ab to *M. sexta* larvae. These results show that we have identified the amino acid region of Bt-R_1 and Bt-R_{175} involved in Cry1A toxin interaction.

Synthetic insecticides cause not only environmental problems, but many have lost their efficacy due to resistance development in the pest insects. *Bacillus thuringiensis* (Bt),[1] a biopesticide, is a viable alternative for the control of insect pests in agriculture and disease vectors of importance in public health. Bt use is also compatible with sustainable and environmentally friendly agricultural practices. Bt produces insecticidal proteins (Cry toxins) during sporulation as parasporal crystals. These crystals are predominantly composed of one or more proteins, also called δ-endotoxins. These toxins are highly specific to their target insect; are safe to humans, vertebrates, and plants; and are completely biodegradable.

The three-dimensional structures of Cry3A and Cry1Aa toxins have been resolved by x-ray diffraction crystallography (1, 2). The two proteins share many similar features and are composed of three domains. Domain I, extending from the N terminus, a seven-helix bundle, is the pore-forming domain. Domain II consists of three anti-parallel β-sheets, and domain III is a β-sandwich of two anti-parallel β-sheets (1, 2). Domains II and III are involved in receptor binding, and domain III additionally protects the toxin from further proteolysis (for reviews, see Refs. 3 and 4).

The mode of action of Cry toxins is a multistage process. Crystal toxins ingested by susceptible larvae dissolve in the alkaline environment of the larval midgut, thereby releasing soluble proteins. The inactive protoxins are then cleaved at specific sites by midgut proteases, yielding 60–70-kDa protease-resistant active fragments. The active toxin then binds to specific membrane receptors on the apical brush border of the midgut epithelium columnar cells (5, 6). Therefore, receptors on the brush border membrane are a key factor in determining the specificity of Cry toxins. This specific binding involves two steps, a reversible followed by an irreversible one (7). After binding, the toxin apparently undergoes a large conformational change leading to its insertion into the cell membrane (1). The Cry toxin molecules then aggregate through toxin-toxin interactions (8), leading to the formation of lytic pores (8–10), which disrupt midgut ion gradients and the transepithelial potential difference. This disruption is accompanied by an inflow of water that leads to cell swelling and eventual lysis, resulting in paralysis of the midgut and subsequent larval death (3, 4).

A number of putative receptor molecules for lepidopteran-specific Cry1A toxins have been identified. In *Manduca sexta*, Cry1Aa, Cry1Ab, and Cry1Ac proteins bind to a 120-kDa aminopeptidase N (APN) (11–13) and to a 210-kDa cadherin-like protein (Bt-R_1) (14, 15). In *Bombyx mori*, Cry1Aa binds to a 175-kDa cadherin-like protein (Bt-R_{175}) (16, 17) and to a 120-kDa APN (18). In *Heliothis virescens*, Cry1Ac binds to two proteins of 120 and 170 kDa, both identified as APN (20, 21). In

* This work was supported in part by Consejo Nacional de Ciencia y Tecnologia (CONACYT) Contract 27637-N, Dirección General de Apoyo al Personal Académico-Universidad Nacional Autónoma de México IN206200 and IN216300, UC MEXUS-CONACYT, United States Department of Agriculture Grant 96-353-0-3820, and the University of California Toxic Substances Research and Training Program. The costs of publication of this article were defrayed in part by the payment of page charges. This article must therefore be hereby marked "*advertisement*" in accordance with 18 U.S.C. Section 1734 solely to indicate this fact.

¶ To whom correspondence should be addressed. Tel.: 52-73-291618; Fax: 52-73-172388; E-mail: mario@ibt.unam.mx.

[1] The abbreviations used are: Bt, *B. thuringiensis*; APN, aminopeptidase N; BBMV, brush border membrane vesicles; SPR, surface plasmon resonance; CDR, complementary determinant region; PAGE, polyacrylamide gel electrophoresis; scFv, single-chain variable fragment; HBS-P, HEPES-buffered saline with surfactant P-20; LB, Luria broth; NB, nutrient broth.

Plutella xylostella and *Lymantria dispar* APNs were identified as Cry1Ac receptors (11, 22–24). All of these receptor molecule proteins are glycosylated (12, 15, 16, 19). The interaction between toxin and its receptor can be complex. For example, Cry1Ac binds to two sites on the APN purified from *M. sexta*, and only one of these sites is also recognized by Cry1Aa and Cry1Ab (25). Interestingly, binding of Cry1Ac to both receptor sites is inhibited by sugars, which do not inhibit the binding of Cry1Aa and Cry1Ab (25).

There is little information on the receptor domains involved in Cry toxin binding. In *B. mori*, Cry1Aa toxin binds to a conserved APN domain (26). However, the precise regions that are involved in toxin-receptor interactions, including that of the cadherin-like protein, are not known. In an attempt to identify the receptor molecules and map the receptor epitopes involved, we decided to use the phage display technique. Among several approaches used for epitope mapping, phage display has proven to be highly successful (27–31).

In this study, we focused on the interaction of Cry1A toxins with brush border membrane vesicles from susceptible insects. We report here the identification of one scFv antibody whose CDR3 region shares extensive homology with an 8-amino acid region present in the cadherin-like receptors Bt-R_1 and Bt-R_{175} from two lepidopteran insects. This 8-amino acid region competes with the binding of Cry1Ab and Cry1Aa to Bt-R_1 and Bt-R_{175}, suggesting that we identified the Cry1A toxin-binding epitopes in the cadherin-like receptor protein.

MATERIALS AND METHODS

Bacterial Strains, Plasmids, and Media—Escherichia coli strains were grown in Luria broth (LB) at 37 °C either with ampicillin (100 μg/ml) or erythromycin (250 μg/ml), while Bt strains were grown in nutrient broth sporulation medium (NB) at 30 °C with or without erythromycin (7.5 μg/ml). The acrystalliferous strain 407*cry*$^-$ (32) transformed with pHT409 (33) harboring the *cry1Aa* gene or pHT315–1Ab harboring the *cry1Ab* gene was used for Cry1Aa and Cry1Ab production. Cry1Ac was produced from the wild type Bt strain HD73.

Purification of Cry1A Toxins and Cry1Ab Protein Fragments—Bt strains containing the *cry1Ab*, *cry1Aa*, and *cry1Ac* genes were grown for 3 days in NB. The spores and crystals were harvested and washed with buffer containing 0.01% Triton X-100, 50 mM NaCl, 50 mM Tris-HCl, pH 8.5. Crystals were isolated by sucrose gradients as previously described (34). These crystals were solubilized and activated by trypsin (1:50, w/w) for 2 h, and the proteins were purified by anion exchange chromatography (Q-Sepharose) as described (34, 35). The purified toxins were concentrated in dialysis bags (Spectra/Por, cut-off 12–14 kDa; Fisher) covered with polyethylene glycol 8000, dialyzed against 1000 volumes of buffer A (150 mM *N*-methylglucamine chloride, 10 mM HEPES, pH 8), and stored at 4 °C until used. Toxins were apparently homogeneous as determined by SDS-PAGE and silver staining.

Phage Display Library, Selection, and Sequencing of Clones—The Nissim synthetic phage-antibody library used in this work was kindly provided by the Cambridge Center for Protein Engineering (Cambridge, UK). This library, with a diversity of 1×10^8 clones, contains a diverse repertoire of *in vitro* rearranged VH genes containing a random VH-CDR3 of 4–12 amino acid residues in length (36). Cry1Ab-binding phages were isolated by panning using immunotubes (Nunc), which were coated with (100 μg/ml) Cry1Ab toxin overnight at room temperature. After each round of selection, individual clones were analyzed for their ability to bind Cry1Ab by enzyme-linked immunosorbent assay. The helper phage VCS-M13 (Stratagene) was used to rescue phages from individual colonies of infected *E. coli* TG-1. Expression of soluble fragments from single infected *E. coli* HB2151 colonies (36–38) was induced by isopropyl thiogalactoside. Bacterial supernatants containing phage or scFv fragments were screened for toxin binding by enzyme-linked immunosorbent assay. DNA fingerprinting was performed by amplifying the scFv insert using primers LMB3 (5′-CAGGAAACAGCTATGAC) and fd-SEQ1 (5′-GAATTTTCTGTATGAGG) followed by digestion with the frequently cutting enzyme *Bst*NI as described (37). CDR3 sequence was determined using the primer CDRFOR (5′-CAGGGTACCTTGGCCCCA) (38).

Purification and Characterization of scFvs—For purification of scFv molecules, scFv genes were subcloned into the pSyn vector (38) and used to transform *E. coli* TG1. scFv fragments were purified to homogeneity as follows. Selected clones were cultured at 37 °C in 2× TY (supplemented with 100 μg/ml ampicillin and 0.1% glucose) until they reached an OD of 0.7 at 600 nm. Production of soluble scFv was induced by the addition of 0.5 mM isopropyl thiogalactoside to the culture and grown for 4 h at 25 °C. The scFv was collected from the periplasm. Soluble periplasmic extracts were obtained by osmotic shock at 4 °C using lysis buffer containing 200 mg/ml sucrose, 1 mM EDTA, 300 mM Tris-HCl, pH 8. The supernatant was applied to a nickel-agarose column, which was washed with PBS, and the scFv was eluted with 2 ml of 250 mM imidazole, 0.2% azide in PBS.

Western Blotting of Cry1Ab Domain I and Domain II-III Polypeptides—DomI and DomII-III-H6 of the Cry1Ab toxin were individually expressed in BL21 *E. coli* cells as described (39).[2] Briefly, an overnight culture of pDomII-III-H6 (or pDomI) transformed cells was grown at 37 °C in LB medium (200 μg/ml ampicillin). This culture was used to inoculate 100 ml of LB medium (1:100 dilution). The cells were grown to an OD of 0.5–0.6 and induced with 1 mM isopropyl thiogalactoside. After 3 h of growth, the cells were centrifuged and suspended in 3 ml of buffer A (50 mM $NaSO_4$, 300 mM NaCl, pH 8). Cells were then sonicated on ice (two 1-min bursts) and centrifuged (10 min at 12,000 × *g*). Soluble proteins (10 μg) were separated by 10% SDS-PAGE, and Western blot analysis was performed as described (35), using bacterial supernatants containing phage or scFv fragments. For scFv fragments, a c-Myc antibody (Sigma) (1:1000 dilution) was used, followed by incubation with a secondary goat anti-mouse antibody conjugated with peroxidase (Sigma) (1:1000 dilution). For clone M13–19, an anti-M13 antibody conjugated to peroxidase (Sigma) (1:1000 dilution) was utilized as described (34, 35). Blots were visualized using luminol (ECL; Amersham Pharmacia Biotech).

Preparation of Brush Border Membrane Vesicles (BBMVs)—M. sexta eggs were kindly supplied by Dr. Jorge Ibarra (CINVESTAV, Irapuato), and *B. mori* eggs were obtained from Carolina Biological Supply Co. *M. sexta* and *B. mori* larvae were reared on an artificial diet and fresh mulberry leaves, respectively. BBMVs from fifth instar *M. sexta* or *B. mori* larvae were prepared as reported (41) except that neomycin sulfate (2.4 μg/ml) was included in the buffer (300 mM mannitol, 2 mM dithiothreitol, 5 mM EGTA, 1 mM EDTA, 0.1 mM phenylmethylsulfonyl fluoride, 150 μg ml^{-1} pepstatin A, 100 μg ml^{-1} leupeptin, 1 μg ml^{-1} soybean trypsin inhibitor, 10 mM HEPES-HCl, pH 7.4).

Qualitative Binding Assays with Isolated BBMV—Binding and competition analyses of Cry1Aa-c toxins to *M. sexta* and *B. mori* BBMV were performed as previously described (35). Amino acid sequences of synthetic peptides used for competition experiments were the following: CDR3–73 (RITQTTNRAA), BtR1-CRY (HITDTNNKAA), BtR175-CRY1 (QIIDTNNKAA), BtR175-CRY2 (LDETTNVLAA), and PepL1 (TDAHRGEYYW). Toxins were biotinylated using biotinyl-*N*-hydroxysuccinimide ester (Amersham Pharmacia Biotech), and binding analyses were performed in 100 μl of binding buffer (PBS, 0.1% (w/v) BSA, 0.1% (v/v) Tween 20, pH 7.6). Ten micrograms of BBMV protein were incubated with 10 nM biotinylated toxin, and the unbound toxin was removed by centrifugation for 10 min at 14,000 × *g*. The pellet containing BBMV and the bound biotinylated toxin was suspended in 100 μl of binding buffer and washed twice. Finally, the BBMVs were suspended in 10 μl of PBS, pH 7.6, and an equal volume of 2× sample loading buffer (0.125 M Tris-HCl, pH 6.8, 4% SDS, 20% glycerol, 10% 2-mercaptoethanol, 0.01% bromphenol blue) was added. The samples were separated by SDS-polyacrylamide gels and electrotransferred to nitrocellulose membranes. The biotinylated protein was visualized by incubating with streptavidin-peroxidase conjugate (1:4000 dilution) for 1 h, followed by luminol (ECL; Amersham Pharmacia Biotech). For competition experiments, biotinylated Cry1A toxins were incubated with different concentrations of scFvs or peptides in PBS for 1 h at room temperature before incubating toxin with BBMV.

Toxin Overlay Assays—Protein blot analysis of BBMV preparations was performed as described previously (35, 41). Ten micrograms of BBMV protein were separated by 9% SDS-PAGE and electrotransferred to nitrocellulose membranes. After blocking, the membranes were incubated for 2 h with 10 nM biotinylated Cry1A toxins. Unbound toxin was removed by washing the membrane three times with washing buffer for 10 min, and the bound toxin was identified by incubation with streptavidin-peroxidase conjugate (1:5000) for 1 h and visualized using luminol (ECL; Amersham Pharmacia Biotech). For competition experiments, biotinylated Cry1A toxins were incubated with different concentrations of scFvs or peptides in washing buffer (0.1% Tween 20, 0.2%

[2] A. Bravo, R. Meza, and A. Lorence, unpublished results.

BSA in PBS) for 1 h at room temperature before incubating toxin with nitrocellulose membranes.

Biosensor (SPR) Analysis of scFv73 Affinities to Cry1A—All surface plasmon resonance (SPR) measurements were performed using a Biacore X and CM5 sensor chips (Biacore). HBS-P buffer (10 mM HEPES, pH 7.4, 0.15 M NaCl, 3 mM EDTA, 005% surfactant P20) was used throughout the analyses. The ligand, scFv73 (30 kDa, apparently homogeneous based on SDS-PAGE) at a concentration of 25 μg/ml in 20 mM ammonium acetate, pH 5, buffer, was immobilized on flow cell 2 using a standard amine-coupling kit (Biacore) at densities of less than 150 response units. The surfaces of both flow cells were activated for 5 min at a flow rate of 10 μl/min. Following ligand immobilization on flow cell 2, both flow cells were blocked with a 5-min injection of 1 M ethanolamine at a flow rate of 10 μl/min. The analytes (65 kDa, apparently homogenous based on SDS-PAGE) were injected over both flow cells at a flow rate of 30 μl/min. The complex was allowed to associate and dissociate for 120 and 180 s, respectively. The surfaces were regenerated with a 1-min injection of 1 mM HCl. Triplicate injections of each toxin concentration were injected in random order over both surfaces, and the responses were corrected by double referencing (42). The data were fitted using global analysis software available within Biaevaluation 3.1 (Biacore). Competition experiments were performed by injection of a 10- and 200-fold molar excess of scFv in combination with Cry1Ab and Cry1Aa toxins. Carbohydrate inhibition studies with GalNAc were carried out using 600 nM Cry1Ac and 20 μM GalNAc. As an additional control, we immobilized a non-Cry1A-binding scFv4E that was obtained by panning against a different antigen onto flow cell 1 at similar levels as scFv73. Various concentrations of toxin were injected over both flow cells, and the response curve on flow cell 1 was subtracted from flow cell 2. Using this control flow cell configuration, identical Cry1Ab binding curves were obtained compared with using the ethanolamine-blocked control surface.

Insect Bioassay—Bioassays were performed with *M. sexta* neonate larvae using surface-treated food with 9 ng/cm^2 as reported (5), and mortality was recorded after 7 days.

RESULTS

Characterization of scFv Antibodies That Bind Cry1Ab Toxin—A library of 10^8 human single chain antibody fragments (scFv) with variability in the CDR3 region (5–12 amino acids) (36) was used to select a population of phages that bound Cry1Ab toxin. After eight rounds of panning, 98% of the M13 phages bound Cry1Ab (data not shown). To characterize the phages isolated, we amplified the variable regions by PCR and digested the products with *Bst*NI restriction enzyme. Analysis of 50 phage clones showed three different restriction patterns (data not shown). One of these patterns was found in 48 of the clones analyzed (representative clone scFv45), while the other two patterns were each represented by one clone. DNA sequence analysis of the CDR3 region was determined for 10 clones of the most abundant restriction pattern (including scFv45) and also for the two clones representing the other two unique restriction patterns (scFv19 and scFv73). Three different amino acid sequences were present in the CDR3 regions of the clones analyzed (scFv19, RTSPRLTPKHR; scFv73, ITQTTNR; scFv45, NPRIPP).

We used Western blot analysis to determine which Cry1Ab toxin domain bound the three scFv antibodies. This analysis was performed using the scFv antibodies against membrane blots containing protein extracts from *E. coli* expressing either Cry1Ab domain I or domains II-III. Fig. 1 shows that the three scFv clones recognized the 44-kDa domain II-III polypeptide but not the 30-kDa domain I polypeptide. To analyze whether domain II or III was recognized by these scFv proteins, we determined if the three M13-scFv phages bound Cry1Ac toxin, since this toxin shares 98% identity with Cry1Ab toxin in domain II but only 38% identity in domain III. Enzyme-linked immunosorbent assay binding analysis showed that the three scFv antibodies also recognized Cry1Ac toxin (data not shown), suggesting that the three scFv fragments bound to domain II of Cry1Ab toxin.

Competition of Cry1Ab Toxin Binding to M. sexta BBMV with

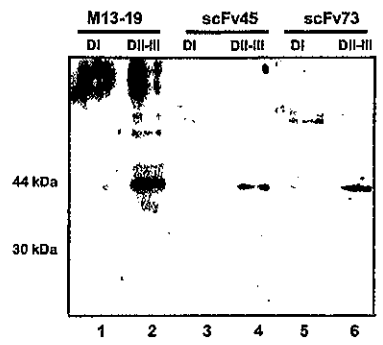

FIG. 1. **Binding of scFv molecules to Cry1Ab toxin domains.** Protein extracts of *E. coli* strains expressing domain I (*lanes 1, 3,* and *5*) or domains II-III (*lanes 2, 4,* and *6*) were detected with M13–19 (*lanes 1* and *2*), scFv45 (*lanes 3* and *4*), or scFv73 (*lanes 5* and *6*) as described under "Materials and Methods." Molecular masses of domain I and domain II-III polypeptides are 30 and 44 kDa, respectively.

Selected scFv Antibodies—The three anti-Cry1Ab scFv genes were subcloned into a plasmid to incorporate a hexahistidine tag and then expressed and purified from *E. coli*. Only scFv73 and scFv45 were produced in *E. coli* in high quantities, and scFv19 was therefore not analyzed further. To determine if the selected scFv antibodies could compete with the binding of Cry1Ab toxin to its receptor, we performed two different binding assays. In the first protocol, a qualitative binding assay, biotinylated Cry1Ab toxin was incubated in solution with BBMV. The bound toxin was visualized following SDS-PAGE and electrotransfer of the proteins to nitrocellulose membranes. Fig. 2*A* shows that both scFv antibodies compete with the binding of Cry1Ab toxin to *M. sexta* BBMV, although scFv73 competes more efficiently than scFv45 (Fig. 2*A*, *lanes 4* and *6*). The second protocol, toxin overlay assays, allows the identification of BBMV proteins that interact with Cry1Ab. BBMV proteins were separated by SDS-PAGE and electrotransferred to nitrocellulose. Then biotinylated Cry1Ab toxin was incubated with the membranes, and the proteins that bound the toxin were detected with streptavidin coupled to peroxidase. Fig. 2*B* shows that both the 120-kDa aminopeptidase (APN) (13) and the 210-kDa cadherin-like (Bt-R_1) (15) proteins bound biotinylated Cry1Ab. The scFv45 did not compete with Cry1Ab binding to either the 120- or 210-kDa proteins. In contrast, scFv73 competed with the binding of Cry1Ab to the 210-kDa protein but not to the 120-kDa protein.

The scFv73 CDR3 Shares Significant Homology with M. sexta and B. mori Cadherin-like Proteins—Since scFv73 competed with the binding of Cry1Ab toxin to the Bt-R_1 receptor from *M. sexta*, we compared the amino acid sequence of the CDR3 region to that of Bt-R_1 and APN. The CDR3 amino acid sequence of scFv73 (RITQTTNR) shares 71% similarity with an 8-amino acid region present in Bt-R_1 (GenBank™ accession number AAG37912, ^{869}HITDTNNK^{876}) from *M. sexta* and 66% similarity to the corresponding region of Bt-R_{175} protein from *B. mori* (GenBank™ accession number BAA77212, ^{873}IIDTNNK^{880}). In addition, a second 6-amino acid region in Bt-R_{175} (^{1296}LDETTN^{1301}) shares 71% similarity with scFv73 CDR3. No significant homology with APN was found. The CDR3 regions of scFv45 and scFv19 had no homology with either Bt-R_1 or APN.

Binding Affinities of scFv73 to Cry1A—The binding affinity of Cry1Ab toxin to purified Bt-R_1 has been reported to be 0.7 nM using ^{125}I-labeled toxin (15). To determine the binding affinity of the scFv73 CDR3 region to Cry1A toxins we performed real time binding kinetics by SPR. SPR analyses showed that Cry1Aa, Cry1Ab, and Cry1Ac toxins bound immobilized scFv73. Toxin binding curves were globally fitted to various

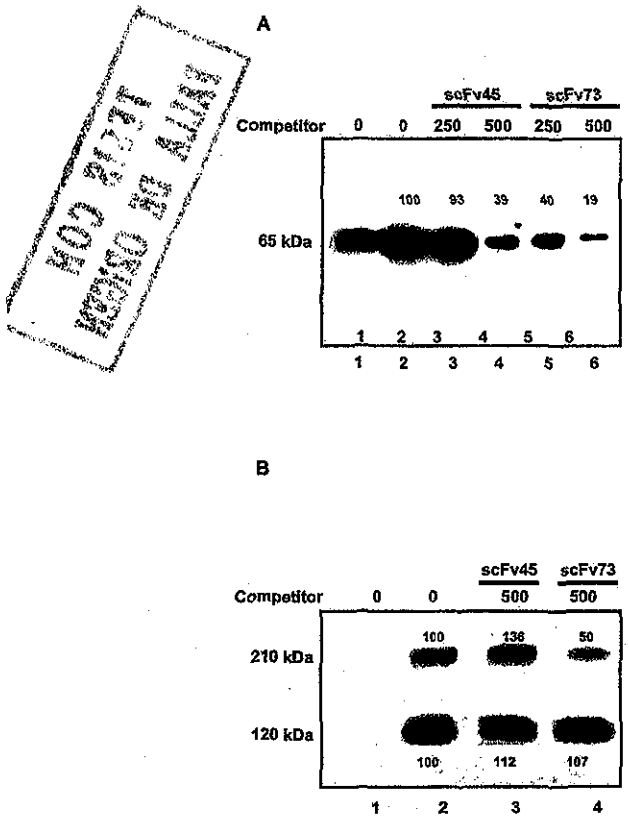

FIG. 2. **The scFv73 antibody competes binding of Cry1Ab to *M. sexta* BBMV and to Bt-R_1.** *A*, qualitative binding of Cry1Ab to *M. sexta* BBMV. *Lane 1*, biotinylated Cry1Ab toxin as marker; *lane 2*, binding of Cry1Ab to BBMV; *lanes 3* and *4*, binding of Cry1Ab with a 250- and 500-fold molar excess of scFv45, respectively; *lanes 5* and *6*, binding of Cry1Ab with a 250- and 500-fold molar excess of scFv73, respectively. *B*, toxin overlay assays of Cry1Ab to *M. sexta* BBMV. *Lane 1*, *M. sexta* BBMV; *lane 2*, binding of Cry1Ab; *lane 3*, competition of Cry1Ab with a 500-fold molar excess of scFv45; *lane 4*, binding of Cry1Ab with a 500-fold molar excess of scFv73. Cry1Ab (10 nM) was used in *lanes 2–6*. Molecular weights of Cry1Ab-binding proteins are indicated on the *left*. *Numbers within the images* represent the percentage of signal relative to Cry1Ab binding without competitors as determined by scanning optical density of bands in blots.

binding models and the best fit (χ^2 value of 1) was found using a Langmuir binding model that indicated a 1:1 toxin/receptor stoichiometry. The binding responses were reproducible during three separate scFv73 immobilizations, which indicated that amine coupling did not affect the Cry1Ab binding site on scFv73. The overall affinity (K_d of 39.7 nM) for Cry1Ab binding to scFv73 was obtained from the apparent rate constants (k_{on} and k_{off} values) generated by the binding model (Fig. 3*A*, Table I). The Cry1Aa and Cry1Ac affinities were 51.1 and 20.5 nM, respectively (Table I). scFv73 coinjected with Cry1Ab or Cry1Aa toxin completely inhibited (100%) toxin binding to the immobilized scFv73 (Fig. 3*B*). In contrast, scFv45, only inhibited 5% of the Cry1Ab and Cry1Aa binding to scFv73. These results indicate that the scFv73 and scFv45 bind to different sites on Cry1Aa and Cry1Ab. Bovine serum albumin, a protein of similar size as the Cry1A toxins did not bind scFv73 at any of the concentrations tested.

Cry1Ac binding to immobilized scFv73 was identical in the absence or presence of GalNAc (data not shown). GalNAc efficiently competes the binding of Cry1Ac to APN by binding to a pocket located in domain III (25, 44, 45). This suggests the Cry1Ac epitope that binds scFv73 is different than that known for initially binding to APN, and as our results suggest, is located on domain II.

Identification of the Binding Region of Bt-R_1 and Bt-R_{175} to Cry1Ab and Cry1Aa Toxins by Competition Experiments with Synthetic Peptides—We performed binding competition experiments to determine if the Bt-R_1 region that shares sequence homology with scFv73 CDR3 plays a role in receptor binding to Cry1Ab. Synthetic peptides corresponding either to scFv73 CDR3 (CDR3–73) or to the corresponding region in Bt-R_1 (BtR1-CRY) were used as competitors. Two alanine residues were added to each peptide at the C terminus to facilitate synthesis. Fig. 4*A* shows that the two synthetic peptides, CDR3–73 and BtR1-CRY, decreased Cry1Ab toxin binding to *M. sexta* BBMV (*lanes 4* and *6*). This competition was specific, since an unrelated ten amino acid peptide (PepL1, *lane 2*) did not compete the binding of Cry1Ab. In contrast, Cry1Ac binding to *M. sexta* BBMVs was not competed by BtR1-CRY (*lane 8*). Cry1Aa binding to *M. sexta* BBMVs was also inhibited by BtR1-CRY peptide (data not shown). Toxin overlay assays also confirmed that both synthetic peptides competed Cry1Ab binding to the 210-kDa protein and that the BtR1-CRY synthetic peptide competed more efficiently (Fig. 4*B*, *lanes 6–8*) than CDR3–73 (Fig. 4*B*, *lanes 2–5*). However, these peptides did not substantially inhibit Cry1Ab binding to the 120-kDa protein (Fig. 4*B*). Fig. 4*C* shows that the BtR1-CRY peptide also competed binding of Cry1Aa toxin to the 210-kDa protein. In contrast to that observed with Cry1Ab binding, CDR3–73 showed greater competition than with BtR1-CRY. In our experimental conditions, we could not detect binding of Cry1Ac to the 210-kDa protein (data not shown).

As mentioned previously, scFv73 CDR3 shares significant amino acid homology with two regions in the *B. mori* Cry1Aa receptor Bt-R_{175}. To determine if the regions identified in Bt-R_{175} could also compete with the binding of Cry1Ab and Cry1Aa toxins to *B. mori* BBMV, competition binding experiments of Cry1Aa and Cry1Ab to *B. mori* BBMV were performed. Fig. 5*A* (*lanes 2–7*) shows that binding of Cry1Aa toxin to BBMV in solution was not competed efficiently with either of the two synthetic peptides: one that corresponds to the similar region mapped for Bt-R_1 (BtR175-CRY1) and the second that corresponds to the amino acid sequence of the second site in Bt-R_{175} (BtR175-CRY2). Toxin overlay assays showed that BtR175-CRY2 peptide competed with Cry1Ab binding to the 175-kDa protein (Fig. 5*B*, *lanes 7* and *8*) more efficiently than competition of Cry1Aa binding (Fig. 5*C*, *lanes 7* and *8*). In contrast, BtR175-CRY1 competed poorly with both Cry1Ab and Cry1Aa binding to the 175-kDa protein (Fig. 5, *B* and *C*, *lanes 5* and *6*).

Involvement of the Epitope Mapped in Bt-R_1 in Cry1Ab Toxicity—To determine if the epitope mapped in Bt-R_1 involved in Cry1Ab toxin interaction interferes with Cry1Ab toxicity to *M. sexta* larvae, bioassays were performed using the different scFv antibodies and synthetic peptides in combination with Cry1Ab toxin. First instar larvae were fed Cry1Ab toxin either alone or the Cry1Ab toxin previously incubated with a 300-fold molar excess of the different proteins or peptides. Table II shows that the toxicity of Cry1Ab toxin was reduced by 50% when the toxin was incubated with scFv73 or the synthetic peptides CDR3–73 or BtR1-CRY. In contrast, treatment with scFv45, which has a different epitope, had little effect on Cry1Ab toxicity. None of the peptides were toxic to *M. sexta* larvae (data not shown).

DISCUSSION

In susceptible insects, Cry toxin specificity correlates with receptor recognition (8, 9). The identification of epitopes involved in Cry toxin-receptor interactions could provide insights into the mechanism of insect specificity and the mode of action of these toxins. Furthermore, receptor epitope mapping offers tools for improving the specificity and toxicity of Bt toxins. To facilitate the identification of these receptor epitopes, we uti-

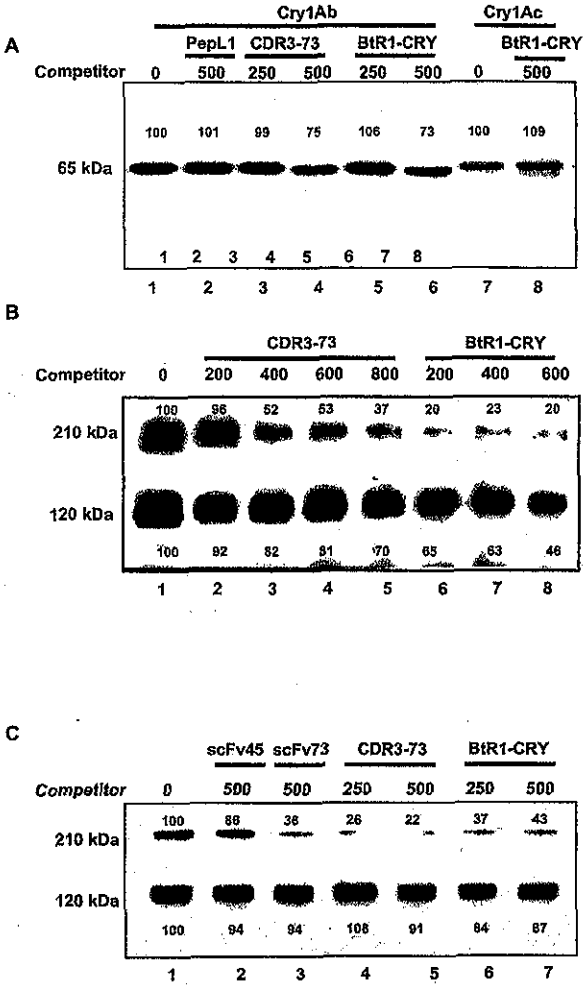

FIG. 4. **Synthetic peptides homologous to scFv73 CDR3 and to Bt-R_1 compete with Cry1Ab binding to Bt-R_1.** *A*, qualitative binding of Cry1Ab to *M. sexta* BBMV. *Lane 1*, binding of Cry1Ab to BBMVs; *lane 2*, binding of Cry1Ab with a 500-fold molar excess of peptide PepL1; *lanes 3* and *4*, binding of Cry1Ab with a 250- and 500-fold molar excess of peptide CDR3–73, respectively; *lanes 5* and *6*, binding of Cry1Ab with a 250- and 500-fold molar excess of peptide BtR1-CRY, respectively; *lane 7*, binding of Cry1Ac to BBMV; *lane 8*, binding of Cry1Ac with a 500-fold molar excess of peptide BtR1-CRY. *B*, toxin overlay assays of Cry1Ab to *M. sexta* BBMV. *Lane 1*, binding of Cry1Ab; *lanes 2–5*, competition of Cry1Ab with a 200-, 400-, 600- and 800-fold molar excess of peptide CDR3–73, respectively; *lanes 6–8*, competition of Cry1Ab with a 200-, 400-, and 600-fold molar excess of peptide BtR1-CRY, respectively. *C*, toxin overlay assays of Cry1Aa to *M. sexta* BBMV. *Lane 1*, binding of Cry1Aa; *lane 2*, competition with a 500-fold molar excess of scFv45; *lane 3*, competition with a 500-fold molar excess of scFv73; *lanes 4* and *5*, competition of Cry1Aa with a 250- and 500-fold molar excess of peptide CDR3–73, respectively; *lanes 6* and *7*, competition of Cry1Aa with a 250- and 500-fold molar excess of peptide BtR1-CRY, respectively. Molecular weights of Cry1A proteins are indicated on the *left*. *Numbers within* the *images* represent the percentage of signal relative to Cry1A binding without competitors as determined by scanning optical density of bands in blots.

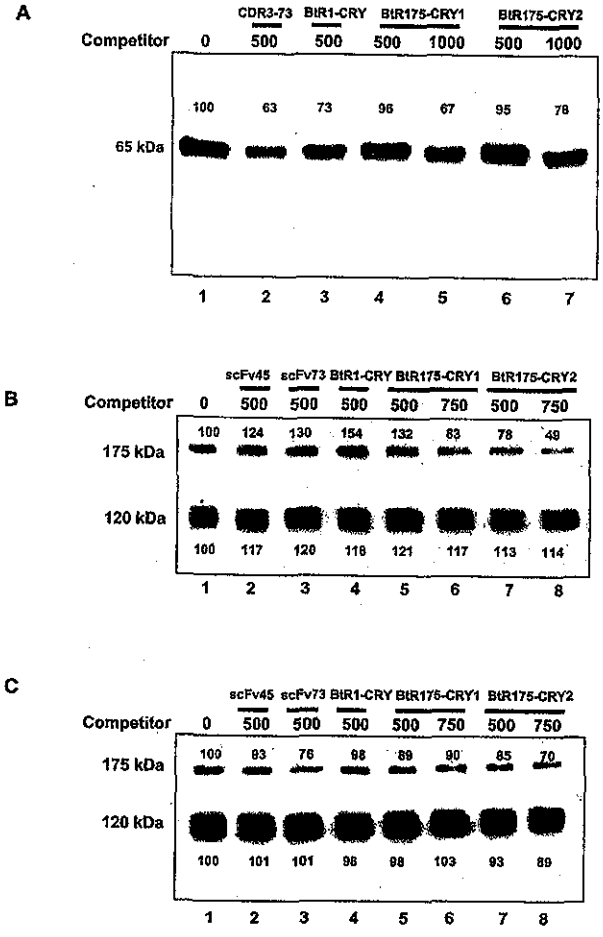

FIG. 5. **Synthetic peptides homologous to *B. mori* Bt-R_{175} compete binding of Cry1Ab and Cry1Aa to the receptor.** *A*, binding of Cry1Aa to *B. mori* BBMV; *lane 1*, binding of Cry1Aa; *lane 2*, binding of Cry1Aa with a 500-fold molar excess of peptide CDR3–73; *lane 3*, binding of Cry1Aa with a 500-fold molar excess of peptide BtR1-CRY; *lanes 4* and *5*, binding of Cry1Aa with a 500- and 1000-fold molar excess of peptide BtR175-CRY1; *lanes 6* and *7*, binding of Cry1Aa with a 500- and 1000-fold molar excess of peptide BtR175-CRY2. *B*, toxin overlay assays of Cry1Ab to *B. mori* BBMV. *Lane 1*, binding of Cry1Ab; *lane 2*, competition of Cry1Ab with a 500-fold molar excess of scFv45; *lane 3*, competition of Cry1Ab with a 500-fold molar excess of scFv73; *lane 4*, competition of Cry1Ab with a 500-fold molar excess of peptide BtR1-CRY; *lanes 5* and *6*, competition of Cry1Ab with a 500- and 750-fold molar excess of peptide BtR175-CRY1, respectively; *lanes 7* and *8*, competition of Cry1Ab with a 500- and 750-fold molar excess of peptide BtR175-CRY2, respectively. *C*, toxin overlay assays of Cry1Aa to *B. mori* BBMV. *Lane 1*, binding of Cry1Aa; *lane 2*, competition of Cry1Aa with a 500-fold molar excess of scFv45; *lane 3*, competition of Cry1Aa with 500-fold molar excess of scFv73; *lane 4*, competition of Cry1Aa with a 500-fold molar excess of peptide BtR1-CRY; *lanes 5* and *6*, competition of Cry1Aa with a 500- and 750-fold molar excess of peptide BtR175-CRY1, respectively; *lanes 7* and *8*, competition of Cry1Aa with a 500- and 750-fold molar excess of peptide BtR175-CRY2, respectively. Molecular weights of Cry1A proteins are indicated on the *left*. *Numbers within* the *images* represent the percentage of signal relative to Cry1A binding without competitors as determined by scanning optical density of bands in blots.

M. sexta Bt-R_1 (Figs. 4*B* and 5*B*). This could also explain the low competition observed with synthetic peptides in Cry1Aa and Cry1Ab binding to *B. mori* BBMV (Fig. 5*A*). Cry1Aa and Cry1Ab toxins share the same binding site in *B. mori* BBMV, with Cry1Aa toxin having at least a 10-fold higher toxicity due to a higher binding affinity (47). These affinity differences may explain why the peptide BtR175-CRY2 competes more efficiently with Cry1Ab binding to Bt-R_{175} than the binding of Cry1Aa (Fig. 5, *B* and *C*), since less peptide is needed to compete the binding of a protein with lower affinity.

The epitope of Cry1Ab toxin involved in the interaction of

TABLE II
Toxicity of Cry1Ab protein to M. sexta larvae in the presence or absence of competitors

Treatment	Mortality[a]
Cry1Ab[b]	97 ± 2.3
Cry1Ab + scFv45	89 ± 4.6
Cry1Ab + scFv73	55 ± 1.1
Cry1Ab + CDR3–73	48 ± 5.9
Cry1Ab + BtR1CRY	49 ± 4.2
Control	0

[a] Percentage of 48 larvae per treatment ± S.D. of three experiments.
[b] 9 ng/cm^2 of toxin; competitors used were 300-fold molar excess.

this toxin with the Bt-R_1 receptor has not been mapped. However, mutations in loop 2 and loop 3 of Cry1Ab domain II affect initial binding to *M. sexta* BBMV (7, 42, 44). Mapping the epitopes in Cry1Aa and Cry1Ab toxins that interact with scFv73 antibody could help in determining the epitopes of these toxins involved in the interaction with cadherin-like receptors.

This is the first report that has mapped the receptor epitopes involved in Cry toxin binding and toxicity. Defining the toxin and the receptor epitopes involved in the specific interaction of these proteins could have a significant impact in the design of more efficient Bt toxins and also help explain the high specificity of these toxins.

Acknowledgments—We thank Baltazar Becerril for scFv4E and discussions; Didier Lereclus for Bt strain 407*cry*$^-$ and pHT409; Juan Carlos Almagro and Juan Miranda for fruitful discussions; Martín Peralta for performing initial experiments; and Laura Lina, Jorge Sanchez, and Oswaldo Lopez for technical assistance.

REFERENCES

1. Li, J., Carroll, J., and Ellar, D. J. (1991) *Nature* **353,** 815–821
2. Grochulski, P., Masson, L., Borisova, S., Pusztai-Carey, M., Schwartz, J. L., Brousseau, R., and Cygler, M. (1995) *J. Mol. Biol.* **254,** 447–464
3. Pietrantonio, P. V., and Gill, S. S. (1996) in *Biology of the Insect Midgut* (Lehane, M. J., and Billingsley, P. F., eds) pp. 345–372, Chapman and Hall, London
4. Schnepf, H. E., Crickmore, N., Van Rie, J., Dereclus, D., Baum, J., Feitelson, J., Zeigler, D. R., and Dean, D. H. (1998) *Microbiol. Mol. Biol. Rev.* **62,** 775–806
5. Bravo, A., Jansens, S., and Peferoen, M. (1992) *J. Invertebr. Pathol.* **60,** 237–246
6. Hofmann, C., Vanderbruggen, H., Höfte, H., Van Rie, J., Jansens, S., and Van Mellaert, H. (1988) *Proc. Natl. Acad. Sci. U. S. A.* **85,** 7844–7848
7. Dean, D. H., Rajamohan, F., Lee, M. K., Wu, S.-J., Chen, X. J., Alcántara, E., and Hussain, S. R. (1996) *Gene (Amst.)* **179,** 111–117
8. Soberón, M., Perez, R. V., Nuñez-Valdéz, M. E., Lorence, A., Gómez, I., Sánchez, J., and Bravo, A. (2000) *FEMS Microbiol. Lett.* **191,** 221–225
9. Lorence, A., Darszon, A., Díaz, C., Liévano, A., Quintero, R., and Bravo A. (1995) *FEBS Lett.* **360,** 217–222
10. Schwartz, J. L., Garneau, L., Masson, L., Brousseau, R., and Rousseaeu, E. (1993) *J. Membr. Biol.* **132,** 53–62
11. Denolf, P., Hendrickx, K., VanDamme, J., Jansens, S., Peferoen, M., Egheele, D., and VanRie, J. (1997) *Eur. J. Biochem.* **248,** 748–761
12. Garczynski, S. F., and Adang, M. J. (1995) *Insect Biochem. Mol. Biol.* **25,** 409–415
13. Knight, P. J. K., Crickmore, N., and Ellar, D. J. (1994) *Mol. Microbiol.* **11,** 429–436
14. Belfiore, C. J., Vadlamudi, R. K., Osman, Y. A., and Bulla, L. A., Jr. (1994) *Biochem. Biophys. Res. Commun.* **200,** 359–364
15. Vadlamudi, R. K., Weber, E., Ji, I., Ji, T. H., and Bulla, L. A., Jr. (1995) *J. Biol. Chem.* **270,** 5490–5494
16. Nagamatsu, Y., Toda, S., Yagamuchi, F., Ogo, M., Kogure, M., Nakamura, M., Shibata, Y., and Katsumoto, T. (1998) *Biosci. Biotechnol. Biochem.* **62,** 718–726
17. Nagamatsu, Y., Koike, T., Sasaki, K., Yoshimoto, A., and Furukawa, Y. (1999) *FEBS Lett.* **460,** 385–390
18. Yaoi, K., Kadotani, T., Kuwana, H., Shinkawa, A., Takahashi, T., Iwahana, H., and Sato, R. (1997) *Eur. J. Biochem.* **246,** 652–657
19. Knowles, B. H., Knight, P. J. K., and Ellar., D. J. (1991) *Proc. R. Soc. Lond. B* **245,** 31–35
20. Gill, S. S., Cowles, E. A., and Francis, V. (1995) *J. Biol. Chem.* **270,** 27277–27282
21. Oltean, D. I., Pullikuth, A. K., Lee, H-K., and Gill, S. (1999) *Appl. Environ. Microbiol.* **65,** 4760–4766
22. Luo, K., Tabashnik, B. E., and Adang, M. J. (1997) *Appl. Environ. Microbiol.* **63,** 1024–1027
23. Lee, M. K., You, T. H., Young, B. A., Cotrill, J. A., Valaitis, A. P., and Dean, D. H. (1996) *Appl. Environ. Microbiol.* **62,** 2845–2849
24. Valaitis, A. P., Lee, M. K., Rajamohan, F., and Dean, D. H. (1995) *Insect Biochem. Mol. Biol.* **25,** 1143–1151
25. Masson, L., Lu, Y.-J., Mazza, A., Brousseau, R., and Adang, M. J. (1995) *J. Biol. Chem.* **270,** 20309–20315
26. Nakanishi, K., Yaoi, K., Shimada, N., Kadotani, T., and Sato, R. (1999) *Biochim. Biophys. Acta* **1432,** 57–63
27. Cortese, R., Felici, F., Galfre, G., Luzzago, A., Monaci, P., and Nicosia, A. (1994) *Trends Biotechnol.* **12,** 262–267
28. DeLeo, F., Yu, L., Burritt, J. B., Loetterle, L. R., Bond, C. B., and Jesaitis, A. J. (1995) *Proc. Natl. Acad. Sci. U. S. A.* **92,** 7110–7114
29. Demangel, C., Maroun, R. C., Rouyre, S., Bon, C., Mazié, J. -C., and Choumet, V. (2000) *Eur. J. Biochem.* **267,** 2345–2353
30. Luzzago, A., Felici, F., Tramontano, A., Pessi, A., and Cortese, R. (1993) *Gene (Amst.)* **128,** 51–57
31. Szardenings, M., Törnoth, S., Mutulis, F., Muceniece, R., Keinänen, K., Kuusinen, A., and Wikberg, J. E. S. (1997) *J. Biol. Chem.* **272,** 27943–27948
32. Lereclus, D., Arantès, O., Chaufaux, J., and Lecadet, M.-M. (1989) *FEMS Microbiol. Lett.* **60,** 211–218
33. Arantès, O., and Lereclus, D. (1991) *Gene (Amst.)* **108,** 115–119
34. Thomas, W. E., and Ellar, D. J. (1983) *J. Cell Sci.* **60,** 181–197
35. Aranda, E., Sanchez, J., Perferoen, M., Güereca, L., and Bravo, A. (1996) *J. Invertebr. Pathol.* **68,** 203–212
36. Nissim, A., Hoogenboom, H. R., Tomlinson, I. M., Flynn, G., Lidgley, C., Lane, D., and and Winter, G. (1994) *EMBO J.* **13,** 692–698
37. Hoogenboom, H. R., and Winter, G. (1992) *J. Mol. Biol.* **227,** 381–388
38. Marks, J. D., Hoogenboom, H. R., Bonnert, T. P., MacCafferty, J., Griffiths, A. D., and Winter, G. (1991) *J. Mol. Biol.* **222,** 581–597
39. Flores, H., Soberón, X., Sánchez, J., and Bravo, A. (1997) *FEBS Lett.* **414,** 313–318
40. Low, N. M., Holliger, P., and Winter G. (1996) *J. Mol. Biol.* **260,** 359–368
41. Wolfersberger, M., Lüthy, P., Maurer, A., Parenti, P., Sacchi, F. V., Giordana, B., and Hanozet, G. M. (1987) *Comp. Biochem. Physiol.* **86A,** 301–308
42. Myszka, D. G. (1999) *J. Mol. Recognit.* **12,** 279–284
43. Burton, S. L., Ellar, D. J., Li, J., and Derbyshire, D. J. (1999) *J. Mol. Biol.* **287,** 1011–1022
44. Jenkins, J. L., Lee, M. K., Valaitis, A. P., Curtiss, A., and Dean, D. H. (2000) *J. Biol. Chem.* **275,** 14423–14431
45. Garczynski, S. F., Crim, J. W., and Adang, M. J. (1991) *Appl. Environ. Microbiol.* **57,** 2816–2820
46. Keeton, T. P., and Bulla, L. A. (1997) *Appl. Environ. Microbiol.* **63,** 3419–3425
47. Ihara, H., Kuroda, E., Wadano, A., and Himeno, M. (1993) *Biosci. Biotechnol. Biochem.* **57,** 200–204

ANEXO II

Cadherin-like receptor binding facilitates proteolytic cleavage of helix α-1 in domain I and oligomer pre-pore formation of *Bacillus thuringiensis* Cry1Ab toxin.

Gómez, I., Sánchez, J., Miranda, R., Bravo, A., and Soberón M.

FEBS Letters. (2002).513:242-246.

FEBS Letters 513 (2002) 242–246 FEBS 25809

Cadherin-like receptor binding facilitates proteolytic cleavage of helix α-1 in domain I and oligomer pre-pore formation of *Bacillus thuringiensis* Cry1Ab toxin

Isabel Gómez, Jorge Sánchez, Raúl Miranda, Alejandra Bravo*, Mario Soberón**

Instituto de Biotecnología, Departamento de Microbiología Molecular, UNAM, Apdo postal 510-3, Cuernavaca, Morelos 62250, Mexico

Received 18 December 2001; revised 11 January 2002; accepted 13 January 2002

First published online 31 January 2002

Edited by Maurice Montal

Abstract **Cry toxins form lytic pores in the insect midgut cells. The role of receptor interaction in the process of protoxin activation was analyzed. Incubation of Cry1Ab protoxin with a single chain antibody that mimics the cadherin-like receptor and treatment with *Manduca sexta* midgut juice or trypsin, resulted in toxin preparations with high pore-forming activity in vitro. This activity correlates with the formation of a 250 kDa oligomer that lacks the helix α-1 of domain I. The oligomer, in contrast with the 60 kDa monomer, was capable of membrane insertion as judged by 8-anilino-1-naphthalenesulfonate binding. Cry1Ab protoxin was also activated to a 250 kDa oligomer by incubation with brush border membrane vesicles, presumably by the action of a membrane-associated protease. Finally, a model where receptor binding allows the efficient cleavage of α-1 and formation of a pre-pore oligomeric structure that is efficient in pore formation, is presented.** © 2002 Published by Elsevier Science B.V. on behalf of the Federation of European Biochemical Societies.

Key words: δ-Endotoxin; Protoxin activation; Receptor binding; Pre-pore; Membrane insertion

1. Introduction

Bacillus thuringiensis (Bt) is a bacterium that produces insecticidal proteins (Cry) toxic to different insect orders [1]. Cry toxins exert their pathological effect by forming lytic pores in the membrane of insect midgut cells [2].

The Cry proteins are solubilized within the insect gut due to the highly alkaline and reducing conditions of gut lumen. The liberated protoxins are activated by midgut proteases to release the toxin fragment [3]. The three-dimensional structures of some Cry toxins have been resolved [4–6] showing that they are comprised of three domains. Domain I, a seven-α helix bundle, is the pore-forming domain. Domain II and domain III, composed of β-sheets, are involved in receptor binding [7]. Cry toxin binds specifically to its receptors. Two Cry1A toxin receptors have been identified as aminopeptidase-*N* (APN) and cadherin-like ($Bt\text{-}R_1$, $Bt\text{-}R_{175}$) [8–14]. The debate on whether these are functional receptors leading to pore formation is still on-going. In contrast to APN, the expression of the cadherin-like protein from *Bombyx mori*, $Bt\text{-}R_{175}$, on the surface of Sf9 insect cells rendered them sensitive to Cry1Aa toxin [11]. Also, an *Heliothis virescens* population resistant to Cry1Ac toxin is mutated in a cadherin-like gene [15]. In previous work, a scFv antibody (scFv73) that inhibits binding of Cry1A toxins to cadherin-like receptors, but not to APN, and reduced the toxicity of Cry1Ab to *Manduca sexta* larvae was characterized. Interestingly, the CDR3 region of scFv73 shared homology with an eight amino acid epitope of *M. sexta* cadherin-like receptor, $Bt\text{-}R_1$ [16]. Overall, these results suggested that binding to cadherin-like receptor is an important step in the Cry1A toxins mode of action.

Following binding, it is proposed that at least part of the toxin inserts into the membrane resulting in pore formation [1,2]. The intermolecular interaction of Cry1Ab monomers is a necessary step for toxicity [17,18] and a tetrameric oligomer of Cry1Ac was observed in synthetic membranes [19]. However, it has not been established if oligomer formation occurs before (pre-pore) or after toxin insertion. Previous observations in our laboratory showed that trypsin-activated Cry1A protoxins, resulted in toxin preparations with low pore formation activity in vitro, despite the fact that they retained toxicity [20], suggesting an incomplete activation. Also, *M. sexta* midgut juice (MJ) treatment of Cry1Ab protoxin produced proteolytic cleavages inside the toxin. Two additional nicks were identified which remove helices α-1 and α-2 of domain I. The highest in vitro pore formation activity was observed after helix α-1 was removed [20]. Similar results were obtained for Cry1Ac protoxin activated with MJ from *Pieris brassica* [21]. These results suggest that in vivo, further proteolytical cleavages may occur for toxin activation.

In this work we analyzed if receptor interaction, using the scFv73 antibody as model receptor, is a necessary step for an efficient proteolytic activation of Cry1A toxins. We show that Cry1Ab toxin binding to the cadherin-like receptor promotes complete proteolytic activation and a pre-pore formation that is insertion competent leading to the formation of functional ionic pores in vitro.

2. Materials and methods

2.1. MJ isolation and activation of Cry1Ab protoxin

M. sexta larvae were reared on artificial diet. Midgut tissue was dissected from 5th instar larvae. MJ was separated from solid material by centrifugation and filtered through 0.22 μm filters.

*Corresponding author. Fax: (52)-777-3 172388.
**Corresponding author.
E-mail addresses: bravo@ibt.unam.mx (A. Bravo), mario@ibt.unam.mx (M. Soberón).

Abbreviations: BBMV, brush border membrane vesicles; APN, aminopeptidase-*N*; MJ, midgut juice; ANS, 8-anilino-1-naphthalenesulfonate hemimagnesium; Dis-C_3-(5), 3,3′-dipropylthiodicarbocyanine

0014-5793/02/$22.00
PII: S0014-5793(02)02321-9

Cry1Ab crystals were produced in *Bt* strain 407*cry*$^-$ transformed with pHT315-1Ab [16]. Cry1Ab crystal purification and protoxin solubilization were done as described [16]. For activation, 1–2 mg/ml Cry1Ab protoxin was incubated 1 h with 1/1 ratio of scFv73. Trypsin (1/20 ratio) or MJ (5%) was added and incubated 1 h at 37°C. PMSF (1 mM) was added and samples centrifuged (20 min at 12000×*g*). For protoxin activation with brush border membrane vesicles (BBMV), 100 nM Cry1Ab protoxin was incubated 15 min with 10 μg BBMV, stopped with PMSF and centrifuged as above. Purification of the activated toxins was done by size exclusion chromatography with Superdex 200 HR 10/30 (Amersham Pharmacia Biotech, Sweden) FPLC size exclusion as described [22]. N-terminal sequencing was performed at the Harvard Microchemistry Facility of Harvard University (Cambridge, MA, USA) after 7% SDS–PAGE and transfer onto polyvinylidene difluoride membranes.

2.2. Western blot of Cry1Ab toxin

Activated toxin was separated in SDS–PAGE, transferred onto a nitrocellulose membrane PVDF, blocked with slimed milk (5%) and detected with anti-Cry1Ab polyclonal antibody (1/80000; 1 h) and visualized with a goat anti-rabbit antibody coupled with horseradish peroxidase (HR) (Sigma, St. Louis, MO, USA) (1/1000; 1 h), followed by SuperSignal chemiluminescent substrate (Pierce, Rockford, IL, USA) as described by the manufacturers.

2.3. Purification and characterization of scFv

Escherichia coli scFv fragments were purified to homogeneity by an Ni-agarose column, as described [16].

2.4. Preparation of BBMV

BBMV from 5th instar *M. sexta* larvae were prepared and dialyzed against 150 mM KCl, 2 mM EGTA, 0.5 mM EDTA, 10 mM HEPES–HCl pH 7.5 as reported [16]. BBMV for activation of Cry1A protoxins were prepared as above without protease inhibitors.

2.5. Fluorescence measurements

Membrane potential was monitored with the fluorescent positively charged dye, 3,3′-dipropylthiodicarbocyanine (Dis-C_3-(5)), in an Aminco Bowman luminescence spectrometer (Urbana, IL, USA) as in [24].

2.6. ANS binding

Binding of 8-anilino-1-naphthalenesulfonate hemimagnesium (ANS, 15 μM, Sigma, St. Louis. MO, USA) was measured as reported [25] at 380/480 nm excitation/emission wavelengths pair.

2.7. Insect bioassay

Bioassays were performed with *M. sexta* neonate larvae as reported [26]. The effective doses were calculated using PROBIT analysis.

3. Results

3.1. Proteolytic activation of Cry1Ab protoxin in the presence of scFv73 antibody

We isolated a single chain antibody (scFv73) that interfered the interaction of Cry1Ab toxin with BBMV from *M. sexta* [16]. The characterization of scFv73 led to the identification of two discrete eight residue regions present in cadherin-like receptors from *M. sexta* and *B. mori*, that were sufficient to compete binding of Cry1Ab and Cry1Aa to cadherin proteins and to negatively affect toxicity of Cry1Ab against *M. sexta* larvae [16]. Therefore scFv73 can be used as a surrogate of cadherin-like receptors.

To analyze the effect of Cry toxin binding to this epitope in the activation process, Cry1Ab protoxin was preincubated with scFv73 at room temperature and treated afterwards with trypsin or with MJ from *M. sexta* larvae. As control, Cry1Ab protoxin was incubated with scFv45 that binds Cry1Ab but has no effect on Cry1Ab binding to Bt-R_1 or in toxicity [16]. MJ or trypsin completely degrade scFv as

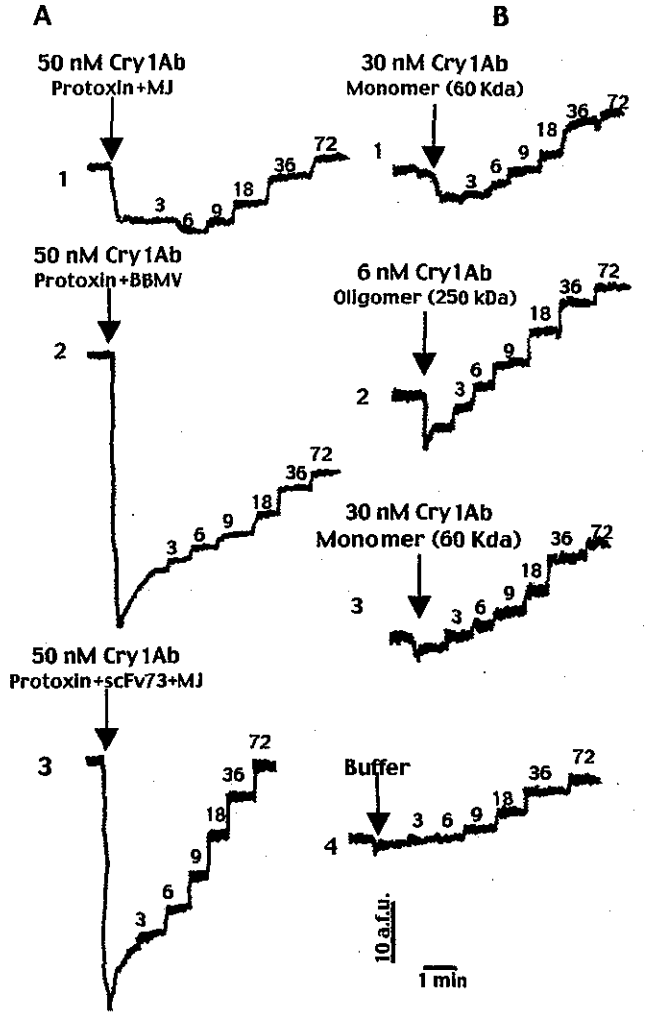

Fig. 1. K^+ permeability across *M. sexta* BBMV induced by Cry1Ab-activated toxins. Changes in distribution of a fluorescent dye (Dis-C_3-(5)) sensitive to change in membrane potential were recorded as 2.5. A: Trace 1, Cry1Ab toxin activated with MJ (50 nM); trace 2, Cry1Ab toxin activated with BBMV (50 nM); trace 3, Cry1Ab toxin activated with scFv73 and MJ (50 nM). B: K^+ permeability of purified Cry1Ab toxins by size exclusion. Trace 1, Cry1Ab 60 kDa monomer (30 nM) (fraction 17 of Fig. 2C); trace 2, Cry1Ab 250 kDa oligomer (6 nM) (fraction 9* of Fig. 2C); trace 3, Cry1Ab 60 kDa monomer (30 nM) (fraction 17* of Fig. 2C); trace 4, control, buffer addition. The arrow on the top of the traces corresponds to the time of toxin addition. An upward deflection indicates a membrane depolarization. Numbers in traces indicate the final K^+ concentrations (mM).

judged by SDS–PAGE and Western blot (see below). In vitro K^+ permeability assays were performed using a fluorescent positively charged dye (Dis-C_3-(5)) sensitive to changes in membrane potential as reported [24] in isolated *M. sexta* BBMV with the different toxin preparations (Fig. 1A, Table 1). Proteolytic activation of Cry1Ab protoxin incubated with scFv73 and treatment with MJ or trypsin resulted in toxin preparations with high pore formation activities, in contrast with the Cry1Ab protoxin incubated with scFv45 or treated only with MJ or trypsin (Table 1). Also, Cry1Ab protoxin or scFv73 alone or a mixture of both without further treatment with proteases, showed no pore formation activity in vitro (data not shown). Addition of 50 nM of scFv73-MJ-activated Cry1Ab toxin to BBMV loaded with 150 mM KCl and sus-

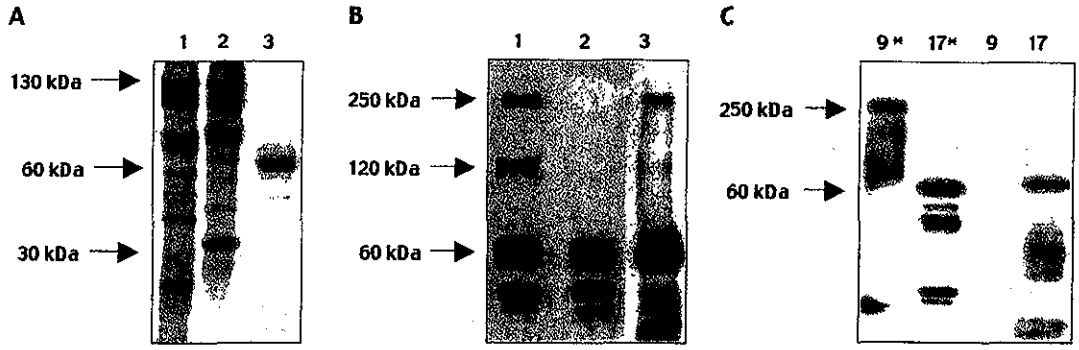

Fig. 2. SDS–PAGE and Western blots of activated Cry1Ab toxin. A: SDS–PAGE (10% acrylamide): lane 1, Cry1Ab protoxin; lane 2, Cry1Ab protoxin with scFv73; and lane 3, Cry1Ab protoxin with scFv73 and treated 1 h with MJ. B: Western blotting (SDS–PAGE 7% acrylamide) detected with an anti-Cry1Ab polyclonal antibody. Lane 1, Cry1Ab protoxin activated with scFv73 and MJ; lane 2, Cry1Ab protoxin activated only with MJ; lane 3, Cry1Ab protoxin activated with *M. sexta* BBMV. C: Western blotting (SDS–PAGE 12% acrylamide) of samples from size exclusion chromatography of Cry1Ab protoxins activated with scFv73 and MJ (*) or with MJ. Proteins were revealed with anti-Cry1Ab polyclonal antibody. Numbers in C are the retention times of the different fractions.

pended in 150 mM MeGluCl produced a fast hyperpolarization (Fig. 1A). The response of the Dis-C_3-(5) dye to KCl additions also increased, when compared to the control in which the same amount of buffer was added. After each KCl addition a new membrane potential is established, and a depolarization is produced. Preincubation of Cry1Ab protoxin with scFv73 was necessary since simultaneous addition of scFv73 and MJ proteases resulted in no pore formation (Table 1). Activation was further improved when scFv73 was preincubated with Cry1Ab protoxin at 37°C, suggesting a better interaction at this temperature (Table 1).

Bioassays were performed with toxin preparations obtained by MJ treatment in the presence or absence of scFv73. Table 2 shows that toxin preparations obtained in the presence of scFv73 showed similar LC_{50} than Cry1Ab protoxin and 10 times higher toxicity than toxin treated with MJ in absence of scFv73.

3.2. *In vitro pore formation activity correlates with oligomer formation*

Fig. 2A shows a SDS–PAGE of different samples of Cry1Ab protoxin. A major band of 130 kDa was observed in the Cry1Ab protoxin samples in the absence or presence of scFv73 (Fig. 2A, lanes 1 and 2), an additional 30 kDa band was also observed in the sample incubated with scFv73 that corresponds to the molecular mass of the scFv molecule. In contrast, in the Cry1Ab protoxin sample incubated with scFv73 and treated with MJ only a 60 kDa band was observed suggesting that scFv73 was degraded by the protease treatment (Fig. 2A, lane 3). Western blot of Cry1Ab-activated proteins, using an anti-Cry1Ab polyclonal antibody, was performed. Fig. 2B shows that a major 60 kDa protein and lower molecular mass proteins were obtained as reported [20]. However, additional higher molecular mass bands (120 and 250 kDa) that reacted with poly-Cry1Ab, were observed in toxin preparations obtained in the presence of scFv73. The molecular sizes of these proteins correspond to dimers and tetramers of Cry1Ab. The samples containing the oligomers were treated at different temperatures before loading the gels. The same amount of the 250 kDa oligomer was observed at 50°C, 80°C or boiling, implying that oligomers were highly stable (data not shown). To analyze if scFv73 was part of the oligomer, a Western blot using anti-mic tag antibody was performed showing that the scFv73 was not part of the oligomer (data not shown). To further characterize the putative oligomers, Cry1Ab toxin preparations obtained by MJ treat-

Table 1
K^+ permeability of Cry1Ab-activated toxins

Sample	$m-m^a_{int}$ (K^+ permeability)	% K^+ permeability
Protox. Cry1Ab+scFv73+trypsin	0.202	41
Protox. Cry1Ab+scFv73+MJ	0.392	78
Protox. Cry1Ab+scFv45+trypsin	0.049	10
Protox. Cry1Ab+scFv45+MJ	0.027	5
Protox. Cry1Ab+MJ	0.045	9
Protox. Cry1Ab+scFv73+MJ at 37°C	0.498	100
Protox. Cry1Ab+scFv73+MJ (mixed)[b]	0.087	18
Protox. Cry1Ab+BBMV	0.143	29
Protox. Cry1Ab+MJ (monomer)[c]	0.049 (0.079)[e]	10 (16)
Protox. Cry1Ab+scFv73+MJ (monomer)[c]	0.047 (0.076)	10 (16)
Protox. Cry1Ab+scFv73+MJ (oligomer)[d]	0.122 (1.02)	25 (207)

Values are means of four different determinations. Standard deviations were less than 10%. 50 nM toxin for each assay except where indicated.
[a]The differences of the slope of the curve of each activated toxin (m_{tox}) minus the slope of the control trace in which the same amount of buffer was added [m_{int}] are presented.
[b]Cry1Ab protoxin and scFv73 were not preincubated and were mixed along with the MJ.
[c]30 nM toxin. Proteins after size excusion chromatography of activated Cry1Ab toxin as indicated.
[d]60 nM toxin. Proteins after size excusion chromatography of activated Cry1Ab toxin as indicated.
[e]Numbers in parentheses are values obtained considering 50 nM protein concentration as the rest of the treatments.

ment in the presence or absence of scFv73 were subject to size exclusion chromatography and poly-Cry1Ab detection. Fig. 2C shows that a major fraction containing the monomer (60 kDa) was obtained in both toxin preparations (retention time 17 min). In this fraction, lower molecular mass proteins that co-eluted with the 60 kDa monomer were observed. These smaller proteins are the product of proteolysis within domain II that co-eluted with the monomer since they remain attached after nicking [20]. However, in the toxin preparation obtained in the presence of scFv73 the 250 kDa oligomer (retention time 9 min), was observed (Fig. 2C). The 120 kDa protein was not observed after size exclusion. The same samples of the chromatography were blotted and revealed using a monoclonal 4D6 that recognizes an epitope in domain I of Cry1Ab [23]. 4D6 only recognized the Cry1Ab monomer (data not shown).

Finally, pore formation activity of the 250 kDa oligomer and of 60 kDa monomers obtained after size exclusion chromatography was determined. Fig. 1B and Table 1 show that only the oligomer had pore formation activity in vitro.

3.3. Oligomer formation involves cleavage after helix α-1

The amino-terminal sequences of the 60 kDa monomer and the 250 kDa oligomer were determined. The amino terminal sequence of the monomer (^{29}IETGYTP) corresponds to the beginning of helix α-1, in contrast to the oligomer (^{51}VPGAG) that was located between helices α-1 and α-2, showing that the helix α-1 was removed.

3.4. ANS binding to Cry1Ab monomer and oligomer

ANS binds to solvent-accessible clusters of non-polar residues [27], which are relatively rare in the native state of soluble proteins. We analyzed ANS binding to the 250 kDa oligomer, and to the 60 kDa monomer. Fig. 3 shows that only the toxin preparation containing the oligomer bound ANS.

3.5. Activation of Cry1Ab toxin with membrane-associated proteases

Cry1Ab protoxin was activated by incubation with BBMV preparations isolated without protease inhibitors for different times and analyzed by SDS–PAGE and Western blot with poly-Cry1Ab. Incubation of Cry1Ab protoxin with BBMV prepared in the absence of proteinase inhibitors for 15 min was enough to digest the protoxin to a 60 kDa polypeptide (Fig. 2B) suggesting the existence of proteases associated with the BBMV. The formation of the 250 kDa oligomer (Fig. 2B), which showed in vitro pore formation activity (Fig. 1A, Table 1) was also observed.

4. Discussion

The accepted mode of action of Cry toxins involves solubilization of Cry proteins, proteolytic activation, receptor binding, membrane insertion, toxin oligomerization and finally pore formation leading to cell swelling and lysis [7]. It is accepted that the pore is formed by the aggregation of several monomers [17–19]. However, it is still unclear if oligomer formation occurs before or after membrane insertion. Neither is clear if receptor binding is important in the process of oligomer formation. In this work we provide evidences for an active role of receptor binding in the process of proteolytic activation. Moreover, our data support the formation of a pre-pore structure that is capable of inserting into membranes. Thus, the proposed mode of action of Cry toxins now resembles the one proposed for several other pore-forming toxins in which proteolytic cleavage after receptor binding promotes pre-pore oligomer formation as a prerequisite for membrane insertion [25,28–31]. We show here that cadherin binding promotes efficient proteolytic activation of Cry1Ab toxin that leads to dimer and tetrameric oligomer formation. However, the dimer was consistently observed in lower amounts than the tetramer (Fig. 2B) and could not be detected after separation by size exclusion suggesting that the dimer could be an unstable intermediate in the formation of the tetramer. The tetrameric oligomer correlates with higher in vitro pore formation activity and enhanced Cry1Ab toxicity (Fig. 1B). The similar activation with scFv73 and MJ was obtained for Cry1Aa protoxin (data not shown).

Cry toxins do not form spontaneous oligomers in solution in vitro [22], suggesting that in vivo the oligomer formation may occur either after receptor binding or by lateral movement of monomers in the membrane. Our data support that the Cry1Ab oligomer is formed after receptor binding and before membrane insertion, forming a pre-pore structure that is insertion competent. The oligomer preferentially bound ANS that specifically reacts with solvent-accessible clusters of non-polar residues suggesting that oligomerization is accompanied by exposure of a hydrophobic surface. Binding of Cry1Ab toxin to the cadherin epitope analyzed in this work [16] seems to be a key step in the process of protease cleavage and pre-pore formation. However, the efficiency of Cry1Ab activation in vitro in the presence of scFv73 was low since a large proportion of the toxin remained monomeric (Fig. 2). Affinity of scFv73 to Cry1A toxins was in the range of 20–50 nM [16] in contrast with 1 nM of purified Bt-R_1 [10], suggesting that additional epitopes in the receptor may contribute to the binding interaction, or other receptors might be involved

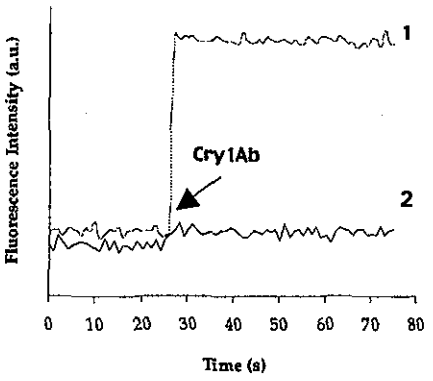

Fig. 3. ANS binding to Cry1Ab protoxin activated in the presence of scFv73 and MJ (1) or with MJ (2). Samples correspond to proteins shown in Fig. 2B, lanes 1 and 2 respectively. After 25 s 1.5 μg protein of the Cry1Ab samples was added.

Table 2
Toxicity of Cry1Ab-activated toxins to *M. sexta*

Treatment	LC_{50} (ng/cm^2)[a]
Protoxin Cry1Ab	1 (0.5–1.7)
Protoxin Cry1Ab+scFv73+MJ	1.6 (0.78–3.01)
Protoxin Cry1Ab+MJ	20.7 (14.3–67.4)

[a]LC_{50} values and (95% confidence limits) calculated by probit analysis.

(e.g. APN). Another possibility, to explain the low efficiency is that since scFv73 is degraded by the protease treatment, most of the Cry1Ab proteins loose scFv73 binding before a proper cleavage. The activation with BBMV was less efficient than with scFv73. It is likely that cadherin concentration in BBMV was low compared with the excess of scFv73 used (1/1 ratio). Also, the fact that BBMV were purified in the absence of proteinase inhibitors could reduce even more the concentration of active receptor. This remains to be analyzed.

Our data indicate that cadherin receptor binding is involved in proteolytic activation of Cry1Ab protoxin, promoting the formation of an oligomeric structure which exposes hydrophobic residues and is active for pore formation activity.

Acknowledgements: Oswaldo Lopez is acknowledged for technical assistance. This work was supported by CONACyT 27637-N and G36505N, DGAPA IN206200 and IN216300 and EC-INCO ERB3514PL972673. IG to CONACyT for PhD fellowship.

References

[1] Crickmore, N., Zeigler, D.R., Feitelson, J., Schnepf, E., Van Rie, J., Lereclus, D., Baum, J. and Dean, D.H. (1998) Microbiol. Mol. Biol. Rev. 62, 807–813.
[2] DeMaagd, R.A., Bravo, A. and Crickmore, N. (2001) Trends Genet. 17, 193–199.
[3] Choma, C.T., Surewicz, W.K., Carey, P.R., Pozsgay, M., Raynor, T. and Kaplan, H. (1990) Eur. J. Biochem. 189, 523–527.
[4] Li, J., Carroll, J. and Ellar, D.J. (1991) Nature 353, 815–821.
[5] Grochulski, P., Masson, L., Borisova, S., Pusztai-Carey, M., Schwartz, J.L., Brousseau, R. and Cygler, M. (1995) J. Mol. Biol. 254, 447–464.
[6] Morse, R.J., Yamamoto, T. and Stroud, R.M. (2001) Structure 9, 409–417.
[7] Schnepf, H.E., Crickmore, N., Van Rie, J., Lereclus, D., Baum, J., Feitelson, J., Zeigler, D.R. and Dean, D.H. (1998) Microbiol. Mol. Biol. Rev. 62, 775–806.
[8] Garczynski, S.F. and Adang, M.J. (1995) Insect. Biochem. Mol. Biol. 25, 409–415.
[9] Knight, P.J.K., Crickmore, N. and Ellar, D.J. (1994) Mol. Microbiol. 11, 429–436.
[10] Vadlamudi, R.K., Weber, E., Ji, I., Ji, T.H. and Bulla Jr., L.A. (1995) J. Biol. Chem. 270, 5490–5494.
[11] Nagamatsu, Y., Koike, T., Sasaki, K., Yoshimoto, A. and Furukawa, Y. (1999) FEBS Lett. 460, 385–390.
[12] Yaoi, K., Kadotani, T., Kuwana, H., Shinkawa, A., Takahashi, T., Iwahana, H. and Sato, R. (1997) Eur. J. Biochem. 246, 652–657.
[13] Gill, S.S., Cowles, E.A. and Francis, V. (1995) J. Biol. Chem. 270, 27277–27282.
[14] Oltean, D.I., Pullikuth, A.K., Lee, H-K. and Gill, S.S. (1999) Appl. Environ. Microbiol. 65, 4760–4766.
[15] Gahan, L.J., Gould, F. and Heckel, D.G. (2001) Science 293, 857–860.
[16] Gomez, I., Oltean, D.I., Gill, S.S., Bravo, A. and Soberón, M. (2001) J. Biol. Chem. 276, 28906–28912.
[17] Aronson, A., Geng, Ch. and Wu, L. (1999) Appl. Environ. Microbiol. 65, 2503–2507.
[18] Soberón, M., Perez, R.V., Nuñez-Valdéz, M.E., Lorence, A., Gómez, I., Sánchez, J. and Bravo, A. (2000) FEMS Microbiol. Lett. 191, 221–225.
[19] Vie, V., Van Mau, N., Pomarede, P., Dance, C., Schwartz, J.L., Laprade, R., Frutos, R., Rang, C., Masson, L., Heitz, F. and Le Grimellec, C. (2001) J. Membr. Biol. 180, 195–203.
[20] Miranda, R., Zamudio, F. and Bravo, A. (2001) Insect. Biochem. Mol. Biol. 31, 1153–1155.
[21] Lightwood, D.J., Ellar, D. and Jarret, P. (2000) Appl. Environ. Microbiol. 66, 5174–5181.
[22] Guereca, L. and Bravo, A. (1998) Biochim. Biophys. Acta 1429, 342–350.
[23] Höfte, H., Van Rie, J., Jansens, S., Van Houtven, A., Vanderbruggen, H. and Vaeck, M. (1988) Appl. Environ. Microbiol. 54, 2010–2017.
[24] Lorence, A., Darszon, A., Díaz, C., Liévano, A., Quintero, R. and Bravo, A. (1995) FEBS Lett. 360, 217–222.
[25] van der Goot, F.G., Pattus, F., Wong, K.R. and Buckley, T. (1993) Biochemistry 32, 2636–2642.
[26] Bravo, A., Jansens, S. and Peferoen, M. (1992) J. Invertebr. Pathol. 60, 237–246.
[27] Stryer, L. (1965) J. Mol. Biol. 13, 482.
[28] Klimpel, K.P., Molloy, S.S., Thomas, G. and Leppla, S.H. (1992) Proc. Natl. Acad. Sci. USA 89, 10277–10281.
[29] Walker, B., Krishnasastry, M., Zorn, L. and Bayley, H. (1992) J. Biol. Chem. 267, 21782–21786.
[30] Chiron, M.F., Frylin, C.M. and FitzGerald, D.J. (1994) J. Biol. Chem. 269, 18167–18176.
[31] Abrami, L., Fivaz, M., Decroly, E., Seidah, N.G., Jean, F., Thomas, G., Leppla, S.H., Buckley, J.T. and van der Goot, F.G. (1998) J. Biol. Chem. 273, 32656–32661.

ANEXO III

Hydropathic complementarity determines interaction of epitope ^{869}HITDTNNK^{876} in *Manduca sexta* Bt-R_1 receptor with loop 2 of domain II of *Bacillus thuringiensis* Cry1A toxins.

Gómez I., Miranda-Rios J.,Rudiño-Piñera E., Oltean D. I., Gill S. S., Bravo A. and Soberón M.

Journal of Biological Chemistry. (2002). 277:30137-30143.

THE JOURNAL OF BIOLOGICAL CHEMISTRY
© 2002 by The American Society for Biochemistry and Molecular Biology, Inc.

Vol. 277, No. 33, Issue of August 16, pp. 30137–30143, 2002
Printed in U.S.A.

Hydropathic Complementarity Determines Interaction of Epitope ^{869}HITDTNNK^{876} in *Manduca sexta* Bt-R_1 Receptor with Loop 2 of Domain II of *Bacillus thuringiensis* Cry1A Toxins*

Received for publication, April 1, 2002, and in revised form, May 3, 2002
Published, JBC Papers in Press, June 5, 2002, DOI 10.1074/jbc.M203121200

Isabel Gomez‡§, Juan Miranda-Rios‡, Enrique Rudiño-Piñera¶, Daniela I. Oltean‖, Sarjeet S. Gill‖, Alejandra Bravo‡, and Mario Soberón‡**

From the ‡Departamento de Microbiología Molecular and ¶Departamento de Reconocimiento Molecular y Bioestructura, Instituto de Biotecnología, Universidad Nacional Autónoma de México, Apdo postal 510-3, Cuernavaca, Morelos 62250, México and the ‖Department of Cell Biology and Neuroscience, University of California, Riverside, California 92521

In susceptible insects, Cry toxin specificity correlates with receptor recognition. In previous work, we characterized an scFv antibody (scFv73) that inhibits binding of Cry1A toxins to cadherin-like receptor. The CDR3 region of scFv73 shared homology with an 8-amino acid epitope (^{869}HITDTNNK^{876}) of the *Manduca sexta* cadherin-like receptor Bt-R_1 (Gomez, I., Oltean, D. I., Gill, S. S., Bravo, A., and Soberón, M. (2001) *J. Biol. Chem.* 276, 28906–28912). In this work, we show that the previous sequence of scFv73 CDR3 region was obtained from the noncoding DNA strand. However, most importantly, both scFv73 CDR3 amino acid sequences of the coding and noncoding DNA strands have similar binding capabilities to Cry1Ab toxin as Bt-R_1 ^{869}HITDTNNK^{876} epitope, as demonstrated by the competition of scFv73 with binding to Cry1Ab with synthetic peptides with amino acid sequences corresponding to these regions. Using synthetic peptides corresponding to three exposed loop regions of domain II of Cry1Aa and Cry1Ab toxins, we found that loop 2 synthetic peptide competed with binding of scFv73 to Cry1A toxins in Western blot experiments. Also, loop 2 mutations that affect toxicity of Cry1Ab toxin are affected in scFv73 binding. Toxin overlay assays of Cry1A toxins to *M. sexta* brush border membrane proteins showed that loop 2 synthetic peptides competed with binding of Cry1A toxins to cadherin-like Bt-R_1 receptor. These experiments identified loop 2 in domain II of as the cognate binding partner of Bt-R_1 ^{869}HITDTNNK^{876}. Finally, 10 amino acids from β-6-loop 2 region of Cry1Ab toxin (^{363}SSTLYRRPFNI^{373}) showed hydropathic pattern complementarity to a 10-amino acid region of Bt-R_1 (^{865}NITIHITDTNN^{875}), suggesting that binding of Cry1A toxins to Bt-R_1 is determined by hydropathic complementarity and that the binding epitope of Bt-R_1 may be larger than the one identified by amino acid sequence similarity to scFv73.

Bacillus thuringiensis (Bt)[1] is an aerobic, spore-forming bacteria that produces crystalline inclusions during the sporulation phase (1, 2). These inclusions, which are toxic to larvae of several insects orders as well as to other invertebrates, are composed of proteins known as Cry toxins (1, 2).

The inclusions are solubilized within the lepidopteran gut lumen to its highly alkaline pH and reducing conditions. Cry proteins are produced as protoxins that are activated by midgut proteases to release the toxin fragment (3). It is generally accepted that Cry toxins exert their pathological effect by forming lytic pores in the membrane of insect midgut epithelial cells (1, 2).

The three-dimensional structures of Cry3A (coleopteran-specific), Cry1Aa (lepidopteran-specific) trypsin-activated toxins, and of Cry2A (dipteran-specific) protoxin have been resolved by x-ray diffraction crystallography (4–6). The three proteins share many similar features and are comprised of three domains. In particular, Cry1Aa and Cry3A structures are more similar and have the following characteristics. The N-terminal domain I, a seven-α-helix bundle in which helix α-5 is encircled by the other helices, is the pore-forming domain. Domain II consists of three anti-parallel β-sheets with exposed loop regions, and domain III is a β-sandwich (4, 5). Domains II and III are involved in receptor binding (for reviews, see Refs. 1, 2, and 7).

The activated Cry toxin binds specifically to its receptors located on the midgut epithelium. In susceptible insects, Cry toxin specificity correlates with receptor recognition (8, 9). The identification of epitopes involved in Cry toxin-receptor interactions could provide insights into the mechanism of insect specificity and the mode of action of these toxins. Also, this knowledge could offer tools for improving the specificity and toxicity of Cry toxins. Two Cry1A toxin receptors from various lepidopteran insects have been identified as aminopeptidase N (APN) and cadherin-like proteins (Bt-R_1, Bt-R_{175}) (10–16). In *Lymantria dispar*, besides APN and cadherin-like receptors, a high molecular weight anionic protein (Bt-R_{270}) that binds Cry1A toxins with high affinity was identified (17). However, an on-going debate is whether these are functional receptors leading to toxin pore formation activity. In contrast to APN, expression of the cadherin-like protein from *Bombyx mori*, Bt-R_{175}, on the surface of Sf9 insect cells made these cells sensitive to Cry1Aa toxin (13). Also, a *Heliothis virescens* population

* This work was supported in part by Consejo Nacional de Ciencia y Tecnologia Contracts 27637-N and G36505-N, Dirección General de Asuntos del Personal Académico-Universidad Nacional Autónoma de México Grants IN206200 and IN216300, UC MEXUS-CONACYT, and the University of California Toxic Substance Research Teaching program. The costs of publication of this article were defrayed in part by the payment of page charges. This article must therefore be hereby marked "*advertisement*" in accordance with 18 U.S.C. Section 1734 solely to indicate this fact.

§ Supported in part by a Consejo Nacional de Ciencia y Tecnologia Ph.D. fellowship.

** To whom correspondence should be addressed. Tel.: 52-777-329-16-18; Fax: 52-777-317-23-88; E-mail: mario@ibt.unam.mx.

[1] The abbreviations used are: Bt, *B. thuringiensis*; APN, aminopeptidase N; BBMV, brush border membrane vesicles; SPR, surface plasmon resonance; CDR, complementary determinant region; scFv, single-chain variable fragment.

resistant to Cry1Ac toxin contained a mutation in a cadherin-like coding gene (18). Moreover, in previous work we identified a scFv antibody (scFv73) that inhibited binding of Cry1A toxins to cadherin-like receptors, but not to APN, and reduced the toxicity of Cry1Ab to *Manduca sexta* larvae. Interestingly the CDR3 region of scFv73 shared homology with an eight-amino acid epitope of *M. sexta* cadherin-like receptor, Bt-R_1, involved in Cry1A interaction (19). Evidence was obtained that showed Cry1A toxin binding to this cadherin epitope facilitates proteolytic cleavage of helix α-1 in domain I and formation of a tetramer oligomer pre-pore that is insertion-competent (20). Overall, these results suggest that binding to cadherin-like receptor is an important step in the mode of action Cry1A toxins.

Site-directed mutagenesis studies of Cry1A toxins revealed that loop α-8, located in the junction of domains I and II, and loop 2 and loop 3 regions of domain II are involved in receptor recognition and toxicity (21–26). Interestingly enough, Cry1Aa and Cry1Ab toxins have different loop 2 and loop 3 amino acid sequences despite the fact that they interact with the same *M. sexta* receptors, APN and Bt-R_1 (10–12, 24, 27, 28).

In regard to the receptor binding epitopes, in *B. mori* APN, a region of 63 residues involved in Cry1Aa binding was identified. This site was specific for Cry1Aa toxin since it was not involved in Cry1Ac binding (29). In cadherin-like receptors, a region located between residues 1245 and 1391 of Bt-R_{175} was identified as a binding region important for Cry1Aa interaction (13). We identified an 8-amino acid epitope in Bt-R_1 (^{869}HITDTNNK^{876}) and 2 amino acid epitopes in *B. mori* Bt-R_{175} (^{873}IIDTNNK^{880} and ^{1296}LDETTN^{1301}) involved in binding of Cry1A toxins (19). To study the mechanism of receptor interaction it is important to identify the Cry1A cognate binding partner for Bt-R_1 ^{869}HITDTNNK^{876} epitope.

The molecular basis of protein-protein interactions remains largely unknown, although accumulating evidence indicates that proteins can interact through amino acid sequences displaying inverse hydropathic profiles leading to the concept of hydropathic complementarity (30). One model for interacting complementary structures postulates secondary structures, β-strands and α-helices, in which the hydrophilic surfaces are oriented toward the aqueous phases, whereas hydrophobic surfaces face each other (31), and another model suggests complementary surface contour (32). This concept has been crucial for the molecular recognition theory that proposes that peptides whose sequences are obtained from the noncoding DNA strands likely bind the amino acid sequence of the coding strand since they have inverted hydropathic patterns (30, 33). Among more than 40 examples (for review, see Ref. 34) hydropathic complementarity has been successfully applied to produce biologically active synthetic analogs of receptor binding sites (33, 35, 36) and ligands (37) and to map binding epitopes of natural ligands with their receptors (38, 39). Also, hydropathic complementarity has been shown to determine several peptide-antibody interactions (40). However, there are few examples of naturally occurring peptides or proteins whose similarity in binding properties is correlated with similar hydropathic patterns.

In this work, we demonstrate that the scFv73 CDR3 region interacts with the same epitope in Cry1Ab toxin as the ^{869}HITDTNNK^{876} epitope of Bt-R_1. Also, we identified domain II loop 2 of Cry1A toxins as the cognate binding partner of the Bt-R_1 ^{869}HITDTNNK^{876} epitope. Finally, hydropathic profiles analyses of the loop 2 regions in the toxins and of the cadherin-like receptor Bt-R_1 binding epitope revealed that hydropathic complementarity could account for the interaction of Cry1A toxins with their cadherin-like receptors and that the binding epitope in Bt-R_1 is likely to include residues ^{865}NITIHITDTNN^{875}.

MATERIALS AND METHODS

Bacterial Strains, Plasmids, and Media—*Escherichia coli* strains and Bt strains producing Cry1Aa and Cry1Ab toxins, acrystalliferous strain 407*cry*$^-$ (41) transformed with pHT409 (42) harboring the *cry1Aa* gene or pHT315–1Ab (19), were grown in Luria broth or in nutrient broth sporulation medium (nutrient broth) as described (19). An *E. coli* strain harboring *cry*1Ab F371A was kindly supplied by Dr. Dean (Ohio State University).

Purification of Cry1A Toxins—The Cry1Aa and Cry1Ab crystals produced by Bt strains were isolated, trypsin-activated, and purified by Q-Sepharose as described (19, 43, 44). Mutant F371A was expressed in *E. coli* and purified as previously described (45).

Sequencing of Clones—CDR3 sequence was determined using primers CDRFOR (5′-CAGGGTACCTTGGCCCCA-3′) as reported previously (19). From the sequence obtained, another primer was designed CDRb (5′-AGCCTGAGATCTGACGACAC-3′) to read the coding strand. A third primer that overlaps with CDRFOR, CDRa (5′-TCGAGACGGTGACCAGGGTA-3′), was used to read the noncoding DNA strand.

Purification and Characterization of scFv73—scFv73 antibody was purified from *E. coli* cells to homogeneity by a nickel-agarose column as described (19).

Western Blotting of Cry1Ab with scFv73—Trypsin-activated Cry1Aa or Cry1Ab toxin was separated in 9% SDS-PAGE, transferred onto a nitrocellulose membrane polyvinylidene difluoride, and blocked with skim milk (5%). The membranes were then incubated in 200 nM scFv73 antibody followed by anti-c-Myc antibody (Sigma) (1:5000 dilution) and then a secondary goat anti-mouse antibody conjugated with peroxidase (Sigma) (1:5000 dilution). Blots were visualized using luminol (ECL, Amersham Biosciences). Amino acid sequences of synthetic peptides used for competition experiments are shown in Table I. Quantification of competition with synthetic peptides was determined by scanning the optical density of bands in blots. Fig. 2 blots were replicated at least twice, and representative results are shown. Data points of Fig. 3 are the means of three replicates, and error deviations are shown.

Preparation of Brush Border Membrane Vesicles (BBMV)—*M. sexta* were reared on an artificial diet from eggs kindly supplied by Dr. Jorge Ibarra (Centro de Investigación y de Estudios Avanzados, Irapuato, Mexico). BBMV from fifth instar *M. sexta* larvae were prepared as reported (19, 46).

Toxin Overlay Assays—Toxins were biotinylated using biotinyl-*N*-hydroxysuccinimide ester (Amersham Biosciences) according to the manufacturer's instructions. Protein blot analysis of BBMV preparations was performed as described previously (19, 44). To determine the ability of peptides to compete with the Cry1A toxin, different concentrations of the peptides were incubated with biotinylated Cry1A toxins in washing buffer (0.1% Tween 20, 0.2% bovine albumin in phosphate-buffered saline) for 1 h at room temperature before adding the mixture to nitrocellulose membranes. Fig. 4 blots were replicated at least twice, and representative results are shown.

Biosensor Analysis of scFv73 Affinities to Cry1A—All surface plasmon resonance (SPR) measurements was performed using a Biacore X and CM5 sensor chips (Biacore) as described (19). HBS-P buffer (10 mM HEPES, pH 7.4, 0.15 M NaCl, 3 mM EDTA, 0.05% surfactant P20) was used throughout the analyses. Briefly, the 30-kDa ligand, scFv73 in 20 mM ammonium acetate pH 5 buffer, was immobilized on flow cell 2, giving densities of less than 150 relative units. The experimental and control surfaces were then blocked with a 5-min injection of 1 M ethanolamine. Cry1Ab wild type and the F371A mutant (65 kDa, apparently homogenous based on SDS-PAGE) were injected over both flow cells at a flow rate of 30 μl/min. Association and dissociation were monitored for 120 and 180 s, respectively, before the surfaces were regenerated (47). The data obtained from triplicate injections of each toxin concentration (15–750 nM) over both surfaces were corrected by double referencing (47) and fitted using global analysis software available within Biaevaluation 3.1 (Biacore). A variety of controls were done as previously described (19).

Docking Construction—Using coordinates for the insecticidal toxin Cry1Aa (PDB code 1CIY) as template, an initial three-dimensional model for Cry1Ab was constructed using module homology from Insight II (Biosym/MSI). Subsequently, energy of the model was minimized using the CNS program (48). A fragment of Bt-R_1 (residues 864–880) was used to perform a Fasta search using the PDB data base. The resulting highest score fragment (residues 153–169 from ADP ribosyl cyclase, PDB code 1LBE) was used as template to structure the Bt-R_1

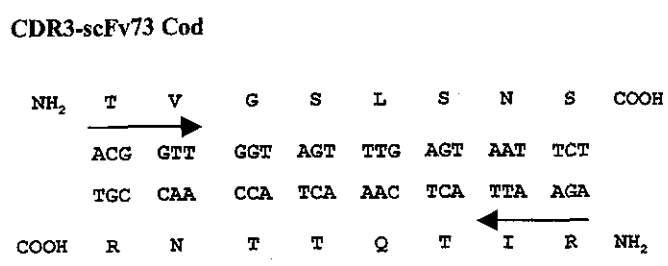

FIG. 1. Amino acid sequences of the coding and noncoding DNA strands of scFv73 CDR3 region.

fragment using Insight II. Hydrophobic docking was performed using the GRAMM program by applying the recommended parameters (49). The first 100 BtR_1 fragment positions were explored selecting those that bind close to loop 2 of domain II of Cry1Ab model. The positions of selected results were adjusted by performing an annealing procedure (CNS), fixing the position of Cry1Ab atoms, and adjusting the position of $Bt\text{-}R_1$ fragment atoms.

Hydropathic Pattern Determination—Hydropathic profiles based on the Kyte-Doolittle algorithm were calculated using Hypscan software kindly provided by Dr. J. E. Blalock (University of Alabama, Birmingham, AL).

RESULTS

scFv73 CDR3 and Bt-R_1 Epitope ^{869}HITDTNNK^{876} Bind the Same Region in Cry1Ab Toxin—To generate a strategy to mutate CDR3 of scFv73, both DNA strands of the CDR3 region were sequenced since the previous sequence was short and corresponded to only one DNA strand. The new sequence revealed that the previous CDR3 amino acid sequence (RITQTTNR) was obtained from the noncoding DNA strand (5′ to 3′) (Fig. 1). The amino acid sequence of the CDR3 coding strand (TVGSLSNS) shares no identity with the sequence of the binding epitope in $Bt\text{-}R_1$ ^{869}HITDTNNK^{876} (named here BtR_1-Cry1A). Previously, we demonstrated that synthetic peptides corresponding to the epitope BtR_1-Cry1A or to the amino acid sequence of the noncoding scFv73 CDR3 peptide (CDR non-cod, Table I) competed with binding of Cry1Aa and Cry1Ab toxins to $Bt\text{-}R_1$ (19). To determine whether scFv73 binds to the same regions in Cry1Ab toxin as epitope BtR_1-Cry1A, competition assays of scFv73 binding to Cry1Ab with synthetic peptides corresponding to scFv73 CDR3 (coding and noncoding) and to the BtR_1-Cry1A epitope were performed. Fig. 2*A* shows a Western blot of Cry1Ab toxin detected with scFv73, indicating that peptides homologous to scFv73 coding or noncoding CDR3 and BtR_1-Cry1A epitope competed with binding of scFv73 to Cry1Ab. A non-relevant peptide (scramble of scFv73 CDR3 sequence) did not compete with binding of scFv73 to Cry1Ab (Fig. 2*A*). This result shows that the coding and noncoding CDR3 amino acid sequences bind to the same epitope in Cry1Ab toxin as the BtR_1-Cry1A binding epitope.

scFv73 Binds to Loop 2 of Domain II of Cry1A Toxins—Previously we demonstrated that scFv73 binds to domain II of Cry1Ab toxin (19). Site-directed mutagenesis of Cry1A domain II sequences demonstrated that the exposed loops of this domain are involved in receptor interaction (21–26). To map the Cry1A cognate binding epitope of BtR_1-Cry1A, synthetic peptides corresponding to the three loops of Cry1A toxins were synthesized and used to compete with binding of scFv73 to Cry1A toxins in Western blots. Fig. 2, *B* and *C*, shows that loop 2 peptides of Cry1Aa and Cry1Ab toxins competed with binding of scFv73 to their corresponding Cry1A toxin in contrast to peptides corresponding to loop 1 and loop 3. Moreover, loop 2 peptide of Cry1Ab competed the binding of scFv73 to Cry1Aa although in a lesser extent (Fig. 2*C*).

TABLE I
Synthetic peptide sequences

Name	Description	Sequence
CDR3 (non-cod)	Amino acid sequence obtained from non-coding DNA strand	RITQTTNRAA
CDR3 (cod)	Amino acid sequence obtained from coding DNA strand	RTVGSLSNS
CDR3 (scr)	Scramble amino acid sequence of CDR3 (cod)	SGRNSTSLV
BtR1-Cry	Amino acid sequence homologous to $Bt\text{-}R_1$ epitope	HITDTNNKAA
L2-Aa	Amino acid sequence of Cry1Aa loop 2	LYRRIILGSGPNNQQ
L3-Aa	Amino acid sequence of Cry1Aa loop 3	LSQAAGAVYTLR
L1-Ab	Amino acid sequence of Cry1Ab loop 1	TDAHRGEYYW
L2-Ab	Amino acid sequence of Cry1Ab loop 2	RRPFNIGINNQQ
L3-Ab	Amino acid sequence of Cry1Ab loop 3	FRSGSAQQIEGS
L2F371A	Amino acid sequence of Cry1Ab loop 2 with F371A	RRPANIGINNQQ
L2RR-EE	Amino acid sequence of Cry1Ab loop 2 with R368E/R9E	EEPFNIGINNQQ

Cry1Ab Loop 2 Amino Acids Involved in Receptor Binding and Toxicity Affect scFv73 Binding—The biological significance of the binding of Cry 1A loop 2 to scFv73 was addressed by the use of synthetic peptide representing known mutants of Cry1Ab toxin to determine whether mutant loop 2 peptides binding to scFv73 correlated with the characteristic of known mutants in terms of binding and toxicity. Cry1Ab loop 2 F371A and double mutant R368E/R9E showed decreased *M. sexta* toxicity and binding to BBMV (22, 26). Synthetic peptides containing F371A and R368E/R9E double mutations were synthesize to determine their ability to compete with scFv73 binding to Cry1Ab toxin. Optical density of Cry1Ab toxin bands in Western blots was scanned to quantify the degree of binding in the presence of different concentrations of peptides used as competitors. Synthetic loop 2 peptides containing the R368E/R9E or F371A mutations did not compete with scFv73 binding to Cry1Ab toxin in contrast to the wild-type loop 2 synthetic peptide, L2Ab (Fig. 3). To determine whether scFv73 binds the Cry1Ab F371A mutant, Western blots of F371A mutant detected with scFv73 were performed that showed that scFv73 binds Cry1Ab F371A mutant (data not shown). However, lower concentrations of the wild-type loop 2 peptide are required to compete with binding of scFv73 to F371A toxin than are needed to compete with scFv73 binding to wild-type Cry1Ab (Fig. 3). These data suggest that scFv73 binds F371A mutant with lower affinity than Cry1Ab toxin.

The binding affinity of Cry1A toxins to scFv73 was in the range of 20–50 nM (19). To determine the effect of the loop 2 mutation F371A in the interaction with scFv73, we performed real time binding kinetics by SPR. Fig. 4 show sensograms of Cry1Ab and F371A mutant binding to scFv73. Cry1Ab F371A has a lower affinity compared with wild-type Cry1Ab toxin, 114 *versus* 55.8 nM (Table II). The apparent lower affinity, 114 nM, was due to differences in the association as well as the dissociation rates (Fig. 4). This result shows that F371A moderately affects the interaction of Cry1Ab with scFv73.

Loop 2 Peptides Compete Binding of Cry1Ab Toxin to Bt-R_1—We showed scFv73 and the BtR_1-Cry1A epitope bind to the same Cry1Ab epitope (Fig. 2*A*) and that this region corresponds

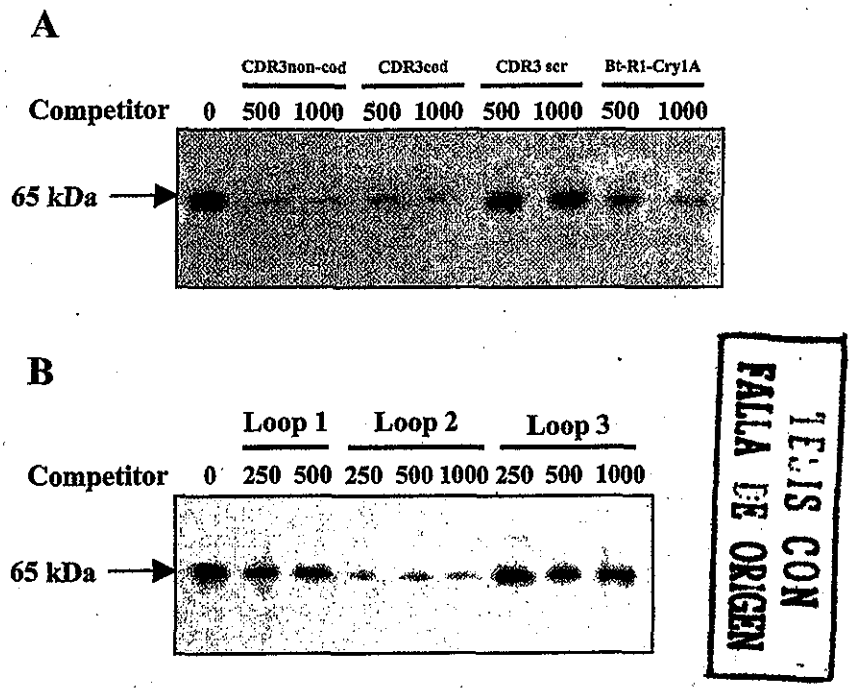

FIG. 2. **Loop 2 of Cry1A toxins bind to Bt-R_1-Cry1A epitope and to CDR3 coding and noncoding amino acid sequences.** Western blots of Cry1A toxins detected with scFv73. *A*, competition of scFv73 binding to Cry1Ab with a molar excess of synthetic peptides corresponding to CDR3 coding sequence (*CDR3 cod*), CDR3 noncoding (*CDR3 non-cod*) sequence, BtR_1-Cry1A epitope (*BtR1-Cry*), and scramble of scFv73 CDR3 (*CDR3 scr*). *B*, competition of scFv73 binding to Cry1Ab with a molar excess of synthetic peptides corresponding to Cry1Ab loop 1 (L1Ab), loop 2 (L2Ab), and loop 3 (L3Ab). *C*, competition of scFv73 binding to Cry1Aa with a molar excess of synthetic peptides corresponding to Cry1Aa loop 1 (L1Ab), loop 2 (L2Ab), loop 3 (L3Aa), and Cry1Ab loop 2 (L2Ab). Blots were replicated at least twice, and representative results are shown.

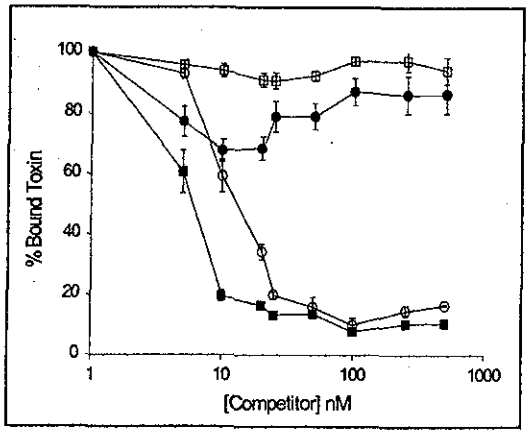

FIG. 3. **Loop 2 mutations of Cry1Ab affect binding of scFv73 to Cry1Ab.** scFv73 binding to Cry1Ab toxin competed with L2Ab (○), L2F371A (●), or L2R-EE (□) synthetic peptides. scFv73 binding to Cry1Ab F371A mutant competed with L2Ab synthetic peptide (■). Data points are means of three replicates, and S.E. deviations are shown.

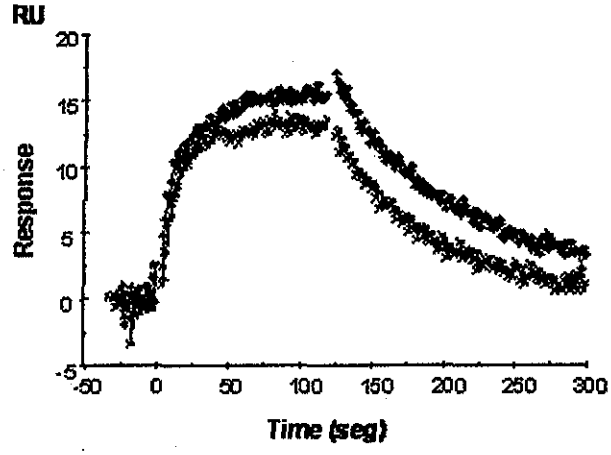

FIG. 4. **Comparison of 750 nM Cry1Ab (*gray*) and Cry1Ab F371A (*black*) binding to immobilized scFv73 by SPR.** *RU*, relative units.

to loop 2 of domain II (Fig. 2*B*). To corroborate these data, we performed toxin overlay assays to determine whether Cry1Aa and Cry1Ab loop 2 peptides could compete with the interaction of Cry1A toxins to Bt-R_1. Fig. 5 shows the Cry1Aa and Cry1Ab toxins bind APN (120 kDa) and Bt-R_1 (210 kDa) of *M. sexta* BBMV as previously reported (10–12, 19). Competition with synthetic peptides corresponding to loop regions of these toxins showed that synthetic peptides corresponding to loop 2 of Cry1Aa and Cry1Ab competed with binding of their corresponding toxin to Bt-R_1 and not to APN. Interestingly, whereas the loop 3 peptide of Cry1Aa toxin also competed with binding of Cry1Aa toxin to Bt-R_1, the Cry1Ab toxin loop 3 peptide did not compete. Neither loop 1 peptide had an effect on binding of the corresponding toxin to Bt-R_1 (Fig. 5).

Inverse Hydropathy Determines Interaction of Cry1A Loop 2 Sequences with Bt-R_1—As shown above, BtR_1-Cry1A epitope

TABLE II
Binding kinetics of Cry1Ab and F371A Cry1Ab to scFv73

Toxin	k_{on}	k_{off}	K_d
	$\times 10^{6}\ M^{-1}\ s^{-1}$	$\times 10^{-3}\ s^{-1}$	$\times 10^{-8}\ M$
Cry1Ab	2.09	11.7	5.58
F371A Cry1Ab	1.16	13.2	11.50

k_{on} is the association rate constant; k_{off} is the dissociation rate constant and K_d is the apparent affinity (k_{on}/k_{off}). Values are representative of triplicate injections that were analyzed globally.

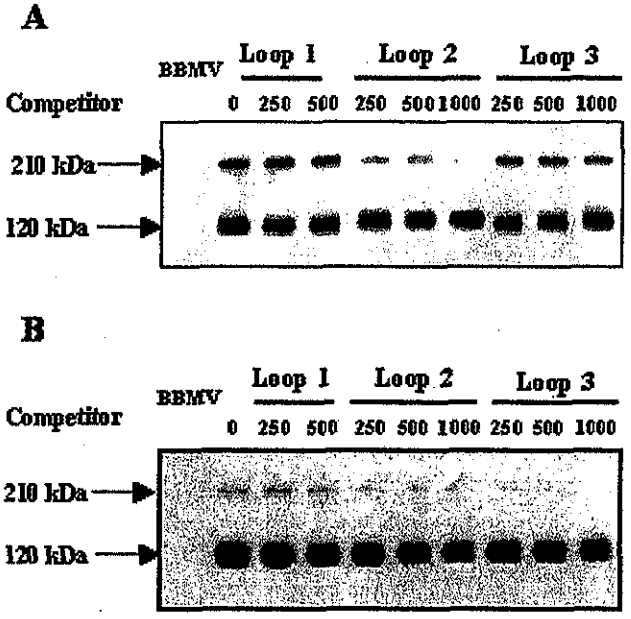

FIG. 5. **Loop 2 synthetic peptides of Cry1A toxins compete with binding of Cry1A to Bt-R_1.** Toxin overlay assays of competition of Cry1A with molar excess of different loop Cry1A peptides. *A*, toxin overlay of Cry1Ab to *M. sexta* BBMV. *B*, toxin overlay of Cry1Aa to *M. sexta* BBMV. Blots were replicated at least twice, and representative results are shown.

binds to Cry1Aa and Cry1Ab toxins at loop 2 despite the fact that these loop 2 epitopes share low amino acid identity. To determine whether the interaction of loop 2 regions with BtR_1-Cry1A epitope involves inverted hydropathic patterns, the hydropathic profiles of loop 2 Cry1A epitopes were determined as well as those of Bt-R_1-Cry1A and the CDR3 regions. The patterns were compared for similarity or complementarity between them using the computer program Hypscan as indicated under "Materials and Methods." Fig. 6*A* shows that the hydropathic profile of the scFv73 coding and noncoding CDR3 amino acid sequences and that of BtR_1-Cry1A are very similar. Fig. 6, *B* and *C*, shows Cry1Aa and Cry1Ab loop 2 regions have inverted hydropathic profiles relatives to the Bt-R_1 epitope, with Cry1Ab loop 2 more complementary to the BtR_1-Cry1A epitope than the Cry1Aa loop 2 region. Regions of Cry1A toxins that showed inverse hydropathic patterns to the BtR_1-Cry1A epitope included five residues of β-6 and five residues of loop 2 in Cry1Ab ^{363}SSTLYRRPFNI^{373}, whereas Bt-R_1 included residues ^{865}NITIHITDTNN^{875}. The amino acid sequence identity between the Cry1Aa and Cry1Ab regions that have inverted hydropathic complementarity to Bt-R_1 is 60%, where 5 of 6 identical residues are from the β-6 structure and one from the loop 2 region.

DISCUSSION

Understanding the molecular basis of Cry toxin specificity will help in the rational design of improved toxin formulations useful in insect pest management. The identification of epitopes involved in Cry toxin-receptor interaction could pro-

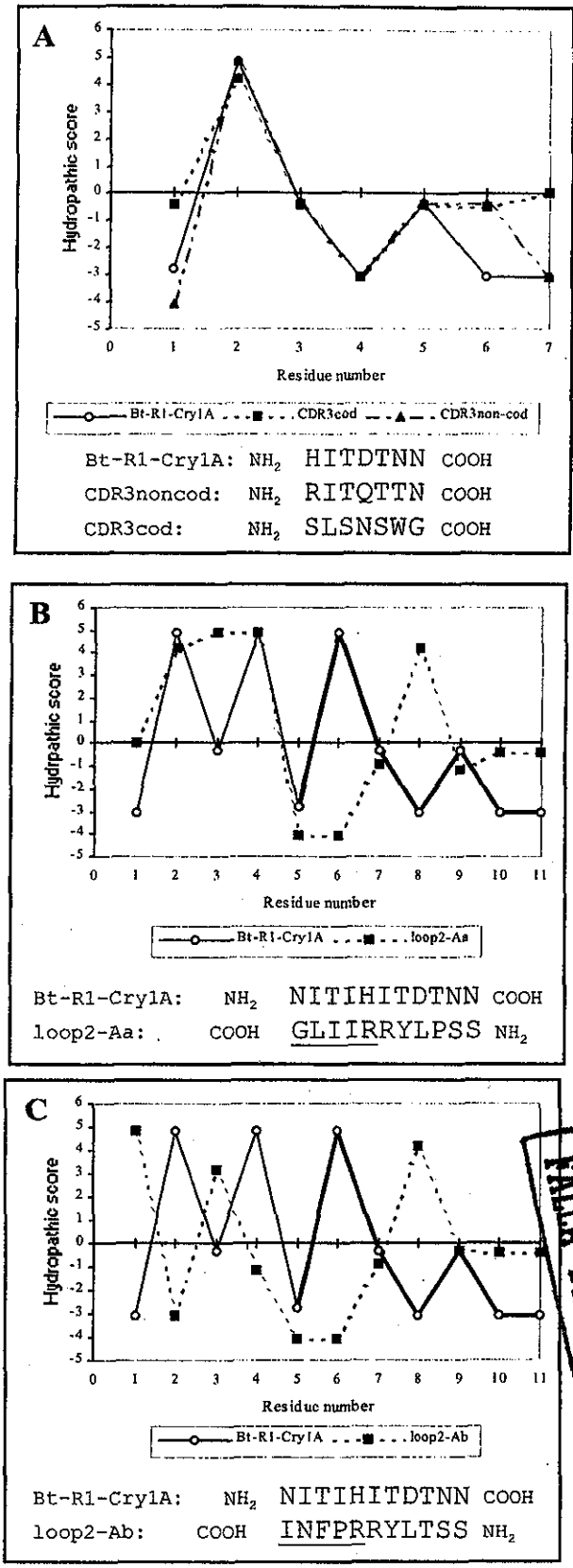

FIG. 6. **Hydropathic profile of BtR_1-Cry1A epitope is inverted to that of β-6-loop 2 of Cry1A toxins.** *A*, comparison of hydropathic profiles of scFv73 CDR3 coding, non-coding, and BtR_1-Cry1A epitope (*A*), BtR_1-Cry1A and β-6-loop 2 of Cry1Aa (*B*), and BtR_1-Cry1A and β-6-loop 2 of Cry1Ab (*C*). The *bold lines* of *B* and *C* represent region depicted on *A* of BtR_1-Cry1A. Amino acids *underlined* in *B* and *C* are residues of loop 2 regions, whereas residues not underlined are from β-6 region.

vide insights into the mechanism of insect specificity and the mode of action of these toxins. In this work we identified loop 2 of domain II of Cry1A toxins as the cognate binding epitope of the *M. sexta* receptor Bt-R_1 ^{869}HITDTNNK^{876}. This finding highlights the importance of BtR_1-Cry1A binding epitope since extensive mutagenesis of loop 2 of Cry1A toxins has shown that this loop region is important for receptor binding and toxicity (22, 23). Besides loop 2, loop α-8 and loop 3 of Cry1A toxins are also important for receptor interaction and toxicity (21, 24–26). The Bt-R_1 epitopes involved in binding loop α-8 and loop 3 regions still remains to be identified. In this work we analyzed the role of the three exposed loop regions of domain II on receptor interaction. The role of loop α-8 on receptor Bt-R_1 interaction still remains to be analyzed since mutagenesis of this region has been shown to have an important role on receptor interaction (21). Loop 2 peptides of Cry1Aa and Cry1Ab toxins competed with binding of both toxins to Bt-R_1 in toxin overlay assays (Fig. 5). However, only the peptide corresponding to loop 3 of Cry1Aa but not that of Cry1Ab competed with binding of the corresponding Cry1A toxin to Bt-R_1 (Fig. 5). Cry1Aa loop 3 shares no amino acid sequence identity with Cry1Ab or Cry1Ac loop 3 regions (24). Therefore, our results suggest that loops 2 and 3 of Cry1Ab and Cry1Aa toxins contribute differentially to the binding of these toxins to Bt-R_1, with Cry1Aa loop 3 more important in the interaction with Bt-R_1 receptor than Cry1Ab loop 3. However, we cannot rule out the possibility that Cry1Ab loop 3 has structural constraints for receptor interaction, therefore explaining the lack of competition by the Cry1Ab loop 3 peptide in Cry1Ab binding to Bt-R_1 (Fig. 5).

CDR3 of scFv73 exhibits similar binding properties as Bt-R_1 since scFv73 binding to Cry1Ab toxin is affected by loop 2 mutations that also affect Cry1Ab receptor binding (Fig. 3). In addition, by using scFv73 as a surrogate for Bt-R_1, we found that binding of Cry1A toxins to this epitope facilitates proteolytic cleavage of helix α-1 of domain I and the formation of a tetramer oligomer pre-pore structure, showing that scFv73 has functional activity similar to that of the natural Bt-R_1 receptor (20).

Prior SPR binding analysis showed the binding of the Cry1Ab loop 2 F371A mutant to APN is barely affected (50), and this mutant has a 2-fold lower affinity for Bt-R_1 as judged by binding to scFv73 (Table II, Fig. 4). However, the irreversible binding and toxicity is affected (22, 23). As mentioned above, binding to Bt-R_1 facilitates proteolytic cleavage of helix α-1 and the formation of a pre-pore structure that is membrane insertion-competent, probably by inducing a conformational change that makes helix α-1 accessible for proteolytic degradation (20). Therefore, it is possible that binding of Cry1Ab F371A mutant to Bt-R_1 does not promote the conformational change that facilitates helix α-1 degradation, thus affecting the formation of the pre-pore structure. This hypothesis could explain the effect of the F371A mutation on irreversible toxin binding since it is postulated that formation of the pre-pore is a prerequisite for membrane insertion (20). Analysis of pre-pore formation by the Cry1Ab F371A mutant induced by scFv73 binding will enable us to determine whether this step is affected (work in progress).

Competition of Cry1Aa and Cry1Ab toxins to APN and Bt-R_1 in toxin overlay assays in the presence of loop 2 synthetic peptides showed that loop 2 is important for interaction of the Cry1A toxin to Bt-R_1 but not for APN (Fig. 5). These data support the fact that Bt-R_1 has an important role in insect toxicity. However, we cannot rule out the possibility that the APN receptor has a role in Cry1Ab toxicity since several loop 2 point mutations affect both APN binding and toxicity (26, 50).

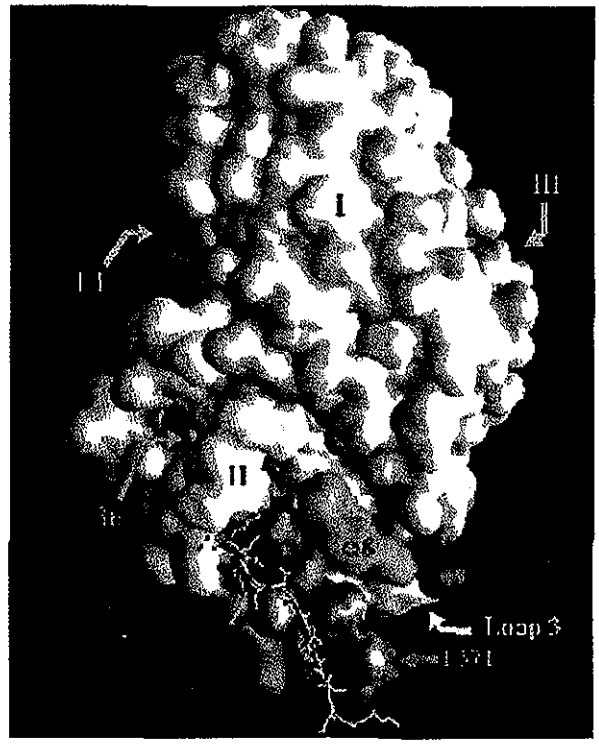

FIG. 7. **Molecular surface model of Cry1Ab toxin.** Exposed surfaces of helix α-8 (residues 275–293 (*blue*); Arg-281 (*deep blue*)), loop 1 (residues 310–314 (*violet*)), loop 2 (368–375, *red*), residues R-368–R-369 and Phe-371 (*orange*)), β-6 (360–367 (*green*)), and loop 3 (residues 438–443 (*yellow*)). The lowest potential energy docking of Bt-R_1 864–880 peptide to Cry1Ab β-6-loop 2 region (rank 70) is shown.

The fact that some Cry1A loop 2 mutations affect APN binding suggests that a similar binding epitope as BtR_1-Cry1A could be present in APN. However, the loop 2 peptides did not compete with Cry1Ab binding to APN. These data are in apparent contradiction. An important methodological difference is that SPR binding studies (26, 50) determined binding of native proteins in contrast to toxin overlay assays, which determine binding to denatured proteins after SDS-PAGE electrophoresis. Thus, structural differences could account for the lack of competition of loop 2 peptide on Cry1A toxins binding to APN observed in this work.

Accumulating evidence indicates that proteins can interact through amino acid sequences displaying inverted hydropathic profiles, implying that amino acid sequences that share low amino acid sequence identity can interact with the same epitopes if they share a similar hydropathic profile (30). Analysis of hydropathic patterns of Cry1A loop 2 regions and that of BtR_1-Cry1A epitope showed that the interaction of these regions is determined by inverse hydropathic patterns (Fig. 6). Hydropathic profiles of amino acid sequences of scFv73 CDR3 and BtR_1-Cry1A epitope were similar (Fig. 6*A*) and inverted to a region of Cry1A that corresponds to the end of β-6 and loop 2 (Fig. 6, *B* and *C*). If we analyze the hydropathic pattern of the amino acid region adjacent to the Bt-R_1-Cry1A epitope, we find an inverse pattern with Cry1Ab region including five residues of β-6 and five residues of loop 2 in both toxins. This analysis predicts that mutations of Cry1A β-6 residues ^{363}SSTLY^{367} would affect receptor binding and toxicity (work in progress). The Bt-R_1 included residues ^{865}NITIHITDTNN^{875}, suggesting that the binding epitope could be larger than the one previously mapped based on amino acid sequence identity with scFv73 CDR3 (19). Using a computer-simulated docking method, we analyzed the binding of a peptide corresponding to Bt-R_1 ^{864}GNITIHITDTNNKVPQAE^{880} to Cry1Ab. We observed that

the binding of this Bt-R_1 amino acid sequence to β-6-loop 2 region was favorable in steric and energy-pairing analyses among several other favorable binding possibilities obtained (Fig. 7). This result provides support to this region of Bt-R_1 interacting with β-6-loop 2 of Cry1A toxins. The inverted hydropathic pattern of Cry1Ab loop 2 sequences with that of Bt-R_1-Cry1A was more complementary than that of loop 2 of Cry1Aa (Fig. 6, *B* and *C*); these data correlates with a slightly lower affinity of Cry1Aa to Bt-R_1 compared with the binding affinities of Cry1Ab and Cry1Ac toxins (51). The finding that inverse hydropathic patterns could determine the interaction of loop 2 of Cry1A toxins with Bt-R_1 could be used in the rational design of more toxic Cry1A mutant proteins by optimizing the profile of β-6 loop 2 to that of the epitope in the receptor. Mutants with optimized inverted hydropathic patterns are predicted to have improved affinity toward its receptor as has been shown for other examples of interacting proteins (34).

In this study we show that amino acid sequences obtained from the coding and noncoding DNA strands of scFv73 CDR3 bind to loop 2 of Cry1A toxins. The molecular recognition theory predicts that peptides obtained from noncoding DNA strands (anti-peptides) bind to amino acid sequence epitopes of the coding strand (30, 52). In the case of scFv73 CDR3, the amino acid sequence of the noncoding strand has similar binding properties as the coding DNA strand CDR3 amino acid sequence (Fig. 2*A*). There are other examples of anti-peptides that have similar binding properties as the coded amino acid sequence in the literature (35, 51). The analysis of hydropathic profiles of the coding and noncoding scFv73 CDR3 amino acid sequences revealed that they share a similar hydropathic pattern (Fig. 6*A*), explaining their ability to interact with the same epitope in the toxin even though they share no sequence identity. The noncoding amino acid sequence of scFv73 CDR3 (RITQTTNR) shares amino acid sequence identity with Bt-R_1 ^{869}HITDTNNK^{876} epitope (19). Isolation of peptides that mimic natural ligands by phage display have been successful in mapping protein epitopes by searching amino acid sequence similarities (53). Nevertheless, as was pointed out before (39), the most reliable way to map binding epitopes is to search hydropathic profile similarities rather than amino acid sequences similarities. We propose that amino acid sequence similarities could also be searched considering both amino acid sequences of the coding and noncoding DNA strands of the interacting epitopes.

Acknowledgments—We thank Dr. J. E. Blalock and Dr. Douglas Barker for Hypscan software, Didier Lereclus for Bt strain 407*cry*$^-$ and pHT409, and Lizbeth Cabrera and Cludia Morera for technical assistance.

Note Added in Proof—Recently a different Cry1A toxin-binding site in Bt-R_1 receptor was mapped by heterologous expression of deletion derivatives: Cry1A toxins of *B. thuringiensis* bind specifically to a region adjacent to the membrane-proximal extracellular domain of BT-R_1 in *M. sexta*. Involvement of a cadherin in the entomopathogenicity of *B. thuringiensis* (54). This result suggests that toxin-receptor interactions may involve multiple structural determinants on both molecules.

REFERENCES

1. Crickmore, N., Zeigler, D. R., Feitelson, J., Schnepf, E., Van Rie, J., Lereclus, D., Baum, J., and Dean, D. H. (1998) *Microbiol. Mol. Biol. Rev.* **62,** 807–813
2. DeMaagd, R. A., Bravo, A., and Crickmore, N. (2001) *Trends Genet.* **17,** 193–199
3. Choma, C. T., Surewicz, W. K., Carey, P. R., Pozsgay, M., Raynor, T., and Kaplan, H. (1990) *Eur. J. Biochem.* **189,** 523–527
4. Li, J., Carroll, J., and Ellar, D. J. (1991) *Nature* **353,** 815–821
5. Grochulski, P., Masson, L., Borisova, S., Pusztai-Carey, M., Schwartz, J. L., Brousseau, R., and Cygler, M. (1995) *J. Mol. Biol.* **254,** 447–464
6. Morse, R. J., Yamamoto, T., and Stroud, R. M. (2001) *Structure (Lond.)* **9,** 409–417
7. Pietrantonio, P. V., and Gill, S. S. (1996) *in Biology of the Insect Midgut* (Lehane, M. J., and Billingsley, P. F., eds) pp. 345–372, Chapman & Hall, London
8. Bravo, A., Jansens, S., and Peferoen, M. (1992) *J. Invertebr. Pathol.* **60,** 237–246
9. Hofmann, C., Vanderbruggen, H., Höfte, H., Van Rie, J., Jansens, S., and Van Mellaert, H. (1988) *Proc. Natl. Acad. Sci. U. S. A.* **85,** 7844–7848
10. Garczynski, S. F., and Adang, M. J. (1995) *Insect Biochem. Mol. Biol.* **25,** 409–415
11. Knight, P. J. K., Crickmore, N., and Ellar, D. J. (1994) *Mol. Microbiol.* **11,** 429–436
12. Vadlamudi, R. K., Weber, E., Ji, I., Ji, T. H., and Bulla, L. A., Jr. (1995) *J. Biol. Chem.* **270,** 5490–5494
13. Nagamatsu, Y., Koike, T., Sasaki, K., Yoshimoto, A., and Furukawa, Y. (1999) *FEBS Lett.* **460,** 385–390
14. Yaoi, K., Kadotani, T., Kuwana, H., Shinkawa, A., Takahashi, T., Iwahana, H., and Sato, R. (1997) *Eur. J. Biochem.* **246,** 652–657
15. Gill, S. S., Cowles, E. A., and Francis, V. (1995) *J. Biol. Chem.* **270,** 27277–27282
16. Oltean, D. I., Pullikuth, A. K., Lee, H-K., and Gill, S. S. (1999) *Appl. Environ. Microbiol.* **65,** 4760–4766
17. Valaitis, A. P., Jenkins, J. L., Lee, M. K., Dean, D. H., and Garner, K. J. (2001) *Arch. Insect Biochem. Physiol.* **46,** 186–200
18. Gahan, L. J., Gould, F., and Heckel, D. G. (2001) *Science* **293,** 857–860
19. Gomez, I., Oltean, D. I., Gill, S. S., Bravo, A., and Soberón, M. (2001) *J. Biol. Chem.* **276,** 28906–28912
20. Gómez, I., Sánchez, J., Miranda, R., Bravo A., and Soberón, M. (2002) *FEBS Lett.* **513,** 242–246
21. Lee, M. K., Jenkins, J. L., You, T. H., Curtiss, A., Son, J. J., Adang, M. J., and Dean, D. H. (2001) *FEBS Lett.* **497,** 108–112
22. Rajamohan, F., Alcantara, E., Lee, M. K., Chen, X. J., Curtiss, A., and Dean, D. H. (1995) *J. Bacteriol.* **177,** 2276–2282
23. Rajamohan, F., Cotrill, J. A., Gould, F., and Dean, D. H. (1996) *J. Biol. Chem.* **271,** 2390–2396
24. Rajamohan, F., Hussain, S-R. A., Cotrill, J. A., Gould, F., and Dean, D. H. (1996) *J. Biol. Chem.* **271,** 25220–25226
25. Jenkins, J. L., LeeM. K., Valaitis, A. P., Curtiss, A., and Dean, D. H. (2000) *J. Biol. Chem.* **275,** 14423–14431
26. Lee, M. K., Rajamohan, F., Jenkins, J. L., Curtiss, A., and Dean, D. H (2000) *Mol. Microbiol.* **38,** 289–298
27. Denolf, P., Hendrickx, K., VanDamme, J., Jansens, S., Peferoen, M., Egheele, D., and VanRie, J. (1997) *Eur. J. Biochem.* **248,** 748–761
28. Belfiore, C. J., Vadlamudi, R. K., Osman, Y. A., and Bulla L. A., Jr. (1994) *Biochem. Biophys. Res. Commun.* **200,** 359–364
29. Yaoi, K., Nakanishi, K., Kadotani, T., Imamura, M., Koizumi, N., Iwahana, H., and Sato, R. (1999) *FEBS Lett.* **463,** 221–224
30. Blalock, J. E. (1995) *Nat. Med.* **1,** 876–878
31. Markus, G., Trisch, G. L., and Parthasarathy, R. (1989) *Arch. Biochem. Biophys.* **272,** 433–439
32. Villain, M., Jackson, P. L., Manion, M. K., Dong, W-J., Su, Z., Fassina, G., Johnson, T. M., Sakai, T. T., Krishna, N. R., and Blalock, J. E. (2000) *J. Biol. Chem.* **274,** 2676–2685
33. Bost, K. L., Smith, E. M., and Blalock, J. E. (1985) *Proc. Natl. Acad. Sci. U. S. A.* **82,** 1372–1375
34. Blalock, J. E. (1999) *Cell. Mol. Life Sci.* **55,** 513–518
35. Dillon, P. F., Root-Bernstein, R. S., and Holsworth, D. D. (1998) *Hypertension* **31,** 854–860
36. Heal, J. R., Bino, S., Ray, K. P., Christie, G., Miller, A. D., and Raynes, J. G. (1999) *Mol. Immunol.* **36,** 1141–1148
37. Dillon, J., Woods, W. T., Guarcello, V., LeBoeuf, R. D., and Blalock, J. E. (1991) *Proc. Natl. Acad. Sci. U. S. A.* **88,** 9726–9729
38. Ruiz-Opazo, N., Akimoto, K., and Herrera, M. L. A. (1995) *Nat. Med.* **1,** 1074–1081
39. Sagot, M-A., Wijkhuisen, A., Créminon, C., Tymciu, S., Frobert, Y., Turbica, I., Grassi, J., Couraud, J-Y., and Boquet, D. (2000) *Mol. Immunol.* **37,** 423–433
40. Boquet, D., Déry, O., Frobert, Y., Grassi, J., Couraud, J. Y. (1995) *Mol. Immunol.* **32,** 303–308
41. Lereclus, D., Arantès, O., Chaufaux, J., and Lecadet, M.-M. (1989) *FEMS Microbiol. Lett.* **60,** 211–218
42. Arantes, O., and Lereclus, D. (1991) *Gene* **108,** 115–119
43. Thomas, W. E., and Ellar, D. J. (1983) *J. Cell Sci.* **60,** 181–197
44. Aranda, E., Sanchez, J., Perferoen, M., Güereca, L., and Bravo, A. (1996) *J. Invertebr. Pathol.* **68,** 203–212
45. Lee, M. K., Milne, R. E., Ge, A. Z., and Dean, D. H. (1992) *J. Biol. Chem.* **267,** 3115–3121
46. Wolfersberger, M., Lüthy, P., Maurer, A., Parenti, P., Sacchi, F. V., Giordana, B., and Hanozet, G. M. (1987) *Comp. Biochem. Physiol.* **86,** 301–308
47. Myszka, D. G. (1999) *J. Mol. Recognit.* **12,** 279–284
48. Brunger, A. T. Adams, P. D., Clore, G. M., Delano, W. L., Gros, P., Grosse-Kunstleve, R. W. Jiang, J-S., Kuszewski, J., Nilges, M., Pannu, N. S., Read, R. J., Rice, L. M., Simonson, T., and Warren, G. L. (1998) *Acta Crystallogr. Sect. D Biol. Crystallogr.* **54,** 2444–2448
49. Vakser, I. A., and Aflalo, C. (1994) *Proteins* **20,** 320–329
50. Jenkins, J. L., and Dean D. H. (2000) *Genetic Engineering: Principles and Methods* (Setlow, J. K., ed) pp. 33–54, Plenum Press, New York
51. Keeton, T. P., and Bulla, L. A. (1997) *Appl. Environ. Microbiol.* **63,** 3419–3425
52. Root-Bernstein, R., and Holswortn, D. D. (1998) *J. Theor. Biol.* **190,** 107–119
53. Kay, B. K., Kasanov, J., Knight, S., and Kurakin, A. (2000) *FEBS Lett.* **480,** 55–62
54. Dorsch, J. A., Candas, M., Griko, N. B., Maaty, W. S. A., Midbo, E. G., Vadlamudi, R. K., and Bulla, L. A., Jr. (2002) *Insect Biochem. Mol. Biol.*, in press

ANEXO IV

Evidences for inter-molecular interaction as a necessary step for pore-formation activity and toxicity of *Bacillus thuringiensis* Cry1Ab toxin.

Soberón, M., Perez, R. V., Nuñez-Valdéz, M. E., Lorence, A., **Gómez, I.**, Sánchez, J., Bravo, A.

FEMS Microbiology Letters. (2000). 191:221-225.

Heliothis virescens and *Manduca sexta* lipid rafts are involved in Cry1A toxin binding to the midgut epithelium and subsequent pore formation.

Zhuang, M. Oltean, D.I. **Gómez, I.** Pullikuth, A.K. Soberón, M. Bravo, A. Gill, S.S.

Journal of Biological Chemistry. (2002). 277:13863-13872.

Pore formation activity of Cry1Ab toxin from *Bacillus thuringiensis* in an improved membrane vesicle preparation from *Manduca sexta* midgut cell microvilli.

Bravo, A. Miranda, R. **Gómez, I.** Soberón, M.

Biochim. Biophys. Acta. (2002). 1562:63-69.

Mecanismo de Acción de las Toxinas Cry de *Bacillus thuringiensis*.

Miranda, R., **Gómez, I.**, Soberón, M. y Bravo, A.

TIP Revista Especializada en Ciencias Químico-Biológicas. (2002). 5:5-13.

ELSEVIER

FEMS Microbiology Letters 191 (2000) 221–225

FEMS MICROBIOLOGY Letters

www.fems-microbiology.org

Evidence for intermolecular interaction as a necessary step for pore-formation activity and toxicity of *Bacillus thuringiensis* Cry1Ab toxin

Mario Soberón [a,*], Rigoberto V. Pérez [a], María E. Nuñez-Valdéz [a], Argelia Lorence [b], Isabel Gómez [a], Jorge Sánchez [a], Alejandra Bravo [a]

[a] *Instituto de Biotecnología, U.N.A.M., Apdo Postal 510-3, Cuernavaca, Morelos 62271, Mexico*

[b] *Centro de Investigación en Biotecnología, U.A.E.M., Av. Universidad 1000, Col. Chamilpa, Cuernavaca, Morelos 62210, Mexico*

Received 20 May 2000; received in revised form 21 July 2000; accepted 15 August 2000

Abstract

Based on the observation of large conductance states formed by *Bacillus thuringiensis* Cry toxins in synthetic planar lipid bilayers and the estimation of a pore size of 10–20 Å, it has been proposed that the pore could be formed by an oligomer containing four to six Cry toxin monomers. However, there is a lack of information regarding the insertion of Cry toxins into the membrane and oligomer formation. Here we provide direct evidence showing that the intermolecular interaction between Cry1Ab toxin monomers is a necessary step for pore formation and toxicity. Two Cry1Ab mutant proteins affected in different steps of their mode of action (F371A in receptor binding and H168F in pore formation) were affected in toxicity against *Manduca sexta* larvae. Binding analysis showed that F371A protein bound more efficiently to *M. sexta* brush border membrane vesicles when mixed with H168F in a one to one ratio. These mutant proteins also recovered pore-formation activity, measured with a fluorescent dye with isolated brush border membrane vesicles, and toxicity against *M. sexta* larvae when mixed, showing that monomers affected in different steps of their mode of action can form functional hetero-oligomers.

Keywords: δ-Endotoxin oligomerization; Pore formation; *Bacillus thuringiensis*; *Manduca sexta*

1. Introduction

Bacillus thuringiensis (Bt) is an aerobic, spore-forming soil bacterium that produces crystalline inclusions during the sporulation phase of growth. Crystal inclusions are composed of proteins known as insecticidal crystal proteins (ICP) or δ-endotoxins, which are toxic to larval forms of several insects of different orders as well as to other invertebrates [1]. The ICPs form two very different multigene families, *cry* and *cyt* [2–4], which have been classified into 28 different Cry subgroups and two different Cyt subgroups [5], based on amino acid identity.

In the case of the lepidopteran-specific Cry1 toxins, after ingestion by susceptible larvae, the ICPs are solubilized in the alkaline and reducing conditions of the midgut lumen, releasing the protoxin from the crystal. The protoxin is further processed by the insect gut proteases into a protease-resistant active toxin fragment. The activated toxin binds to specific receptors located on the apical membrane of the midgut epithelial cells [6–8] and inserts irreversibly into the membrane, forming pores that allow a net uptake of ions and water that causes the swelling and osmotic lysis of the cells [9–11]. These events lead to a breakdown in the integrity of the midgut cells and to the insect's death [11].

The three-dimensional structures of the Cry3A and Cry1Aa ICPs have been resolved by X-ray diffraction crystallography [2,3]. They share many similar features and are comprised of three domains. Domain I, extending from the N-terminus, is a seven-α-helix bundle with helix α-5 in the center encircled by the other helices. This domain has been implicated in the channel formation in the membrane. Domain II consists of three anti-parallel β-sheets and domain III is a β-sandwich of two anti-parallel β-sheets [2,3]. Domains II and III are involved in receptor

* Corresponding author. Tel.: +52 (73) 291618; Fax: +52 (73) 172388; E-mail: mario@ibt.unam.mx

0378-1097/00/$20.00
PII: S0378-1097(00)00394-3

binding [2,3]. Domain III also protects the toxin from further proteolysis [2].

Based on the observation of large conductance states formed by Cry1Ac, Cry3A, Cry3B and Cry1C toxins in synthetic planar lipid bilayers [12–14] and the estimation of a pore size of 10–20 Å [15], it has been proposed that the pore could be formed by an oligomer of Cry toxins containing four to six toxin monomers [16,17]. The oligomeric state of some Cry toxins in solution has been analyzed. A recent report showed that Cry proteins in solution do not form oligomers of a defined subunit number suggesting that oligomers form after the toxin is inserted into the membrane [18]. Also, Cry1Ac oligomeric state was analyzed after binding to brush border membrane vesicles where multimers were identified [19]. In the binary toxin, produced by *Bacillus sphericus*, evidence for oligomer formation was obtained by recovering toxicity of point mutant toxins after mixing them, showing that altered binary toxins can functionally complement each other by forming oligomers [20].

In this study we provide direct evidence showing that the intermolecular interaction between Cry1Ab monomers is a necessary step for pore formation and toxicity. Two Cry1Ab mutant proteins affected in different steps of their mode of action (receptor binding and pore formation) recovered binding, pore-formation activity and toxicity against *Manduca sexta* larvae when mixed, showing that monomers affected in different steps of their mode of action can form functional hetero-oligomers.

2. Materials and methods

2.1. Bacterial strains, plasmids and media

Plasmids pC34 [21], pBluescript-SK (Stratagene, La Jolla, CA) and pTH315 [22] were used for cloning. An *Escherichia coli* strain harboring *cry1Ab* F371A was kindly supplied by Dr. Dean (Ohio State University, USA). Acrystalliferous Bt strain 407 [23] was provided by Dr. Lereclus (Institut Pasteur, France). *E. coli* strains were grown in Luria broth at 37°C and Bt in nutrient broth sporulation medium (NB) [24] at 30°C. Antibiotics were as follows: ampicillin 100 μg ml^{-1} (for *E. coli*); erythromycin 250 μg ml^{-1} for *E. coli* and 7.5 μg ml^{-1} for Bt.

2.2. Construction of the H168F mutant

The H168F mutant was constructed by overlap-extension PCR site-directed mutagenesis as described [25]. Plasmid pC375 containing a 375-bp *Xba*I fragment from the *cry1Ab* gene (480–813 bp, α-helix 5) was used as template, in two sequential PCRs. The first round of PCR involved two separate PCRs, using T3 primer and the mutagenic primer RM11 (5′-TCT CAA AAC TGA TAA AAA TAA ATT TGC AGC TTG) (residues 631–663), to amplify the first portion of the fragment and mutagenic primer RM7 (5′-CTT TTA TCA GTA NNS GTT CAA GCT GCA AAT TTA C) (residues 610–643), and T7 to amplify the second part of the fragment. PCRs were done with 3 U *Pfu* (Stratagene) with the program: one cycle of 94°C, 5 min; 53°C, 2 min and 72°C, 3 min; followed by 23 cycles of 94°C, 1 min; 53°C, 1 min and 72°C, 1 min. The resulting fragments overlap by 16 bp.

The second round of PCR involved the purification of both PCRs and treatment with Klenow. 50 ng of each PCR product was mixed, boiled for 10 min, and cooled on ice for 5 min. Extension of the overlapping products was allowed by adding PCR buffer and 3 U *Pfu*: 72°C for 3 min, followed by 10 cycles of 94°C, 1 min; 53°C, 1 min and 72°C, 1 min. Then, 20 pmol of T3 and T7 primers were added in addition of 3 U *Pfu* and allowed to amplify for 25 cycles. The final PCR product was 567 bp. This fragment was digested with *Xba*I and cloned into pBluescript-SK. *E. coli* DH5α was transformed and plasmid from the resulting colonies was sequenced. The 375-bp *Xba*I H168F mutated fragment was subcloned into the *cry1Ab* protoxin gene, cloned in pHT315 [22] and transformed into Bt strain 407.

2.3. Purification of wild-type Cry1Ab, and Cry1Ab F371A and H168F mutant toxins

Bt strains containing *cry1Ab* or *cry1Ab* H168F were grown for 3 days in NB until complete sporulation. Crystals were purified by sucrose gradients as in [26]. Purified crystals were solubilized and activated by trypsin 1:10 w/w for 2 h and purified by anion exchange chromatography (Q-Sepharose) as described [27]. The purified toxins were dialyzed against 1000 volumes of 150 mM *N*-methylglucamine chloride (MeGluCl), 10 mM HEPES pH 8 and stored at 4°C until used. Toxin purity was examined by SDS–PAGE. Mutant F371A was expressed in *E. coli* and purified as previously described [28]. Protein was measured by a protein dye method [29].

2.4. Toxicity assay of Manduca sexta

M. sexta larvae used in this study were supplied by Dr. J. Ibarra (CINVESTAV, Irapuato, Mexico). Toxicity assays were performed with first-instar larvae. Twenty-four larvae were fed with 20 ng cm^{-2} of toxin on an artificial diet (Bio-Serv). The mortality was recorded after 5 days.

2.5. Preparation of brush border membrane vesicles (BBMV)

BBMV from fifth-instar *M. sexta* larvae were prepared and analyzed as previously reported [30]. BBMV were dialyzed overnight against 500 volumes of 150 mM KCl, 2 mM EDTA, 10 mM HEPES–HCl pH 7.6 and stored at −70°C until used.

98

2.6. Binding assay

Homologous competition of biotinylated Cry1Ab, H168F and F371A toxins to *M. sexta* BBMV was performed as previously described [31].

2.7. Fluorescence measurements

Membrane potential was monitored with the positively charged fluorescent dye, 3,3'-dipropyl-thiodicarbocyanine (dis-C_3-(5) (Molecular Probes, Eugene, OR, USA), as previously described [10]. Fluorescence was recorded at the 620/670 nm excitation/emission wavelength pair using a Hansatech system (Norfolk, UK). Hyperpolarization causes dye internalization into the BBMV and fluorescence decrease. Dye calibration and determination of resting membrane potential were performed in the presence of valinomycin (2 mM) by successive additions of KCl to BBMV (20 μg) in 140 mM MeGluCl, 10 mM HEPES–HCl pH 8.0. Resting membrane potential was determined from a ΔF (%) vs. K^+ equilibrium potential (E_{K^+}) (mV) curve ($n=4$). E_{K^+} was calculated with the Nernst equation.

3. Results and discussion

In order to obtain evidence for the interaction of different Cry1Ab monomers during pore-formation activity and toxicity, we decided to explore if two independent mutants affected in different regions could recover toxicity and pore formation when assayed as protein mixtures. Mutant F371A of Cry1Ab protein was chosen since previous reports showed that this mutant was affected in receptor binding and toxicity [32]. The mutation F371A maps in loop 2 of domain II and it is affected primarily in the irreversible binding step of the toxin. Also, no effects on stability to trypsin treatment were observed in this mutant and it presented a 400-fold reduction in toxicity against *M. sexta* larvae [32]. In this study we show that mutant F371A could not form pores on BBMV prepared from *M. sexta* larvae (see below).

3.1. Isolation of Cry1Ab H168F

In order to have a different mutant affected exclusively in pore-formation activity and not in binding to the receptor, we decided to mutagenize His 168 localized within helix α-5 of domain I. In the closely related Cry1Ac toxin, several mutations in the conserved residue H168 showed altered toxicity to *M. sexta* larvae [33]. The positive charge seemed to be important for toxicity since a mutant with a change to negative charge (H168D) or a change to no charge (H168N) showed reduced toxicity in contrast to a conservative change (H168R) that showed three-fold increased toxicity against *M. sexta* larvae [33]. Mutations that reduced toxicity (H168D, H168N) did not affect binding while toxicity was diminished [33]. We decided to change H168 for a non-charged amino acid. H168 was mutagenized and changed to phenylalanine. The H168F crystals were purified, solubilized and trypsinized. A 55-kDa trypsin-resistant fragment was produced in low yield.

Bioassays done with the H168F mutant protein showed that this protein had reduced toxicity to *M. sexta* larvae in contrast to Cry1Ab toxin (Table 1).

3.2. Binding analysis of H168F and F371A to M. sexta BBMV

Analysis of binding of biotinylated H168F protein to BBMV prepared from *M. sexta* showed that this protein was able to bind to BBMV (Fig. 1A). This interaction is specific since heterologous competition using 100-fold excess of unlabeled Cry1Ab protein competed for binding with H168F to *M. sexta* BBMV. Also, we analyzed the binding of biotinylated F371A to *M. sexta* BBMV. In our binding conditions, F371A did not bind to BBMV (Fig. 1A); previously it was shown that although F371A is affected in receptor binding it was not affected in initial reversible binding using a similar protocol for binding [32]. This difference could be due to the fact that in our assay toxin was labeled with biotin, while ^{125}I-labeled toxin was used previously [32]. Nevertheless, binding of F371A was evident when a 100-fold excess of unlabeled Cry1Ab protein was incubated along with F371A (Fig. 1A). We also analyzed if mutant F371A could bind to BBMV when mixed with H168F. Fig. 1B shows that F371A bound efficiently to BBMV when mixed with H168F in a one to one ratio. F371A also bound to BBMV when mixed with 100-fold excess of H168F although less efficiently (Fig. 1B). These results showed that mutant F371A binds efficiently to BBMV when mixed with toxin proteins that are not affected in receptor binding, suggesting that intermolecular interaction between monomers could occur after receptor binding.

3.3. Pore-formation activity and toxicity of F371A and H168F protein mixtures

In order to determine if proteins F371A and H168F

Table 1
Toxicity of Cry proteins to *M. sexta* larvae

Mutant[a]	Mortality (%)[b]
Cry1Ab	100
F371A	0
H168F	4
F371A+H168F[c]	*25*
None	0

[a]All proteins were tested as pure trypsin-activated toxins.
[b]Mortality as percent of 24 larvae treated with 20 ng cm^{-2} after 5 days.
[c]1:1 protein mixture.

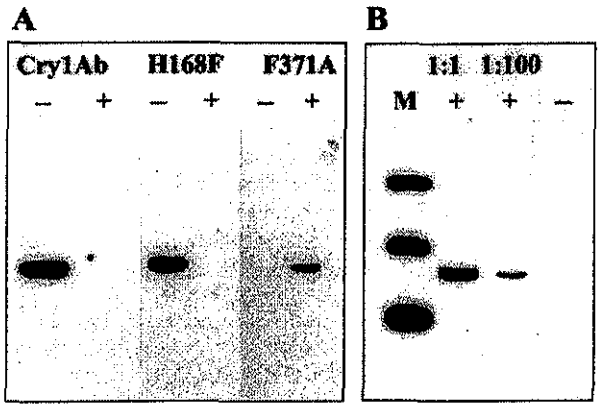

Fig. 1. Homologous competition binding assays on BBMV isolated from *M. sexta* larvae. A: Biotinylated Cry1Ab (lanes 1, 2), H168F (lanes 3, 4) and F371A (lanes 5, 6) toxins were incubated with the BBMV in the absence (–) or in the presence (+) of 100-fold excess of unlabeled Cry1Ab toxin. After 1 h of incubation, unbound toxins were removed and vesicles containing bound toxins were loaded onto a SDS–PAGE and blotted to a nitrocellulose membrane. Labeled proteins were visualized by means of streptavidin–peroxidase conjugate. B: Biotinylated F371A was incubated with the BBMV in the absence (–) or in the presence (+) of 1-fold (1:1) or 100-fold (1:100) unlabeled H168F toxin. Molecular size markers (lane M) are 98, 68 and 46 kDa respectively.

could form functional hetero-oligomers, the pore-formation activity of wild-type Cry1Ab and F371A–H168F mixtures was analyzed in BBMV from *M. sexta* larvae. BBMV were loaded with 150 mM KCl and assayed with the membrane potential-sensitive fluorescent dye dis-C_3-(5) as previously reported [10]. The resting membrane potential was -42.3 ± 3 mV ($n=4$) and the potassium equilibrium potential (E_K) calculated with the Nernst equation was -115.8 mV. Addition of 100 nM of Cry1Ab toxin to BBMV suspended in 150 mM MeGluCl produced a fast hyperpolarization (-66.7 ± 5 mV, $n=4$). After toxin exposure, the vesicles also increased their response to KCl additions ($m=0.19$), when compared to the control ($m=0.017$) to which the same amount of buffer was added (Fig. 2). The slope of the trace after KCl addition reflects the K^+ permeability of BBMV. In contrast to Cry1Ab toxin, proteins F371A ($m=0.02$) or H168F ($m=0.035$) did not induce an increased K^+ permeability when compared to control ($m=0.017$) (Fig. 2), showing that both mutants are affected in pore-formation activity. Addition of 100 nM of a 1:1 mixture of F371A–H168F to BBMV showed an increased K^+ permeability ($m=0.174$) very similar to that induced by wild-type Cry1Ab toxin, and also produced a fast hyperpolarization of -80.4 ± 3 mV, $n=3$. These data showed that the protein mixture of F371A and H168F recovered their capacity to form ionic channels in vitro.

Finally the toxicity against *M. sexta* larvae was analyzed. *M. sexta* larvae were fed with a 1:1 mixture of F371A–H168F proteins as described in Section 2. Table 1 shows that the mixture of both proteins recovered toxicity to some extent since mortality was 25% in contrast to larvae fed with F371A or H168F mutants, which showed no mortality, or with Cry1Ab protein, which showed 100% mortality (Table 1).

The pore-formation activity by the F371A–H168F protein mixture was very similar to the pore-formation activity of Cry1Ab. However, toxicity was only partially recovered by the F371A–H168F protein mixture (Fig. 2, Table 1). This result could be explained by a reduced stability of H168F mutant toxin in the midgut. Nevertheless, the fact that the F371A–H168F protein mixture presented increased mortality in comparison with toxicity displayed by individual mutant proteins clearly shows that functional hetero-oligomers could also be formed in vivo. These data also suggest that residue H168 is not involved in oligomer formation since mutant H168F is capable of interacting with F371A protein. Finally, these data are the first to show that the interaction of more than one monomer is fundamental for pore formation and toxicity of Cryl proteins. Also, assays of protein mixtures to recover pore formation and toxicity could be useful to identify

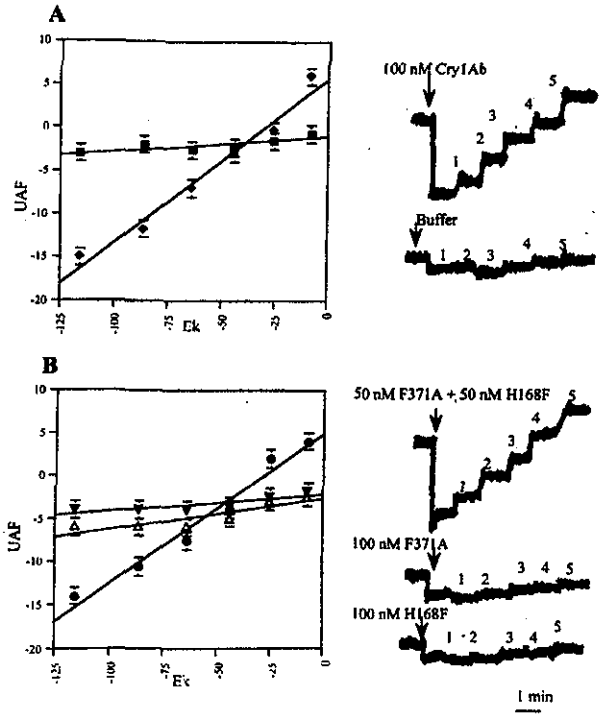

Fig. 2. Effect of the Cry1Ab, F371A, H168F and F371A–H168F toxins on the membrane potential in *M. sexta* midgut BBMV. Membrane potentials of BBMV (20 μg) loaded with (mM) 150 KCl, 2 EGTA, 0.5 EDTA, 10 HEPES–HCl pH 7.6 were recorded as described in Section 2. Pre-equilibration with 1.5 mM dis-C_3-(5) (9 min) is not shown. The arrow at the top of the traces corresponds to the time of toxin or buffer addition. Final K^+ concentrations were (mM): 1=6; 2=12; 3=24; 4=48 and 5=96. FAU=fluorescence arbitrary units. A: Response of BBMV suspended in buffer A (140 mM MeGluCl, 10 mM HEPES–HCl pH 8) to Cry1Ab toxin. In the control, buffer A was added instead of toxin. B: Response of BBMV to H168F toxin, F371A toxin and 1:1 F371A–H168F toxin mixture.

100

specific regions that might be involved in Cry1 protein–protein interactions for oligomer formation.

Acknowledgements

We thank Dr. Donald Dean for kindly providing us with the F317A mutant and Dr. Didier Lereclus for Bt strain 407 Cry$^-$ and plasmid pTH315. We thank Laura Lina and Leopoldo Güereca for technical assistance. This work was partially supported by CONACyT Contracts 27637-N and 25248-N, DGAPA-UNAM IN217597 and UC MEXUS-CONACYT.

References

[1] Feitelson, J.S. (1993) in: Advanced Engineered Pesticides (Kim, L., Ed.), pp. 63–72. Marcel Dekker, New York.
[2] Li, J., Carroll, J. and Ellar, D.J. (1991) Nature 353, 815–821.
[3] Grochulski, P., Masson, L., Borisova, S., Pusztai-Carey, M., Schwartz, J.L., Brousseau, R. and Cygler, M. (1995) J. Mol. Biol. 254, 447–464.
[4] Li, J., Koni, P.A. and Ellar, D.J. (1996) J. Mol. Biol. 257, 129–152.
[5] Crickmore, N., Zeigler, D.R., Schnepf, E., Van Rie, J., Lereclus, D., Baum, J., Bravo, A. and Dean, D.H. (1999) *Bacillus thuringiensis* toxin nomenclature. http://www.biols.susx.ac.uk/Home/Neil_Crickmore/Bt/index.html.
[6] Bravo, A., Jansens, S. and Peferoen, M. (1992) J. Invertebr. Pathol. 60, 237–246.
[7] Hofmann, C., Lüthy, P., Hütter, R. and Pliska, V. (1988) Eur. J. Biochem. 173, 85–91.
[8] Van Rie, J., Jansens, S., Höfte, H. and Degheele, D. (1990) Appl. Environ. Microbiol. 56, 1378–1385.
[9] Sacchi, V.F., Parenti, P., Hanozet, G.M., Giordana, B., Lüthy, P. and Wolfersberger, M. (1986) FEBS Lett. 204, 213–218.
[10] Lorence, A., Darszon, A., Díaz, C., Liévano, A., Quintero, R. and Bravo, A. (1995) FEBS Lett. 360, 217–222.
[11] Knowles, B.H. (1994) Adv. Insect Physiol. 24, 275–308.
[12] Schwartz, J.L., Garneau, L., Savaria, D., Masson, L., Brousseau, R. and Rousseau, E. (1993) J. Membr. Biol. 132, 53–62.
[13] Slatin, S.L., Abrams, C.K. and English, L.H. (1990) Biophys. Res. Commun. 169, 765–772.
[14] Von-Tersch, M.A., Slatin, S.L. and Kulesza, C.A. (1994) Appl. Environ. Microbiol. 60, 3711–3717.
[15] Knowles, B.H. and Ellar, D.J. (1987) Biochim. Biophys. Acta 924, 509–518.
[16] Pietrantonio, P.V. and Gill, S.S. (1996) in: Biology of the Insect Midgut (Lehane, M.J. and Billingsley, P.F., Eds.), pp. 345–372. Chapman and Hall, London.
[17] Schwartz, J.L., Juteau, M., Grochulski, P., Cygler, M., Préfontaine, G., Brousseau, R. and Masson, L. (1997) FEBS Lett. 410, 397–402.
[18] Güereca, L. and Bravo, A. (1999) Biochim. Biophys. Acta 1429, 342–350.
[19] Aronson, A., Geng, Ch. and Wu, L. (1999) Appl. Environ. Microbiol. 65, 2503–2507.
[20] Sanimugavelu, M., Rajamohan, F., Kathrivel, M., Eñlangovan, G., Dean, D.H. and Jayaraman, K. (1998) Appl. Environ. Microbiol. 64, 756–759.
[21] Wabiko, H., Raymond, K.C. and Bulla Jr., L.A. (1986) DNA 5, 305–314.
[22] Arantes, O. and Lereclus, D. (1991) Gene 108, 115–119.
[23] Lereclus, D., Arantes, O., Chaufaux, J. and Lecadet, M.-M. (1989) FEMS Microbiol. Lett. 60, 211–218.
[24] Lereclus, D., Agaisse, H., Gominet, M. and Chaufaux, J. (1995) Bio/Technology 13, 67–71.
[25] Meza, R., Nuñez-Valdez, M.-E., Sanchez, J. and Bravo, A. (1996) FEMS Microbiol. Lett. 145, 333–339.
[26] Thomas, W.E. and Ellar, D.J. (1983) J. Cell Sci. 60, 181–197.
[27] Masson, L., Lu, Y.-J., Mazza, A., Brosseau, R. and Adang, M.J. (1995) J. Biol. Chem. 270, 20309–20315.
[28] Lee, M.K., Milne, R.E., Ge, A.Z. and Dean, D.H. (1992) J. Biol. Chem. 267, 3115–3121.
[29] Bradford, M.M. (1976) Anal. Biochem. 72, 248–254.
[30] Wolfersberger, M., Lüthy, P., Maurer, A., Parenti, P., Sacchi, F.V., Giordana, B. and Hanozet, G.M. (1987) Comp. Biochem. Physiol. 86A, 301–308.
[31] Aranda, E., Sanchez, J., Peferoen, M., Güereca, L. and Bravo, A. (1996) J. Invertebr. Pathol. 68, 203–212.
[32] Rajamohan, F., Alcantara, E., Lee, M.K., Chen, X.J. and Dean, D.H. (1995) J. Bacteriol. 177, 2276–2282.
[33] Wu, D. and Aronson, A.I. (1992) J. Biol. Chem. 267, 2311–2317.

THE JOURNAL OF BIOLOGICAL CHEMISTRY
© 2002 by The American Society for Biochemistry and Molecular Biology, Inc.

Vol. 277, No. 16, Issue of April 19, pp. 13863–13872, 2002
Printed in U.S.A.

Heliothis virescens and *Manduca sexta* Lipid Rafts Are Involved in Cry1A Toxin Binding to the Midgut Epithelium and Subsequent Pore Formation*

Received for publication, October 18, 2001, and in revised form, February 6, 2002
Published, JBC Papers in Press, February 8, 2002, DOI 10.1074/jbc.M110057200

Meibao Zhuang‡§, Daniela I. Oltean‡§, Isabel Gómez¶, Ashok K. Pullikuth§, Mario Soberón¶, Alejandra Bravo¶, and Sarjeet S. Gill‡§‖

From the ‡Environmental Toxicology Graduate Program and the §Department of Cell Biology and Neuroscience, University of California, Riverside, California 92521 and the ¶Instituto de Biotecnología, Departamento de Microbiología, Universidad Nacional Autónoma de México, Apdo. postal 510-3, Cuernavaca, Morelos 62250, México

Lipid rafts are characterized by their insolubility in nonionic detergents such as Triton X-100 at 4 °C. They have been studied in mammals, where they play critical roles in protein sorting and signal transduction. To understand the potential role of lipid rafts in lepidopteran insects, we isolated and analyzed the protein and lipid components of these lipid raft microdomains from the midgut epithelial membrane of *Heliothis virescens* and *Manduca sexta*. Like their mammalian counterparts, *H. virescens* and *M. sexta* lipid rafts are enriched in cholesterol, sphingolipids, and glycosylphosphatidylinositol-anchored proteins. In *H. virescens* and *M. sexta*, pretreatment of membranes with the cholesterol-depleting reagent saponin and methyl-β-cyclodextrin differentially disrupted the formation of lipid rafts, indicating an important role for cholesterol in lepidopteran lipid rafts structure. We showed that several putative *Bacillus thuringiensis* Cry1A receptors, including the 120- and 170-kDa aminopeptidases from *H. virescens* and the 120-kDa aminopeptidase from *M. sexta*, were preferentially partitioned into lipid rafts. Additionally, the leucine aminopeptidase activity was enriched approximately 2–3-fold in these rafts compared with brush border membrane vesicles. We also demonstrated that Cry1A toxins were associated with lipid rafts, and that lipid raft integrity was essential for *in vitro* Cry1Ab pore forming activity. Our study strongly suggests that these microdomains might be involved in Cry1A toxin aggregation and pore formation.

Cry proteins, major components of parasporal crystals produced by *Bacillus thuringiensis*, are specifically toxic against insect pests and widely used in agriculture as biological insecticides or in transgenic plants (1, 2). These proteins exert their toxic effects through a receptor-dependent process (1, 3, 4). Both glycosylphosphatidylinositol (GPI)[1]-anchored aminopeptidases and cadherin-like proteins have been identified as putative Cry1A receptors. In *Heliothis virescens*, the cadherin-like protein was found to be associated with Cry1A toxin resistance and consequently plays a role in *B. thuringiensis* toxicity (5). In this insect four aminopeptidases, which differentially bind the Cry1Aa, Cry1Ab, and Cry1Ac toxins, are also putative receptors for these toxins (6–9).[2] Similarly, in *Manduca sexta* and *Bombyx mori*, aminopeptidases and the cadherin-like proteins bind Cry1A toxins as well (10–14). Carbohydrate modification of these proteins may also be critical in insect resistance to Cry1 toxins, because impaired glycosylation was a factor in Cry5B-resistant *Caenorhabditis elegans* (15).

Binding to membrane receptors and subsequent pore formation are critical for Cry toxicity (1). However, the process by which Cry toxin-receptor binding leads to membrane pore formation remains ambiguous. Previous studies suggested that Cry toxin aggregates on the midgut epithelial membrane (16, 17), but the mechanism of toxin aggregation is unknown. With some mammalian pore-forming toxins, lipid rafts play an essential role in toxin aggregation (18–20). These rafts function as platforms to recruit proteins from distinct classes, such as GPI-anchored proteins and palmitoylated or diacylated transmembrane proteins (21–23). For example, the pore-forming toxin lysenin binds sphingomyelin in raft membranes (24), whereas cholera toxin requires both cholesterols and sphingolipids in rafts for its action (25). Binding to cholesterol by listerolysin O, another pore-forming toxin, is important in triggering a conformational change required for toxin oligomerization and channel formation (19). Moreover, aerolysin of *Aeromonas hydrophila*, one of the more widely studied pore-forming toxins, functions via a GPI-anchored protein present in lipid rafts (18). In regard to Cry toxins, phospholipase C treatment of *Trichoplusia ni* brush border membrane vesicles (BBMV) cleaved GPI-anchored membrane proteins and reduced pore formation by Cry1Ac toxin (26). Binding of these toxins to their respective membrane receptors, which are preferentially associated with lipid rafts, promotes an increase in local toxin concentration within the cell membrane favoring toxin oli-

* This work was supported in part by the University of California Agricultural Experimental Station; United States Department of Agriculture Grant 96-353-0-3820; fellowships from the University of California Toxic Substances Research and Teaching Program (to M. Z. and D. I. O.); and Consejo Nacional de Ciencia y Tecnologia (CONACYT) Grant 27637-N; Dirección de Apoyo al Personal Académico-Universidad Nacional Autónoma de México IN206200 and IN216300; and the University of California Mexico-United States CONACYT grant. The costs of publication of this article were defrayed in part by the payment of page charges. This article must therefore be hereby marked "*advertisement*" in accordance with 18 U.S.C. Section 1734 solely to indicate this fact.

‖ To whom correspondence should be addressed: 5429 Boyce Hall, Dept. of Cell Biology and Neuroscience, Environmental Toxicology Graduate Program, University of California, Riverside, CA 92521. Fax: 909-787-3087; E-mail: sarjeet.gill@ucr.edu.

[1] The abbreviations used are: GPI, glycosylphosphatidylinositol; BBMV, brush border membrane vesicle; MβCD, methyl-β-cyclodextrin; NSF, *N*-ethylmaleimide-sensitive factor; SM, sphingomyelin; PES, ethanolamine phosphosphingolipid; PS, phosphatidylserine; PC, phosphatidylcholine; PI, phosphatidylinositol; PE, phosphatidylethanolamine; TOA, toxin overlay assay; CRD, cross-reacting determinant.

[2] D. I. Oltean, M. Zhuang, and S. S. Gill, unpublished data.

gomerization required for pore formation, a key step in toxin action.

Lipid rafts are detergent-insoluble microdomains enriched in cholesterol, sphingolipids, and GPI-anchored proteins (22, 27–29). Several lines of evidence show the presence of lipid rafts *in vivo* (30–34). In fact, the formation of the liquid ordered phase results in membrane insolubility in the nonionic detergent Triton X-100 (22, 27). Hence, insolubility in Triton X-100 has been widely used as a criterion for isolation of rafts from cellular membranes (28, 35).

Although lipid rafts have been widely studied in mammalian cells (27, 29, 35), and have been isolated from *Saccharomyces cerevisiae* (36, 37), *Tetrahymena* (38), and *Drosophila melanogaster* (39), their constituents differ widely between species. Currently there are no data on the nature of lipid rafts from any other insect species, including lepidopterans. In this study, we isolated and characterized lipid rafts from the midgut epithelium of two lepidopteran insects, *H. virescens* and *M. sexta*. Additionally, we investigated the role of lipid rafts in the toxicity of Cry toxins to *H. virescens* and *M. sexta*. We demonstrated that Cry1A toxin-binding molecules, including aminopeptidases and some higher molecular weight bands, and the toxin molecules themselves show differential localization in lipid rafts isolated from these insects. We also showed lipid rafts play an important role in pore formation. This is the first study that suggests a role for lipid rafts in the mechanism of action of Cry toxins.

EXPERIMENTAL PROCEDURES

Bacterial Strains, Insects, and Media—Cry1Ac was produced from wild-type *B. thuringiensis* strain HD73 grown in nutrient broth sporulation medium for 72 h at 30 °C. Cry1Ab was produced from the acrystalliferous strain 4Q7cry transformed with pHT315-cry1Ab and grown in HCO medium (40) for 96 h at 30 °C. Both *H. virescens* and *M. sexta* were reared on artificial diet (Southland Bioproducts and Ref. 41, respectively).

Purification of Cry1Ab and Cry1Ac Toxins and the Activated Protein Fragments—Spores and crystals were harvested and washed with buffer containing 0.01% Triton X-100, 50 mM NaCl, and 50 mM Tris-HCl, pH 8.5. Crystals were isolated by NaBr gradients as previously described (42), solubilized in 10 mM Na_2CO_3, pH 10, at 37 °C for 1 h, and then activated with trypsin (1:5 w/w) at 18 °C for 6 h. The proteins were further purified by anion exchange chromatography (SMART, Amersham Biosciences) as previously described (8), and the purified toxins were dialyzed against appropriate buffers.

Toxin Biotinylation—Cry1Ab and Cry1Ac toxins, 100 μg, were biotinylated using the protein biotinylation module kit (Amersham Biosciences) and then purified with Sephadex G25 columns. Protein concentration in the collected fractions was determined by BCA (Pierce). The biotinylated toxins were detected with horseradish peroxidase-streptavidin and ECL® (Amersham Bioscience).

Purification of Detergent-insoluble Lipid Rafts—BBMV were prepared from early (day 1–2) 5th instar *H. virescens* and *M. sexta* midguts as described (43). Purified BBMV were suspended in TNE buffer (100 mM Tris, pH 7.5, 150 mM NaCl, and 0.2 mM EGTA). An equal volume of BBMV (100 μg) and pre-chilled 2% Triton X-100 were aliquoted into a SW41 tube and mixed. After solubilization for 30 min on ice, the mixture was brought to a final concentration of 60% sucrose and then overlaid with 2 ml each of 50, 40, 30, and 15% sucrose in TNE buffer. The samples were then centrifuged at 2 °C for 18 h at 80,000 × *g*. Insoluble lipid rafts, present in the middle of the sucrose gradients, were collected from the top of the tube, washed twice with TNE buffer, and centrifuged at 2 °C for 30 min at 150,000 × *g*. Soluble fractions were collected from the bottom of the tubes. BBMV pretreatments with detergents were performed with 10 mM methyl-β-cyclodextrin (MβCD) (Sigma) at 37 °C for 30 min or with 0.2% saponin (Sigma) on ice for 30 min, with subsequent addition of an equal volume of 2% Triton X-100 (Sigma). Direct treatment of isolated lipid rafts was done using the same conditions. Isolated lipid rafts were treated with MβCD or saponin and centrifuged at 100,000 × *g* for 30 min, and the supernatants and pellets were collected respectively, without subsequent Triton X-100 addition. Toxin association experiments were performed using different concentrations of biotinylated toxins, which were pre-incubated with BBMV at 4 °C for 1 h with subsequent isolation of lipid rafts by Triton X-100 treatment and separated by the sucrose gradient mentioned above.

Western Blotting—Proteins were electrotransferred to Immobilon membranes (Amersham Biosciences), which were then blocked with 5% powdered milk in phosphate-buffered saline and 0.05% Tween 20 (Sigma) for 1 h and then incubated with primary antibody diluted in 3% milk, phosphate-buffered saline, and 0.05% Tween 20. Dilutions of antibodies used were: anti-*M. sexta* fasciclin II, 1:2000 (44); anti-*H. virescens*-APN120 (6), 1:8000; anti-*Culex quinquefasciatus* V-ATPase B subunit (45), 1:5000; anti-*H. virescens* APN170 (8), 1:5000; anti-*H. virescens* APN180,[2] 1:3000; anti-*M. sexta* *N*-ethylmaleimide-sensitive factor (NSF) (46), 1:5000; and anti-cross-reacting determinant (anti-CRD) (Glyko), 1:200. Blots were subsequently incubated with horseradish peroxidase-conjugated secondary antibodies (goat anti-rabbit (Amersham Biosciences) or goat anti-guinea pig (Jackson)), and the signal was detected by ECL® (Amersham Biosciences). Toxin overlay assays (TOAs) for Cry1Ab and Cry1Ac were performed as described (8) using 1:3,000 diluted Cry1A antibodies (47).

Phosphatidylinositol Phospholipase C Digestion and GPI Anchor Detection—Proteins prepared as above were transferred to Immobilon membranes, which were then digested with phosphatidylinositol phospholipase C (Glyko, 1.5 units/10 ml) according to Guther *et al.* (48). The presence of a cleaved GPI anchor was detected with anti-CRD antibody (Glyko).

Protein Concentration Determination and Enzyme Assays—Protein concentrations were determined by BCA. Leucine aminopeptidase activities were assayed as previously described (43) using leucine-*p*-nitroanilide as substrate (Sigma).

Lipid Quantification—BBMV samples were treated with 10 mM MβCD at 37 °C for 30 min, with 0.2% saponin on ice for 30 min, or with 1% Triton X-100 on ice for 30 min. These detergent-treated samples were then centrifuged at 100,000 × *g* for 30 min, the supernatants (S) and pellets (P) were collected, and both fractions were used for quantification of total cholesterols and phospholipids. Cholesterol quantification was performed with the Infinity cholesterol reagent from Sigma using the manufacturer's protocol. Cholesterol standards were purchased from Sigma. Total phospholipid quantification was performed using Barlett's method (49). Briefly, samples and standards were hydrolyzed in 0.2 ml of perchloric acid for 2 h at 180 °C, cooled to room temperature, and subsequently mixed with 1.25 ml of reducing reagent (1% sodium bisulfite, 0.2% sodium sulfite, and 0.017% 1-amino-2-naphthol-4-sulfonic acid) and 1.25 ml of molybdate reagent (0.44% ammonium molybdate, 1.4% sulfide acid). The mixtures were then treated in boiling water bath for 10 min. The absorbance determined at 820 nm represents the amount of phospho groups, which indicates the amount of phospholipids present in the sample.

Lipid Analysis—Lipid extractions were performed as described (50). Briefly, total lipids were extracted from the isolated lipid rafts with chloroform:methanol (2:1), purified with chloroform:methanol:H_2O (3:48:47), and subsequently dried. Electrospray ionization tandem mass spectrometry was performed as described (51). Lipid samples were infused into the source via a 50-μm fused silica transfer line at 3 μl/min. Spectra from samples containing 5 ng/μl lipid or more were acquired in less than 10 s of total acquisition time. Negative ion ms/ms was run with an orifice voltage from −60 to −80 V. Samples were scanned between 500 and 900 atomic mass units in the negative ionization mode. Spectra were subsequently collected and analyzed using proprietary software from Sciex Corp. Because the total area of the spectra (S_t) represents the total amount of lipids, the area of an individual peak (S_i) represents the relative amount of a specific lipid; the relative ratio of a specific lipid was thus determined as S_i/S_t, and the data obtained are given in Fig. 3.

Measurements of Membrane Potential and Pore Formation Activity—Membrane potentials were monitored with the fluorescent positively charged dye, 3,3′-dipropylthiodicarbocyanine (Molecular Probes; 1.5 μM final, 1 mM stock in Me_2SO). Lipid raft vesicles were centrifuged at 100,000 × *g* for 1 h, suspended in 150 mM KCl, 10 mM HEPES, pH 8.0, buffer, and sonicated with six pulses of 30 s each at 25 °C (Branson 1200 sonic bath) in the same solution. Fluorescence was recorded at the 620/670 nm excitation/emission wavelength pair using an Aminco SLM spectrofluorometer (26). Hyperpolarization causes dye internalization into the membrane vesicles and a fluorescence decrease, whereas depolarization has the opposite effect. Dye calibration and determinations of the resting membrane potentials were performed in the presence of valinomycin (2 μM) by successive additions of KCl to raft vesicles (10 μg) suspended in 150 mM *N*-methyl-D-glucamine chloride (MeGluCl), 10 mM HEPES-HCl, pH 8.0, buffer (1.8 ml). All measurements were made at

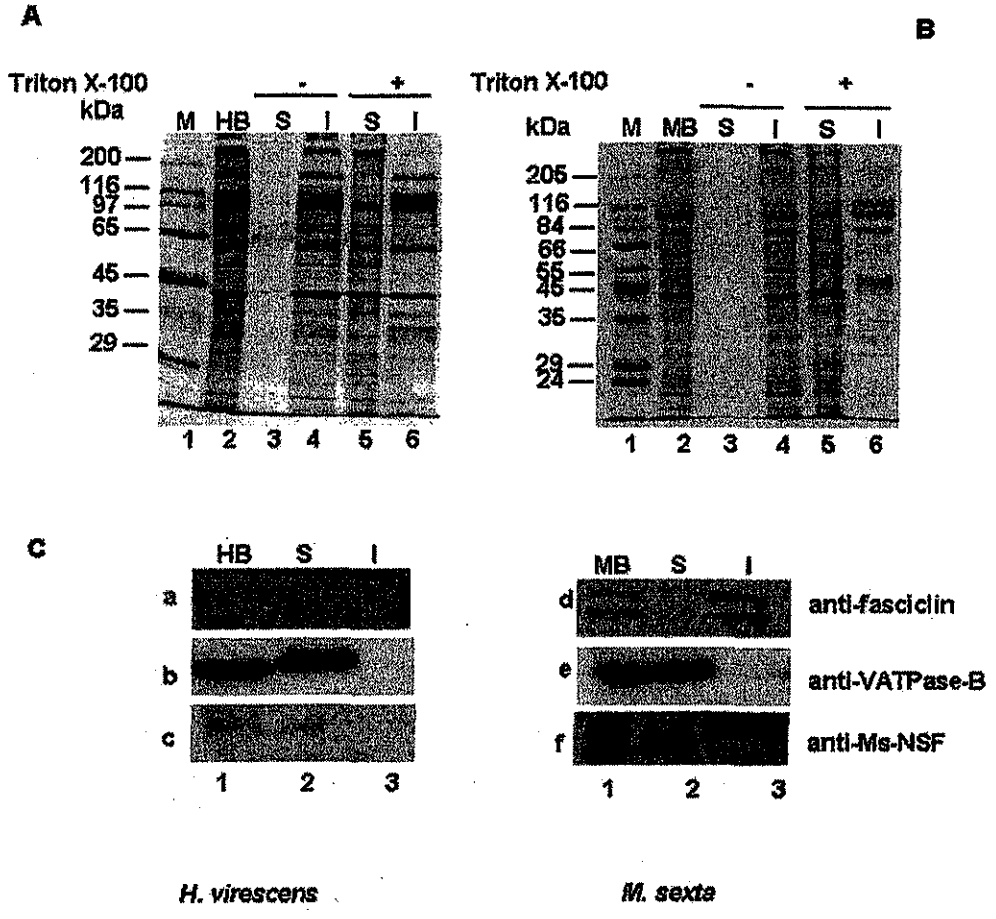

FIG. 1. **Isolation of Triton X-100-insoluble lipid rafts from lepidopteran insect midgut BBMV.** *HB*, *H. virescens* BBMV; *MB*, *M. sexta* BBMV; *S*, soluble fractions; *I*, insoluble fractions isolated from the sucrose gradient. *Panels A* and B show silver-stained gels following 10% SDS-PAGE. *A*, comparison of the Triton X-100-soluble and -insoluble lipid raft fractions obtained from *H. virescens* BBMV. Upon Triton X-100 treatment, the insoluble fraction (*lane 6*) had a distinct protein profile from that of the soluble fraction (*lane 5*). Lipid rafts differ from intact BBMV (*lane 2*) or control without detergent treatment (*lanes 3* and *4*). *B*, similar results were observed with *M. sexta* samples and *H. virescens*. *C*, immunoblot analysis of Triton X-100-insoluble (lipid rafts) and -soluble fractions. *M. sexta* fasciclin antibody recognized the 110- and 90-kDa isoforms present exclusively in *M. sexta*-insoluble fractions (*panel C, d, lane 3*). Similar results were obtained with *H. virescens* (*a, lane 3*). The B subunit of V-ATPase and the 84-kDa NSF homolog partitioned into the soluble fraction (*b–f, lane 2*). Interestingly, the *M. sexta* NSF antibody recognized another 97-kDa protein, which was present only in lipid rafts from *M. sexta* (*f, lane 3*). In *A–C*, each lane contains 10 μg of protein, except in lanes where negligible protein was present, in which case the maximum volume (40 μl) was loaded.

25 °C with constant stirring. Time 0 (t) was when raft vesicles were added, and subsequently toxin (50 nM) was added after 2 min. After the first hyperpolarization produced, successive additions of KCl (4, 8, 12, 16, 32, and 64 mM, final concentration) to the raft vesicles were performed. The slope (m) of the curves ΔF (%) *versus* K^+ equilibrium potential (E_{K^+}) (mV) or *versus* external K^+ concentration was determined. E_{K^+} was calculated using the Nernst equation. Changes in fluorescence determinations were repeated three times. Pore formation activity was also analyzed in raft vesicles that were treated with 10 mM MβCD (for *H. virescens*) or 20 mM MβCD (for *M. sexta*) at 37 °C for 30 min. Excess MβCD was removed from the membranes by centrifugation at 100,000 × *g* for 30 min, and raft vesicles were resuspended in 150 mM KCl, 10 mM HEPES, pH 8.0, buffer.

RESULTS

Separation of H. virescens and M. sexta Midgut Epithelial Membrane Lipid Rafts—Plasma membranes of numerous cell types contain microdomains commonly referred to as lipid rafts, which are biochemically distinct from the bulk plasma membranes (22, 27). Lipid rafts are resistant to solubilization at low temperature by nonionic detergents, such as Triton X-100 and, because of their low buoyant density, can be isolated by density gradient ultracentrifugation (22, 27, 28). In this study, we isolated Triton X-100-insoluble lipid rafts from *H. virescens* and *M. sexta* BBMV. After Triton X-100 treatment and overnight centrifugation, the *H. virescens* insoluble band (I) was collected from the interface of 50 and 40% sucrose layers, whereas the soluble fraction (S) was collected from the bottom sucrose layer. The *M. sexta* insoluble band was collected from the interface of 40 and 30% sucrose layers. *H. virescens* and *M. sexta* Triton X-100-insoluble lipid rafts migrated to different positions in the sucrose gradient suggesting the lipid components or lipid-protein ratios of these rafts were different. Subsequent lipid analysis supported these observations (see below, and Fig. 3). BBMV subjected to sucrose gradient centrifugation alone were apparently unchanged and consistently isolated in the insoluble fraction (Fig. 1, *panels A* and *B*, *lanes 2–4*). However, addition of Triton X-100 solubilized some proteins, whereas others remained in the insoluble fraction (Fig. 1, *panels A* and *B*, *lanes 5* and *6*). The protein profiles of BBMV from *H. virescens* (*HB*) and *M. sexta* (*MB*), soluble fractions (*S*), and insoluble fractions (*I*) obtained upon Triton X-100 treatment were significantly different. Two isotypes of *M. sexta* fasciclin, a lipid raft-marker protein (39), were recognized by the *M. sexta* anti-fasciclin antibody and were present exclusively in the insoluble fractions (Fig. 1, *panel C, d*). Similar results were obtained with *H. virescens* (Fig. 1, *panel C, a*).

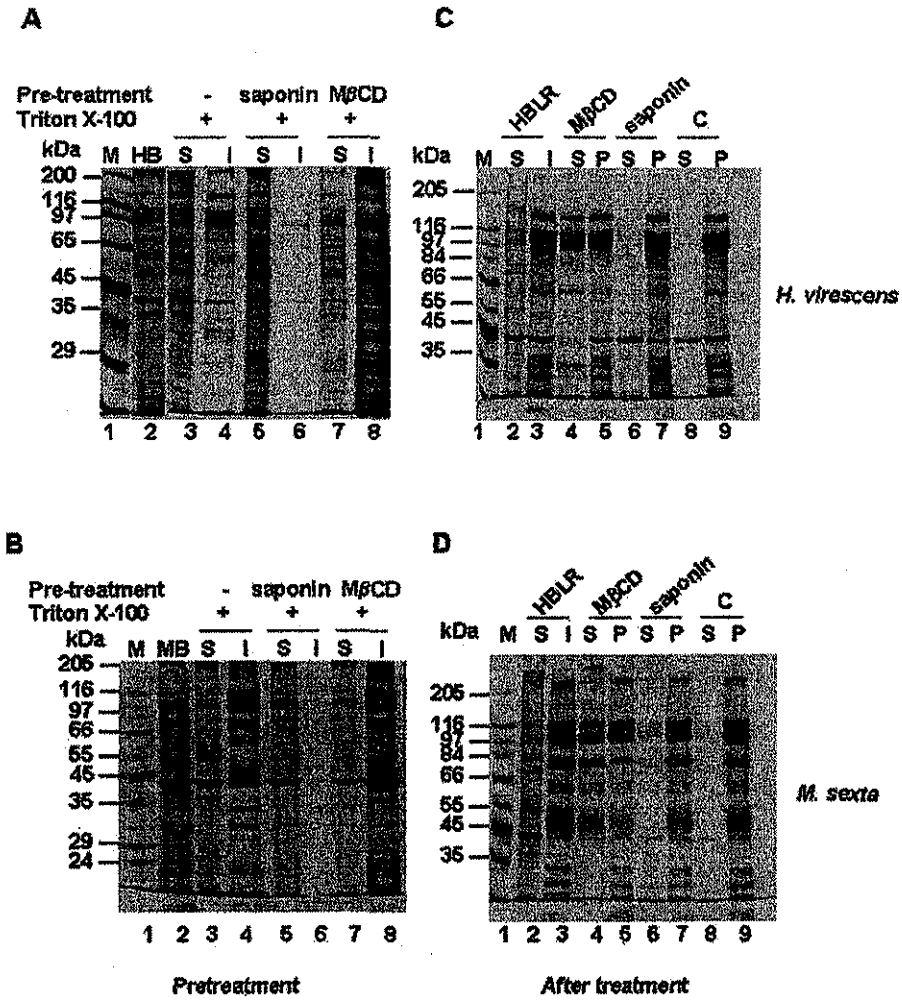

FIG. 2. **Effect of cholesterol-depleting reagents on protein distribution in lipid rafts.** 10% SDS-PAGE of *H. virescens* (*A*) and *M. sexta* (*B*) BBMV pretreated with saponin and MβCD before lipid raft isolation. *Lane 2* represents intact BBMV, BBMV solubilized with Triton X-100 without any pretreatment; *lanes 3* and *4* represent the soluble fraction (*S*) and lipid rafts (*I*), respectively. Pretreatment of BBMV with saponin caused most of the lipid raft-associated proteins to become soluble, thereby disrupting lipid rafts (*lanes 5* and *6*). Pretreatment of BBMV with MβCD caused most proteins to be Triton X-100-insoluble (*lanes 7* and *8*). *C* and *D*, effect of MβCD and saponin on the isolated lipid rafts from *H. virescens* (*C*) and *M. sexta* (*D*). Isolated lipid rafts were treated with MβCD or saponin and centrifuged at 100,000 × *g* for 30 min, and the resultant supernatants (*S*) and pellets (*P*) were collected respectively, without subsequent Triton X-100 addition. Further treatment of isolated lipid rafts with MβCD solubilized some of the lipid raft-associated proteins (*lanes 4* and *5*), whereas further treatment with saponin did not affect protein association with lipid rafts (*lanes 6* and *7*). Controls were isolated lipid rafts (*C* and *D*, *lanes 2* and *3*, HBLR/MBLR) and lipid rafts undergone the same process as in *lanes 4–7* but without MβCD nor saponin further treatment (*C* and *D*, *lanes 8* and 9). In *A–D*, each lane contained 10 μg of protein, except in lanes where negligible protein was present, in which case the maximum volume (40 μl) was loaded.

These data confirmed that the Triton X-100-insoluble fractions isolated from sucrose gradients were lipid rafts. In contrast, the 57-kDa V-ATPase B subunit and the 84-kDa NSF homolog were exclusively partitioned into the soluble fraction (Fig. 1, *panel C*, *b–f*). In *M. sexta*, another 97-kDa protein, which is likely the p97/CDC48 homolog (53), was detected exclusively in lipid rafts (Fig. 1, *panel C*, *f*). Collectively, these data show that proteins are not uniformly distributed within the plasma membrane, but some are selectively localized into lipid raft microdomains.

Cholesterol Plays a Structural Role in Lipid Rafts—Both MβCD and saponin are cholesterol-depleting reagents. MβCD is an effective extracellular cholesterol acceptor that extracts cholesterol from membranes (54), whereas saponin binds cholesterol and sequesters it from other interactions, but does not extract it from the membrane (55). In our study, pretreatment of the BBMV sample with MβCD and saponin before lipid rafts isolation differentially affected the resultant lipid rafts (Fig. 2, *panels A* and *B*). Addition of MβCD resulted in BBMV becoming resistant to detergent solubilization. In addition, the protein profile of the isolated Triton X-100-insoluble fraction from MβCD-treated BBMV was similar to that of the control BBMV (without Triton X-100 treatment), but not to the profile of typical lipid rafts (Fig. 2, *panels A* and *B*, *lanes 8* and *2*, and *lane 4*). However, pretreatment of membranes with saponin disrupted lipid rafts. Most raft-associated proteins became Triton X-100-soluble upon saponin pretreatment and thus partitioned into the soluble fractions (Fig. 2, *panels A* and *B*, *lanes 5* and *6*), suggesting that cholesterol is essential for lipid raft formation in lepidopteran insects.

Treatment of isolated lipid rafts with MβCD and saponin (Fig. 2, *panels C* and *D*) had different effects compared with detergent pretreatment of BBMV (*panels A* and *B*). Extraction of cholesterol from the isolated lipid rafts with MβCD led to solubilization of proteins previously associated with cholesterol (Fig. 2, *panels C* and *D*, *lanes 4* and *5*). Although saponin affects lipid-protein interactions and weakens membrane liquid-ordered forces (which results in Triton X-100 solubility), it does

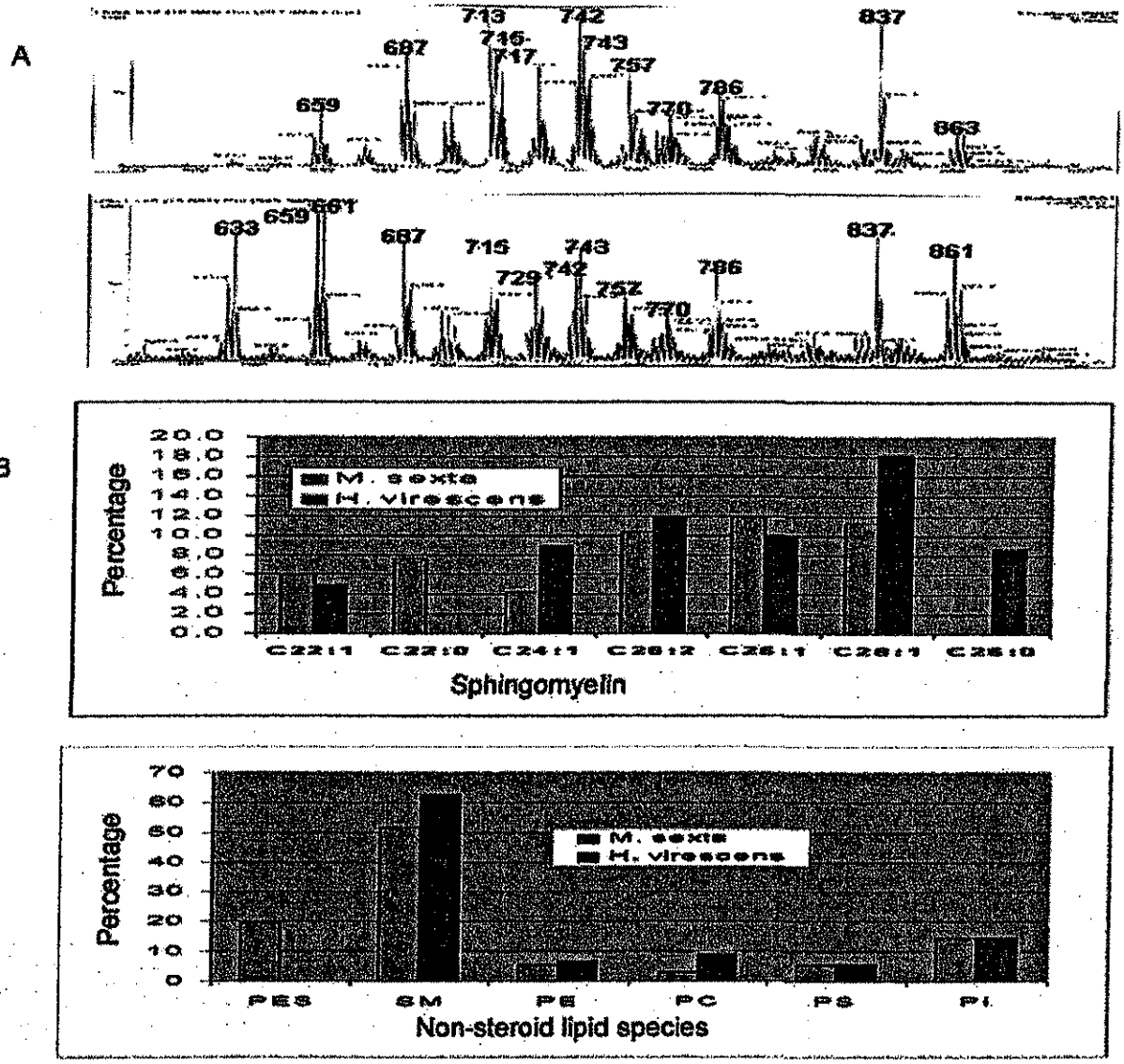

FIG. 3. **Electrospray ionization mass spectrometry analysis of lipid components from the isolated lipid rafts.** *A*, mass spectrum of raft lipids from *H. virescens* (*1*) and *M. sexta* (*2*). *B*, fatty acid acyl chain length of sphingomyelins from *H. virescens* and *M. sexta* lipid rafts. *C*, major nonsteroid lipid species isolated from lepidopteran insect midgut epithelium lipid rafts.

not extract cholesterol from the membrane. Thus, as expected, direct treatment of the isolated lipid rafts with saponin did not affect protein partitioning (Fig. 2, *panels C* and *D*, *lanes 6* and *7*).

Both cholesterol and phospholipids are enriched in lepidopteran lipid rafts (22, 28, 29). However, MβCD and saponin extracted cholesterol and phospholipid differently. Under the experimental conditions used, MβCD extracted 38.7 and 48.1% of cholesterol from *H. virescens* and *M. sexta* BBMV, respectively, but it did not extract phospholipids from BBMV. In contrast, saponin extracted 11.7 and 13.2% of phospholipids from *H. virescens* and *M. sexta* BBMV, respectively, but it did not extract cholesterol from BBMV.

Lipid Composition—By using electrospray ionization tandem mass spectrometry, major nonsteroid lipid components of lepidopteran lipid rafts were determined. As summarized in Fig. 3 and Table I, the major non-steroid lipids of lepidopteran insect midgut epithelium lipid rafts are sphingomyelin (SM), phosphatidylserine (PS), phosphatidylcholine (PC), phosphatidylinositol (PI) and phosphatidylethanolamine (PE). Some of these lipid acyl chains are saturated, which facilitate formation of a liquid order phase when mixed with cholesterol (56). Our data also showed that the lipid acyl chain length from the *H. virescens* and *M. sexta* lipid rafts were shorter (Table I) than those from mammalian plasma membranes (57), but were similar to those from *D. melanogaster* lipid rafts (39).

The major nonsteroid lipid components of both *H. virescens* and *M. sexta* lipid rafts are sphingomyelins. Loss of the head group in sphingomyelins in negative mode results in ion 168, whereas loss of the head group in ethanolamine phosphosphingolipids results in ion 140. Both of these lipids were detected in *M. sexta*, but only sphingomyelins were detected in the *H. virescens*. Fragment 208, a typical derivative of the hexadeca-4-sphingenine backbone, was detected in *D. melanogaster* lipid rafts (39). However, in both *H. virescens* and *M. sexta* samples, this ion was not detected. Collectively, these data showed that the lipid components of *H. virescens* and *M. sexta* lipid rafts are similar but not identical. Additionally, the amount of total lipids extracted from the same amount of *H. virescens* and *M.*

106

TABLE I
Major non steroid lipid species in lepidopteran insect lipid rafts

A. *H. virescens*

m/z	Species	Acyl chain
659	SM	C22:1
687	SM	C24:1
713	SM	C26:2
715	SM	C26:1
717	SM	C26:0
742	PE	C18:0/C18:2
742	PC	C16:0/C18:2
743	SM	C28:1
757	SM	C28:1
770	PC	C18:0/C18:2
786	PS	C18:0/C18:2
837	PI	C16:0/C18:0
863	PI	C18:0/C18:1

B. *M. sexta*

m/z	Species	Acyl chain
633	PES	C22:2
659	SM	C22:1
659	PES	C24:1
661	SM	C22:0
661	PES	C24:0
687	SM	C24:1
687	PES	C26:1
713	SM	C26:2
715	SM	C26:1
729	SM	C26:1
729	PES	C28:1
742	PE	C18:0/C18:2
743	SM	C28:1
757	SM	C28:1
770	PC	C18:0/C18:2
786	PS	C18:0/C18:2
837	PI	C16:0/C18:0
861	PI	C18:0/C18:2

sexta lipid rafts were significantly different. The lipid-protein ratio (w/w, 0.55) from *M. sexta* lipid rafts was larger than that observed from *H. virescens* (w/w, 0.42) lipid rafts. Taken together, these differences explain why lipid rafts from *H. virescens* and *M. sexta* were isolated from different positions of the sucrose gradients. Differences in the lipid components from these two lepidopteran insects could arise from differences in the diet of these two insects.

Lipid Rafts Are Enriched in GPI-anchored Proteins—GPI-anchored proteins are enriched in mammalian lipid rafts (28, 58, 59). Similarly, Western blots showed that, in both *H. virescens* and *M. sexta*, most of the GPI-anchored proteins are partitioned into the lipid rafts (I) rather than into the soluble fractions (S). In *H. virescens* five GPI-anchored proteins of 170, 120, 66, 50, and 35 kDa were recognized by the anti-CRD antibody and partitioned into isolated lipid rafts (Fig. 4, *panel A, lane 3*), whereas a protein of 180-kDa was present in the soluble fraction (Fig. 4, *panel A, lane 2*). Western blot analysis with anti-APN180 antiserum suggested this protein is the 180-kDa aminopeptidase.[2] In case of *M. sexta*, four GPI-anchored proteins of 120, 100, 70, and 50 kDa were found exclusively in lipid rafts (Fig. 4, *panel B, lane 3*), consistent with lipid rafts being enriched in GPI-anchored proteins.

Distribution of Cry1A-binding Proteins in Lipid Rafts—One group of Cry1A-binding molecules in *H. virescens*, the aminopeptidases, are GPI-anchored proteins (6–9). Western blot analysis showed that the 120- and 170-kDa *H. virescens* aminopeptidases (Fig. 4, *panel C, a* and *b*) were preferentially associated with lipid rafts, whereas the 180-kDa aminopeptidase was partitioned into the soluble fraction (Fig. 4, *panel C, c*). Similarly, the *M. sexta* 120- and 106-kDa aminopeptidases were preferentially partitioned into lipid rafts (Fig. 4, *panel C, d*). Because the 120- and 170-kDa aminopeptidases have high leucine aminopeptidase activity (6–8), this enzymatic activity was monitored. Table II shows that the isolated lipid rafts have 2–3-fold enriched leucine aminopeptidase activity as compared with the untreated BBMV in *H. virescens* and *M. sexta*. These data confirmed that most of the aminopeptidases were preferentially associated with lipid rafts.

Furthermore, toxin overlay assays provided a general pattern of distribution of Cry1Ab- and Cry1Ac-binding proteins. In *H. virescens*, the 170- and 110-kDa Cry1Ab-binding proteins are apparently associated with lipid rafts, the 205-kDa Cry1Ab-binding protein partitioned into the soluble fraction, whereas the 190-kDa protein partitioned into both fractions (Fig. 5, *panel A*). As for Cry1Ac-binding proteins, the abundant 170- and 120-kDa proteins were preferentially partitioned into lipid rafts (Figs. 4*C* (*a* and *b*) and 5*B*). Other *H. virescens* lipid raft-associated Cry1Ac-binding proteins have sizes of 110, 85, and 60 kDa, whereas the 205- and 180-kDa Cry1Ac-binding proteins preferentially were partitioned into the soluble fraction (Fig. 5, *panel B*). In *M. sexta*, the 210-kDa Cry1Ab-binding proteins partitioned into both lipid rafts and the soluble fraction, whereas the 120-kDa protein partitioned exclusively into lipid rafts (Figs. 4*C* (*d*) and 5*C*). The rest of the Cry1Ab-binding proteins, including the 195-, 140- and 130-kDa proteins, were partitioned into the soluble fraction (Fig. 5, *panel C, lane 2*). Similarly, the *M. sexta* Cry1Ac-binding proteins of 210, 190, 140, and 106 kDa partitioned into both fractions, whereas the 120-kDa protein was exclusively lipid raft-associated (Fig. 5, *panel D*).

Cry1A Toxin Is Associated with H. virescens Lipid Rafts—Our data showed that several of the Cry1Ac-binding proteins are associated with *H. virescens* and *M. sexta* lipid rafts. Cry1Ab does not bind to *M. sexta* brush border membrane uniformly, but preferentially binds the tip of the microvilli (60). These results suggested that distribution of receptors is not uniform in these membranes and specific microdomains in microvilli could be involved in Cry toxin binding. To determine whether Cry toxin itself is associated with lipid rafts, biotinylated Cry1Ac was incubated with BBMV prior to Triton X-100 treatment. Fig. 6 shows that, at low toxin concentrations (1 nM), most of the Cry1Ac toxin fractionated with lipid rafts (Fig. 6, *panel A, lane 4*). At 10 nM, higher levels of Cry1Ac toxin were detected in lipid rafts than in the soluble fraction (Fig. 6, *panel A, lanes 5* and *6*). At even higher toxin levels (40 nM), the toxin was present in both fractions (Fig. 6, *panel A, lanes 7* and *8*). These data suggest Cry1Ac associated with *H. virescens* lipid rafts specifically, and the toxin association in lipid rafts was saturated between 1 and 10 nM. Similar experiments performed with *M. sexta* membrane samples produced the same results (data not shown). Pretreatment of BBMV-Cry1Ac with MβCD and saponin, before Triton X-100 treatment, affected the distribution of Cry1Ac as expected. Pretreatment with saponin caused the lipid raft-associated Cry1Ac to partition into the soluble fraction (Fig. 6, *panel B, lanes 3* and *4*). However, no change in the association of the Cry1Ac toxin was observed if BBMV were pretreated with MβCD (Fig. 6, *panel B, lanes 5* and *6*).

MβCD Disrupts Cry1Ab Pore Formation Activity—Cry toxins have been shown to alter K^+ permeability in liposomes and BBMV (17). We thus tested whether lipid rafts have a role in pore formation. We have shown in Fig. 2 (*panels C* and *D*) that MβCD treatment disrupted the isolated lipid rafts; thus, MβCD was used in this experiment. Cry1Ab-dependent K^+ permeability was determined in lipid rafts isolated from *H. virescens* and *M. sexta* before and after extraction of cholesterol by MβCD. As a control to determine vesicle integrity after

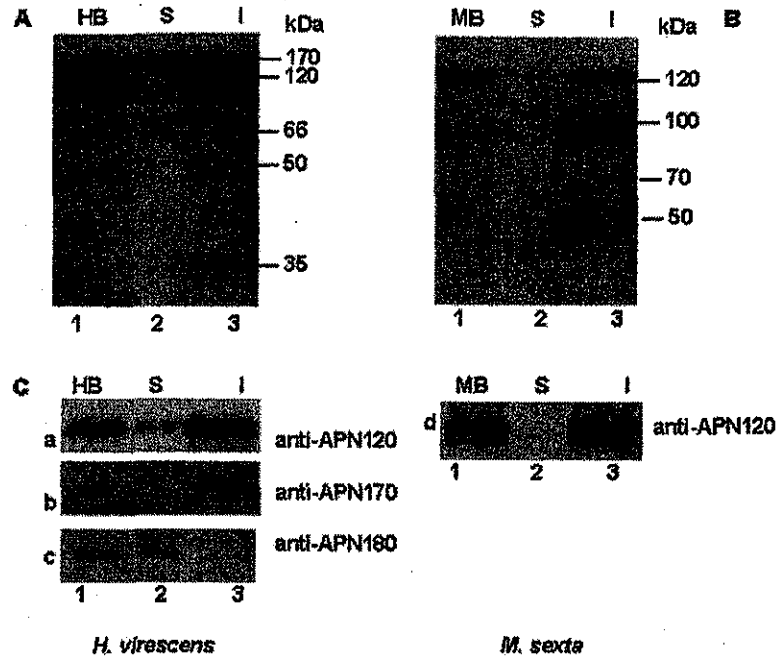

FIG. 4. **Immunoblot analyses of protein components in lipid rafts from *H. virescens* (*A* and *C*) and *M. sexta* (*B* and *D*).** Each lane contains 10 μg of protein. *HB*, *H. virescens* BBMV; *MB*, *M. sexta* BBMV; *S*, soluble fractions; *I*, insoluble fractions isolated from the sucrose gradient. *A* and *B*, immunoblot analyses with anti-CRD antibody indicated that most of the GPI-anchored proteins were partitioned into the lipid raft fraction. *C*, localization of aminopeptidases (*APN*) in Triton X-100 treated *H. virescens* BBMV sample fractions; *a–c*, *H. virescens* samples. *H. virescens* 120-kDa APN preferentially partitioned into the lipid rafts (*a*). 170-kDa APN exclusively partitioned into the lipid rafts (*b*). The 180-kDa APN, however, was exclusively Triton X-100-soluble (c). *D*, anti-*H. virescens*-120-kDa APN antiserum recognized two *M. sexta* BBMV proteins with sizes of 120 and 106 kDa, which were preferentially associated with lipid rafts.

TABLE II
Leucine aminopeptidase activities in isolated lipid rafts obtained from H. virescens and M. sexta midgut BBMVs

Sample	Aminopeptidase activities	
	H. virescens	*M. sexta*
	μmol/min/mg of protein	
Midgut homogenate	0.39 ± 0.08	0.53 ± 0.09
Unsolubilized BBMVs	3.82 ± 0.04	3.93 ± 0.05
Lipid rafts	7.36 ± 0.07	10.66 ± 0.11
Soluble fraction	0.031 ± 0.01	0.047 ± 0.01

MβCD treatment, the effect of the ionophore, valinomycin, on K^+ permeability was analyzed. Fig. 7 shows that the valinomycin dependent K^+ permeability was only slightly affected with MβCD treatment in vesicles obtained from lipid rafts (Table III). In contrast, Cry1Ab-dependent K^+ permeability was severely affected by MβCD treatment (Fig. 7 and Table III). These results show that lipid rafts integrity is essential for Cry1Ab pore formation activity. At the levels of Cry1Ab used in these experiments, this toxin was associated with lipid rafts (data not shown).

DISCUSSION

Lipid rafts occur in a variety of mammalian cells, including fibroblasts, lymphoma, endothelial cells, muscle cells, thymocytes, epithelium, neuron, and T cells (22, 23, 28, 35, 61, 62). Their presence was also reported in *Drosophila melanogaster* (39), *Saccharomyces cerevisiae* (36, 37), and *Tetrahymena* (38). Our data showed that lipid rafts are also present in the lepidopteran insects, *H. virescens* and *M. sexta*. However, the precise compositions of proteins and lipids in rafts isolated from these organisms differ. For example, in *H. virescens* lipid rafts, the percentage of long fatty acid acyl chains was higher than that in *M. sexta* lipid rafts, even though these rafts were isolated from midgut epithelium. Furthermore, the lipid-to-protein ratio from *H. virescens* lipid rafts was lower than that observed in *M. sexta* lipid rafts. However, as noted with mammalian lipid rafts, those isolated from *H. virescens* and *M. sexta* were also enriched with GPI-anchored proteins.

Cholesterol has profound effects on the packing properties of lipids, and a certain level of cholesterol is required to form a liquid-ordered phase, which is known as lipid rafts (63, 64). Cholesterol-depleting reagents including MβCD and saponin disrupt lipid rafts, but they affect the rafts differently. Although saponin caused lipid raft-associated proteins to solubilize upon Triton X-100 treatment, pretreatment with MβCD caused more membrane proteins to become Triton X-100-insoluble, and the resultant insoluble fraction was no longer typical lipid rafts. We also showed that saponin caused lipid raft-associated Cry1Ac to partition into the soluble fraction, whereas MβCD did not affect the distribution of Cry1Ac. Abrami *et al.* (20) also observed similar effects with MβCD. Using immunofluorescence to detect proaerolysin distribution, they showed MβCD treatment did not affect the ability of the toxin to bind microdomains, whereas treatment with saponin affected toxin association with lipid rafts. Therefore, the toxins were highly enriched in lipid rafts after MβCD treatment, but not after saponin treatment. It is likely that saponin causes the receptors and their bound toxin molecules to become evenly distributed in the plane of the plasma membrane by preventing any clustering.

Interestingly, direct treatment of isolated *H. virescens* and *M. sexta* lipid rafts with saponin had no effect on protein-raft association, whereas MβCD caused some of the lipid raft-associated proteins to become soluble. This solubilization could occur because MβCD extracts cholesterol nonspecifically from the membrane, resulting in insufficient cholesterol levels to maintain the liquid-ordered structure of lipid rafts. Because saponin does not extract cholesterol from the membrane, the lipid raft structure was weakly maintained even with saponin treatment. But addition of Triton X-100 did disrupt the saponin-treated rafts (data not shown).

Moreover, quantification of cholesterol and phospholipid levels in detergent-treated BBMV revealed significant differences of these two cholesterol-depleting reagents. MβCD extracts cholesterol from BBMV, but saponin prevents interactions between cholesterol and other lipids/proteins without extracting it from BBMV membranes, and these interactions have profound effects on formation of lipid rafts (21, 29). Both cholesterol and phospholipids are enriched in lipid rafts. However,

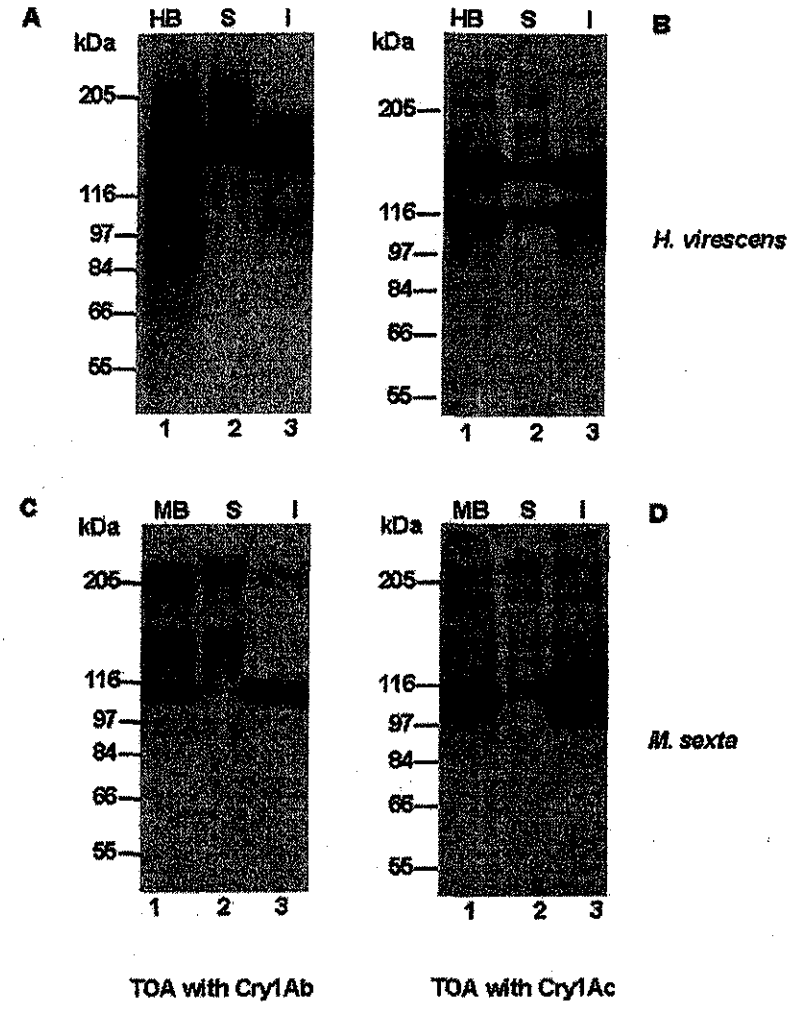

FIG. 5. **TOAs of *H. virescens* (*A* and *B*) and *M. sexta* samples (*C* and *D*) with Cry1Ab and Cry1Ac.** Each lane contains 10 μg of protein. *HB*, *H. virescens* BBMV; *MB*, *M. sexta* BBMV; *S*, soluble fractions; *I*, insoluble fractions isolated from the sucrose gradient. *A*, TOA of *H. virescens* samples with Cry1Ab. *B*, TOA of *H. virescens* samples with Cry1Ac. *C*, TOA of *M. sexta* samples with Cry1Ab. *D*, TOA of *M. sexta* samples with Cry1Ac. Anti-Cry1 antibody detected the bound toxin.

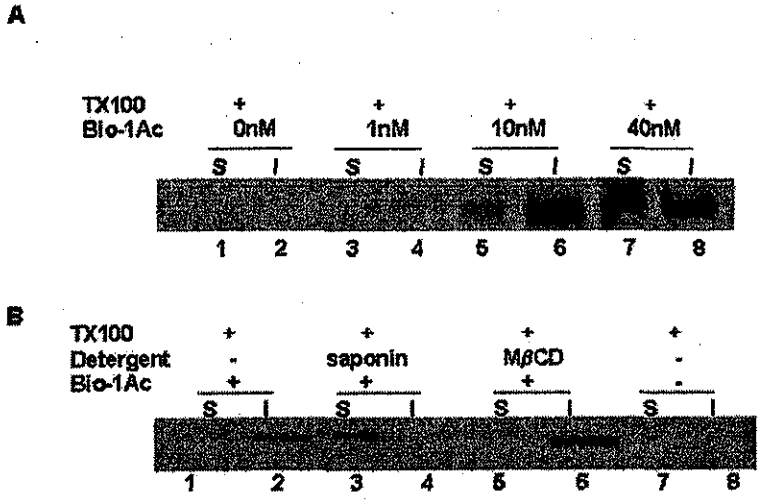

FIG. 6. **Association of biotinylated Cry1Ac toxins with *H. virescens* lipid rafts.** Each lane contains 10 μg of protein. *A*, at 1 nM, Cry1Ac was only associated with *H. virescens* lipid rafts (*lane 4*). With increasing toxin concentrations, some of the toxins partitioned to the soluble fraction (*lanes 5–8*). *B*, association of Cry1Ac with *H. virescens* lipid rafts was disrupted by saponin. With saponin pretreatment prior to isolation of lipid rafts by Triton X-100, all the Cry1Ac toxins partitioned to the soluble fraction (*lane 3*). MβCD-pretreated sample showed that Cry1Ac remained in the insoluble fraction (*lane 6*).

cholesterol levels in lipid rafts vary widely because its role in maintenance of lipid raft structure is remediable by saturated long fatty acyl chains of phospholipids and sphingomyelins (55, 56). Thus, partial depletion of membrane cholesterol by MβCD pretreatment of BBMV does not completely disrupt the isolation of lipid rafts. On the other hand, pretreatment of BBMV with saponin not only prevents interactions between cholesterol and other lipids/proteins, it also extracts phospholipids from BBMV, which accordingly disrupts further isolation of lipid rafts with Triton X-100.

Clustering of sphingolipids and cholesterol in the form of lipid rafts can recruit a specific set of membrane proteins and exclude others (21, 22, 65). These lipid rafts could act as platforms for increased concentration of receptors to interact with

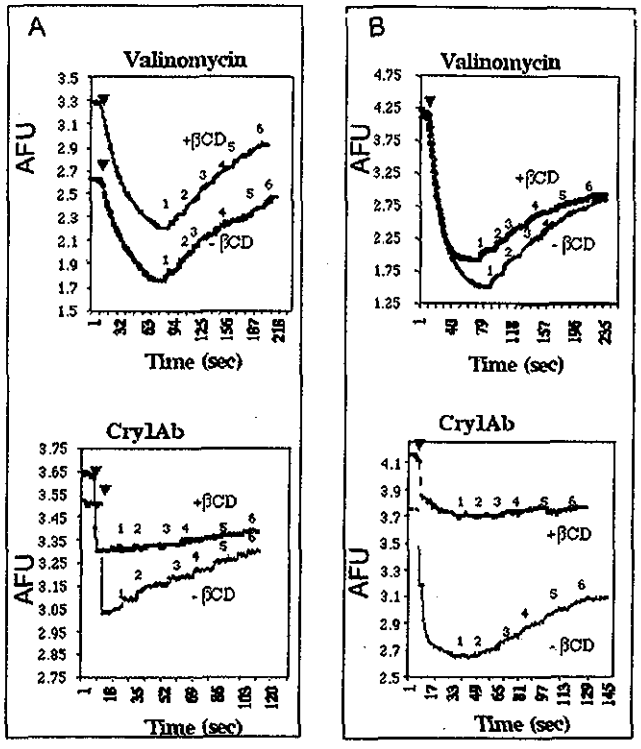

FIG. 7. **Effect of MβCD on the K_+ permeability of raft membrane vesicles isolated from *H. virescens* (*A*) and *M. sexta* (*B*).** *Upper panels* show the K^+ permeability induced by valinomycin, and *lower panels* show that induced by activated Cry1Ab. Changes in the distribution of a fluorescent dye (3,3′-dipropylthiodicarbocyanine) sensitive to changes in membrane potential were recorded as described under "Experimental Procedures." Midgut juice-activated Cry1Ab toxin (50 nM) was added to membrane vesicles, which were previously loaded with 150 mM KCl, 10 mM HEPES-HCl, pH 8.0, and suspended in 150 mM MeGluCl, 10 mM HEPES-HCl, pH 8.0, buffer (1.8 ml). The *arrow* on *top* of the *traces* corresponds to the time of valinomycin or toxin addition. An upward deflection indicates a membrane potential depolarization, whereas a downward one indicates a hyperpolarization. *AFU*, arbitrary fluorescence units. Final K^+ concentrations (mM) were as follows: 4 (*1*), 8 (*2*), 12 (*3*), 16 (*4*), 32 (*5*), and 64 (*6*).

TABLE III
Pore formation by Cry1Ab in membrane vesicles of lipid rafts isolated from H. virescens and M. sexta midgut

	Slope arbitrary fluorescence units/K^+ equilibrium potential	
	−MβCD	+MβCD
Valinomycin-dependent K^+ permeability		
H. virescens lipid rafts	0.13 ± 0.02	0.13 ± 0.02
M. sexta lipid rafts	0.22 ± 0.01	0.19 ± 0.03
Cry1Ab-dependent K^+ permeability		
H. virescens lipid rafts	0.043 ± 0.01	0.015 ± 0.004
M. sexta lipid rafts	0.091 ± 0.02	0.010 ± 0.002

ligands and effectors on both sides of the membrane. This would allow for efficient and rapid coupling of receptors to the effector system and prevent inappropriate cross-talk between pathways (22). Our data showed that proteins associated with lipid rafts differently. Most of GPI-anchored proteins from *H. virescens* and *M. sexta* were preferentially partitioned into the lipid raft fractions, as observed in mammalian lipid rafts.

Lipid rafts also play critical roles in the action of several pore-forming toxins, including aerolysin (18), cholera toxin (25), lysenin (24), and thiol-activated toxins (19, 66–68), such as streptolysin O, lysteriolysin O, and perfringolysin O. Toxin association with lipid rafts probably triggers a conformational change necessary for pore formation. At the juncture between lipid rafts and liquid phase phosphoglyceride domains, unfavorable energetic effects probably locally weaken the lipid bilayer and might favor membrane penetration (18, 20, 27, 64). By providing receptor-binding sites for these toxins, lipid rafts appears to play multiple roles: targeting, promotion of oligomerization, triggering a membrane insertion-competent form, and stabilizing the toxin-induced pore (64, 69).

The currently accepted mode of action of *B. thuringiensis* Cry toxins suggests that binding of activated Cry toxin to membrane receptors is crucial for pore formation (1). Cry toxin pores are likely to be composed of four to six toxin molecules (52), which suggests that Cry toxin aggregation occurs before the membrane pore is formed, but it is not clear how the Cry toxin aggregates. However, it is clearly established that many of the processes that lead to toxic action of Cry proteins involve the insect midgut epithelium, including activation, toxin insertion, aggregation, and pore formation (17). In this report we show that detergent-insoluble lipid rafts are present in the midgut epithelium of insects susceptible to the Cry1A toxins, and several of the Cry1Ac-binding proteins, including the 120- and 170-kDa aminopeptidases from *H. virescens* and the 120-kDa aminopeptidase from *M. sexta*, were preferentially associated with lipid rafts. Interestingly, the *H. virescens* 180-kDa aminopeptidase, which binds the Cry1Ab toxin is not enriched in lipid rafts. Specific antibodies to the cadherin-like proteins of *H. virescens* are needed to determine whether these proteins partition into the lipid rafts or the soluble fraction. Our data suggest that Cry1A toxicity is likely mediated via lipid rafts.

Indeed, at very low toxin concentrations, at which toxicity occurs, most of the Cry1Ac toxin was detected in lipid rafts. This toxin-lipid raft association is specific because the toxin partitioned into the lipid raft fraction upon Triton X-100 treatment. When the toxin concentration was increased to 10 nM, some of the toxin was detected in the soluble fraction, suggesting Cry1Ac-lipid raft binding is saturated between 1 and 10 nM.

Lipid rafts also play critical roles in the formation of toxin pores, which are required for insect toxicity. Our study revealed that the integrity of lipid rafts is important for Cry1Ab pore formation activity, because MβCD inhibited toxin-induced K^+ permeability in isolated lipid rafts. The effect observed with MβCD was not the result of membrane vesicle disruption because K^+ permeability induced by valinomycin was not affected by MβCD treatment. MβCD's effect on the Cry1Ab pore formation activity could be caused by disruption of lipid rafts that would alter the local toxin concentration and, thus, toxin oligomerization as proposed for other pore-forming toxins (20). Alternatively, we cannot exclude the possibility that cholesterol could have a role in triggering Cry1Ab conformational change that renders the toxin capable of oligomerization and membrane insertion as suggested for listerolysin O (19). These data collectively suggest that lipid rafts are important elements in the mode of action of Cry1Ab toxin. This study provides supplemental biochemical information to the mode of action of *B. thuringiensis* Cry toxins.

Acknowledgments—We thank Ana Soderini Coviella for maintaining and dissecting *H. virescens*, Didier Lereclus for Bt strain 407*cry*⁻ and pHT409, Philip Copenhaver for the fasciclin antibody, Ruud de Maagd for the Cry1A antibody, Paul Mayer for mass spectrometry services, and Jean Wong for critically reading the manuscript.

REFERENCES

1. Schnepf, E., Crickmore, N., Van Rie, J., Lereclus, D., Baum, J., Feitelson, J., Zeigler, D. R., and Dean, D. H. (1998) *Microbiol. Mol. Biol. Rev.* **62**, 775–806
2. Van Rie, J. (2000) *Int. J. Med. Microbiol.* **290**, 463–469
3. Gill, S. S., Cowles, E. A., and Pietrantonio, P. V. (1992) *Annu. Rev. Entomol.*

37, 615–636
4. de Maagd, R. A., Bravo, A., and Crickmore, N. (2001) *Trends Genet.* **17,** 193–199
5. Gahan, L. J., Gould, F., and Heckle, D. G. (2001) *Science* **293,** 857–860
6. Gill, S. S., Cowles, E. A., and Francis, V. (1995) *J. Biol. Chem.* **270,** 27277–27282
7. Luo, K., Sangadala, S., Masson, L., Mazza, A., Brousseau, R., and Adang, M. J. (1997) *Insect Biochem. Mol. Biol.* **27,** 735–743
8. Oltean, D. I., Pullikuth, A. K., Lee, H. K., and Gill, S. S. (1999) *Appl. Environ. Microbiol.* **65,** 4760–4766
9. Banks, D. J., Jurat-Fuentes, J. L., Dean, D. H., and Adang, M. J. (2001) *Insect Biochem. Mol. Biol.* **31,** 909–918
10. Knight, P. J., Knowles, B. H., and Ellar, D. J. (1995) *J. Biol. Chem.* **270,** 17765–17770
11. Vadlamudi, R. K., Weber, E., Ji, I., Ji, T. H., and Bulla, L. A., Jr. (1995) *J. Biol. Chem.* **270,** 5490–5494
12. Yaoi, K., Kadotani, T., Kuwana, H., Shinkawa, A., Takahashi, T., Iwahana, H., and Sato, R. (1997) *Eur. J. Biochem.* **246,** 652–657
13. Nagamatsu, Y., Toda, S., Yamaguchi, F., Ogo, M., Kogure, M., Nakamura, M., Shibata, Y., and Katsumoto, T. (1998) *Biosci. Biotechnol. Biochem.* **62,** 718–726
14. Gomez, I., Oltean, D. I., Gill, S., Bravo, A., and Soberon, M. (2001) *J. Biol. Chem.* **276,** 28906–28912
15. Griffitts, J. S., Whitacre, J. L., Stevens, D. E., and Aroian, R. V. (2001) *Science* **293,** 860–864
16. Aronson, A. I., Geng, C., and Wu, L. (1999) *Appl. Environ. Microbiol.* **65,** 2503–2507
17. Aronson, A. I., and Shai, Y. (2001) *FEMS Microbiol. Lett.* **195,** 1–8
18. Abrami, L., Fivaz, M., Glauser, P. E., Parton, R. G., and van der Goot, F. G. (1998) *J. Cell Biol.* **140,** 525–540
19. Jacobs, T., Darji, A., Frahm, N., Rohde, M., Wehland, J., Chakraborty, T., and Weiss, S. (1998) *Mol. Microbiol.* **28,** 1081–1089
20. Abrami, L., and van Der Goot, F. G. (1999) *J. Cell Biol.* **147,** 175–184
21. Harder, T., and Simons, K. (1997) *Curr. Opin. Cell Biol.* **9,** 534–542
22. Simons, K., and Ikonen, E. (1997) *Nature* **387,** 569–572
23. Galbiati, F., Razani, B., and Lisanti, M. P. (2001) *Cell* **106,** 403–411
24. Nakai, Y., Sakurai, Y., Yamaji, A., Asou, H., Umeda, M., Uyemura, K., and Itoh, K. (2000) *J. Neurosci. Res.* **62,** 521–529
25. Orlandi, P. A., and Fishman, P. H. (1998) *J. Cell Biol.* **141,** 905–915
26. Lorence, A., Darszon, A., and Bravo, A. (1997) *FEBS Lett.* **414,** 303–307
27. Brown, D. A., and London, E. (1998) *Annu. Rev. Cell Dev. Biol.* **14,** 111–136
28. Hooper, N. M. (1999) *Mol. Membr. Biol.* **16,** 145–156
29. Brown, D. A., and London, E. (2000) *J. Biol. Chem.* **275,** 17221–17224
30. Varma, R., and Mayor, S. (1998) *Nature* **394,** 798–801
31. Jacobson, K., and Dietrich, C. (1999) *Trends Cell Biol.* **9,** 87–91
32. Pralle, A., Keller, P., Florin, E., Simons, K., and Horber, J. (2000) *J. Cell Biol.* **148,** 997–1007
33. Kenworthy, A. K., Petranova, N., and Edidin, M. (2000) *Mol. Biol. Cell* **11,** 1645–1655
34. Schutz, G. J., Kada, G., Pastushenko, V. P., and Schindler, H. (2000) *EMBO J.* **19,** 892–901
35. London, E., and Brown, D. A. (2000) *Biochim. Biophys. Acta* **1508,** 182–195
36. Kubler, E., Dohlman, H. G., and Lisanti, M. P. (1996) *J. Biol. Chem.* **271,** 32975–32980
37. Bagnat, M., Keranen, S., Shevchenko, A., and Simons, K. (2000) *Proc. Natl. Acad. Sci. U. S. A.* **97,** 3254–3259
38. Zhang, X., and Thompson, G. A., Jr. (1997) *Biochem. J.* **323,** 197–206
39. Rietveld, A., Neutz, S., Simons, K., and Eaton, S. (1999) *J. Biol. Chem.* **274,** 12049–12054
40. Lecadet, M. M., Blondel, M. O., and Ribier, J. (1980) *J. Gen. Microbiol.* **121,** 203–212
41. Bell, R. A., and Joachim, F. G. (1976) *Ann. Entomol. Soc. Am.* **69,** 365–373
42. Cowles, E. A., Yunovitz, H., Charles, J. F., and Gill, S. S. (1995) *Appl. Environ. Microbiol.* **61,** 2738–2744
43. Wolfersberger, M., Luethy, P., Maurer, A., Parenti, P., Sacchi, F. V., Giordana, B., and Hanozet, G. M. (1987) *Comp. Biochem. Physiol.* **86A,** 301–308
44. Wright, J. W., and Copenhaver, P. F. (2000) *Dev. Biol.* **225,** 59–78
45. Filippova, M., Rosa, L. S., and Gill, S. S. (1998) *Insect Mol. Biol.* **7,** 223–232
46. Pullikuth, A. K., and Gill, S. S. (1999) *Gene (Amst.)* **240,** 343–354
47. de Maagd, R. A., Kwa, M. S., van der Klei, H., Yamamoto, T., Schipper, B., Vlak, J. M., Stiekema, W. J., and Bosch, D. (1996) *Appl. Environ. Microbiol.* **62,** 1537–1543
48. Guther, M. L., de Almeida, M. L., Rosenberry, T. L., and Ferguson, M. A. (1994) *Anal. Biochem.* **219,** 249–255
49. Barlett, G. R. (1959) *J. Biol. Chem.* **234,** 466–468
50. Folch, J., Lees, M., and Sloane Stanley, G. H. (1956) *J. Biol. Chem.* **194,** 497–508
51. Kerwin, J. L., Tuininga, A. R., and Ericsson, L. H. (1994) *J. Lipid Res.* **35,** 1102–1114
52. Vie, V., Van Mau, N., Pomarede, P., Dance, C., Schwartz, J. L., Laprade, R., Frutos, R., Rang, C., Masson, L., Heitz, F., and Le Grimellec, C. (2001) *J. Membr. Biol.* **180,** 195–203
53. Latterich, M., Frohlich, K. U., and Schekman, R. (1995) *Cell* **82,** 885–893
54. Kilsdonk, E. P., Yancey, P. G., Stoudt, G. W., Bangerter, F. W., Johnson, W. J., Phillips, M. C., and Rothblat, G. H. (1995) *J. Biol. Chem.* **270,** 17250–17256
55. Schroeder, R. J., Ahmed, S. N., Zhu, Y., London, E., and Brown, D. A. (1998) *J. Biol. Chem.* **273,** 1150–1157
56. Sankaram, M. B., and Thompson, T. E. (1990) *Biochemistry* **29,** 10676–10684
57. Klenk, H. D., and Choppin, P. W. (1969) *Virology* **38,** 255–268
58. Brown, D. (1994) *Braz. J. Med. Biol. Res.* **27,** 309–315
59. Abrami, L., Fivaz, M., Kobayashi, T., Kinoshita, T., Parton, R. G., and van Der Goot, F. G. (2001) *J. Biol. Chem.* **276,** 30729–30736
60. Bravo, A., Hendrickx, S., Jansen, S., and Peferoen, M. (1992) *J. Invertebr. Pathol.* **60,** 247–254
61. Yasuda, K., and Kosugi, A. (2000) *Tanpakushitsu Kakusan Koso* **45,** 1812–1822
62. Ikonen, E. (2001) *Curr. Opin. Cell Biol.* **13,** 470–477
63. Simons, K., and Ikonen, E. (2000) *Science* **290,** 1721–1726
64. van der Goot, F. G., and Harder, T. (2001) *Semin. Immunol.* **13,** 89–97
65. Peskan, T., Westermann, M., and Oelmuller, R. (2000) *Eur. J. Biochem.* **267,** 6989–6995
66. Kurashima, K., D'Souza, S., Szaszi, K., Ramjeesingh, R., Orlowski, J., and Grinstein, S. (1999) *J. Biol. Chem.* **274,** 29843–29849
67. Billington, S. J., Jost, B. H., and Songer, J. G. (2000) *FEMS Microbiol. Lett.* **182,** 197–205
68. Waheed, A. A., Shimada, Y., Heijnen, H. F., Nakamura, M., Inomata, M., Hayashi, M., Iwashita, S., Slot, J. W., and Ohno-Iwashita, Y. (2001) *Proc. Natl. Acad. Sci. U. S. A.* **98,** 4926–4931
69. Coconnier, M. H., Lorrot, M., Barbat, A., Laboisse, C., and Servin, A. L. (2000) *Cell. Microbiol.* **2,** 487–504

ELSEVIER

Biochimica et Biophysica Acta 1562 (2002) 63–69

BIOCHIMICA ET BIOPHYSICA ACTA
BBA

www.bba-direct.com

Pore formation activity of Cry1Ab toxin from *Bacillus thuringiensis* in an improved membrane vesicle preparation from *Manduca sexta* midgut cell microvilli

Alejandra Bravo*, Raúl Miranda, Isabel Gómez, Mario Soberón

Departamento de Microbiología, Instituto de Biotecnología, Universidad Nacional Autónoma de México, Apartado Postal 510-3, Cuernavaca, Morelos 62250, Mexico

Received 30 October 2001; received in revised form 15 January 2002; accepted 15 January 2002

Abstract

The pore formation activity of Cry1Ab toxin is analyzed in an improved membrane preparation from apical microvilli structures of *Manduca sexta* midgut epithelium cells (MEC). A novel methodology is described to isolate MEC and brush border membrane vesicles (BBMV) from purified microvilli structures. The specific enrichment of apical membrane enzyme markers aminopeptidase (APN) and alkaline phosphatase (APh) were 35- and 22-fold, respectively, as compared to the whole midgut cell homogenate. Ligand-blot and Western-blot experiments showed that Cry1A specific receptors were also enriched. The pore formation activity of Cry1Ab toxin was fourfold higher in the microvilli membrane fraction that showed low intrinsic K^+ channels and higher APN and APh activities than in the basal-lateral membrane fraction harboring high intrinsic K^+ channels. These data suggest that basal-lateral membrane was separated from apical membrane. This procedure should allow more precise studies of the interaction of Cry toxins with their target membranes, avoiding unspecific interaction with other cellular membranes, as well as the study of the pore formation activity induced by Cry toxins in the absence of endogenous channels from *M. sexta* midgut cells.

Keywords: *Bacillus thuringiensis*; Pore formation; Microvilli; Brush border membrane vesicle

1. Introduction

Studies with isolated brush border membranes represent a powerful tool in the analysis of cellular mechanism involved in the transmembrane and transepithelial transport of various solutes, and in the analysis of the interaction of bacterial toxins with their receptors and their pore formation activity. However, data obtained with isolated membrane fractions need careful interpretation since cross-contamination and vesicle heterogeneity can lead to conclusions not related with intact ephitelia.

The midgut of lepidopteran larvae is composed of two major cell types, the columnar cells with an apical brush border microvilli and the goblet cells containing a large cavity which is joined to the apical surface by a complex interdigitated valve [1]. The epithelial cells are joined by septate junctions and gap junctions [2]. The gap junctions provide the electrical and chemical coupling between the globet and columnar cells [3]. The function of the lepidopteran gut is dominated by the vigorous electrogenic transport of K^+ from the blood side to the lumen side [4]. K^+ channels are located in the basal membrane [3–5]. The K^+ proton pump (V-ATPase) and the H^+/K^+ exchanger are located on the apical membrane of the goblet cell [6,7]. Their activity leads to the electrogenic flux of K^+ from the goblet cell cytoplasm to the goblet cell cavity and hence to the gut lumen.

Bacillus thuringiensis (Bt) is an aerobic, spore-forming bacteria that produces crystalline inclusions during the sporulation phase, which are toxic to larvae of several insects orders as well as to other invertebrates [8]. The crystals are composed of proteins known as Cry toxins [9]. It is widely accepted that the primary action of Bt toxins is to lyse midgut ephitelial cells in the target insect [10]. The ingested Cry proteins are dissolved in the alkaline environment of the larval midgut and are cleaved by midgut proteases. The active toxin fragment binds to specific membrane receptors on the apical brush border of the midgut epithelium columnar cells [11,12]. After binding,

* Corresponding author. Tel.: +52-73-291635; fax: +52-73-172388.
E-mail address: bravo@ibt.unam.mx (A. Bravo).

0005-2736/02/$ - see front matter
PII: S0005-2736(02)00360-7

the toxin or part of it, inserts into the cell membrane [13], leading to the formation of lytic pores [14–16], which disrupt midgut ion gradients and the transepithelial potential difference. This disruption is accompanied by an inflow of water that leads to cell swelling and eventual lysis, resulting in paralysis of the midgut and subsequent larval death.

The pore formation activity of purified Cry toxins has been studied in brush border epithelial membranes containing specific receptors [14,17–19]. The method most frequently used to isolate brush border membrane vesicles (BBMV) from lepidopteran insects involves differential Mg^{2+} precipitation introduced by Wolfersberger et al. [20]. However, most BBMV preparations have intrinsic K^+ channels, indicating that the basal-lateral membrane is a cross-contaminant frequently found in the BBMV preparation [14,21,22]. The intrinsic channel activity interferes with the analysis of the pore formation activity of Cry toxins. In this work, we described an improved methodology to purify the brush border membranes from the Cry1A susceptible insect *Manduca sexta*. This novel methodology increases 35- and 22-fold the purification ratio of enzyme markers associated with brush border membranes, aminopeptidase (APN) and alkaline phosphatase (APh), as compared to the whole midgut cell homogenate. Also, the presence of intrinsic K^+ channels is highly reduced. This novel BBMV preparation will be highly useful in the analysis of the Cry toxin ion induced permeability.

2. Materials and methods

2.1. Cry1Ab δ-endotoxin purification

Cry1Ab crystals were produced in the acrystalliferous *Bt* strain 4Q7*cry*$^-$ transformed with pHT315 plasmid [23] harboring the *cry*1Ab gene (pHT315-1Ab) (GenBank accession no. M13898). The transformant strain was grown for 3 days at 29 °C in nutrient broth sporulation medium [24] supplemented with 10 μg/ml erythromycin. After complete sporulation, crystals were purified by sucrose gradients as reported [25], solubilized at 37 °C for 2 h in extraction buffer (50 mM Na_2CO_3 pH 10.5, 0.2% β-mercaptoethanol) and digested with *M. sexta* midgut juice in a 1:10 protease/protoxin mass ratio for 2 h at 30 °C. PMSF was added to a final 1 mM concentration to stop proteolysis. Samples were centrifuged at 16,000 × *g* for 10 min and the toxin-containing supernatant was harvested.

2.2. Isolation of BBMV

M. sexta eggs were kindly supplied by Dr. Jorge Ibarra from CINVESTAV, Irapuato. Larvae were reared on an artificial diet as described [26]. Thirty *M. sexta* larvae in fourth instar were chilled for 10 min on ice and midgut tissue was dissected. The midgut tissue was cleaned from traquea, Malpiglian tubules, peritrophic membrane and midgut content. Then, midguts were cut longitudinally, rinsed with a physiological saline solution (PBS) and incubated for 30–60 min, at room temperature with slow agitation in 100-ml PBS supplemented with Ca^{2+} chelants (EDTA 5 mM and EGTA 5 mM) and protease inhibitors (1 mM PMSF and 100 μg/ml leupeptin). Midgut epithelium cells (MEC) were dissociated using mild agitation of the tissue with forceps, cells were collected by centrifugation 5 min at 120 × *g* (1000 rpm in a bench centrifuge Eppendorf 5804R), washed three times with PBS and suspended in 4-ml cold PBS. Isolated MEC were homogenized by gentle mechanical disruption (2–4 min in vortex maximal velocity) to detach the complete microvilli structure from the disrupted cells. Disrupted cells were loaded in two 10-ml linear density gradient of 0% to 30% Percoll (Sigma Chemical, St. Louis, MO) in PBS, centrifuged 10 min at 2500 × *g* (4500 rpm using a swing rotor in a bench centrifuge Eppendorf 5804R) at 4 °C to purify the microvilli-containing fraction. The two gradients were then fractionated in 10 tubes (1.2 ml each). The microvilli structure sediments in the 25–30% Percoll fractions. The microvilli fraction was suspended in 150 mM KCl, 10 mM HEPES–HCl pH 8, and washed three times by centrifugation for 10 min at 3000 × *g* (5000 rpm Eppendorf 5804R) at 4 °C. Finally, this fraction was sonicated for six periods of 30 s each at 25 °C (Branson 1200 sonic bath, Danbury, CT) in the same solution.

Alternatively, the microvilli fractions were washed and suspended in 300 mM mannitol, 2 mM DTT, 5 mM EGTA, 1 mM EDTA, 0.1 mM PMSF, 150 μg/ml pepstatin, 100 μg/ml leupeptin, 1 μg/ml soybean trypsin inhibitor, 10 mM HEPES–HCl, pH 8.0. BBMV were prepared from this fraction by homogenization in a glass and teflon homogenizer, using nine strokes at 3000 rpm. An equal volume of cold 24 mM $MgCl_2$ solution was added to the microvilli homogenate and incubated 15 min at 4 °C. Then it was centrifuged at 2500 × *g* (4500 rpm in a Beckman JA20 rotor) for 15 min at 4 °C. The supernatant was centrifuged at 30,000 × *g* (16,000 rpm Beckman JA20 rotor) for 30 min at 4 °C; the resulting pellet contains the BBMV. The BBMV preparation was dialyzed overnight against 400 volumes of 150 mM KCl, 10 mM HEPES–HCl pH 8, and sonicated as described above in the same solution.

2.3. Enzyme assays

Cytochrome *c* oxidase activity was determined to ensure that microvilli fraction and BBMV were not contaminated with mitochondrial membranes. It was assayed using reduced cytochrome *c* acid modified from horse heart as substrate in a double beam SIM Aminco DW-2000 [27]. APN activity was assayed using L-leucine-*p*-nitroanilide (LpNA) as substrate [28] and APh using *p*-nitrophenyl phosphate as substrate [29]. Protein content was measured by the D_C protein-dye method (Bio-Rad Richmond, CA) using bovine serum albumin as standard (New England Bio-

Labs, Beverly, MA). The initial rate at 405 nm (Ultrospec II spectrophotometer; Pharmacia LKB) was used to calculate specific enzymatic activity of both enzymes. The absorption coefficient of *p*-nitroanilide used was 9.9×10^{-3} mol l^{-1} [30]. One unit of specific APN activity was defined as the amount of enzyme catalyzing the hydrolysis of 1 μmol of LpNA min^{-1} mg $protein^{-1}$ at 25 °C. One unit of specific alkaline phosphatease (APh) activity was defined as the amount of enzyme producing 1 μmol of nitrophenol min^{-1} mg $protein^{-1}$ at 25 °C. A standard curve of 4-nitrophenol in 0.5 mM $MgCl_2$, 100 mM Tris pH 9.5 was performed.

2.4. Fluorescence measurements

Membrane potential was monitored with the fluorescent positively charged dye, 3,3′-dipropylthiodicarbocyanine (Dis-C_3-(5), Molecular Probes, Eugene, OR; 1.5 μM final, 1 mM stock in DMSO). Fluorescence was recorded at 620/670 nm excitation/emission wavelength pair using an Aminco SLM spectroflorometer, as in Lorence et al. [14]. Hyperpolarization causes dye internalization into the BBMV and fluorescence decrease; depolarization causes the opposite effect. Dye calibration and determination of resting membrane potential were performed in the presence of valinomycin (2 μM) by successive additions of KCl to BBMV (10 μg) suspended in 150 mM *N*-methyl-D-glucamine chloride (MeGluCl), 10 mM HEPES–HCl pH 8 buffer (1.8 ml). All determinations were made at 25 °C with constant stirring. Time zero (t_o) was considered when BBMV were added, and toxin (50 nM) addition was made after 2 min. After the first hyperpolarization produced by the toxin, successive additions of KCl (4, 8, 12, 16, 32 and 64 mM, final concentration) to the BBMV were done. After each KCl addition a new membrane potential is established, and a depolarization is produced. The slope (m) of the curve ΔF (%) vs. K^+ equilibrium potential (E_K+) (mV) or vs. external K^+ concentration was determined. E_K+ was calculated with the Nernst equation. Changes in fluorescence determinations were done four times.

2.5. Detection of APN by Western blot

Sandwich Western blots were used to detect APN. Briefly, homogenate, microvilli and BBMV samples were separated by 9% SDS-PAGE and blotted onto nitrocellulose. The blots were incubated with anti-APN [31] kindly supplied by Dr. Michael Adang (Athens GA) (1:10,000 in PBS), and anti-rabbit horseradish peroxidase (1:3000 in PBS). Blots were developed by enhanced chemiluminescence (ECL, Amersham) as described by manufacturers.

2.6. Toxin overlay assay

Protein blot analysis of microvilli and BBMV preparations was done as previously described [32]. Ten micrograms of BBMV protein was separated by 9% SDS-PAGE and electrotransferred to nitrocellulose membranes. After renaturation and blocking, blots were incubated for 2 h with 10 nM of biotinylated Cry1Ab toxin in washing buffer (0.05% Tween 20 in PBS) at room temperature. Unbound toxin was removed by washing three times for 10 min in washing buffer and bound toxin was identified by incubating the blots in TBS containing streptavidin–peroxidase conjugate (1:5000 in PBS) for 1 h. The excess of streptavidin was removed by washing in three changes of washing buffer and the membrane-bound complex was visualized using luminol as above.

3. Results

3.1. Purification of M. sexta BBMV from isolated microvilli

Pore formation activity of Cry toxins has been assayed in BBMV usually prepared from whole larvae midgut tissues [20]. BBMV are prepared by using a differential precipitation with Mg^{2+} that theoretically separates apical and basal-lateral membranes from epithelial cells according to their difference in surface charge density. In a concentration between 15 and 30 mM the divalent cations aggregate basal-lateral membranes as well as mitochondria, lysosomes, and endoplasmic reticulum. Apical membrane fragments do not aggregate [33]. However, preparation of BBMV using whole midgut homogenates as starting material, only increases the apical membrane enzymes markers APh and APN by 6- and 7-fold, respectively [20], and the membrane vesicles contains endogenous K^+ channels [14,22]. Intrinsic K^+ channels interfere with the characterization of Cry1A-induced K^+ permeability. Therefore, we decided to prepare BBMV from microvilli brush border structures that were purified from MEC. Midguts were isolated from 4th instar *M. sexta* larvae and incubated with Ca^{2+} chelants (EDTA and EGTA) to induce epithelium cell detachment from basal lamina (Fig. 1A). MEC were homogenized by gently mechanical disruption to detach the microvilli from the cells. Microvilli structures were then purified by a density 0–30% Percoll gradient as described in Section 2 (Fig. 1B). Microscopic observation of the different Percoll gradient fractions revealed that fractions 1–3 contain intracellular materials and microsomal membranes, fractions 4–8 contains disrupted midgut cell fragments while the higher density fractions 9 and 10 were enriched in microvilli structures (Fig. 1B).

3.2. BBMV marker enzyme enrichment

APN and APh specific activities were determined in the different fractions obtained from the Percoll density gradient. Fig. 2 shows that both APN and APh were enriched in the fractions where microvilli were isolated. The enrichment of these two enzymes in relation to the initial homogenate was only three and four times for APh and APN, respec-

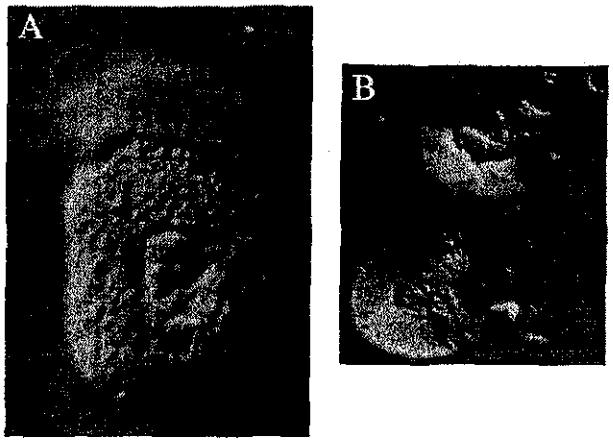

Fig. 1. Light micrographs under Normaski differential interference contrast of isolated *M. sexta* MEC (A) and microvilli structures purified from disrupted cells (B), magnification 100×.

tively (Table 1). However, it is clear from Fig. 2 that the higher activity of both enzymes was found in the fractions of the gradient of higher Percoll concentration that contain the microvilli membranes.

In order to improve the quality of the membrane preparation, membrane vesicles were prepared from isolated microvilli structures using differential Mg^{2+} precipitation. APN and APh enzymatic activities were determined after membrane vesicles isolation. Table 1 shows that BBMV isolated from microvilli have APh and APN enrichments

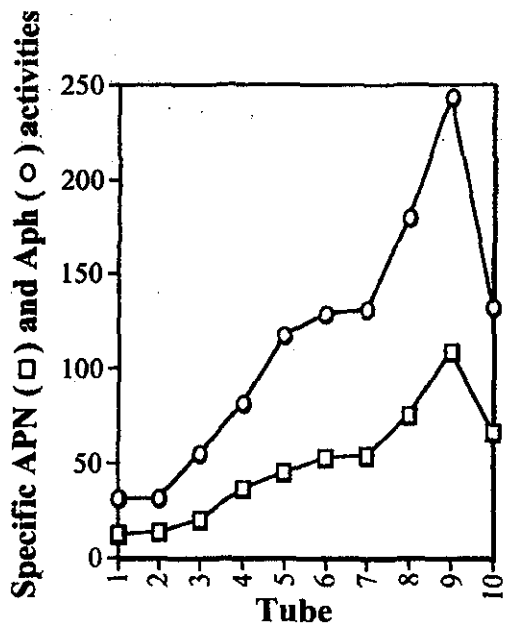

Fig. 2. Microvilli enzyme markers (APN and APh) are enriched in the fractions containing isolated microvilli structures. Analysis of APN (□) and APh (○) specific activities (μmol min^{-1} mg $protein^{-1}$) of the fractions obtained after Percoll gradient centrifugation of disrupted midgut cells.

Table 1
Distribution of APN and APh enzymatic activities in subcellular fractions of *M. sexta* larval midgut

Enzyme	Specific activity (μmol min^{-1} mg $protein^{-1}$)			
	Homogenate	Microvilli	BBMV[a]	BBMV/ homogenate
APh	52 ± 4	249 ± 10	1153 ± 36	22
APN	27 ± 12	109 ± 25	925 ± 52	34

[a] BBMV were purified from isolated microvilli structures as described in Section 2.

of 22- and 34-fold, respectively, in relation to the initial homogenate.

3.3. GPI-anchored APN enrichment and association of Cry1Ab toxin with membrane proteins.

The presence of the Cry1A toxin receptor, a GPI-anchored APN, was analyzed by Western-blot using an antibody raised against a protein fragment of purified *M. sexta* APN [31]. The APN was greatly enriched in the BBMV obtained from isolated microvilli structures (Fig. 3A). Fig. 3B shows a Cry1Ab toxin overlay assay of the three different membrane preparations, initial midgut cells homogenate, microvilli structures and the BBMV isolated from microvilli structures. Toxin overlay assays identify proteins in the membrane that bind Cry1Ab toxin. Fig. 3B shows that besides the 120-kDa APN, the 210-kDa cadherin-like receptor (Bt-R_1) was also present in the microvilli membrane preparations.

3.4. Pore formation activity of Cry1Ab toxin

Pore formation activity of Cry1Ab toxin was assayed in the different fractions obtained after Percoll gradient. The membrane vesicles were loaded with KCl by sonication and pore formation activity was assayed by monitoring changes

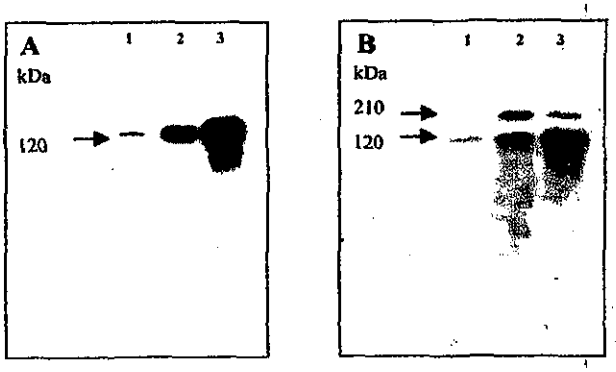

Fig. 3. Cry1A toxin receptors are present in the purified microvilli membranes. Detection of GPI-anchored APN by Western-blot analysis with anti-APN polyclonal antibody (A); toxin overlay assay of biotinylated Cry1Ab to the different membrane samples (B). Homogenate proteins (lines 1), microvilli fraction 9 from the Percoll gradient (lines 2) and BBMV isolated from microvilli structures by the differential Mg^{2+} precipitation method (lines 3).

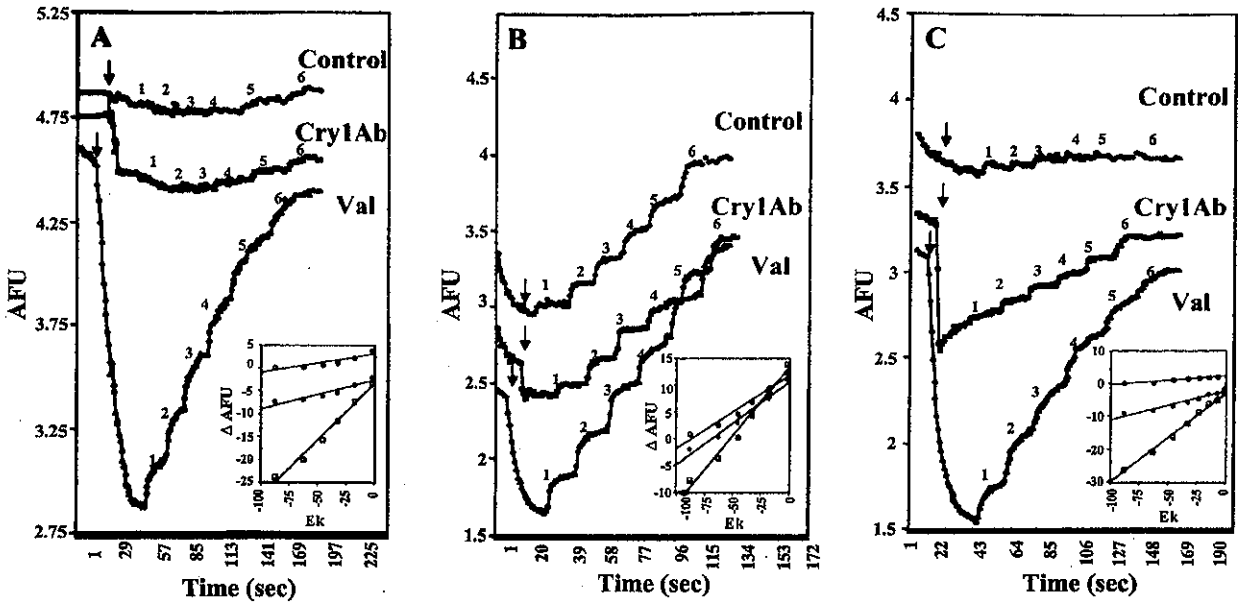

Fig. 4. Analysis of K^+ permeability across membrane vesicles of three different fractions of the Percoll gradient used for purification of microvilli membranes. Membrane vesicles were prepared from fraction 2 that contains intracellular membranes (A), from fraction 5 that contains basal and lateral membranes (B) and from fraction 9 that harbors the purified microvilli membranes (C). Changes in distribution of the fluorescent dye Dis-C_3-(5) sensitive to changes in membrane potential were recorded as described in Section 2. The arrow on top of the traces corresponds to the time of valinomycin, buffer or toxin addition. An upward deflection indicates a membrane potential depolarization; the opposite effect indicates a hyperpolarization. AFU = arbitrary fluorescence units. Final K^+ concentrations (mM) were: 1 = 4, 2 = 8, 3 = 12, 4 = 16, 5 = 32 and 6 = 64. Inserts show the plot of changes in AFU (%) vs. K^+ potential (Ek) (mV) induced by intrinsic K^+ channels (○), valinomycin (□), or by Cry1Ab-activated toxin (◇).

in the fluorescence of a membrane potential-sensitive fluorescent dye Dis-C_3(5) as described in Section 2. Fig. 4 shows the fluorescent traces obtained from three different fractions of the gradient, fraction 2 that contains intracellular membranes (Fig. 4A), fraction 5 that contains principally basolateral membranes (Fig. 4B) and fraction 9 that harbors the purified microvilli membranes (Fig. 4C). All fractions produced similar K^+ permeability response when assayed with the K^+ ionophore valinomycin (Fig. 4). In contrast, the intrinsic K^+ channels were only present in fraction 5 correlating with the presence of basal-lateral membranes (Fig. 4B). Finally, addition of 50 nM of the activated toxin Cry1Ab produced a fast hyperpolarization and an increase in the response of the dye to KCl additions principally in fraction 9 containing the microvilli membranes (Fig. 4C). The plot of the changes in fluorescence vs. K^+ equilibrium potential is shown in the small insert within each panel. The slope of these curves correlates with K^+ permeability across the membrane. Fig. 5 summarizes this information by analyzing the pore formation activity induced by valinomycin, by the intrinsic channels and by the Cry1Ab toxin in all fractions of the Percoll gradient. The Cry1Ab K^+ permeability was calculated by subtracting intrinsic K^+ permeability ($m_{tox} - m_{int}$). This figure shows the percentage of the maximal K^+ permeability obtained from the slope of changes in fluorescence vs. K^+ equilibrium potential. As stated above, all fractions presented similar pore formation when an excess of valinomycin is added; these data indicate

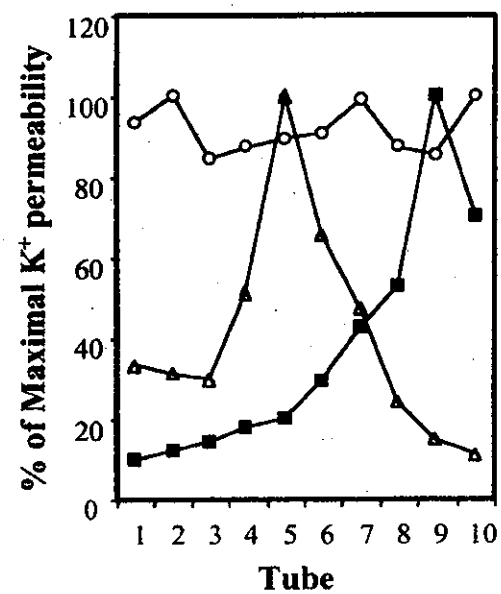

Fig. 5. Percentage of maximal K^+ permeability across membrane vesicle fractions obtained after Percoll gradient centrifugation, produced by intrinsic K^+ channels (△), by valinomycin (○), or by Cry1Ab-activated toxin (■). Changes in distribution of the fluorescent dye (Dis-C_3-(5)) were recorded as described in Section 2. Percentage values were obtained from the slope (m) of the curve ΔF (%) vs. E_{K^+} as in inserts of Fig. 4.

that all fractions contained sealed vesicles that presented a K^+ gradient. The fractions of medium density (fractions 4 to 7) showed a higher intrinsic K^+ permeability, while the Cry1Ab-dependent pore-formation activity was highly increased in the fractions containing the microvilli structures (fractions 9 and 10).

4. Discussion

The pore-forming Cry toxins exert their effect through a multistep process including protoxin proteolytic activation, receptor binding, membrane insertion, oligomerization and finally pore formation. Most of these events have been studied in vitro by the isolation of midgut BBMV, which are the target of the Cry toxins [13]. The purification of BBMV is of key importance to avoid misleading interpretations of the interaction of the toxin with other contaminating cell membranes. For the isolation of BBMV, whole midguts homogenates are differentially precipitated with divalent cations that preferentially precipitate basal-lateral and internal cellular membranes [33]. Using this procedure, enzymatic markers of brush border membranes as APN and APh are enriched sevenfold when compared to the midgut homogenate [20]. In this work we developed a method to purify BBMV from isolated microvilli structures rather than from whole midgut homogenate. The procedure described here showed an enrichment of APN and APh of 34- and 22-fold, respectively, compared with the whole midgut cell homogenate (Table 1), showing that a higher purity preparation of BBMV can be obtained. Ligand-blot and Western-blot experiments demonstrated that Cry1A receptors were enriched in BBMV obtained by this procedure (Fig. 3). In contrast with the 120-kDa APN receptor, the 210 kDa Bt-R_1 receptor was not increased in the final BBMV preparation. This result could suggest a different distribution of these receptors in the midgut cell membrane. The specific enrichment of microvilli by gentle disruption of midgut cells following a density gradient separation (Fig. 1) was illustrated by the separation of membranes harboring low intrinsic K^+ channels, and high Cry1Ab-dependent K^+ permeability (Fig. 4C) of membranes that harbor high intrinsic K^+ channels (Fig. 4B). K^+ ionic channels have been shown to be present in basal-lateral membranes [3,5]. In contrast, purification of BBMV from different larvae (*M. sexta*, *Lymantria dispar* and *Spodoptera frugiperda*) by the differential Mg^{2+} precipitation method had led to the isolation of membranes contaminated with intrinsic channels that were slightly cationic and ranged from 16 to 850 pS [14,21,22].

The procedure described here for BBMV preparation should allow more precise studies of the interaction of Cry toxins with their target membranes avoiding unspecific interaction with other cellular membranes, as well as the study of the pore formation activity induced by Cry toxins in the absence of other intrinsic channels.

Acknowledgements

We thank Oswaldo López, Jorge Sánchez, Lizbeth Cabrera and Javier Luévano for technical assistance. This research was supported in part by DGAPA/UNAM IN216300 CONACyT G36505-N and CONACyT 25248-N.

References

[1] D.F. Moffett, A. Koch, The insect goblet cell: a problem in functional architecture, NIPS 7 (1992) 19–23.
[2] N.J. Lane, H.L. Skaer, Intercellular junctions in insect tissues, Adv. Insect Physiol. 15 (1980) 35–213.
[3] J.A.T. Dow, J.M. Peaccock, Microelectrode evidence for the electrical isolation of Goblet cell cavities in *Manduca sexta* middle midgut, J. Exp. Biol. 143 (1989) 101–114.
[4] D.F. Moffett, A. Koch, Electrophysiology of K^+ transport by midgut epithelium of lepidopteran insect larvae I. The transbasal electrochemical gradient, J. Exp. Biol. 135 (1988) 25–38.
[5] J.A.T. Dow, Insect midgut function, Adv. Insect Physiol. 19 (1986) 187–238.
[6] W.R. Harvey, S. Nedergaard, Sodium independent active transport of potassium in the isolated midgut of the cecropia silkworm, Proc. Natl. Acad. Sci. U.S.A. 51 (1964) 757–765.
[7] D.F. Moffett, A. Koch, Electrophysiology of K^+ transport by midgut epithelium of lepidopteran insect larvae II. The transapical electrochemical gradients, J. Exp. Biol. 135 (1988) 39–49.
[8] R. de Maagd, A. Bravo, N. Crickmore, How *Bacillus thuringiensis* has evolved specific toxins to colonize the insect world, TIG 17 (2001) 193–199.
[9] N. Crickmore, D.R. Zeigler, J. Feitelson, E. Schnepf, J. Van Rie, D. Lereclus, J. Baum, D.H. Dean, Revision of the nomenclature for the *Bacillus thuringiensis* pesticidal crystal proteins, Microbiol. Mol. Biol. Rev. 62 (1998) 807–813.
[10] B.H. Knowles, Mechanism of action of *Bacillus thuringiensis* insecticidal δ-endotoxins, Adv. Insect Physiol. 24 (1994) 274–308.
[11] A. Bravo, S. Jansens, M. Peferoen, Immunocytochemical localization of *Bacillus thuringiensis* insecticidal crystal proteins in intoxicated insects, J. Invertebr. Pathol. 60 (1992) 237–246.
[12] C. Hofmann, H. Vanderbruggen, H. Höfte, J. Van Rie, S. Jansens, H. Van Mellaert, Specificity of *Bacillus thuringiensis* δ-endotoxins is correlated with the presence of high affinity binding sites in the brush border membrane of target insect midgut, Proc. Natl. Acad. Sci. U.S.A. 85 (1988) 7844–7848.
[13] E. Schnepf, N. Crickmore, J. Van Rie, D. Lereclus, J. Baum, J. Feitelson, D.R. Zeigler, D.H. Dean, *Bacillus thuringiensis* and its pesticidal crystal proteins, Microbiol. Mol. Biol. Rev. 62 (1998) 775–806.
[14] A. Lorence, A. Darszon, C. Díaz, A. Liévano, R. Quintero, A. Bravo, δ-endotoxins induce cation channels in *Spodoptera frugiperda* brush border membranes in suspension and in planar lipid bilayers, FEBS Lett. 360 (1995) 217–222.
[15] J.L. Schwartz, L. Garneau, L. Masson, R. Brousseau, E. Rousseaeu, Lepidopteran-specific crystal toxins from *Bacillus thuringiensis* form cation- and anion-selective channels in planar lipid bilayers, J. Membr. Biol. 132 (1993) 53–62.
[16] P.V. Pietrantonio, S.S. Gill, *Bacillus thuringiensis* δ-endotoxins: action on the insect midgut, in: M.J. Lehane, P.F. Billingsley (Eds.), Biology of the Insect Midgut, Chapman & Hall, London, 1996, pp. 345–372.
[17] J. Carroll, D.J. Ellar, An analysis of *Bacillus thuringiensis* delta-endotoxin action on insect midgut membrane permeability using a light scattering assay, Eur. J. Biochem. 214 (1993) 771–778.
[18] J. Carroll, D.J. Ellar, Analysis of the large aqueous pores produced by a *Bacillus thuringiensis* protein insecticide in *Manduca sexta*

117

midgut brush border membrane vesicles, Eur. J. Biochem. 245 (1997) 797–804.
[19] K. Hendrickx, A. de Loof, H. Van Mellaert, Effects of *Bacillus thuringiensis* delta-endotoxin on the permeability of brush border membrane vesicles from tobacco hornworm (*Manduca sexta*) midgut, Comp. Biochem. Physiol. 95C (1990) 241–245.
[20] M. Wolfersberger, P. Lüthy, A. Maurer, F. Parenti, V. Sacchi, B. Giordana, G.M. Hanozet, Preparation and partial characterization of amino acid transporting brush border membrane vesicles from the larval midgut of the cabbage butterfly (*Pieris brassicae*), Comp. Biochem. Physiol. 86A (1987) 301–308.
[21] F.G. Martin, M.G. Wolfersberger, *Bacillus thuringiensis* delta-endotoxin and larval *Manduca sexta* midgut brush border membrane vesicles act synergistically to cause very large increases in the conductance of planar lipid bilayers, J. Exp. Biol. 198 (1995) 91–96.
[22] O. Peyronnet, V. Vachon, J.L. Schwartz, R. Laprade, Ion channel activity from the midgut brush-border membrane of gypsy moth (*Lymantria dispar*) larvae, J. Exp. Biol. 12 (2000) 1835–1844.
[23] O. Arantes, D. Lereclus, Construction of cloning vectors for *Bacillus thuringiensis*, Gene 108 (1991) 115–119.
[24] D. Lereclus, H. Agaisse, M. Gominet, J. Chaufaux, Overproduction of encapsulated insecticidal crystal proteins in a *Bacillus thuringiensis spo*OA mutant, Bio/Technology 13 (1995) 67–71.
[25] W.E. Thomas, D.J. Ellar, *Bacillus thuringiensis* var. israelensis crystal δ-endotoxin: effect in insect and mammalian cells in vitro, J. Cell Sci. 60 (1983) 181–197.
[26] R.A. Bell, F.G. Joachim, Techniques for rearing laboratory colonies of tobacco budworms and pink bollworms, Ann. Entomol. Soc. Am. 69 (1976) 365–373.
[27] J. García-Soto, M. González-Martínez, L. de la Torre, A. Darszon, Sea urchin sperm head plasma membranes: characteristics and egg jelly induced Ca^{2+} and Na^{+} uptake, Biochim. Biophys. Acta 944 (1988) 1–12.
[28] A. Lorence, A. Darszon, A. Bravo, The pore formation activity of *Bacillus thuringiensis* Cry1Ac toxin on *Trichoplusia ni* membranes depends on the presence of aminopeptidase N, FEBS Lett. 414 (1997) 303–307.
[29] E. Harlow, D. Lane, Antibodies: A Laboratory Manual, Cold Spring Harbor Laboratory, New York, 1988, p. 597.
[30] J.C.M. Hafkenscheid, Enzymes 3; peptidases, proteinases and their inhibitors, in: J. Bergemayer (Ed.), Methods of Enzymatic Analysis, vol. V, Verlag Chemie, Weinheim, 1984, pp. 2–34.
[31] K. Luo, J.R. McLachlin, M.R. Brown, M.J. Adang, Expression of glycosylphosphatidylinositol-linked *Manduca sexta* aminopeptidase N in insect cells, Protein Expression Purif. 17 (1999) 113–122.
[32] E. Aranda, J. Sánchez, M. Perferoen, L. Güereca, A. Bravo, Interaction of *Bacillus thuringiensis* crystal protein with the migdut epithelial cells of *Spodoptera frugiperda* (Lepidoptera: Noctuidae), J. Invertebr. Pathol. 68 (1996) 203–212.
[33] R. Kinne, H. Murer, L. Kinne-Saffrano, M. Thees, G. Sachs, Sugar transport by renal plasma membrane vesicles: characterization of the systems in the brush border microvilli and basal-lateral plasma membranes, J. Membr. Biol. 22 (1975) 375–395.